Synthesis and Application of Organotelluroxane Macrocycles and Clusters

A Thesis

Submitted for the Degree of

DOCTOR OF PHILOSOPHY

In

CHEMISTRY

By

Gujju Narsimhulu

(Regd. No. 16CHPH09)

Thesis Advisor

Prof. Viswanathan Baskar

हैदराबाद विश्वविद्यालय
University of Hyderabad

प्रतिष्ठित संस्थान
INSTITUTION OF EMINENCE
राष्ट्रीय अपेक्षाएँ, वैश्विक मानक
National Needs, Global Standards

School of Chemistry
University of Hyderabad
Hyderabad 500046
Telangana
India

2023

Education is a human right with immense power to transform. On its foundation rest the cornerstone of freedom, democracy, and sustainable human development

-Kofi Annan

Dedication

This work is dedicated to my

parents (నరసమ్మ-రాజయ్య) for their endless love and

sacrifices.

Declaration

I, Gujju Narsimhulu hereby declare that this thesis entitled "**Synthesis and Application of Organotelluroxane Macrocycles and Clusters**" submitted by me working with the supervision of **Prof. Viswanathan Baskar** is a bona fide research work carried out by me in the School of Chemistry, University of Hyderabad, India. I also declare that it has not been submitted previously in part or in full to this University or Institution for the award of any degree or diploma.

In keeping with the general practice of reporting scientific observations, due acknowledgment has been made wherever the work described is based on the findings of other investigators. Any omission, which might have occurred by oversight or error, is regretted. This work is free from plagiarism. I hereby agree that my thesis can be deposited in Shodhganga/INFLIBNET.

University of Hyderabad
September 2023

Gujju Narsimhulu
(16CHPH09)

Dr. Viswanathan Baskar
(Thesis Advisor)

School of Chemistry
University of Hyderabad

प्रतिष्ठित संस्थान
INSTITUTION OF EMINENCE

Certificate

This is to certify that the thesis entitled "***Synthesis and Application of Organotelluroxane Macrocycles and Clusters***" submitted by **Gujju Narsimhulu** bearing Registration Number 16CHPH09 in partial fulfillment of the requirements for the award of Doctor of Philosophy in the School of Chemistry is a bonafide work carried out by him under my supervision and guidance.

This thesis is free from plagiarism and has not been submitted previously in part or in full to this or any other University or Institution for an award of any degree or diploma.

Further, the student has the following publications:

1. Pilli V V N Kishore[b], Junaid Ali[a], Gujju Narsimhulu[a] and Viswanathan Baskar[a], *J. Chem. Sci*. (2018) 130:100.
2. *Manuscript Submitted for peer review ID:* DT-ART-08-2023-002746
3. *Manuscript Submitted for peer review ID:* JCSC-D-23-00505
4. *Manuscript under preparation*

And
has made presentations at the following conferences:

1. New Frontiers in chemical science (NFSC) IIT Bombay-2018. (Best poster award)
2. 47th National seminar on crystallography June-2019. BARC Mumbai.
3. MTIC-XVIII, December-2019 IIT Guwahati.
4. Chemfest-2019, Chemfest-2020 (Best Poster award), Chemfest-2021(Oral-presentation).

Further, the student has passed the following courses towards fulfilment of coursework requirement for Ph.D.

Course Code	Name	Credits	Pass/Fail
CY801	Research Proposal	3	Pass
CY802	Chemistry pedagogy	3	Pass
CY805	Instrumental Methods-A	3	Pass
CY806	Instrumental Methods-B	3	Pass

Dean
School of Chemistry

Dr. Viswanathan Baskar
(Thesis Advisor)

Acknowledgments

First and foremost, I want to thank my thesis advisor, Prof. Viswanathan Baskar, for his invaluable advice, unwavering support, and patience throughout my Ph.D. tenure. I am grateful to him for allowing me to think outside the box and work on various projects. I cannot thank him enough for his guidance during my difficult times (professional/ personal). **Prof. Viswanathan Baskar,** I have learned and grown a lot while working with you, and thank you for being a great supervisor, and you have my deepest thanks.

I thank the present dean of the School of Chemistry, Prof. Ashwini Nangia, and former deans, Prof. M. Durga Prasad, Prof. T. P. Radhakrishnan, Prof. Anunay Samanta, and Prof. K. C. Kumara Swamy for providing necessary research facilities.

I am very thankful to my doctoral committee members, Prof. K. Muralidharan and Prof. M. Sathiyendiran, for their encouragement and support during my doctoral tenure. I give special thanks to Prof. D. B. Ramachary for his support, motivation, and encouragement during the M.Sc. project. I would also like to extend my thanks to my M.Sc. Teachers and all the faculty members of the School of Chemistry for their encouragement and cooperation.

I sincerely thank all the non-teaching staff of the School of Chemistry for their cooperation.

My heartfelt gratitude to my lab mates Dr. R. Amaleswari, Dr. Ugandar, Dr. Junaid Ali, Suman Mondal (batchmate), Tokala Navaneetha, Smruthi Prangya Bhehra, Calvin Samuel, Kamala Gangajala, project students Debujana, Dinesh, Gopendra Muduli, Akhil palak, Sabari Nathan (UGC-project).

My sincere thanks to my dearest friends of the School of Chemistry, Dr. Senthil Kumar, Dr. Ramesh Golla, Dr. Sathish Kumar anna, Dr. Arun Kumar Kanakati (MSc. Senior), Praveen (JJ), Dr. Raju mekala, P. Latha, Dr. Surendra, Dr. Sashi anna, Dr. Srinivas Vangara, Shekar, for their unconditional friendship, support, discussions, sittings, and what not.

My heartful thanks to best friends from M.Sc. and well-wishers, Kethavth Ravinayak, Ravi Jada, Anand Golla, Srikanth, Manugonda Srinivas, Barath Kumar Saketh, Anad pali, Surendra, and Ph.D. batchmates Dr. Lakshaman, Ravi, Latha, Shubham, Pritham, jyosna, Anupam, Mamina bhol, Irfan, Anjaneyulu, Prachi Pandey, Sarada Moni Mondal, Shubham Debnath, Shubham Dutta, SK Alim, Soutrick Das, Chinapaka Ravindar, Gorak chand, Akram.

Also thanks my school of chemistry friends and colleagues Ashok, Vamsi, Ali, Praveen, basha, Thamizl anna, Sathish, Obadiah, Babu, Hemanth, Mallesh, Debu Jana, Rameshwari, Manish, Anil, Sudiptho, Sashikanth, Dhanashekar, Suresh, Ramakrishna, Hema, Johar khan, Srinivas and all School of Chemistry senior and Junior Ph.D. scholars.

Sarvepally Radha Krishna Degree college (B.Sc.) lecturers and classmate Raju, Venugopal, Swamy, Naresh, Mounika, Reshma, Sandeep, Madhu (roommate). Navodaya Kranti Coaching Center for giving opportunity for working (part time) to complete my B.Sc. and all the friends during the B.Sc. days.

Bala Vidhya Jyothi junior College Cherial Teachers and friends Srinivas, Mahi, Madhu, Suresh, Hasan, Ravinder reddy, Ramesh, Naveen, Srilatha anumula, Bhargavi, Mahathi, Baghya Lakshmi, and Shahidha begam, Rajitha,Kavitha, Sumathi, Supriya, Ramya, Madavi, Sandhya, Chithra, Srikanth, Lakshmi, all the friends for creating a great environment to have good studies, happy and memorable days.

My school friends Mahi, Raju, Rajesh, Sagar, Babu, Karnakar, Vijju, Mahinder, Vinay, Raju babu, Ramesh, Ravi, Vinod, Naresh, Babu, Santhosh, Anil, Babu raju, Chiranjivi, Rajubabu, Rajireddy, Kiran, Rajalingam, Saikiran, Swapna, venu, Srihari, Lavanya, Lakshaman, Mahesh, PS latha, Madava, Vineeth babu, Kistayya, Narsimha, and all school mates' seniors and juniors my deepest thanks for creating a great enviorment healthy and friendly to complete my schooling.

My deepest gratitude gose to my teachers who inspired and motivated in my education journey from primary school to University of Hyderabd are Sathyanarayana, Srinivasa chary, Narayana Redyy, Padma, Premalatha, Sadandam, Prasanthi madam (inter english), Ram Moorthi sharma (Botany), Rajeshwary (Zoology), Saidulu (Chemistry), Basavaiah, TPR, KCK, Aswini Nangia, Durga prasad, DBR, Mahapatra, RC, PKP, SKD.

My sincere thanks to family relative aunti-uncles Mallavva-Balamallaih, Ellavva-Vemulaiah, Yaddavva-posaiah, Balayya-Uppalamma, Yadayya, lachavva-Anjamma-Balnary, Cousin's Narsimhulu-lavnya, Raju-mangavva, Anil-rani, Elraju-rena, Narsavva-Balamallu, Padma-Anuradha-Mohan das karam chand Gandhi, Mamathi-haribabu, Kankalakshmi-yakayya, Sandhya-Barath, and Mahesh, Hemanth, Abhi, Minnu, Mounika, Nakshu, Charan, Kavya, Deepa, Ram prasad, bakki (Swathika) Vijju, lucky, milky, shiny, Prsasthi, Goldy and latha-ravi, Mamatha-koti, madḥu, navya, chintu, Akhil, Revanth, smiley, lucky, Dinnu.

Also thanks my family members Chinnana-Chinnamma Lakshmi-Narsaiah, Anjavva-Balnari, mama and attamma yadaaih- Lalitha, Anna-Vadina, Nagma-Mahesh, Akhi-babu, Siri, Rakshitha, Ishu, Kushi baby.

I will not be sincere in my acknowldgements if I will not extend it to my late grandparents Posamma-Maisayya, Lingamma-Jalaiah.

I heartily thanks to my beloved wife Chaithanya for her unconditional love and support since June 18,2022 to carry my research work and writing thesis.

I also thank my new born baby girl **Ira**

I have no words to express my heartfelt gratitude, love, and respect to my parents **Narsamma-Rajaiah** for their blessings, endless love, sacrifices and for teaching me essence of education and integrity.

Gujju Narsimhulu
Date 28.06.2023

Table of Contents

List of Acronym

Å	Angstrom
ACS	American Chemical Society
bs	Broad singlet (spectral)
°C	Degree celsius
calcd	Calculated
cat.	Catalytic
cm^{-1}	Wavenumber
CCDC	Cambridge Crystallographic Data Centre
CV	Cyclic Voltammetry
δ	Chemical shift in parts per million
d	Doublet (spectral)
DCM	Dichloromethane
DMF	Dimethylformamide
DOI	Digital object identifier
EADX	Energy dispersive X-ray analysis
ESI	Electrospray ionization
HRMS	High resolution Mass Spectrometry
IR	Infra-red
NMR	Nuclear Magnetic Resonance
PXRD	Powder X-ray diffraction
SCXRD	Single Crystal X-ray Diffraction
SEM	scanning electron microscopy
TGA	Thermal Gravimetric Analysis
UV	Ultra-violet spectroscopy

SYNOPSIS

This thesis is entitled "***Synthesis and Application of Organotelluroxane Macrocycles and Clusters***." It is divided into four chapters, and a detailed description of each chapter is given below.

Chapter 1: Introduction

The work reported in this thesis revolves around organotellurium compounds. Hence a detailed review of organotellurium compounds, their reactivity, and product formed from organotellurium precures are dealt with in detail in this chapter.

Chapter 2: Organotellurium Macrocycles, and Telluronium Salts

In an effort to prepare a macrocycle capped with an octahedral anion, a reaction of Cl-macrocycle $[(p\text{-}MeO\text{-}C_6H_4)_2Te(\mu\text{-}O)(\mu\text{-}PhSeO_2)(\mu_4\text{-}Cl)]_2$ / $[\{(p\text{-}OMeC_6H_4)_2Te\}_2(\mu_2\text{-}O)(\mu\text{-}Ph_3CP(Ph)O_2))(\mu_4\text{-}Cl)]_2$ (**2.1**) was carried out with $AgPF_6$ in a benzene solvent. At room temperature a macrocycle where PF_4^- anions were found bridging and capping $[\{(p\text{-}OMe\ C_6H_4)_2Te\}_2\ (\mu\text{-}O)(\ p\text{-}OMe\ C_6H_4Te)\ (\mu_3\text{-}PF_4)(\mu_2\text{-}PF_4)]_2$ (**2.2**) was confirmed by single crystal X-ray diffraction analysis. When this reaction is done at high temperature it results in the formation of telluronium salt $[(p\text{-}OMe\ C_6H_4)_3Te]^+\ PF_4^-$ (**2.3**) and bis (*p*-methoxy phenyl tellurium di fluoride (R_2TeF_2). Further, we have also been able to expand 12-membred $[(p\text{-}MeO\text{-}C_6H_4)_2Te(\mu\text{-}O)(\mu\text{-}PhSeO_2)(\mu_4\text{-}Cl)]_2$, to 16-membered $[\{(p\text{-}OMeC_6H_4)_2Te\}(\mu_2\text{-}O)_4(\mu\text{-}PhSeO_2)(\mu\text{-}BF_4^-)]_4$ (**2.4**)tellurium macrocycle. Details of the structures will be discussed in this chapter.

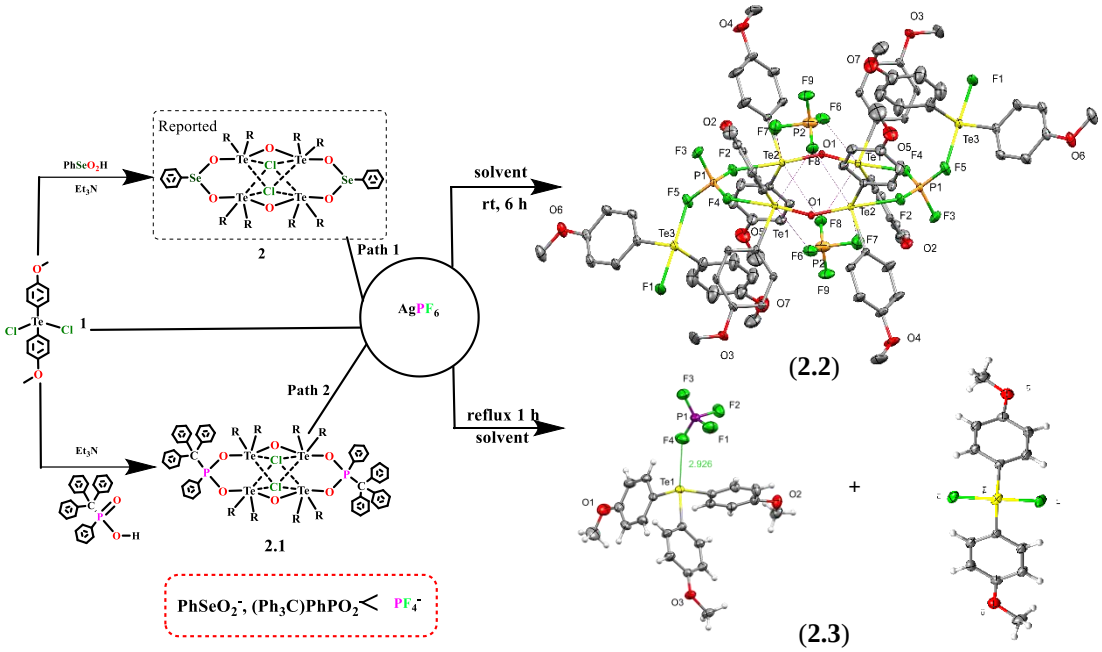

Scheme 1.

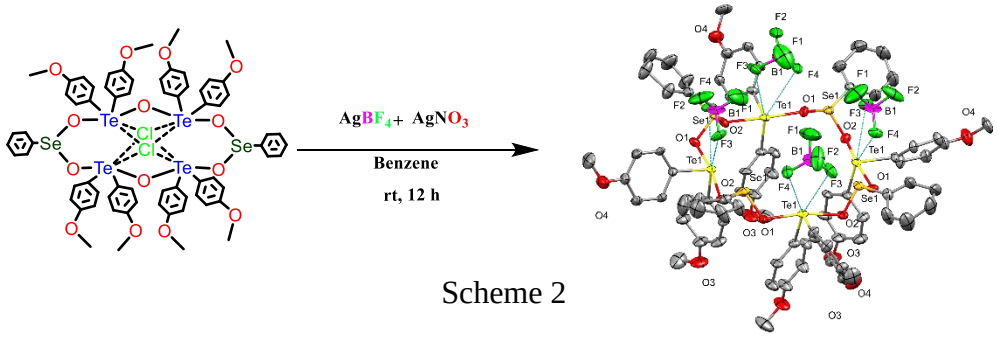

Scheme 2

Chapter 3: Electrocatalytic Hydrogen Evolution Mediated by an Organotelluroxane Macrocycle Stabilized through Secondary Interactions

The macrocycle is synthesized as the chloride abstraction from *bis*(*p*-methoxyphenyl) tellurium dichloride (**1**) by silver salts $AgMX_4$ ($MX_4 = BF_4^-$, and ClO_4^-) results in situ formed di-cationic tetraorganoditelluroxane units two such units are held together

by two weak anions μ_2-MX_4 bridging to create a 12-membered di-cationic macrocycle$[(p\text{-MeO-}C_6H_4)_2Te)_2(\mu\text{-O})(\mu_2\text{-}F_2BF_2)_2]^{2+}$ (**3.1**), $[(p\text{-MeO-}C_6H_4)_2Te)_2(\mu\text{-O})(\mu_2\text{-}O_2ClO_2)_2]^{2+}$ (**3.2**) stabilized via Te-(μ_2-BF_4/ClO_4), secondary interactions. The charge is balanced by two more μ-MX_4 anions present above and below the plane of the macrocycle. The same reaction at higher temperatures led to the formation of telluronium salts R_3TeX [X= BF_4^- (**3.3**), ClO_4^- (**3.4**)] as a significant product. The BF_4^- anion containing macrocycle and telluronium salt was monitored with ^{19}F NMR. The HRMS confirmed the stability of all the compounds in the solution state. Homogeneous electrocatalytic proton reduction is reported using organotellurium macrocycle as electrocatalysis employed in an organic medium with the addition of para-toluene sulfonic acid.

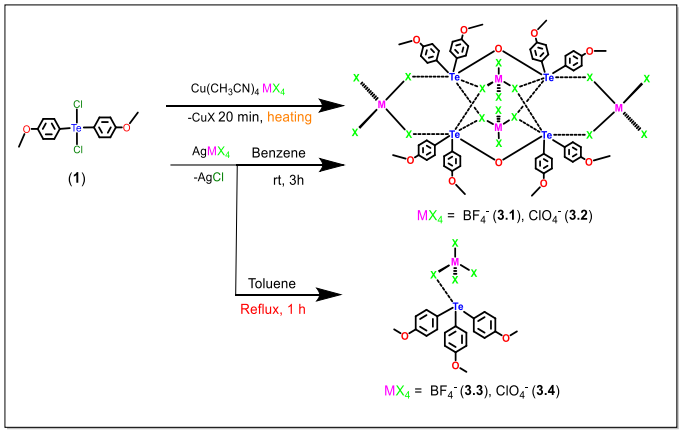

Scheme 3

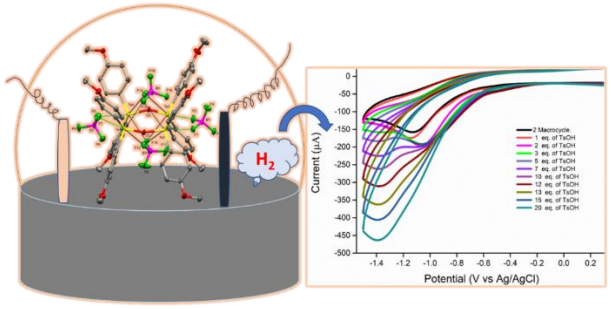

Figure 1: Synthetic scheme and solid-state structures of Organotellurium macrocycle, telluronium salts and homogeneous proton reduction.

Chapter 4: Star-shaped Te(VI)-Te(VI) Complex and an Octanuclear Heterometallic Te_2Sb_6 Oxocluster

The reaction of telluric acid with di-organotellurium di chloride R_2TeCl_2 and tri-organoantimony dichloride R_3SbCl_2 has been carried out in binary solvent using solvothermal synthesis method and isolated high phase purity two novel mixed valent tellurium(VI) containing clusters $Te^{VI}[OTe^{IV}(p\text{-}MeOC_6H_4)_2Cl]_6$ (R = p-$MeOC_6H_4$) (**4.1**) and $[Te(\mu_2\text{-}O_5SbPh_3)(OSbh_3Cl)]_2$ (**4.2**). The products have been analyzed using standard spectroscopic and analytical methods and optical band gap measurements discussed in this chapter.

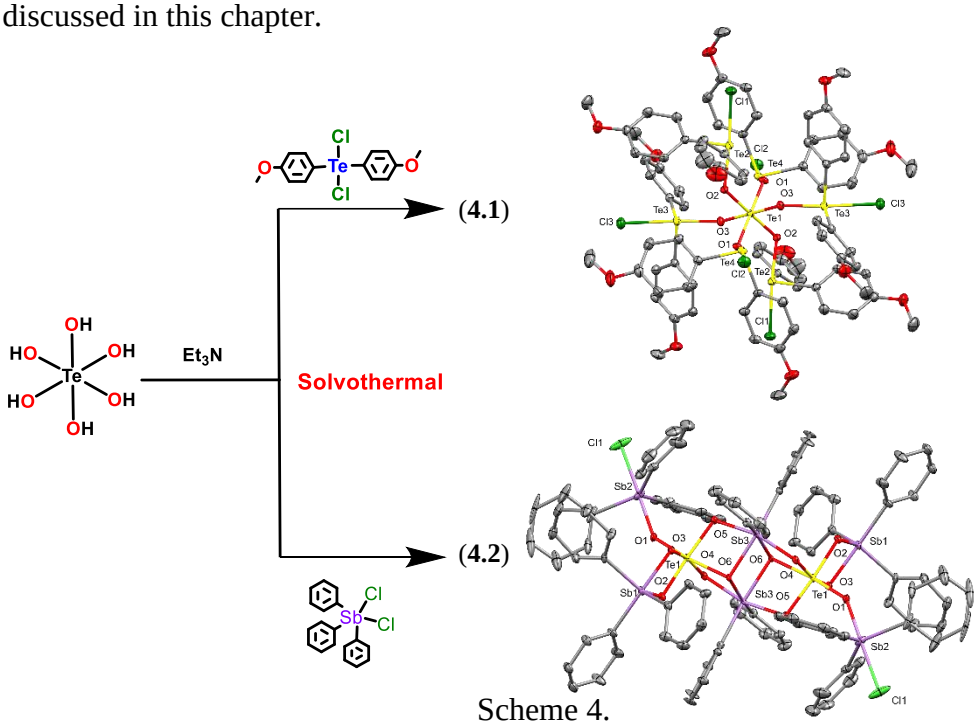

Scheme 4.

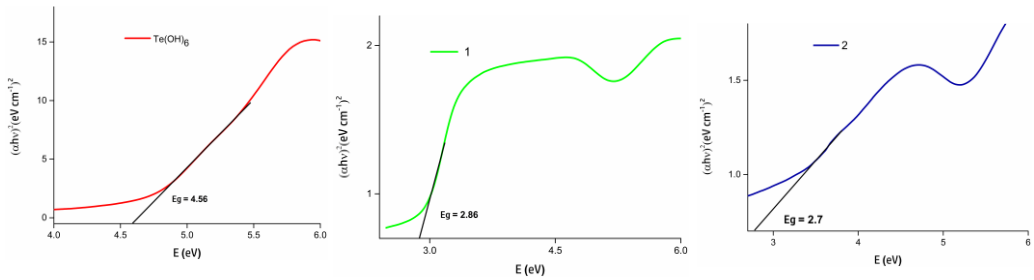

Figure 2. Tauc plot of telluric acid (red), (e) 4.1 (green), (f) 4.2 (blue)

Chapter 1

1. Introduction

The chapter deal with the synthetic methodologies of the starting material of the organotellurium compound in this thesis work. the reaction of the organotellurium compounds with various ligand systems have been dealt with to give the reader an insight in the chemistry of organotellurium compounds. Since the work reported is mainly deals with organotellurium compounds the introduction chapter has been restricting to the various halide and oxides of organotellurium and their reactivity with various ligand systems the protic ligands have been explored in detail.

Tellurium

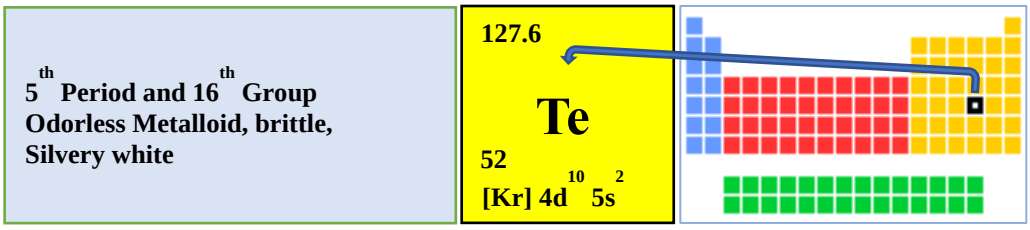

Franz-Joseph Müller von Reichenstein discovered tellurium in Sibiu, Romania, in 1783. He presumed it has bismuth or antimony. However, it turned out to be gold telluride ($AuTe_2$)[1]. Müller researched the ore for three years and found neither antimony nor bismuth. He affirmed that it contained a new element. He sent samples to a German scientist, **Martin Klaproth**, in 1796, whose research results were confirmed. Klaproth synthesized a refined sample and termed as **Tellurium**. The tellurium name from the Latin word "Tellus," which means earth. Tellurium contains eight isotopes that are naturally available, are ^{130}Te, ^{128}Te, ^{126}Te, ^{120}Te, ^{122}Te, ^{123}Te, ^{124}Te, and. ^{125}Te. The most and least naturally abundant isotopes are ^{130}Te (30%) and ^{120}Te (0.89 %), respectively. The NMR activity exists in the nuclei of ^{123}Te and ^{125}Te. However, NMR spectroscopic studies on ^{125}Te (natural abundance: 7.07 %) are more common than ^{123}Te due to its low natural abundance of 0.89 %.

Table 1. List of stable natural isotopes.

Name of isotope	Relative abundance
^{130}Te	34.08
^{128}Te	31.74
^{126}Te	18.84
^{125}Te	7.07
^{124}Te	4.74
^{122}Te	2.55
^{123}Te	0.89
^{120}Te	0.09

Earth's crust has between 60 and 140 parts per billion (ppb) of tellurium, which is about as abundant as platinum. Tellurium exists in several oxidation states, such as -2, 0, +2, +4, and +6.

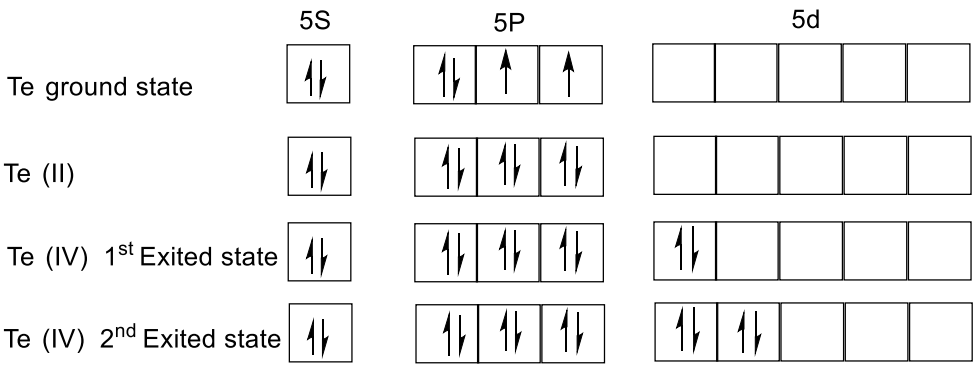

Figure 1a. Tellurium oxidation states

Tellurium possesses distinct physical and chemical properties that's it useful in a wide variety of industrial applications. It is used in the manufacturing of

semiconductors, alloys, and electroplating. it is also used in the production of solar panels, batteries, and rubber.

1.1 Organotellurium Compounds

Wöhler synthesized the first organotellurium compound, diethyl telluride, in 1840.[1] Organotellurium compounds were underdeveloped for a long time (seven decades) due to their foul odor, sensitivity to air and light[2], high reactivity[3] and difficulty in handling.[4] Another reason was a deficit of readily available synthesizing methods and tellurium, which was also thought to be harmful to humans.[5] These might be reasons for the slow evolution of organotellurium chemistry. In spite of that, it was later discovered that only a few compounds (such as alkyl, benzyl, and allyl tellurides) were inherently unstable, and organotellurium compounds were found to be responsible for the foul odor. Lederer's fruitful synthetic efforts led to many aromatic tellurium compounds between 1910 and 1920. Thereafter organotellurium chemistry developed with renowned scientists However, still organotellurium chemistry was less explored than organosulfur and organoselenium chemistry.

Carbon-carbon bond formation reactions, oxidation and reduction reactions of organic compounds, and other applications based on organotellurium compounds in the field of synthetic organic chemistry have all been reported. They are used as reagents alongside other transition metal complexes in cross-coupling reactions. Engman published the first review on synthetic applications of organotellurium compounds in 1985, and Petragnani and his co-workers also published several reviews.[6] In the last three decades, there has been substantial progress made in the area of synthetic research on tellurium-based compounds. Various organotellurium compounds have been synthesized and investigated in the evolution of antioxidants[7,8] and biologically crucial molecules[9] during this time period. Recently reports evidence for C-F bond formation via formal reductive elimination tellurium (IV)[10] and a detailed review on metal complexes using organotellurium compounds and nanosized metal tellurides for photocatalysis,

electrocatalysis, and catalysis[11] Organotellurium-based compounds are divided into various classes based on the number of halides and organo groups connected to tellurium, such as organotellurium trihalide ($RTeCl_3$), diorganotellurium dihalides (R_2TeCl_2), organotellurium mono halide (R_3TeCl), diorganyl tellurides (R_2Te), diorganyl ditelluride (R_2Te_2) and organotelluronium salts ($R_2R´TeX$).[12]

1.2 Preparation of organotellurium compounds

The efficient and high-yield organotellurium preparation can be achieved by using $TeCl_4$ as starting material. Te powder is also used as starting material in a few methods. This section describes a few important preparative methods for the synthesis of organotellurium compounds.

1.2.1 Diorganotellurium dichloride (R_2TeCl_2)

Tellurium tetrachloride as electrophilic reagents form organotellurium trichlorides (at room temperature to 60 °C) and organotellurium dichloride[13] (1) at an elevated temperature of 160 °C when it reacts with an excess of aromatic compounds containing activating groups (e.g., RO-, ROMe-, R2N-, RS-: R = aromatic group). It is a solvent-free method, and after the reaction solution was allowed to solidify/ the remaining aromatic compounds which can be separated using a high vacuum. In the case of less reactive aromatic compounds such as benzene and toluene, high temperatures and a Lewis acidic catalyst ($AlCl_3$) are required.

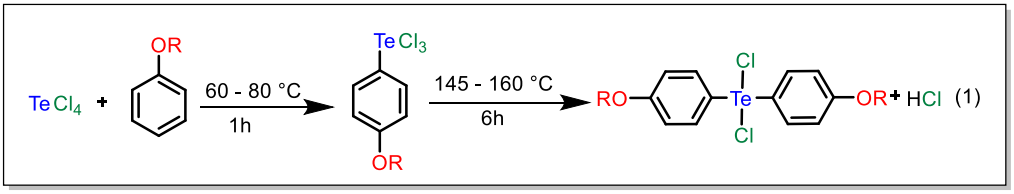

Scheme 1.1

The cleavage of Sn-C (2) and Pb-C (3) facilitates the formation of diorganotellurium di chloride when tetraphenyl tin and tetraphenyl led are reacted

with tellurium tetrachloride in aromatic solvents such as benzene and toluene at high or ambient temperatures respectively.[14]

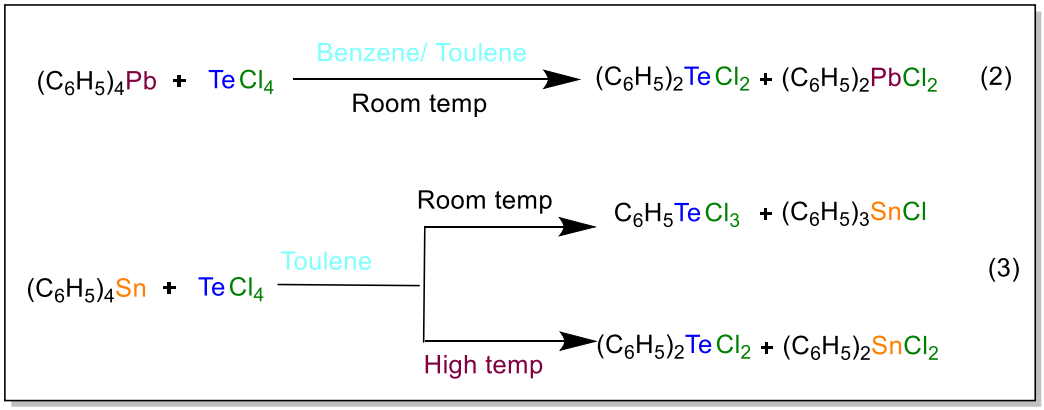

Scheme 1.2

Also, using organometallic reagents such as RHgCl, RMgX, $RN_2^+Cl^-$, or RLi in combination with Te powder or $TeCl_4$, diorganotellurium dihalides have been synthesized. However, the disadvantage of these methods is due to low yields and the formation of other by-products, such as diorganyl tellurides, diorganyl ditellurides, or organotellurium trihalides.[15] The reduction of diorganotellurium di chloride gives the diorganotellurides which further on halogenation can be used to prepare heavier di halides (R_2TeX_2, X = Br, I). Because tetrabromide and tetraiodide do not readily participate in condensation reactions, tellurium tetrachloride is always desired as a starting precursor.

Structural details:

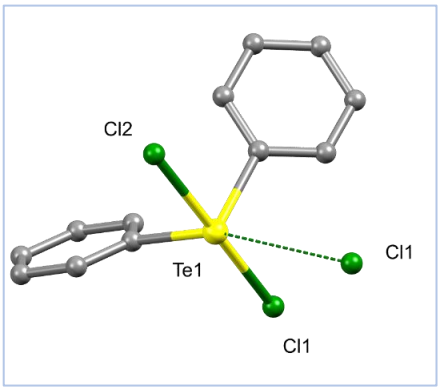

Figure.1.1 Solid state Molecular structure of Ph_2TeCl_2 molecular.

In its solid-state structure, Ph_2TeCl_2 has one Te...Cl interaction, resulting in a distorted octahedral geometry around Te with the sixth position vacant. The asymmetric loan pair in the equatorial position of dimethyl di chloride also shows a distorted-trigonal bipyramid, C—Te---Cl segment of the crystal suggesting a donor-acceptor type

interaction for intramolecular bonding in $(CH_3)TeCl_2$. Para substituted phenyl tellurium dichloride structure is different from those of $(p\text{-}MeC_6H_4)_2TeCl_2$ and $(p\text{-}MeOC_6H_4)_2TeCl_2$ the details of given below.

The structure of $(p\text{-}MeC_6H_4)_2TeCl_2$ is distorted pentagonal bipyramidal, with two primary Cl atoms occupying axial positions. R_2TeCl_2 (R= alky, aryl) solid state molecule structures have distorted trigonal-bipyramidal geometry, with chlorine atoms occupying axial places and a stereo chemically active lone pair, and two carbon atoms filling lateral positions. However, when secondary Te...Cl interactions are taken into account, the geometries around Te change depending on the steric challenge of the organic substituent present on Te.[16] These diorganyl tellurium dihalide compounds, which include a tetrazole unit, operate as a corrosion inhibitor and protect metal surfaces from moisture corrosion.[12]

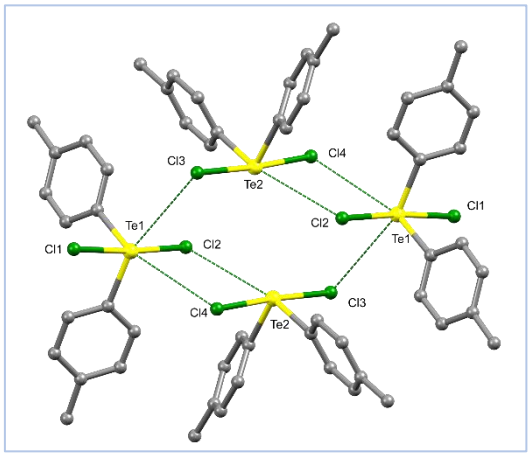

Figure 1.2. Solid state Molecular structure of R_2TeCl_2 Distorted trigonal-bi pyramidal geometry around Te

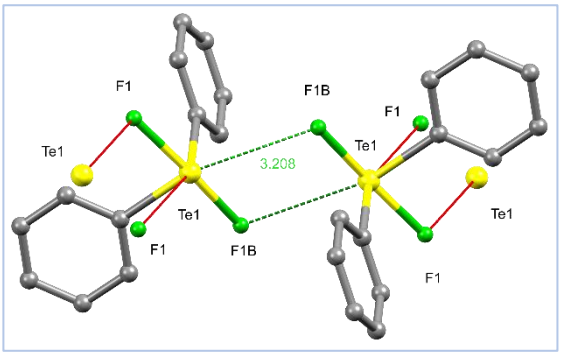

Figure 1.3. Solid state Molecular structure of R_2TeF_2 Trigonal bi pyramid.

The interactions between tellurium and fluorine are weak due to the long contact. The tellurium atom's geometry is distorted trigonal bipyramidal. Here fluorine atoms are in the axial position with a bond angle of 173° and two phenyl rings in the equatorial positions and a bond angle is 96.9° This is due to the repulsion of phenyl rings by loan pair of tellurium.

1.2.2 Organotellurium trichlorides $RTeCl_3$

In Scheme 1, the aromatics (activated) react with tellurium tetrachloride in a 1:1 mole ratio, resulting in the formation of organotellurium trichloride. But less reactive aromatic compounds will not produce the desired products using this method. Tellurium tetrachloride reacts with aryl mercury chlorides to form aryl tellurium trichlorides in this case.[17] In nitromethane reflux, aryl boronic acids were treated with tellurium tetrachloride to produce aryl tellurium trichlorides.[18] A solventless reaction for the preparation of aryl tellurium trichlorides has been reported by treating tellurium tetrachloride with the corresponding activated aromatic compound.[19]

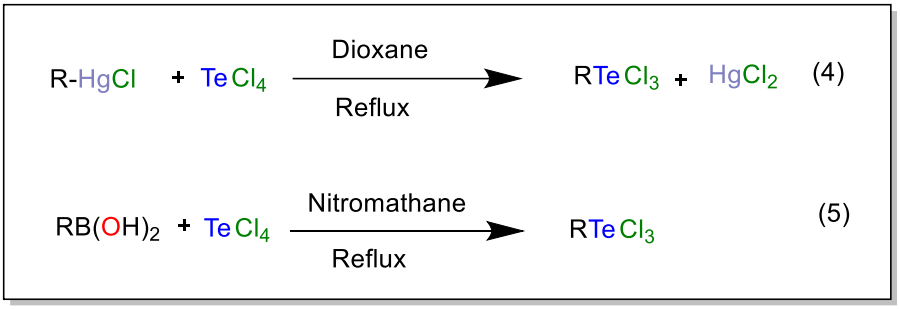

Scheme 1.3

The majority of diorganoditellurides (R_2Te_2) and diorganotellurides (R_2Te) are made by reducing tri organotellurium chloride and di organotellurium tellurium di chloride, respectively.[20] some other methods are also employed for the synthesis of diorganoditellurides in quantitative yields.[20] (as shown in scheme 4)

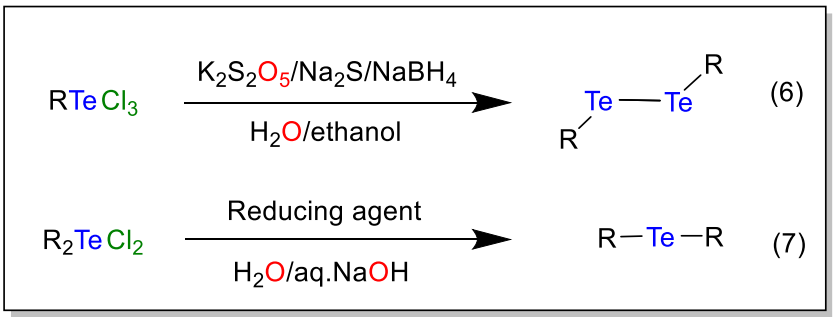

Scheme 1.4

By breaking the Te-Te bond of diaryl tellurides in refluxing toluene with freshly prepared electrolytic copper, diorganotellurides can be synthesized at good yields.

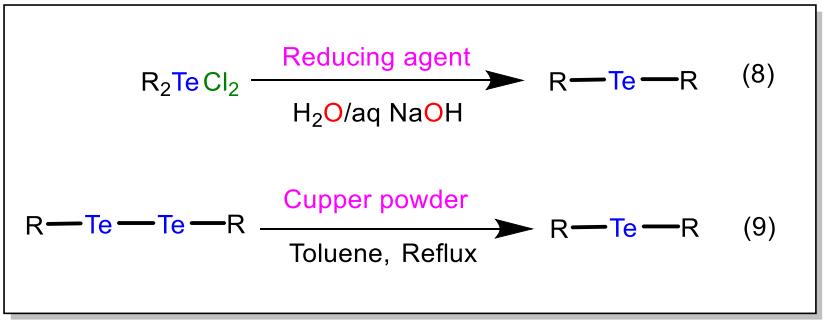

Scheme 1.5

1.2.3 Diorganotellurium oxide structural aspects and diorgano tellurones

The aqueous solution of NaOH (2N or 5%) is used for the hydrolysis of diorganotellurium dihalide to get diorganotellurium oxide. To improve the solubility of the reaction mixture small amount of ethanol is used.[21]

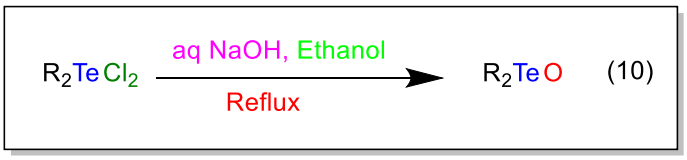

Scheme 1.6

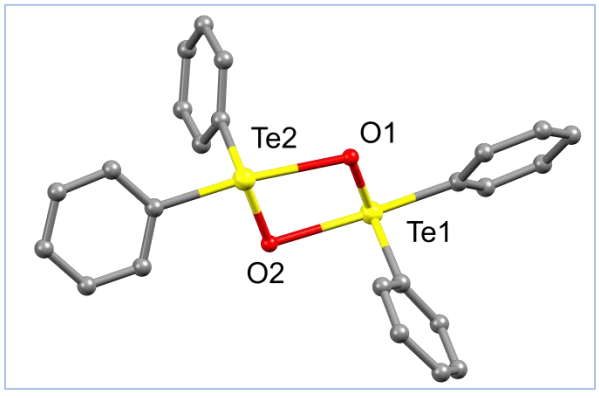

Figure 1.4. Solid state Molecular structure of diphenyl tellurium oxide

Based on the aryl group attached to the Te, diorganotellurium oxides R_2TeO (R= aryl) form different structural patterns in solid state. Ph_2TeO's solid state structure is that of a dimer, which consists of two monomers connected through short Te...O links (average Te-O 2.55(1)) that are then connected through longer

Te...O bonds (average Te-O 3.77(1)). Each Te atom achieves a distorted square-pyramidal geometry by taking into consideration all of these secondary Te...O interactions (Figure 1d). Contrary to this structure, $(p\text{-}MeOC_6H_4)_2TeO$ is a polymeric chain with a Te-O backbone that is zigzag-shaped and devoid of Te...O secondary contacts (Figure 1.4). Te achieves a distorted trigonal-bipyramidal shape with two O atoms occupying axial places by accounting for stereochemically active lone pairs.[22]

Diorgano tellurones (R_2TeO_2):

Using sodium periodate or sodium hypochlorite as an oxidant, diorgano telluroxides or diorgano tellurides can be oxidized to produce diorgano tellurones. The corresponding diorgano tellurone was produced in excellent yields by treating a solution of telluride or telluroxide in ethanol with an aqueous solution of sodium periodate or sodium hypochlorite at room temperature.[23]

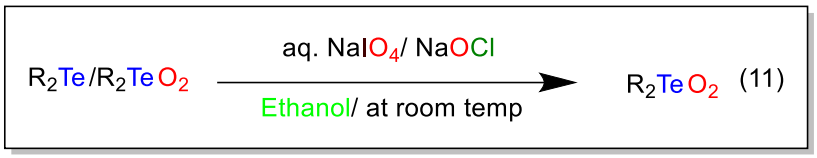

Scheme 1.7

1.3. Reactions of Diorganotellurium dihalide

1.3.1 Reactions of Diorganotellurium dihalide with Etdtc, Etdtp

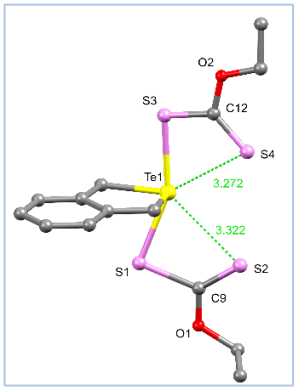

Figure 1.5. Solid state Molecular structure of $C_8H_8Te(S_2COEt_2)_2$.

Dakternieks et al. published their findings in 1988, the reaction of $C_8H_8TeI_2$ with the sodium salt of ethelene bis dithiocarbanate (Etdtc), dithiophosphate (Etdtp), and dithioxanthate (Etxan)/treated in dichloromethane at room temperature produced $C_8H_8Te(S_2COEt_2)_2$, $C_8H_8Te[S_2P(OEt_2]_2$ and $C_8H_8Te(S_2CNEt_2)$ respectively.[24] They demonstrated that whereas dithiophosphate and dithioxanthate complexes contain extra Te-S interactions and form polymeric and dimeric structures, respectively, in the solid state, the dithiocarbamate complex are monomeric. They confirmed that all of these complexes' solid-state structures were retained in solution as well with the aid of solution ^{125}Te NMR. [24] Dakternieks et al. reported that Ph_2TeCl_2 treated in toluene at -40C with sodium salts of dithiocarbamate (Etdtc), dithiophosphate (Etdtp), and dithioxanthate (Etxan), resulting in $Ph_2Te(S_2CNEt_2)_2$, $Ph_2Te[S_2P(OEt)_2]_2$, and $Ph_2Te(S_2COEt)_2$, respectively. (Figur) These complexes were found to be unstable in dichloromethane and decomposed to Ph2Te and $(Etdtc)_2/(Etdtp)_2/(Etxan)_2$.[25]

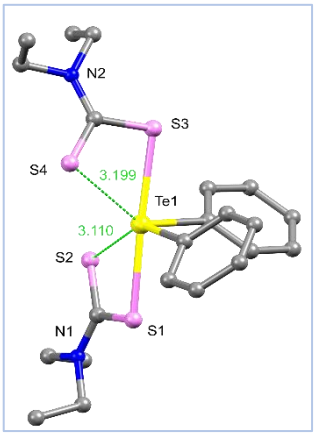

Figure 1.6. Solid state molecular structure of $Ph2Te(S_2CNEt_2)_2$.

1.3.2 Reaction of diorganotellurium di halide with carboxylates

Petragnani et al. reported diorganotellurium dihalides reacting with silver carboxylate in refluxing benzene, leading to the production of diorganotellurium carboxylates (scheme 12).[26] In order to create these compounds, diorganotellurium dihalides were also put through an anion exchange resin that had previously had its ions replaced with carboxylate ions.

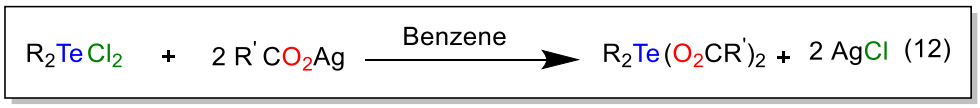

Scheme 1.8

The reactions of acyclic/cyclic tellurium dihalides with freshly prepared silver carboxylates to yield corresponding tellurium dicarboxylates as reported by Srivastava and co-workers.[27]

The reactivity of diorganotellurium dichloride with ferrocene dicarboxylic acid was reported by Chandrasekhar et al., resulting in the formation of a 16-membered tellurium-containing macrocycle (Scheme 9). Two quasi-reversible single-electron oxidations of tellurium ferrocene carboxylate macrocycle were observed. The $E_{1/2}$ value is 0.88 V, and the author proposes that this compound belongs to a class between class I (no coupling) and class II (weakly coupled) systems.[28]

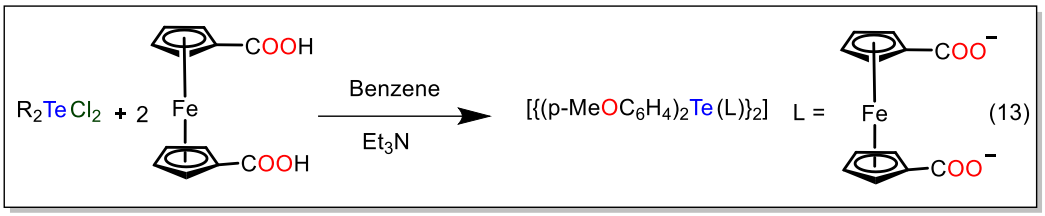

Scheme 1.9

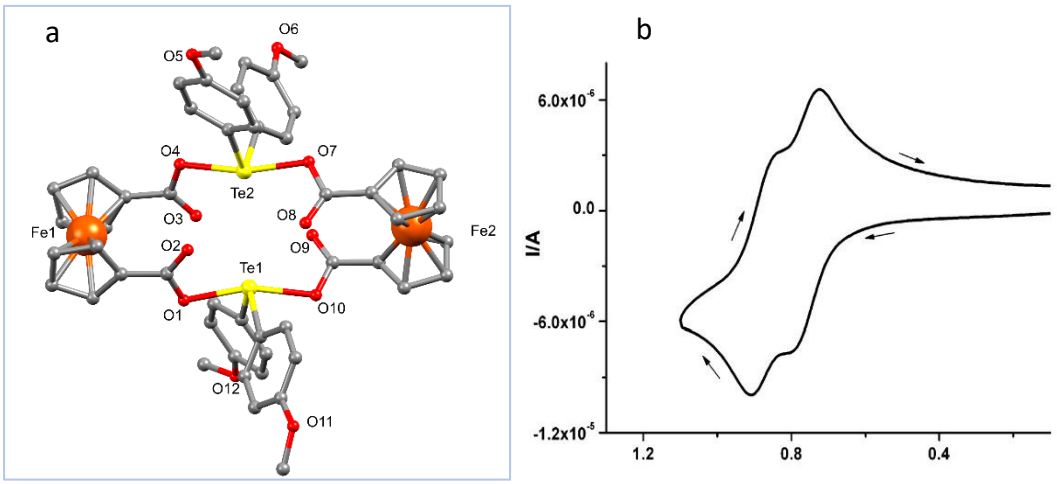

Figure 1.7. (a) Solid state molecular structure of $[R_2TeL]_2$; R=(4-CH_3O-C_6H_4), LH_2=1,1′-ferrocene dicarboxylic acid and (b). cyclic voltammogram

Puddephatt et al. reported the oxidative addition of Ph_2TeCl_2 to form a dimethylplatinum(II) complex. It is well known that telluro ethers and dialkyl/diaryl tellurides can form Te-metal bonds with a variety of transition metal atoms. However, this was the first instance to show the tellurium-halide bond being added oxidatively to a transition metal complex, despite previous reports of oxidative addition of Te-C/Te-M (M= Si, Ge, Sn).[29] In a typical experiment, a 1:1 mole ratio reaction of Ph_2TeCl_2 with [$PtMe_2$(bu_2bpy)] in water is performed. At room temperature, dichloromethane gave rise to [$PtClMe_2$($TePh_2Cl$)(bu_2bpy)]. The trans-oxidative addition of the Te-Cl bond to the platinum(II) complex produced the product.[30]

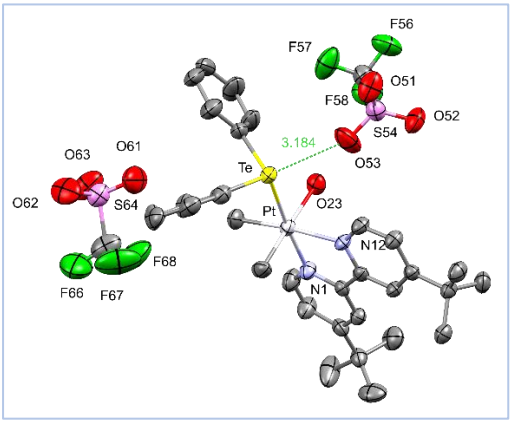

Figure 1.8. solid state molecular structure of [$PtClMe_2$($TePh_2Cl$) (bu_2bpy)]

1.3.3 Reaction of diorganotellurium chloride with protic acid

Chandrashekar et al reported several articles with organotellurium oxide/dihalide with various ligand systems discussion given below. The formation of chloride capped 12- membered Te-containing [((p-$MeOC_6H_4$)Te)$_2$(μ-O)(μ-CyclPO_2(μ$_4$-Cl)]$_2$ macrocycle by reacting with protic cyclic phosphinic acid with para (methoxy phenyl) tellurium di chloride in the presence of Et_3N. This was the first report of an inorganic tellurium-containing macrocycle that could act as a host for halide ions, even though

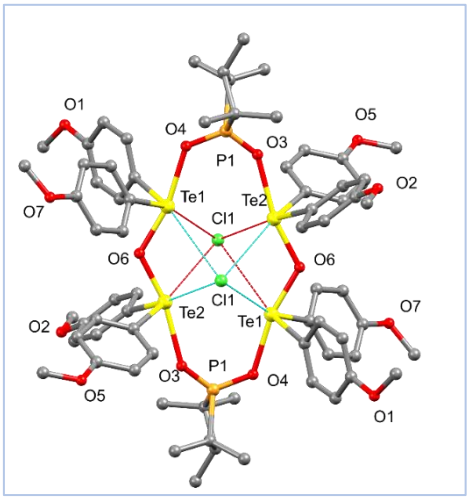

Figure 1.9. Solid state molecular structure of Frist tellurium macrocycle

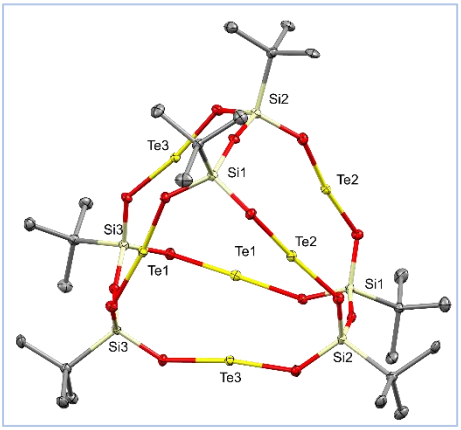

Figure 1.10. Solid state molecular structure of trigonal prismatic core of $[((p\text{-}MeOC_6H_4)_2Te)_6(t\text{-}BuSi)_6O_{15}]$, *p*-methoxy phenyl, hydrogen atoms omitted for clarity

transition metal-containing macrocyclic hosts for halides had previously been described Via Te halide interactions, this macrocycle stabilized the halide ions, and using ESI-MS, they asserted that these secondary contacts also existed in solution[31]. the reaction of organotellurium oxide/halide with ferrocene carboxylic acid (FcCOOH, Fc = C_5H_4-Fe-C_5H_5) in the presence of (triethylamine in case of R_2TeCl_2) toluene/benzene formed organotellurium ferrocene carboxylate $[(4\text{-}OMePh)_2Te(O_2CFc)_2]$/$[(4\text{-}NMe_2\text{-}Ph)_2\text{-}\ Te(O_2CFc)_2]$[31c], subsequently carried out transmetallation of Ar! HgCl and $ArTeCl_3$ synthesized unsymmetrical diorganotellurium (IV) dihalide Ar! (Ar)$TeCl_2$ [Ar! = 2-(R-CH=N-C_6H_3Me; R = 1-pyrenyl, 9-anthracenyl and 9-phenanthrene; Ar = 4-MeO-C_6H_4, 1-$C_{10}H_7$, 2,4,6-Me_3-C_6H_2, C_6H_5, 4-Me-C_6H_4] they studied fluorescent properties of this compounds.[31d] In a 4:6 ratio, silanetriol t-BuSi$(OH)_3$ was combined with (p-$Me_2NC_6H_4)_2TeO$ to create $[((p\text{-}Me_2NC_6H_4)_2Te)_6$ $(t\text{-}BuSiO_3)_4]$, it has a tetrahedron cage structure. with silicon atoms occupying the tetrahedron's vertices. Each pair of silicon atoms is linked together by an R_2TeO_2 pattern. The six O-Te-O bridges occupy the tetrahedron's edges. whereas the reaction of tetrahydroxy-1,3-disiloxane, [*t*-BuSi$(OH)_2$], in a 3:6 ratio with $(p\text{-}MeOC_6H_4)_2TeO$ produced $[((p\text{-}MeOC_6H_4)_2Te)_6(t\text{-}BuSi)_6O_{15}]$. This is a prismatic trigonal cage. The latter is made up of two $Te3Si3O_6$ rings that are linked together by 3 Si-O-Si connections. The molecular structure of $[((p\text{-}MeOC_6H_4)_2Te)_6(t\text{-}BuSi)_6O_{15}]$is similar to the secondary

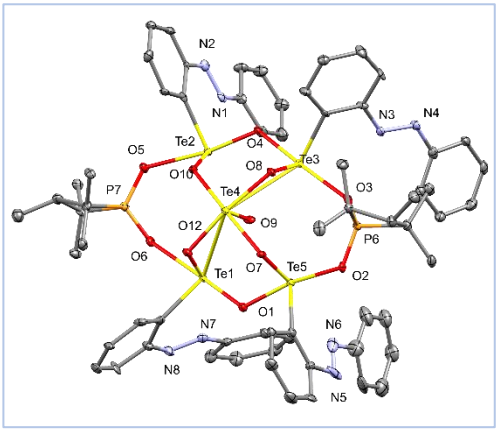

Figure 1.11. Solid state molecular structure of penta nuclear $[(RTe)_4(TeO)(\mu\text{-}O)_6(cycPO_2)_2]$ macrocycle.

architecture framework seen in zeolites such as faujasite.[31e] Same group in 2014 Cyclic phosphinic acid (cyc P(O)(OH)) and diphenyl phosphinic acid (C6H11) were each individually reacted with mono-organotellurium trichloride RTeCl3 (R = 2-phenyl - azo phenyl) to produce two pentanuclear complexes.[31f]

1.3.4 Reaction of diorganotellurium chloride with organo selenic acid

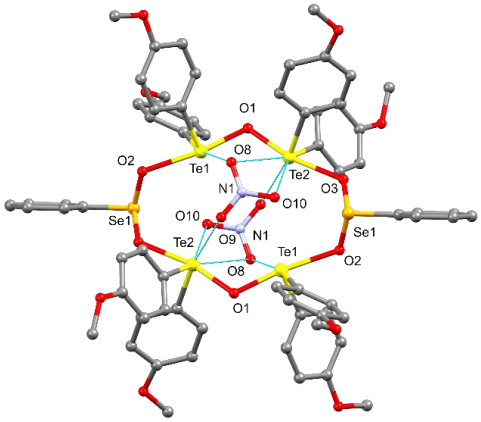

Figure 1.12. Molecular structure of NO_3 capped Te-macrocycle

Our group was involved in the preparation of the organotellurium tellurium macrocycle with benzene seleninic acid, which formed a 12-membered inorganic macrocycle composed of two tetraorganotelluroxane moieties assembled. dicationic $Te_4Se_2O_4$ macrocyclic core stabilized with Te---X (X = spherical anions Cl, Br, and I) with two seleninate Following that, the anion exhibits an exchange reaction of the 12-membered macrocycle with various anions exhibiting variable geometry around the central atom with Te---O and Te---F (NO_3), (ClO_4^-, BF_4^-) interaction give stability.[32]

1.3.5 Hydrolysis of diorganotellurium dichloride

Andrew Docker et. al recently came up with novel telluroxanes, synthesized by hydrolyzing 3,5-bistrifluoromethylphenyl (Ar) substituents containing diaryl tellurium dihalides (Ar_2TeX_2, where X = Cl, Br). Whenever there is a halide templating agent results in the spontaneous formation of a molecular $Ar_{16}Te_8O_6X_4$ cluster (Fig. 1). The clusters are composed of a $Te_8O_6X_4$ core, stabilized by Te--X (X = Cl, Br) Tellurium-anion interactions and characterized by a variety of spectroscopic techniques and X-ray diffraction structural analyses. These Organotelluroxane clusters exist as discrete molecular clusters and have high organic solvents solubility and also chemical stability. In addition, the author claims that fluorescence studies show that organo telluroxanes clusters display aggregation-induced emission (AIE) behavior in organic aqueous solvent combinations. [33]

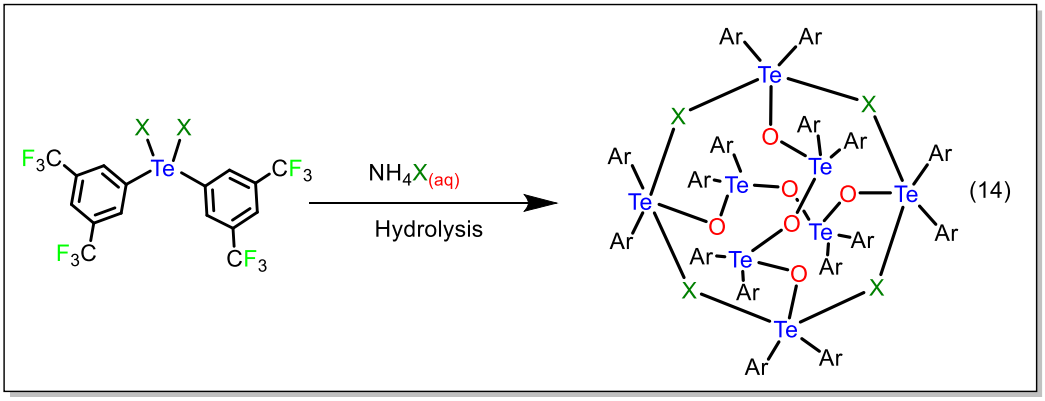

Scheme 1.10

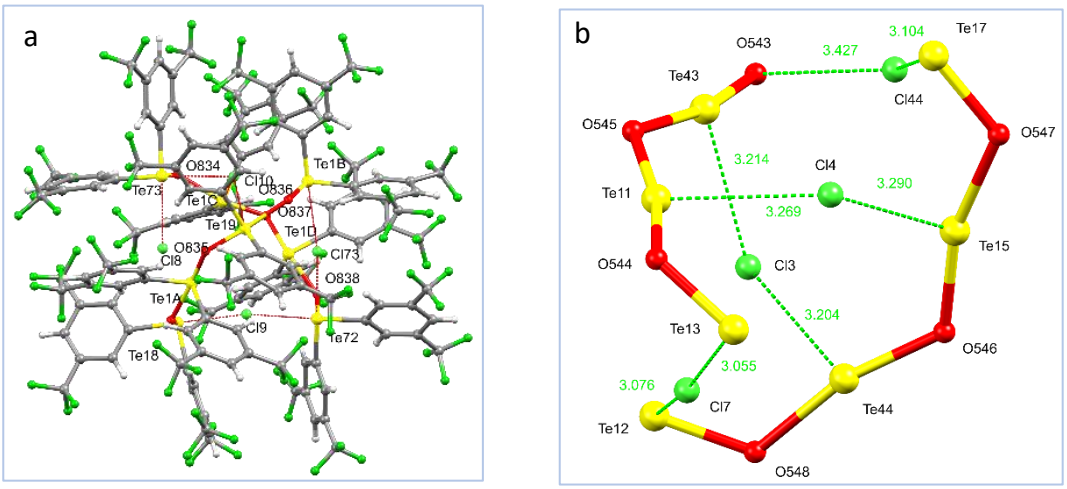

Figure 1.13. Solid state molecular structure of $Ar_{16}Te_8O_6X_4$ (left) and its core structure (right)

1.3.6 Hydrolysis of diorganotellurium iodide/oxidation organotellurium (II) compounds.

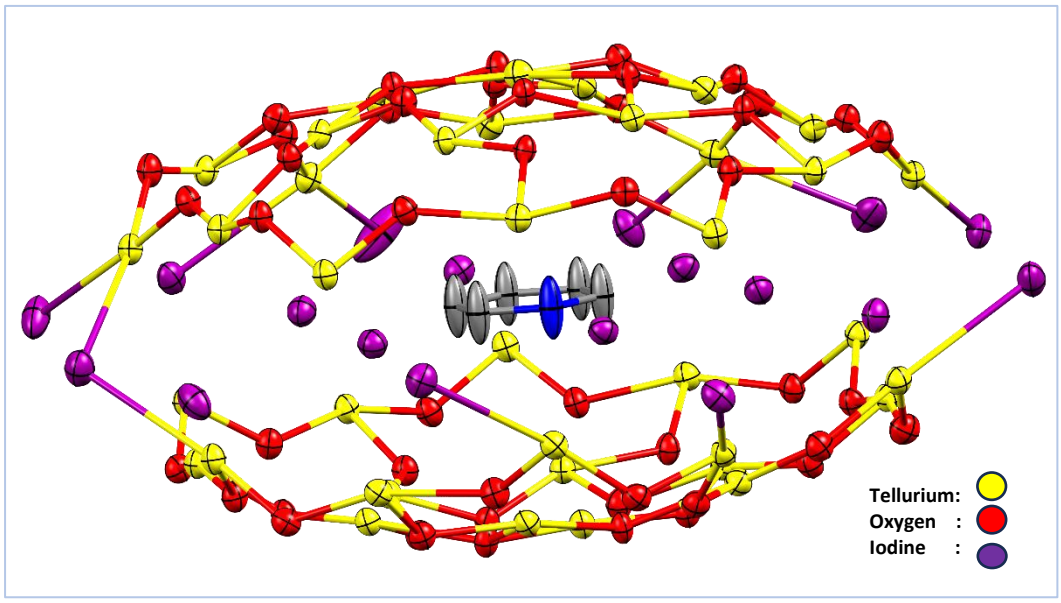

Figure 1.14. Solid state molecular structure of $[\{(PhTe)_{19}O_{24}\}_2I_{18}]$, phenyl rings on tellurium atom and all hydrogen atoms are omitted for clarity.

The controlled hydrolysis of $(PhTeI_3)_2$ produced phenyl telluroxane clusters or this organotelluroxane cluster can be achieved by the hydrolytic oxidation of different

phenyl tellurium (II) compounds in the presence of iodine. This organotelluroxane clusters architecture is made of two half spheres with a formula of $\{(PhTe)_{19}O_{24}\}^{9+}$ these two halves are connected by 18 iodine atoms and the whole structure can accommodate methanol, pyridine solvents. Previously, H.B. Singh and colleagues produced organotelluroxane clusters employing mixed-vallent phenyl tellurenyl bromide bromide.[33a]

1.3.7 Reaction of *p*-(methoxy phenyl) tellurium oxide

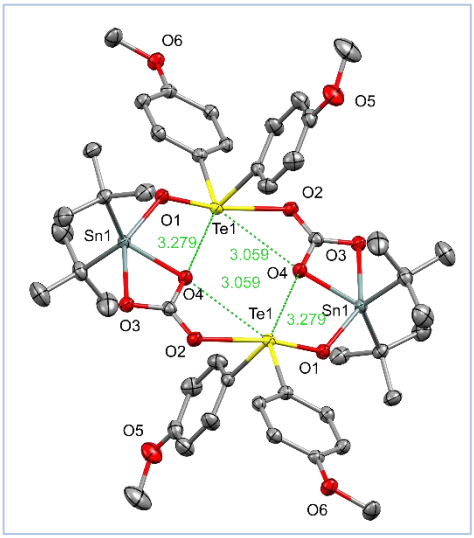

Figure 1.15. solid state molecular structure of [(*p*-$MeOC_6H_4)_2TeOSn(tBu_2)CO_3$]

Kobayashi and Furukawa et al. reported that in dry CH_2Cl_2/CH_3CN at -40°C in an Argon environment for 30 minutes, one equivalent of $NOBF_4$ was added to bis(4-methyl phenyl) telluride to form the quantitative yield of bis[bis(4-methyl phenyl)tellurium(iv)] oxide bis(tetrafluoroborate).[34] The reaction of (p-$MeOC_6H_4)_2TeO$ with triflic acid and phosphinic acid produces tetraorganoditelluroxane$(F_3CSO_3)R_2Te$ and OTe $R_2(O_3SCF_3)$ $(Ph_2PO_2)R_2Te$ and OTe $R_2(O_2PPh_2)_2Ph_2PO_2H$ respectively.[35] Beckmann et al. reported that organotellurium oxide and organotin worked together to fix CO_2. They discovered that a 1:1 solution of p-(methoxy phenyl) tellurium oxide and di-tert-butyl tin oxide readily absorbs carbon dioxide to form [(p-$MeOC_6H_4)_2TeOSn(tBu_2)CO_3$]. (Figure 1.13) At room temperature, air-stable crystalline material forms in 15 minutes and is crystalline material forms in 15 minutes and is when the solution is purged with too much carbon dioxide, a virtually quantitative yield is obtained. two secondary Te---O bonds within a single molecule are observed for tellurium atoms in tellurastannoxane, which involve the carbonate moiety's O_4 and molecular structure identified by ^{29}Sn and ^{125}Te NMR studies.[36]

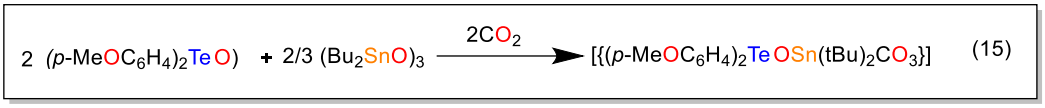

Scheme 1.11

1.4 Tri-organo telluronium salts

R_3TeX, or organo telluronium salts, have been known for over a century. Telluronium salts have sparked considerable interest in recent years due to their role in organic synthetic chemistry. Telluronium salts are two types unsymmetrical telluronium salts and symmetrical telluronium salts, which are starting materials for telluronium ylides, can combine with carbonyl compounds to produce a variety of substances, including oxiranes and secondary alcohols.[37] Ronald.F. Ziolo et. al reported the first triphenyl telluronium chloride $(C_6H_5)_3TeCl$.[38] In the solid state, triphenyl telluronium chloride is predominantly ionic.

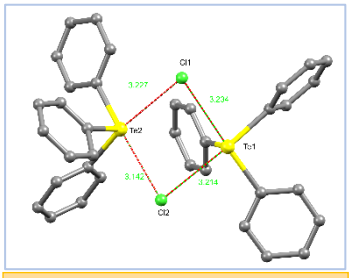

Figure 1.16. solid state molecular structure of Triphenyl telluronium chloride salt

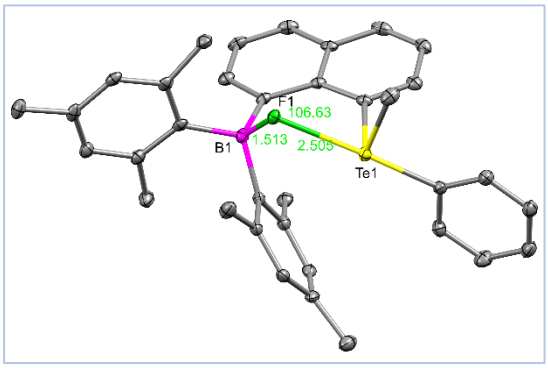

Figure 1.17. solid state molecular structure of Triphenyl telluronium chloride salt

Recently, Gabbai et al. developed novel method for the design of polyfunctional lewis acids by using heavier tellurium ion as lewis acidic sites, with a combination of a boryl moiety.it is capable because of its electropositive, polarizability, and size of the tellurium atom. this bidentate lewis acid telluronium centers show a strong affinity towards fluorine interactions in methanol (Figure 1.15).[39]

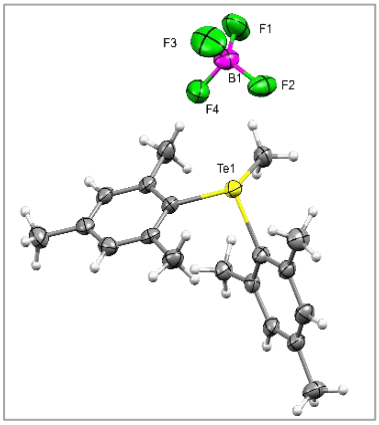

subsequently the same group described the oxidative methylation to diorganotellurides as a strategy to develop telluronium cations of BF_4^- salt which has ability to transport chloride anion in phospholipid bilayers (Figure 1.17). [40]

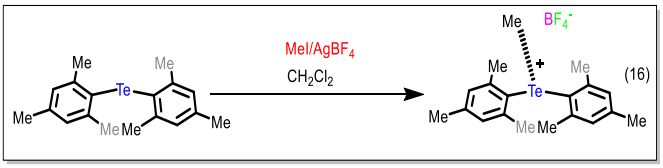

Figure 1.18. solid state molecular structure of Triphenyl telluronium chloride salt and Scheme 1.12

Also, 8-lithio-quinoline reacts with tellurium tetrachloride to form tri(8-quinlinyl) tellurium chloride salt. The bond distance between tellurium and palladium is 2.92, which is more than their covalent radii (2.56-2.77), and the geometry of this complex is a seesaw. this type of telluronium ion complexes can act as sigma acceptors or Z-type ligands with transition metals. [41]

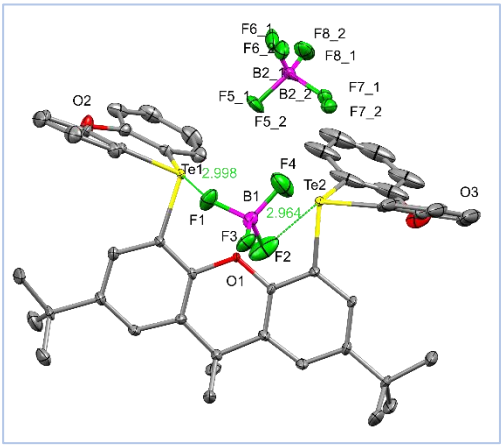

Figure 1.19. solid state molecular structure of Triphenyl telluronium chloride salt

Gabbai pioneering work on this telluronium (salt) ion, structural behavior and its applications have discussed above. Recently in 2022 they reported that the reaction of 2,7-di-tert-butyl-9,9-dimethylxanthene-4,5-diboronic acid with difluoride phenoxatellurine and BF_3OEt_2 for the formation of bis telluronium salt of BF_4^- as a di-cation for anion binding site via secondary interactions. This telluronium di-cation with tetrafluoroborate salt shows a potential application as Lewis acidic site in polydentate chalcogen bond donor construct.[42]

1.5 H. B Singh's work

In the realm of organotellurium chemistry H. B. Singh did pioneering work. in the field of organotellurium derivatives and chalcogenoaza macrocycle. [43] and selenium/tellurium containing Schiff-base macrocycle.[44] Recent work from this group is the preparation of different types of tetraorganotellronic acids by oxidation of unsymmetrical diorganotellurides[45] and The interaction of diorganoiodotelluronium (IV) cation $[(ppy_3Te)]I_3$ with silver perchlorate and silver triflate produced $[(ppy_3Te)].2ClO_4$ and $[(ppy_3Te)].2OTf$, respectively.[46]

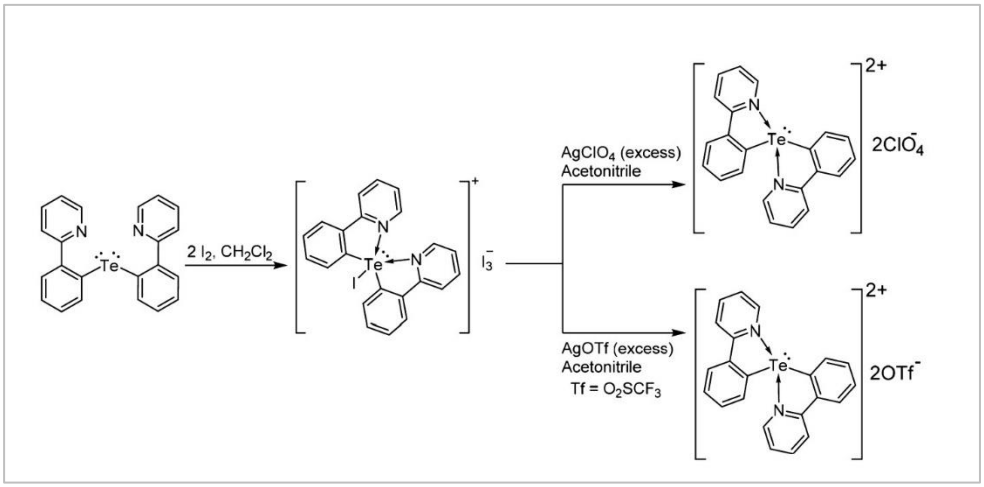

Scheme 1.13

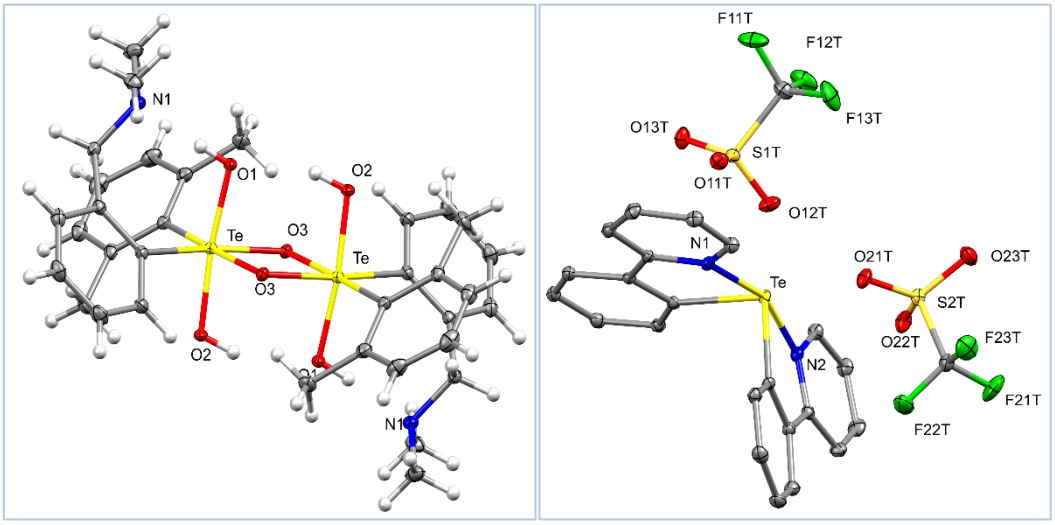

Figure 1.20. Solid state molecular structure of [RR'Te(μ-O) $(OH)_2]_2$ (left) and [(ppy_3Te)].2OTf (right)

1.6 Telluric acid reactions

In 1988 Dakternieks et. al reported the hydrolysis of $C_8H_8Te[S_2P(OCH_2CH_3)_2]_2$ formed under modest conditions. The compound organotellurium $Te[OTe(C_8H_8)(S_2P(O\ CH_2CH_3)_2)]_6$ which contain containing both tellurium (IV) and (VI) first molecule mer-$[(Bu_3SnO)_3Te\text{-}\ (OH)_3]$ was synthesized by reacting of telluric acid with three equivalents of Bu_3SnOMe in good yields. The ^{125}Te NMR spectrum ($CDCl_3$) of confirms the structural integrity in solution, and shows a signal at δ 721.5 with two 2 J(^{125}Te-O-^{119}Sn) couplings of 501 and 432 Hz. Using this product further synthesis continued treated with two times of $(Ph_2SnOH)_2CH_2$ by eliminating one equivalent of tributyltin hydroxide (Bu_3SnOH) and water molecule it formed the spirocyclic tellurastannoxane derivative trans-$[(Bu_3SnO)_2\{CH_2(Ph_2SnO)_2\}_2Te$ reported by the Dakternieks et. al.[47]

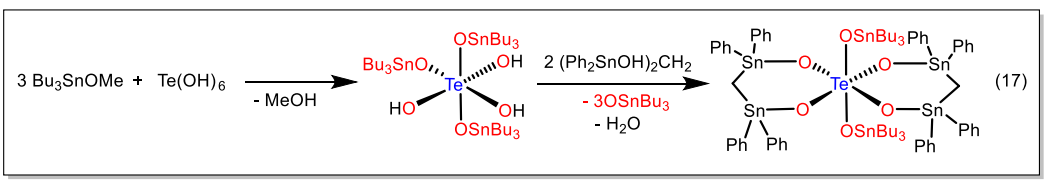

Scheme 1.13

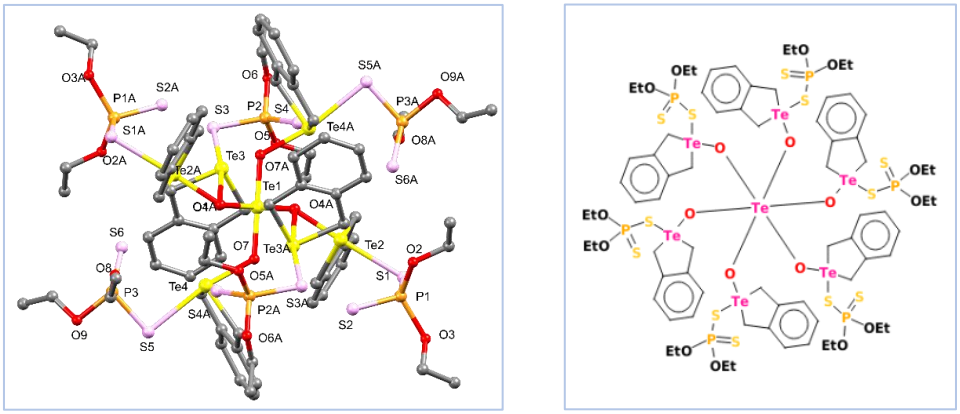

Figure 1.20. Solid state molecular structure of mixed valent Tellurium and chem-draw structure

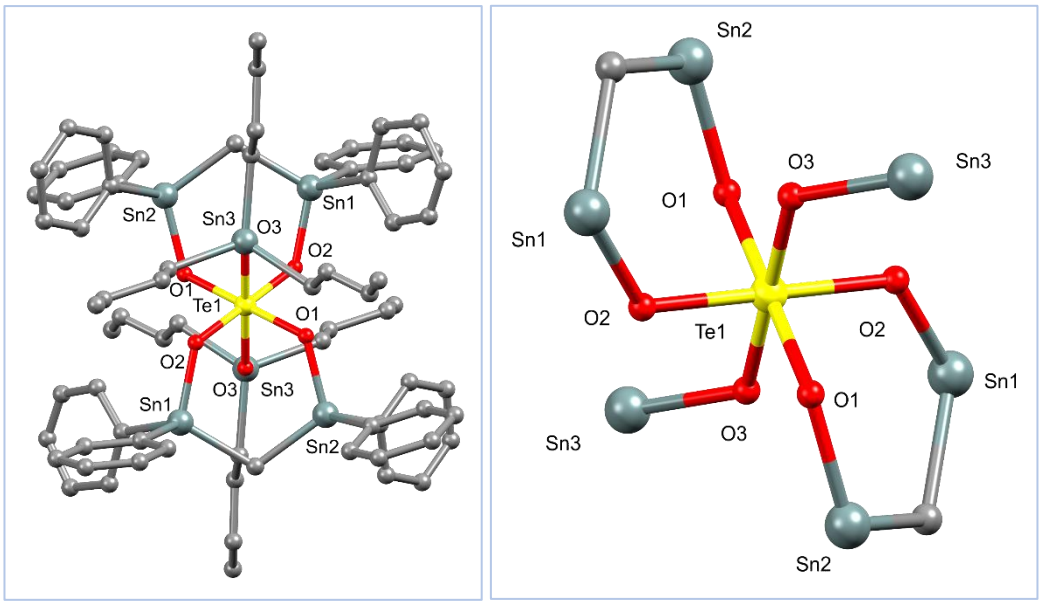

Figure 1.21. molecular structure of -$[(Bu_3SnO)_2\{CH_2(Ph_2SnO)_2\}_2Te$ and its core structure phenyl rings and alkyl groups omitted for clarity.

Domasevitch et. al reported molecular structure that contained six Te-O-Sb bridges.[48] each antimony containing to three phenyls group along with oxygens which are the bonded to tellurium. H_6TeO_6 reacts hydrothermally with $Th(NO_3)_4$,

xH_2O, and V_2O_5 at 200 °C under pressure to form the pure phase $(VO_2)_2(TeO_6)(H_2O)_2$.[49]

Thesis over view

The thesis work mainly focuses on the synthesis of a novel organotellurium Te(IV) based macrocycles, demonstrated inorganic ring expansion 12 to 16 membered organotellurium macrocycle, telluronium salts, where stabilized by secondary interactions and also synthesized tellurate cluster's.

Octahedral PF_6^- anion converting into PF_4^- anion *insitu* and acting as bridging and capping anions in between two ditelluroxane units for the formations of 12-membered macrocycle. Also, we demonstrated inorganic ring expansion of a 12-membered chloro-capped macrocycle to 16-membered BF_4^- capping macrocycle for the first time in the **chapter 2.**

In the **chapter 3**, we have demonstrated that an organotelluroxane macrocycle acting as active site towards HER activity. One of the compound is the first organotellurium containing catalyst for electrochemical hydrogen evolution. Plausible mechanism has been proposed for proton reduction based on the Linear Sweep Voltammetry (LSV) plots which shows two pre-waves corresponding to two successive reductions. Various techniques including CV, LSV, bulk electrolysis have been employed *in the* hydrogen evolution process.

we synthesized high phase purity two novel mixed valent containing main group metal organotellurium and organoantimony with tellurates forming clusters by in non-aqueous medium by using organic binary solvent solvothermal method discussed in the **chapter 4.**

References:

1. Wöhler, Liebigs *Ann. Chem.,* 1840, **35**, 111.
2. a) K. J. Irgolic, *J. Organomet. Chem*., 1978, **158**, 267; b) D. L. J. Clive, G. J. Chittattu, V. Farina, W. A. Kiel, S. M. Menchen, C. G. Russell, A. Singh, C.

K. Wong, N. J. Curtis, *J. Am. Chem. Soc*., 1980, **102**, 4438. (b). M. Irfan, R. Rehman, M.R. Razali, A.-U.-R. Shafiq-Ur-Rehman, M.A. Iqbal, *Rev, Inorg Chem,* 2020, **40**, 193–232. (c). S. Dey, V.K. Jain, A. Knoedler, A. Klein, W. Kaim, S. Zalis, *Inorg. Chem*, 2002, **41**, 2864–2870.

3. R.S. Chauhan, N. Shivran, *RSC Adv*, 2017, **7**, 55175–55198.
4. a) K. J. Irgolic, *J. Organomet. Chem*., 1978, **158**, 267
5. M. Irfan, R. Rehman, M.R. Razali, A.-U.-R. Shafiq-Ur-Rehman, M.A. Iqbal, *Rev, Inorg Chem*, 2020, 40, 193–232.
6. (a) L. Engman, *Acc. Chem. Res.*, 1985, 18, 274. (b). a) N. Petragnani, J. V. Comasseto, *Synthesis*, 1986, ; b) N. Petragnani, J. V. Comasseto, Synthesis, 1991, 793, 897; c) J. V. Comasseto, L. W. Ling, N. Petragnani, H. A. Stefani, Synthesis, 1997, 373; d) N. Petragnani, Tellurium in Organic Synthesis-Best Synthetic Methods, O. Ed. Meth-Cohn, *Academic*, 1994. e) N. Petragnani, *Tetrahedron*, 2005, **61**, 1613.
7. H. Johansson, D. Shanks, L. Engman, R. Amorati, G.F. Pedulli, L. Valgimigli, *J. Org. Chem*, 2010, **75,** 7535–7541.
8. H. Park, L.J. Edgar, M.A. Lumba, L.M. Willis, M. Nitz, *Org. Biomol. Chem*, 2015, **13**, 7027–7033.
9. S.T. Manjare, Y. Kim, D.G. Churchill, *Acc. Chem. Res*, 2014, **47**, 2985–2998. (b). Brown, A.; Hill, A. R.; Boles, J. O. Assessing cell growth in a microtiter plate reader with selective pressure incorporation of unnatural selenium and tellurium containing amino acids. *FASEB J.* 2019, **33**, 461.4, 1. (c). Jamier, V.; Ba, L. A.; Jacob, C. Selenium-and tellurium-containing multifunctional redox agents as biochemical redox modulators with selective cytotoxicity. *Chem. Eur*. 2010, **16**, 10920–10928. (d). Sudesh T. Manjare, Youngsam Kim, and David G. Churchill, *Acc. Chem. Res*, 2014, **47**, 2985−2998.
10. Ragan AN, Kraemer Y, Kong WY, Prasad S, Tantillo D J, Pitts CR. Evidence for C-F Bond Formation through Formal Reductive Elimination from Tellurium (VI). *Angew Chem Int Ed Engl*. 2022 Sep 19;**61**(38): e202208046.
11. (a). Aayushi Arora, Preeti Oswal, Anupama Datta, Arun Kumar, *Coordination Chemistry Reviews*, 2022, **459**, 214406. (b). Kriti Srivastava, Arunashree

Panda, Sagar Sharma, Harkesh B. Singh, *J.Organomet.Chem.,* 2018, **861** 174e206

12. Asmaa B. Sabti; hala Sabry Al-Ttbi; Khawla Sabeeh Bragaal. Synthesis of organotellurium compounds by Transmetallation Reaction of Organomercury compunds/ Review. *Euro.J.ph.Ch.Ma*. 2022, **3**, 3-19.
13. J. Bergman, *Tetrahedron*, 1972, **28**, 3323.
14. (a). C. P. Bhuvan, *J. Organomet. Chem*., 1973, **54**, 191. (b). R. C. Paul, K. K. Bhasin, R. K. Chadha, *J. Inorg. Nucl. Chem*., 1975, **37**, 2337.
15. (a) R. L. O. R. Cunha, A. T. Omori, P. Castelani, F. T. Toledo, J. V. Comasseto, *J. Organomet. Chem*., 2004, **689**, 3631. b) N. Petragnani, *Tetrahedron*, 1960, **11**, 15; b) A. Chieffi, P. H. Menezes, J. V. Comasseto, *Organometallics*, 1997, **16**, 809. (c). K. J. Irgolic, The Organic Chemistry of Tellurium, Gordon, and Breach, New York, 1974.
16. a) F. J. Berry, A. J. Edwards, *J. Chem. Soc. Dalton Trans*., 1980, 2306; b) J. D. Korp, I. Bernal, J. C. Turley, G. E. Martin, *Inorg. Chem*., 1980, **19**, 2556; c) N. W. Alcock, W. D. Harrison, *J. Chem. Soc. Dalton Trans*., 1982, 251; d) R. F. Ziolo, J. M. Troup, *J. Am. Chem. Soc*., 1983, **105**, 229; e) J. Beckmann, D. Dakternieks, A. Duthie, N. A. Smith, *J. Organomet. Chem*., 2003, **149**, 669.
17. (a). L. Engman, *Acc. Chem. Res*., 1985, **18**, 274. (b) E. S. Kostinger, M. L. N. Reddy, D. S. Urch, A. G. Massey, *J. Organomet. Chem*., 1968, **15**, 383; (c) M. D. Moura, N. Petragnani, *Tetrahedron*, 1962, **18**, 521. (d). A. R. Clark, R. Nair, F. R. Fronczek, T. Junk, *Tetrahedron Lett*., 2002, **43**, 1387.
18. A. R. Clark, R. Nair, F. R. Fronczek, T. Junk, *Tetrahedron Lett*., 2002, **43**, 1387.
19. R. L. O. R. Cunha, A. T. Omori, P. Castelani, F. T. Toledo, J. V. Comasseto, *J. Organomet. Chem*., 2004, **689**, 3631
20. (a) N. Petragnani, *Tetrahedron*, 1960, **11**, 15; (b) A. Chieffi, P. H. Menezes, J. V. Comasseto, *Organometallics*, 1997, **16**, 809. (c) W. S. Haller, K. J. Irgolic, *J. Organomet. Chem*., 1972, **38**, 97; (d) M. J. Dabdoub, J. V. Comasseto, *J. Organomet. Chem*., 1988, **344**, 167; (d) L. Engman, J. Persson, *J. Organomet. Chem*., 1990, 388, 71. (e) T. M. Klapötke, B. Krumm, P. Mayer, K. Polborn, I.

Schwab, *Z. Anorg. Allg. Chem*., 2005, **631**, 2677; (f) A. K. S. Chauhan, P. Singh, R. C. Srivastava, R. J. Butcher, A. Duthie, *Inorg. Chim. Acta*., 2011, **376**, 80.

21. J. Beckmann, D. Dakternieks, A. Duthie, F. Ribot, M. Schürmann, N. A. Lewcenko, *Organometallics*, 2003, **22**, 3257.
22. N. W. Alcock, W. D. Harrison, *J. Chem. Soc. Dalton Trans*., 1982, 709.
23. a) J. M. Khurana, B. M. Kandpal, Y. K. Chauhan, *Phosphorus, Sulfur Silicon Relat. Elem*., 2003, **178**, 1369; b) M. Oba, Y. Okada, K. Nishiyama, S. Shimada, W. Ando, *Chem. Commun*., 2008, 5378.
24. D. Dakternieks, R. D. Giacomo, R. W. Gable, B. F. Hoskins, *J. Am. Chem. Soc*., 1988, **110**, 6753.
25. D. Dakternieks, *J. Organomet. Chem*., 1988, **349**, 305.
26. N. Petragnani, J. V. Comasseto, N. H. Varella, *J. Organomet. Chem*., 1976, **120**, 375.
27. (a). P. C. Srivastava, S. Bajpai, R. Lath, C. Ram, S. Bajpai, R. J. Butcher, M. Zimmer, M. Veith, *J. Organomet. Chem*., 2002, **649**, 70; b) P. C. Srivastava, S. Bajpai, R. Lath, C. Ram, S. Bajpai, M. Srivastava, R. J. Butcher, M. Zimmer, M. Veith, *J. Organomet. Chem*., 2002, **658**, 34.
28. V. Chandrasekhar, R. Thirumoorthi, *Organometallics*, 2007, **26**, 5415.
29. a) L. –B. Han, M. Tanaka, *J. Am. Chem. Soc*., 1997, **119**, 1795; b) L. –B. Han, S. Shimada, M. Tanaka, *J. Am. Chem. Soc*., 1997, **119**, 8133.
30. M. C. Janzen, M. C. Jennings, R. J. Puddephatt, *Inorg. Chem*., 2003, **42**, 4553.
31. V. Chandrasekhar, R. Thirumoorthi, *Inorg. Chem*., 2009, **48**, 10330.

(b). Ramesh K. Metre, Subrata Kundu, Dipankar Sahoo, and Vadapalli Chandrasekhar. *Organometallics,* 2014, **33**, 2380−2383. (c). Vadapalli Chandrasekhar, Ramalingam Thirumoorthi, *Eur. J. Inorg. Chem.* 2008, 4578–4585. (d). Vadapalli Chandrasekhar, Arun Kumar, Mrituanjay D. Pandey, *J. Organomet. Chem.*, 2010, **695**, 74–81. (e). Vadapalli Chandrasekhar, Ramalingam Thirumoorthi, *Inorg. Chem*. 2009, **48**, 6236–62401. (f). Ramesh K. Metre, Subrata Kundu, Dipankar Sahoo, and Vadapally Chandrasekhar *Organometallics* 2014, **33**, 2380−2383.

32. (a). N. K. Srungavruksham and V. Baskar, *Eur J Inorg Chem*, 2012, 136–142.(b). N. K. Srungavruksham and V. Baskar, *Dalton Transactions*, 2015, **44**, 4554– 4569.
33. Andrew Docker, Antonio J. Martı´nez Martı´nez, b Heike Kuhna and Paul D. Beer. *Chem. Commun*., 2022, **58**, 3318. (a). Sangeeta Yadav, Harkesh B. Singh, Matthias Zeller, and Ray J. Butcher, *Organometallics* 2017, **36**, 2067−2071
34. K. Kobayashi, N. Deguchi, E. Horn and N. Furukawa, *Angewandte Chemie - International Edition*, 1998, **37**, 984–986.
35. K. Kobayashi, N. Deguchi, O. Takahashi, K. Tanaka, E. Horn, O. Kikuchi and N. Furukawa, *Angewandte Chemie - International Edition*, 1999, **38**, 1638–1640. (b). K. Kobayashi, H. Izawa, K. Yamaguchi, E. Horn and N. Furukawa, *Chemical Communications*, 2001, **1**, 1428–1429.
36. Jens Beckmann, Dainis Dakternieks, Andrew Duthie, Naomi A. Lewcenko, and Cassandra Mitchell, *Angew. Chem. Int. Ed*. 2004, **43**, 6683 –6685.
37. V. Chandrasekhar, R. Thirumoorthi, *Inorg. Chem*., 2009, **48**, 6236.
38. (a). Ronald F. Ziolo and Michael, *Inorganic Chemistry*, **19**, 10, 1980-296; (b). Trotter, J.; Williston, *C. J. Chem. Sor.* 1967, 2018. (c). Ziolo, R. F.; Pritchett, K. J. *Orgunornet. Chern.* 1976, 116, 21 I. (d). Titus, D. D.; Lee, J.-S.; Ziolo, R. F. J. *Orgunornet. Chem*. 1976, 120, 381. (e). Lee, J.6; Titus, D. D. *J. Cryst. Mol. Struct*. 1976, 6, 279. (f). Lee, J.-S.; Titus, D. D.; Ziolo, R. F. *Inorg. Chem*. 1977, 16, 2487; J. Chem. SOC., *Chem. Commun*. 1976, 501. (g). Ash, P. A.; Lee, J.-S.; Titus, D. D.; Bowman, K.; Ziolo, R. F. *J. Organornet. Chem.* 1977, 135, 91. (h). Michael J. Collins, John A. Ripmeester, and Jeffery F. Sawyer, *J. Am. Chem. Soc*. 1988, **110**, 8583-8590. (i). Yoshihiro Matano and Hitomi Suzuki, *Organometallics*, 1996, **15**, 3760-3765. (j). Mao Minoura, Takahiro Mukuda, Takao Sagami, and Kin-ya Akiba, J. Am. Chem. Soc. 1999, 121, 10852-10853.
39. Zhao, H., Gabbaï, F. A bidentate Lewis acid with a telluronium ion as an anion-binding site. *Nature Chem*, 2010, **2**, 984–990.
40. Benyu Zhou and François P. Gabba¨, *Chem. Sci*., 2020, **11**, 7495.

41. Tzu-Pin Lin and FranÅois P. Gabbaï, *Angew. Chem. Int. Ed*.2013,52, 3864 – 3868.
42. Gabbai, *et al. J. Am. Chem. Soc.*, 2021, **143**, 23, 8625–8630.
43. (a). Narasimhan Sudha and Harkesh B. Singh, *Coord. Chem.Rev.*, 1994, **135/136**, 469-515. (b). G Mugesh, Arunashree Panda, and Harkesh B Singh, *Proc. Indian Acad. Sci*. (*Chem. Sci.)*, **112**, No. 3, June 2000, pp. 239–248. (c). Kriti Srivastava, Arunashree Panda b, Sagar Sharma, Harkesh B. Singh *J. Organomet. Chem.*, 2018, **861**, 174e206. (d). Anand Gupta, Rajesh Deka, Saravanan Raju, Harkesh B. Singh, Ray J. Butcher, *J. Organomet. Chem*, 2019, **894**, 10e17.
44. Upali Patel, Harkesh B. Singh, and Ray J. Butcher, *Eur. J. Inorg. Chem*. 2006, 5089–5097. (b). Saija C. Menon, Harkesh B. Singh, Rajan P. Patel and Shailendra K. Kulshreshtha, *J. Chem. SOC., Dalton Trans*., 1996, 1203-1207.
45. Anand Gupta,Rajesh Deka, Arup Sarkar, Harkesh B. Singh, Ray J. Butcher, *Dalton Trans*., 2019, **48**, 10979. (b). Rajesh Deka, Arup Sarkar, Ray J. Butcher, Peter C. Junk, David R. Turner, Glen B. Deacon and Harkesh B. Singh, *Dalton Trans*., 2020, **49**, 1173.
46. Rajesh Deka, Arup Sarkar, Ray J. Butcher, Peter C. Junk, David R. Turner, Glen B. Deacon, and Harkesh B. Singh, *Organometallics* 2020, **39**, 334−343.
47. Kostiantyn V. Domasevitch and Ganna A. Senchyk, *Acta Cryst*. 2021. **E77**, 1229–1233.
48. Tyler A. Sullens and Thomas E. Albrecht-Schmitt, Inorg. Chem. 2005, **44**, 2282−2286.

Chapter 2

Chapter 2

Organotelluroxane Macrocycles and Telluronium salt

Abstract:

Anion exchange reaction of Cl-capped seleninate bridging tellurium twelve-membered macrocycle $[(p\text{-}MeO\text{-}C_6H_4)_2Te(\mu\text{-}O)(\mu\text{-}PhSeO_2)(\mu_4\text{-}Cl)]_2$ with silver salt of hexafluorophosphate was investigate a rare unusual pseudo tetrahedral anion (PF_4^-) replaced the bridging seleninate anion for the formation of 12-membered telluroxane dicationic macrocyclic core. Further the macrocycle was stabilized by two more PF_4^- anions capping both sides of the a dicationic macrocycle with $[\{(p\text{-}OMe\ C_6H_4)_2Te\}_2(\mu\text{-}O)(p\text{-}OMe\ C_6H_4Te)(\mu\text{-}PF_4)(\mu\text{-}PF_4)]_2$ (2.2) with several *in situ* Te-F bonds formation. At high-temperature, the same reaction produces tri (*p*-methoxy phenyl) telluronium PF_4^- salt $[(p\text{-}OMe\ C_6H_4)_3Te]^+\ PF_4^-$ and bis (para methoxy phenyl tellurium di fluoride(R_2TeF_2). Similar products are isolated with $[\{(p\text{-}OMeC_6H_4)_2Te\}_2(\mu_2\text{-}O)(\mu\text{-}Ph_3CP(Ph)O_2))(\mu_4\text{-}Cl)]_2$. The 12-membered macrocycle $[(p\text{-}MeO\text{-}C_6H_4)_2Te(\mu\text{-}O)(\mu\text{-}PhSeO_2)(\mu_4\text{-}Cl)]_2$ was treated with silver salts in a 1:1:1 ratio isolated 16-membered macrocycle$[\{(p\text{-}OMeC_6H_4)_2Te\}(\mu_2\text{-}O)_4(\mu\text{-}PhSeO_2)(\mu\text{-}BF_4^-)]_4$. The obtained results are explained in detail.

2.1 Introduction

For several decades, macrocycles have been a central topic in both synthetic and materials chemistry, for their numerous applications in host–guest chemistry[1], such as gas storage[2], the modeling of biological systems[3] and using macrocycles as counter-anion trapping for improving conductivity.[4] In the last three decades, there has been a growing interest in the area of organo tellurium (IV, II) based chemistry, diorganotellurium/oxide/halides has this ability to form macrocycles[5], by reacting with various protic acids[6] which results in the isolation of new telluroxane frameworks. The potential of the telluraxane moieties is trapping the anions with secondary interaction demonstrating Beckmann et. al by treating organotellurium in atmosphere of the CO_2 was reacted with organo tin at room temperature.[7] Reactivity of diorganotellurium dihalides with benzene seleninic acid, resulted in 12 membered macrocycles $[(p\text{-}MeO\text{-}C_6H_4)_2Te(\mu\text{-}O)(\mu\text{-}PhSeO_2)(\mu_4\text{-}X)]_2$ [X = Cl, Br, I] where the spherical halogen atoms, which are stabilized by Te---X interactions, cap the macrocycles on both sides.[6d] Further anion exchange reaction of chloro-macrocycle $[((p\text{-}MeO\text{-}C_6H_4)_2Te)_2(\mu\text{-}O)(\mu\text{-}PhSeO_2)(\mu_4\text{-}Cl)]_2$ by reacting them with $AgNO_3$, $AgClO_4$, and $AgBF_4$ for targeted macrocycles such chloro cap replaced by the higher anions, which has varying geometries the trigonal planner (NO_3^-), tetrahedral ClO_4^-, BF_4^- structures. Single crystal X-ray diffraction studies confirmed 12-membered macrocycles $[\{(p\text{-}OMeC_6H_4)_2Te\}_2(\mu\text{-}O)(\mu\text{-}PhSeO_2)(\mu_4\text{-}X,\ ]_2$, [X = NO_3, ClO_4, BF_4].[6e] In continuation of the work we wanted to replace chloride cap of Cl- macrocycle $[((p\text{-}MeO\text{-}C_6H_4)_2Te)_2(\mu\text{-}O)(\mu\text{-}PhSeO_2)(\mu_4\text{-}Cl)]_2$ by higher symmetrical geometry octahedral anions like silver salts of PF_6^-, SbF_6^-, and to synthesis mixed anion capped macrocycles. The results obtained are discussed in this chapter.

2.2 Experimental section

2.2.1 Reagents and general procedures:

Tellurium tetrachloride and silver salts were purchased from Sigma-Aldrich Ltd., and the previously mentioned procedure was utilized to synthesize bis-(p-methoxyphenyl) tellurium dichloride and trityl phenyl phosphinic acid.[8] Solvents and other chemicals were purified in line with standard procedures.

2.2.2 Instrumentation:

Rigaku Oxford Xta- Lab synergistic diffractometer with graphite monochromator and a Mo K (=0.71073 A) microfocus sealed tube operated at 50 kV and 1mA acquired single crystal X-ray data at 100K. The data was solved and refined using OLEX software 2-1.2.[9] NMR spectra for ^{1}H, ^{13}C, ^{31}P, ^{19}F, and ^{125}Te were obtained using Bruker AVANCE III 400 and 500 equipment. Infrared spectra were recorded with a NICOLET Is5 FTIR spectrometer. CCDC (xxxxx,xxxx) for **2.1** to **2.4**, Contains the supplementary crystallographic data for this paper. These can be obtained free of charge from the Cambridge crystallographic data center via www.ccdc.cam.ac. Uk/data-request/cif.

2.2.3 Synthetic procedure for 2.1

Trityl phenyl phosphinic acid was taken in 15 ml of dry toluene and triethylamine was added and kept for stirring until it forms a lucid solution. To this *bis*-(*p*-methoxyphenyl) tellurium dichloride (R_2TeCl_2) was added, and the reaction mixture was then left to stir at room temperature for 12 hours. The turbid reaction mixture was filtered, and the filtrate was saved for crystallization. Block-like colorless crystals were obtained in after 4 days' time by slow evaporation and while as well as in diffusion of hexane into toluene solution.

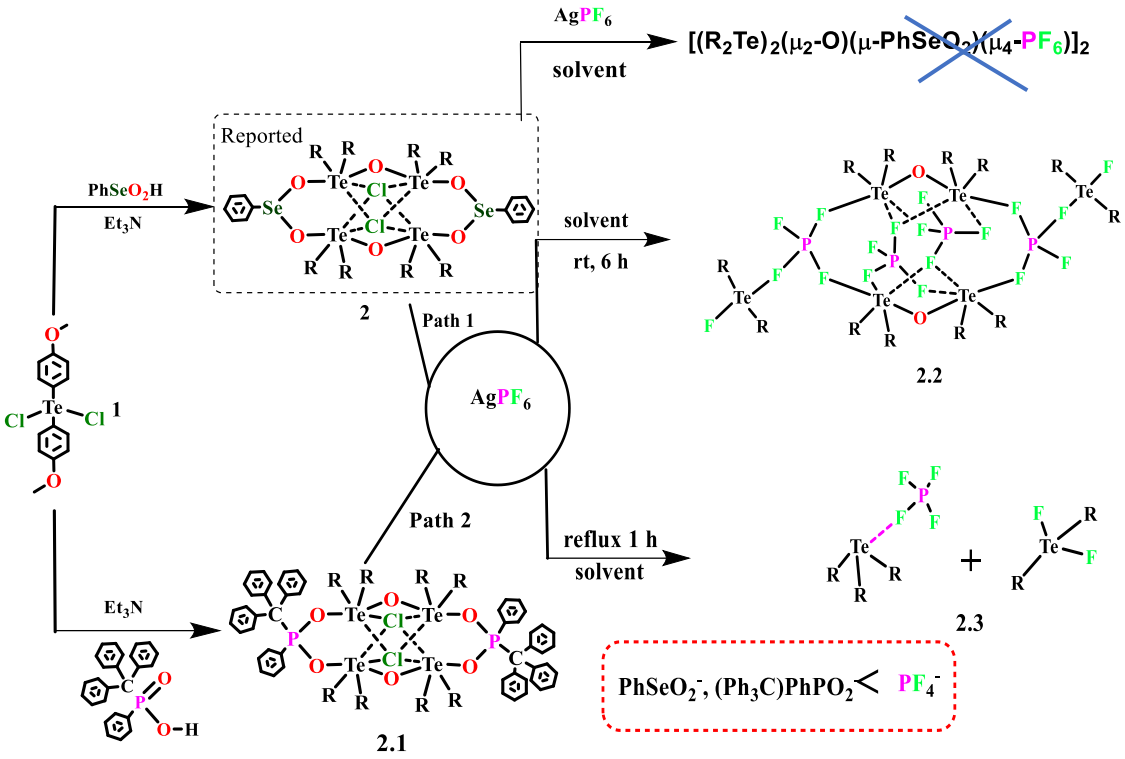

Scheme 2.1

2.2.4 General synthetic procedure for compounds 2.2 and 2.3

These products can be achieved following three methods, first method as follows. Silver hexafluoro phosphate was added to a 100 ml round bottom flask, which was covered with aluminum foil to protect it from light sensitivity, and the round bottom was closed with rubber cork. To this was injected, 30 ml of dry benzene of 12-membered macrocycle (2) solution. After 6 hours of stirring at room temperature the solution was, filtered and the filtrate was kept for crystallization in diffusion hexane into the mother solvent. Block-like brown color crystals formed after two weeks. In the second method 30 ml of dry toluene of 2.1 macrocycle solution added to Silver hexafluoro phosphate, similar procedure to first method. In the third method the procedure as follows. R_2TeCl_2 (1) dissolved in benzene to this silver salt of hexafluoro phosphate added, stirred for 6 hours workup followed as above. At high temperature (90 °C) all these three methods end with telluronium salts product.

2.2.5 Synthetic procedure for 2.4

12- membered macrocycles (2) were taken with silver tetrafluoroborate and silver nitrate, in the equal molar ratio in 40 ml of benzene in a 100 ml round bottom flask. The reaction mixture was stirred overnight, after filtration filtrate kept evaporation at room temperature for crystallization, gave small block-like single crystals in two weeks' time.

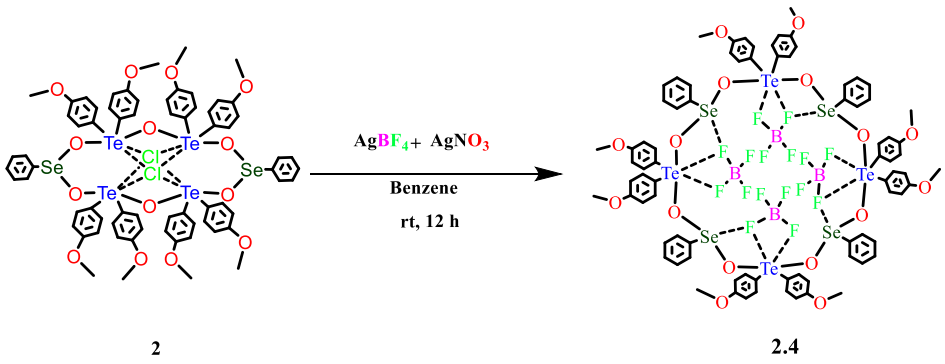

2 2.4

Scheme 2.2

[{(*p*-OMeC_6H_4)$_2$Te}$_2$(μ_2-O)(μ-$Ph_3CP(Ph)O_2$))(μ_4-Cl)]$_2$ (2.1):

Bis-(*p*-methoxy phenyl) Tellurium dichloride (*p*-OMe-C_6H_6)$_2$$TeCl_2$ (0.20 g, 0.49 mmol), Trityl phenyl phosphinic acid (0.19 g, 0.49 mmol), yield: 0.25g (91%) based on *Bis*-(*p*-methoxy phenyl) Tellurium dichloride. MP: 256-258 °C. $C_{106}H_{96}Cl_2O_{14}P_2Te_4$ (2237): ^{1}H NMR (500 MHz, $CDCl_3$, ppm): δ 8.01 (d), δ 7.42 (m), δ 7.28 (m), δ 7.21 (m), δ 7.19 (m), δ 7.18 (m) δ 7.06 (m), δ 3.88 (s). ^{13}C NMR (125 MHz, $CDCl_3$, ppm): δ 162.26, δ 161.91, δ142.52, δ 135.16, δ131.43, δ 131.39, δ 129.05, δ 128.25, δ 127.7, δ 126.61, 125.32, δ 115.07, δ55.58. ^{31}P NMR (158 MHz $CDCl_3$, ppm) δ 37.0 (S): ^{125}Te NMR (126 MHz $CDCl_3$, ppm): δ 1018 (S); IR: 2834 (w), 2493 (m), 1582 (s), 1489 (s), 1459 (s), 1290 (m), 1253 (s), 1173 (s), 1250.5 (s), 1176.2 (m), 1104 (s), 1025 (s), 952 (s), 930 (s), 877 (m), 825 (m), 809 (m), 746 (s), 695 (s), 628 (m), 589 (s), 548 (m), 514 (s), 498 (s), 473(m), 445 (m), 420 (s).

[{(*p*-OMe C_6H_4)$_2$Te}$_2$ (μ-O)(*p*-OMe C_6H_4Te) (μ-PF_4)(μ-PF_4)]$_2$ (2.2):

Cl-macrocycle [((p-MeO-C_6H_4)$_2$Te)$_2$(μ-O)(μ-$PhSeO_2$)(μ_4-Cl)]$_2$, (2), (0.17 g; 0.0920 mmol), silver hexafluorophosphate (0.046 g; 0.1841 mmol), or (2.5), yield: (40 %) based on Cl- macrocycle/. MP: 200-202 °C. ^{1}H NMR (500 MHz, $CDCl_3$, ppm): δ 7.90 (d), δ 7.06 (d), δ 3.84 (s). ^{13}C NMR (125 MHz, $CDCl_3$, ppm): δ 162.30, δ 131.52, δ 129.19, δ 127.73, δ 127.56, δ 115.45, δ 55.43; ^{19}F NMR (471.6 MHz, $CDCl_3$, ppm) δ -72, -109.18, δ -127.03.; ^{31}P NMR (158 MHz, $CDCl_3$, ppm) δ -143. (q); ^{125}Te NMR (126 MHz $CDCl_3$, ppm): δ 1147 (t, J = 572 Hz); IR 2022 (m), 1946 (m), 1582 (m), 1489 (m), 1293 (m), 1248 (s), 1175 (m), 1020 (m), 821 (m), 742 (m), 640 (w), 548 (m), 512 (m), 491 (m), 452 (m), 440 (m).

[(*p*-OMe C_6H_4)$_3$Te]$^+$ PF_4^- and (*p*-OMe C_6H_4)$_2$$TeF_2$ (2.3):

Cl-macrocycle [((p-MeO-C_6H_4)$_2$Te)$_2$(μ-O)(μ-$PhSeO_2$)(μ_4-Cl)]$_2$, (2), (0.17 g; 0.0920 mmol), silver hexafluorophosphate (0.046 g; 0.1841 mmol), or (2.3), mixture compounds yield: (45 %) based on Cl- macrocycle/. MP: 182-184 °C. ^{1}H NMR (500 MHz, $CDCl_3$, ppm): δ 7.90 (d), δ 7.07(d), δ 3.85 (s). ^{13}C NMR (125 MHz, $CDCl_3$,

ppm): δ 162.51, δ 133.02, δ 129.19, δ 128.21, δ 115.51, δ 55.29; ^{19}F NMR (471.6 MHz, $CDCl_3$, ppm) δ -146.2; (s); Hz);

[{(*p*-OMeC_6H_4)$_2$Te} (μ$_2$-O)$_4$(μ-PhSeO_2)(μ-BF_4^-)]$_4$ (2.4):

Cl-macrocycle [((p-MeO-C_6H_4)$_2$Te)$_2$(μ-O)(μ-PhSeO_2)(μ$_4$-Cl)]$_2$, (2), (0.15 g; 0.0811 mmol), silver tetrafluoroborate (0.008 g, 0.0405 mmol), silver nitrate (0.007 g, 0.0405 mmol), yield 51 %, MP: 236-238. ^{1}H NMR (500 MHz, $CDCl_3$, ppm): *δ* 7.75 (d), *δ* 7.59 (d), 7.47 (m), *δ* 7.37 (m), 7.28 (d), *δ* 7.24 (d), 6.93 (d) *δ* 3.71 (s). ^{13}C NMR (125 MHz, $CDCl_3$, ppm): δ 162.30, δ 134.52, δ 134.42, 131.16, δ 130.43, δ 128.73, δ 123.56, δ 115.45, δ 55.43; ^{19}F NMR (471.6 MHz, $CDCl_3$, ppm) δ -127.0. ^{125}Te NMR (126 MHz $CDCl_3$, ppm): δ 1148 (t, J = 572 Hz); IR. 2961 (s), 2840 (m), 1583 (s), 1491 (s), 1440 (m), 1403 (m), 1294 (m), 1256 (s), 1176 (s), 1013 (s), 719 (s), 745 (m), 662 (m), 589 (m).

2.3 Results and discussion:

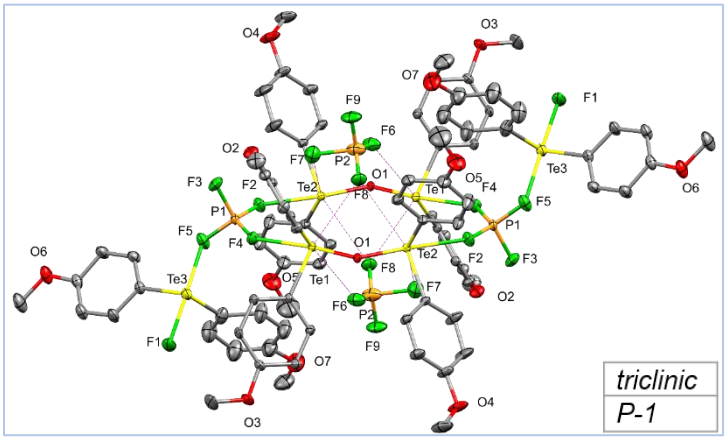

Figure 2.1. Solid state molecular crystal structure of 2.2, hydrogen atoms, and benzene solvate are omitted for clarity. Te shows interactions with Fluorine atoms., and thermal ellipsoids are drawn at 40% probability

An investigation into the reaction between diorganic tellurium dihalides and phenyl seleninic acid led to the formation of inorganic macrocycles with 12 members called [(*p*-MeO-C_6H_4) Te)$_3$(*μ*-O)(*μ*-PhSeO_2)(*μ*-Cl).[1f] Reaction involving the exchange of anions of these Cl-Macrocycle (2) with $AgPF_6$ (path 1) yielded white crystalline powder which on crystallization-afforded block like crystal at low-temperature crystals. The targeted

and expected product was just replacing of chloride anion with a higher symmetrical geometry octahedral anion to the di cationic macrocycle. But single crystal X-ray diffraction studies revealed the formation of 12-membered macrocycle [(*p*-MeO-C_6H_4) $Te)_3(F)_4(\mu\text{-}O)(\mu_3\text{-}PF_4)(\mu\text{-}PF_4^-)]_2$ C_6H_6. (**2.2**) Where two phenyl seleninate were replaced by two unusual R2(F)Te-FPF_3^- bridging anions between two tetarorganotelluroxane units forming as di cationic core macrocycle. This dicationic macrocycle core is countered by two more 2 PF_4^- anions on both sides the of macrocycle and stabilized by Te---F secondary interactions. 2.3 is the first example of a macrocycle that contains two definite chemical motifs. An organotellurium fluoro-phosphinates, $R_2Te—F—P—F—TeR_2$, and a ditelluroxane $R_2Te—O—TeR_2$ So, in xxxxx $RFPF_2^-$ ligand which is generated in situ seems to act as powerful ligand system which could replace ligand like organo-seleninate of phosphate, this generating novel molecular system. On reaction of $[\{(p\text{-}OMeC_6H_4)_2Te\}_2(\mu_2\text{-}O)(\mu\text{-}Ph_3CP(Ph)O_2))(\mu_4\text{-}Cl)]_2$ (**2.1**) with silver salt of hexafluorophosphate. Yielded the same product [(*p*-MeO-C_6H_4) $Te)_3(F)_4(\mu\text{-}O)(\mu_3\text{-}PF_4)(\mu\text{-}PF_4^-)]_2$. We concluded that the (μ_3-PF_4) anion replacing strong ligands (μ-$PhSeO_2$), (μ-$Ph_3CP(Ph)$ < (μ_3-PF_4). Reactions on refluxing forming

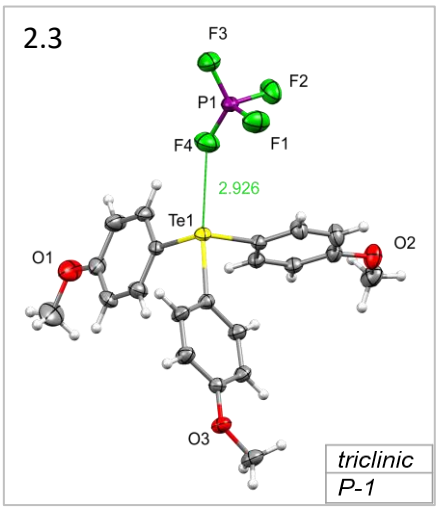

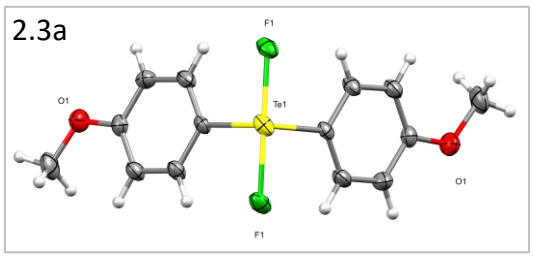

Figure 2.2. Solid state molecular crystal structure of 2.2, and 2.3a and hydrogen atoms are omitted for clarity. Te shows interactions with Fluorine atoms., and thermal ellipsoids are drawn at 40% probability

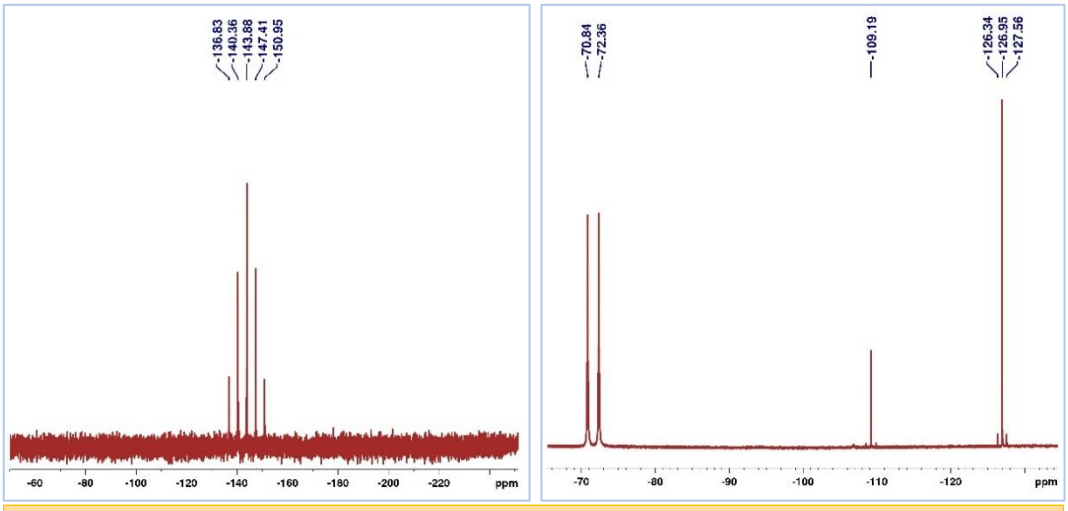

Figure 2.3 Solution of 2.1 ^{19}F NMR showing, two doublet and two singlets along with satellite peaks, respectively.

tri (*p*-methoxy phenyl telluronium tetrafluoro phosphate salt and bis (*p*-methoxy phenyl) tellurium di fluoride compounds isolated. The solution NMR of ^{125}Te shows a triplet signal resonance signal at 1147 ppm by coupling of 2 fluorine atoms to each tellurium with a coupling constant of 574 Hz, which is shifted up field when compare to Cl- macrocycle 1211 ppm. The solution NMR ^{19}F of 2.2 revealed resonance at -72. -109, and -127 ppm in $CDCl_3$ respectively. the solution NMR of ^{125}Te shows a triplet signal resonance. Here -109 ppm with satellite peaks and -72 ppm signals

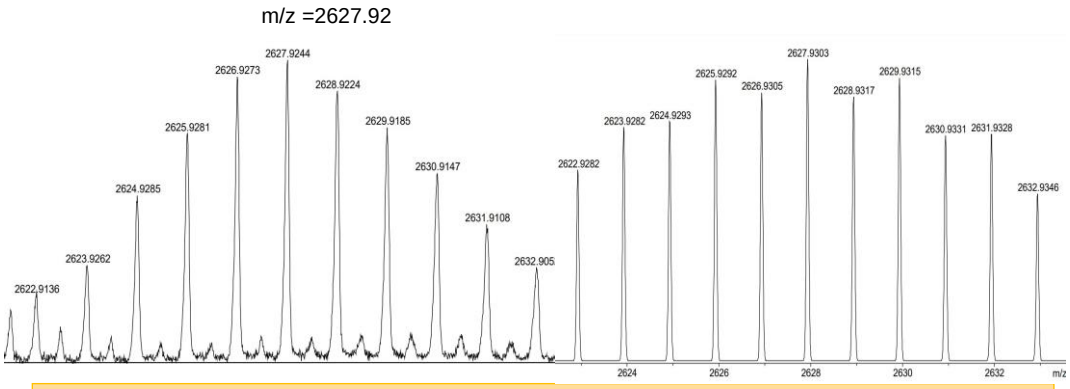

Figure 2.4 Experimental (left) and simulated (right) ESI-MS of 2.2

are assigned to fluorine which is bridging between Tellurium and phosphorus and free fluorine of bridging PF_4^- anion respectively. The signal at -127 ppm is corresponding to 2 fluorine having weak interactions with tellurium showing a signal at up field. ^{31}P at NMR -143 ppm shows a quintet. At room temperature, CDCl3 is used for the recording of each NMR spectrum. The positive ion mode of the HRMS investigation on 2.1 and 2.2 showed ppm peaks at m/z 2627.9 and 557.15 respectively, and these results suggest that the structural integrity of the macrocycle is maintained in the solution as well.

2.4 X-ray single crystal structure description of 2.2 and 2.3:

Standard analytical and spectroscopic methods have been used to characterize Macrocycles **2.2** and telluronium salt **2.3**. the important parameter are given in Table 2.1-2.4. the macrocycle **2.2** crystalizes in triclinic crystal system, space group *P -1* with half of the molecule present in the asymmetric unit. The macrocycle **2.2** is present as by 2 units of tetra (*p*-methoxy phenyl) telluroxanes connected by 2 PF_4^- anions, further one of the Fluorine is attached to di (*p*-methoxy phenyl tellurium fluoride. The dipositive charge of the macrocycle **2.2**, comprises two telluroxane units and two fluoro phosphinates groups. These two fluoro phosphinates ligands link the two di-telluroxane units to produce a 12-membered ($Te_4P_2F_4$) complex in a symmetric bridging way and compensated by the presence of two PF_4^- anions around the macrocycle core ring are in the planar despite their size differences. The interesting part about the presence of this macrocycle is, unusual tetrahedral tetrafluorophophate anions bridging symmetrically between two telluroxane units, also capping on both sides of the macrocycle above and below with secondary bonding interactions Te---F. The interaction distance between Te---F is 3.022 (4) Å, shorter than the total of the sums Vander Waals radii (Te and F ∑vdw (Te---F) = 3.451 (Å)[10] which are present in both macrocycle and telluronium salt.

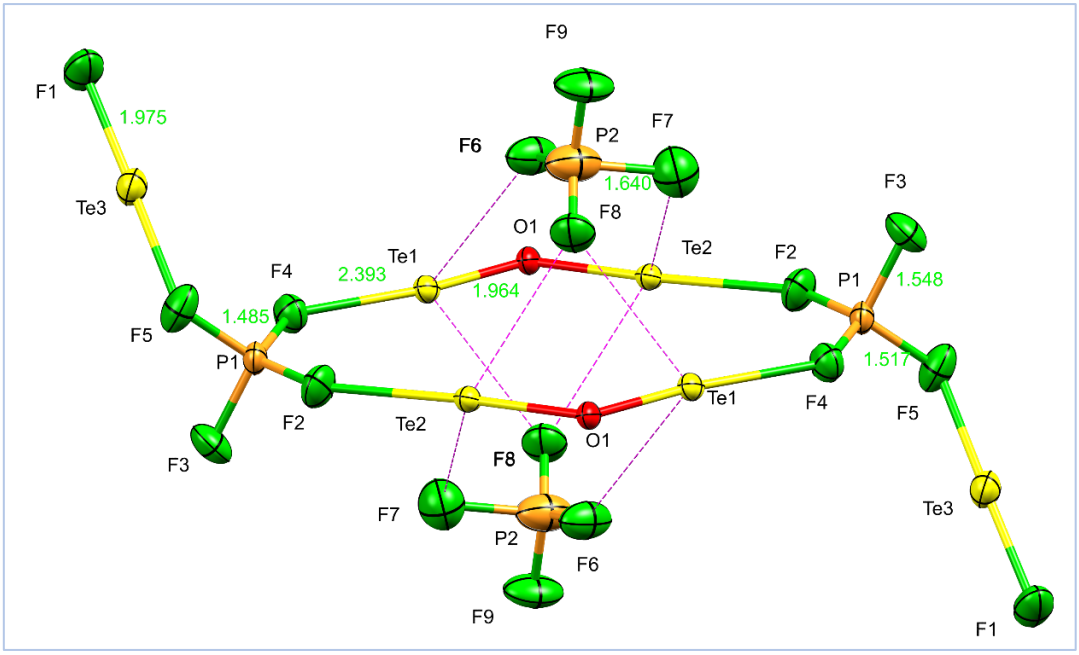

Figure 2.5 Solid state molecular crystal core structure of 2.2

This secondary bond distance falls in the reported literature arrange as seen in macrocycle[6g], telluronium BF_4^- salt[11], telluronium dicationic BF_4^- salt.[12] The in situ formed side chain to telluroxane unit is R_2TeF_2. The bond distance of side chain tellurium atom to fluorine of bridging PF_4^- anion (Te—F) bond distance is 1.978 (11) Å. Te—F (sum of the covalent bond radii Te—F is 1.950 Å) distance is 1.978 (11) Å, here in the average Te—F bond distances fall in the reported literature range. Whereas bond distance of tellurium to fluorine between bridging μ-PF_4^- fluorine to tellurium of core ring telluroxane distance is 2.356 (9) Å is moderately large than its sum of covalent bond radii. This Te—F bond distance can also be compared with Te(IV) monofluoride species, such as [(μ-F)Te$(CF_3)_3$- dimethylformamide][13] a fluoride-bridged polymeric species connected by Te–F linkages of 2.138(2) Å, 2.566(2) Å and a bidentate telluronium ion is also 2.505 (5).[14] The di-telluroxane unit has an average bond length of 1.964 (8), which is comparable to the value that was reported in the past. The average F—Te—O, bond angle is 173.1° (4), Te—O—Te angles 120.2° (4)

larger than previously reported 12-membered tellurium macrocycles (170.45° (6) and 114.39° (7) respectively. the P—F bond length is 1.484 (10) to 1.550(10) Å and the bond angle among F—P—F is 103.2° (7) to 109.9° (7). The geometry around tellurium in the macrocycle and telluronium salt are distorted pseudo-octahedral and Pseudo trigonal pyramidal respectively.

2.5 X-ray single crystal structure description of 2.4:

To achieve a mixed anion-capped macrocycle, the reaction of Chloro-macrocycle [(*p*-$MeOC_6H_4)_2Te(\mu$-O)(μ-$PhSeO_2$)(μ_4-Cl)]$_2$ with silver salts of nitrate and tetrafluoroborate in 1:1:1 ratio in benzene solvent at room temperature for 12 hours, after filtration filtrate on evaporation in a weeks' time small cube type crystal formed. It crystalized in tetragonal space group P4/n. SC-XRD structural studies unfolded an unexpected 16-membered macrocycle- [{(*p*-$OMeC_6H_4)_2Te$}(μ_2-O)$_4$(μ-$PhSeO_2$)(μ-BF_4^-)]$_4$. These 16- membered macrocycle core ring $Te_4Se_4O_8$ is built by four benzene seleninate relate to four bis (*p*-methoxy phenyl) tellurium through oxygens, with Se—O—Te linkage. This core ring is tetra-cationic further stabilized by four tetra-fluoroborate anions attaining neutrality. Unlike the other reported/ synthesized macrocycle capped on both sides, four BF_4^- sitting on the top of each tellurium with secondary interactions Te---F. Each tellurium coupling with two fluorine atoms from BF_4^- anion which splits the tellurium into triplets at 1148 ppm with a coupling constant of 460 Hz. The solution ^{19}F NMR shows resonance at -126.9 ppm with satellite peaks. The ^{11}B NMR resonance at -1 ppm provided conclusive evidence for the presence of the BF^{4-} anion. The distance between Se—O is 1.712 Å no change in it when compared with benzene seleninic acid based macrocycle and Te—O is 2.18 Å is much larger than the reported literature.[6g] Interaction distance between Te---F is 3.174 Å

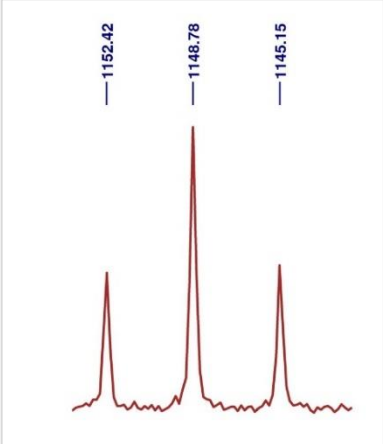

Figure 2.7 Solution of 2.1 ^{19}F NMR showing,

which is also lower relative to its sum of Vander walls radii (Te and F ∑vdw (Te-F) = 3.452 Å).[10] (Tellurium and Fluorine ∑vdw (Te---F) = 3.452 Å)Se---F interaction also has been observed at an

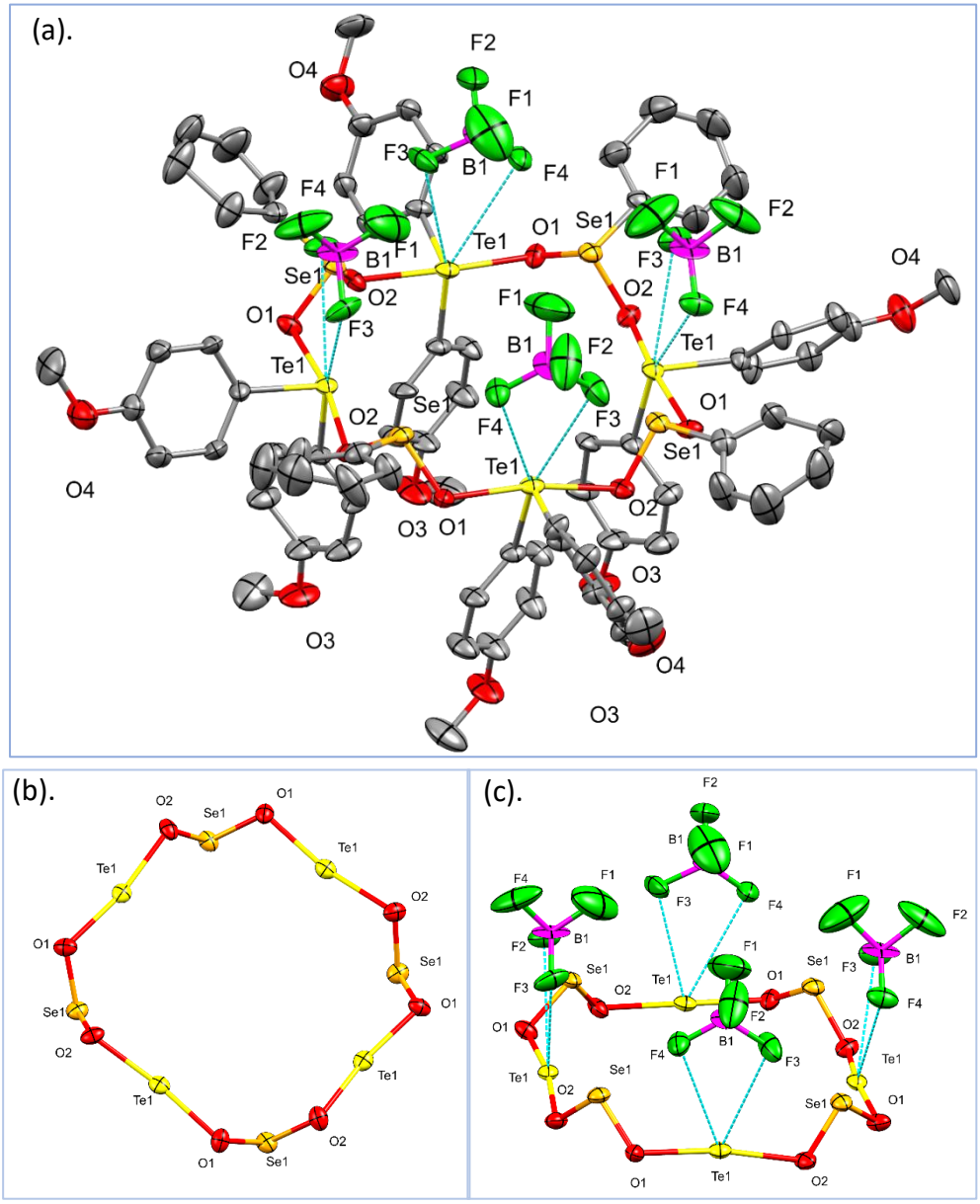

Figure 2.6 (a). Solid state molecular crystal structure of 2.4, hydrogen atoms, are omitted for clarity. Te shows interactions with Fluorine atoms., (b). core structure, (c) Te---F interaction. Thermal ellipsoids are drawn at 40% probability

average distance of Te---F 2.831 Å which is considerably lower than (its sum of Vander wall radii 3.371 Å) reported literature.[15] the average bond angle of O—Te—O are 170.0° (4) matches with our previously reported macrocycle[6g] but higher than literature and the average bond angle of O—Se—O are 101.6° (4). The bond angle and bond distances are mostly like reported macrocycles. The geometry around every tellurium in the macrocycle is distorted pseudo-octahedral.

2.6 Conclusion

We have synthesized a twelve membered macrocycle with a new bridging and capping anions of tetrafluoro phosphate (PF_4^-), and telluronium salt of tetrafluoro phosphate (PF_4^-). Also, we have demonstrated the inorganic twelve membered macrocycle ring expansion to sixteen membered macrocycle which contains organotellurium, organoselenium units and capped by four tetra fluoroborate anions.

Analytical and Spectroscopic data

Table 2.1 Crystal data and structure refinement for **2.2** to **2.3a**

Identification code	2.2	2.3	2.3a
Empirical formula	$C_{84}H_{84}F_{18}O_{14}P_4Te_6$	$C_{21}H_{21}F_4O_3PTe$	$C_{14}H_{14}F_2O_2Te$
Formula weight	2548.99	555.97	379.85
Temperature/K	296	296.	296
Crystal system	*triclinic*	*triclinic*	*monoclinic*
Space group	P-1	P-1	I2/a
a/Å	14.646(3)	10.3656(3)	19.564(4)
b/Å	14.872(3)	10.6864(2)	4.7122(5)
c/Å	15.304(3)	11.3879(3)	15.758(2)
α/°	100.310(7)	112.236(2)	90110.185(19)
β/°	108.902(7)	97.157(2)	110.185(19)
γ/°	116.758(7)	103.226(2)	90
Volume/Å3	2599.6(9)	1105.01(5)	1363.5(4)
Z	1	2	4
ρcalcg/cm3	1.628	1.6708	1.8502
μ/mm-1	1.808	1.471	2.200
F(000)	1234.0	547.7	736.0
Crystal size/mm3	0.08 × 0.08 × 0.06	0.08 × 0.04 × 0.04	00.9 × 0.8 × 0.5
Radiation	MoKα(λ = 0.71073)	MoKα(λ=0.71073)	MoKα(λ=0.71073)
2Θ range for datacollection/°	4.688 to 56.146	3.98 to 53.82	4.436 to 53.442
Index ranges	-18 ≤ h ≤ 18, -19 ≤ k ≤ 19, -19 ≤ l ≤ 19	-13 ≤ h ≤ 12, -13 ≤ k ≤ 13, -14 ≤ l ≤ 13	-24 ≤ h ≤ 24, -5 ≤ k ≤ 5, -19 ≤ l ≤ 19
Reflections collected	123791	26102	47281
Independent reflections	12098[R_{int} =0.0709, R_{sigma} = 0.0387]	4625[R_{int} =0.0496, R_{sigma} = 0.0415]	403 [R_{int} = 0.0512, R_{sigma} = 0.0552]
Data/restraints/ parameters	12098/818/574	4625/2/274	1403/0/88
Goodness-of-fit on F2	1.100	1.068	1.031
Final R indexes [I>=2σ(I)]	R_1 = 0.0937, wR_2 = 0.3008	R_1 = 0.0364, wR_2 = 0.0832	R_1 = 0.0531, wR_2 = 0.1309
Final R indexes	R_1 = 0.1233,	R_1 = 0.0464,	R_1 = 0.0594,

[all data]	wR_2 = 0.3228	wR_2 = 0.0908	wR_2 = 0.1350
Largest diff. peak/hole/e Å^3	3.30/-2.55	0.67/-0.66	1.04/-1.72

Table 2.2 Selected bond lengths [Å] bond Angles for 2.2.

Atom	Atom	Length/Å
Te1	O1	1.964(8)
Te1	C1	2.108(11)
Te1	F4^1	2.394(8)
Te2	O1	1.982(7)
Te2	F2	2.356(9)
Te3	F1	1.978(11)
Te3	F5	2.135(11)
P2	F8	1.306(12)
P2	F6	1.318(12)
P2	F9	1.386(12)
P2	F7	1.640(18)
P1	F2	1.484(10)
P1	F4	1.492(10)
P1	F5	1.516(10)
P1	F3	1.550(10)

Atom	Atom	Atom	Angle/°
O1	Te1	F4^1	172.1(3)
C1	Te1	F4^1	85.8(4)
C8	Te1	F4^1	83.1(4)
O1	Te2	C15	90.2(4)
O1	Te2	C22	89.9(5)
C15	Te2	C22	95.8(5)
O1	Te2	F2	173.1(4)
C15	Te2	F2	85.0(4)
C22	Te2	F2	85.7(5)
F1	Te3	C36	89.3(9)
F1	Te3	C29	88.0(5)
C36	Te3	C29	96.4(7)
F1	Te3	F5	171.3(5)
C36	Te3	F5	85.5(8)
C29	Te3	F5	85.6(5)
Te1	O1	Te2	120.2(4)
F8	P2	F6	125.2(9)
F8	P2	F9	113.9(9)
F6	P2	F9	115.1(9)
F8	P2	F7	96.5(9)
F6	P2	F7	101.4(10)
F9	P2	F7	95.9(10)
F2	P1	F5	109.9(7)
F4	P1	F5	112.6(6)
F2	P1	F3	105.6(7)
F4	P1	F3	105.8(6)
F5	P1	F3	103.2(7)
P1	F2	Te2	145.6(7)

P1	F5	Te3	122.7(6)
P1	F4	Te1[1]	140.3(6)

Table 2.3 PF_4^- bond lengths and bond angles 2.3

Te1	F4	2.393(9)
F2	P1	1.552(3)
F3	P1	1.442(3)
F1	P1	1.540(3)
F4	P1	1.442(3)

	P1	F2	95.9(2)
F3	P1	F2	106.82(18)
F1	P1	F3	108.6(2)
F4	P1	F2	110.03(19)
F4	P1	F3	123.95(19)
F4	P1	F1	107.95(18)

Table 2.4 Bond length and bond angles of 2.3

Te1	F1[1]	1.997(4)
Te1	F1	1.997(4)

F1[1]	Te1	F1	172.3(2)
F1	Te1	C1[1]	87.52(17)
F1[1]	Te1	C1[1]	87.47(17)
F1	Te1	C1	87.47(18)
F1[1]	Te1	C1	87.52(17)

ESI mass spectral analysis of compound 2.2

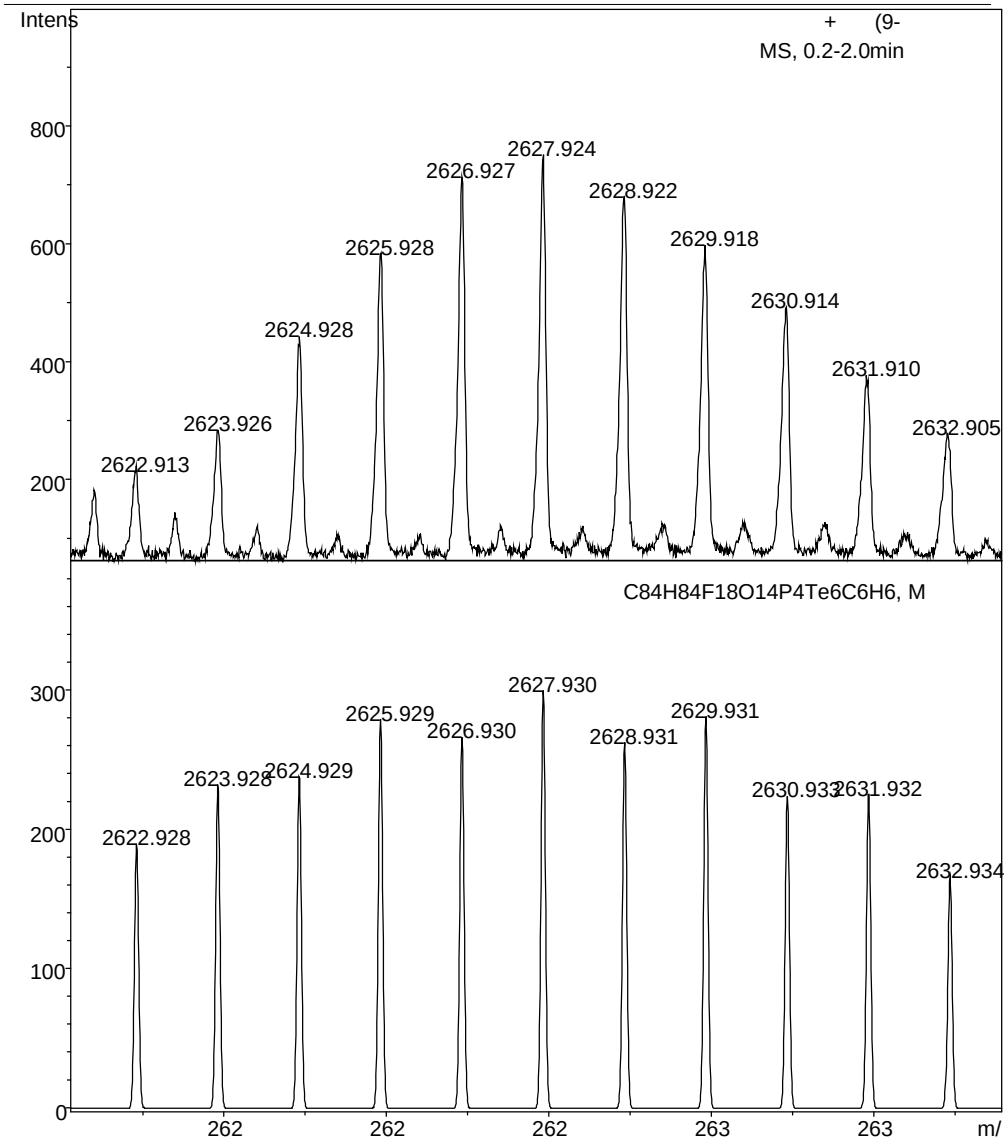

^{125}Te, ^{19}F, ^{11}B, ^{1}H, ^{13}C NMR spectral analysis of compound

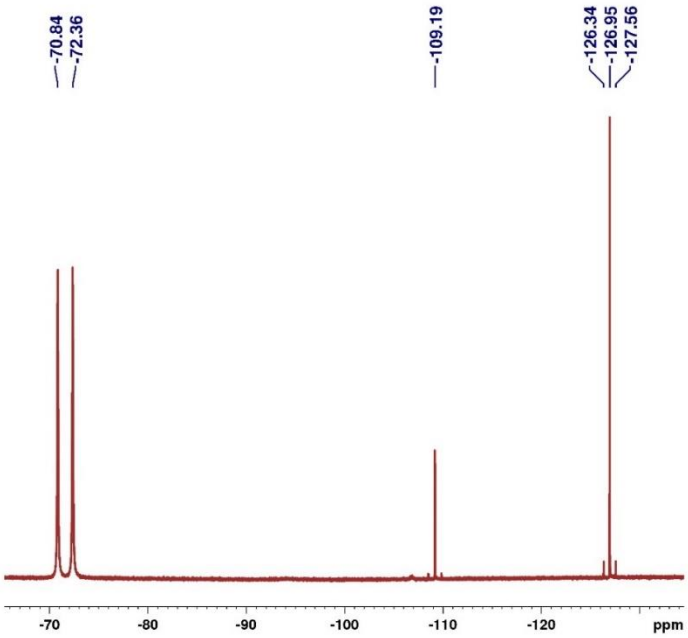

Figure 2.8 ^{19}F NMR spectrum of **2.2** in $CDCl_3$ at room temperature.

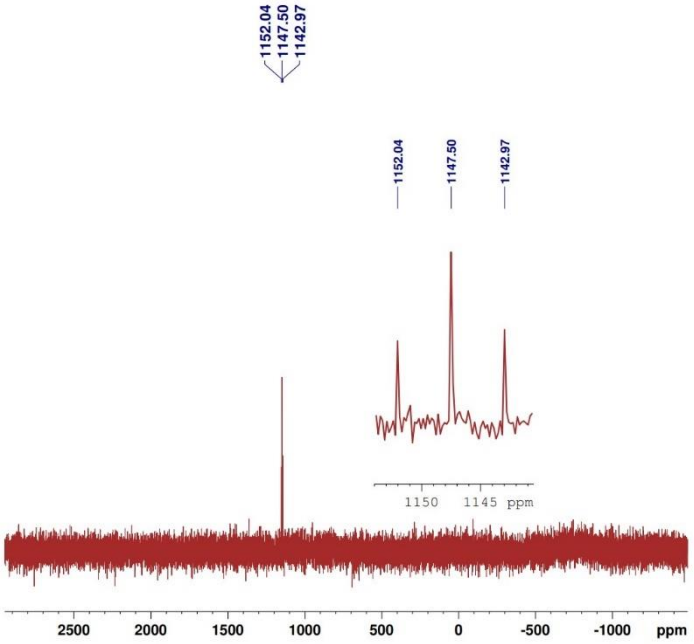

Figure 2.9. ^{125}Te NMR spectrum of **2** in $CDCl_3$ at room temperature.

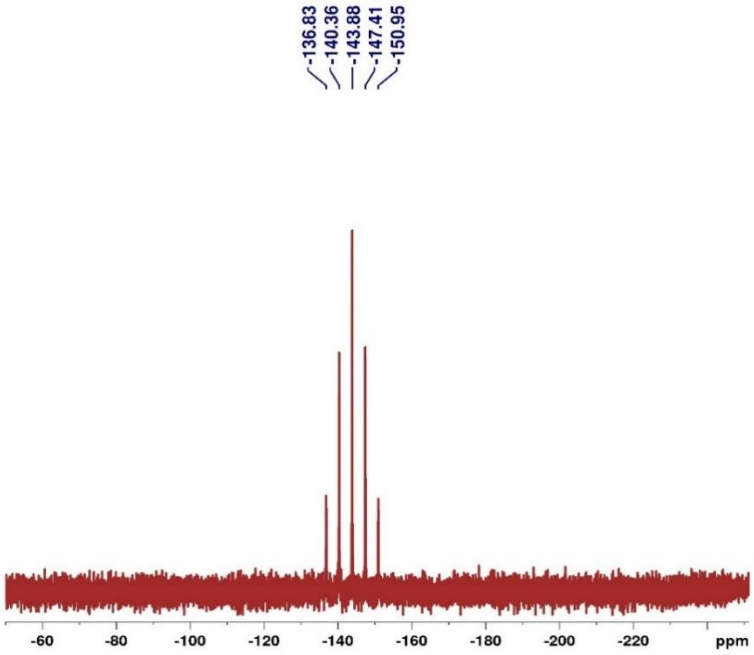

Figure 2.10. ^{31}P NMR spectrum of **2.2** in $CDCl_3$ at room temperature.

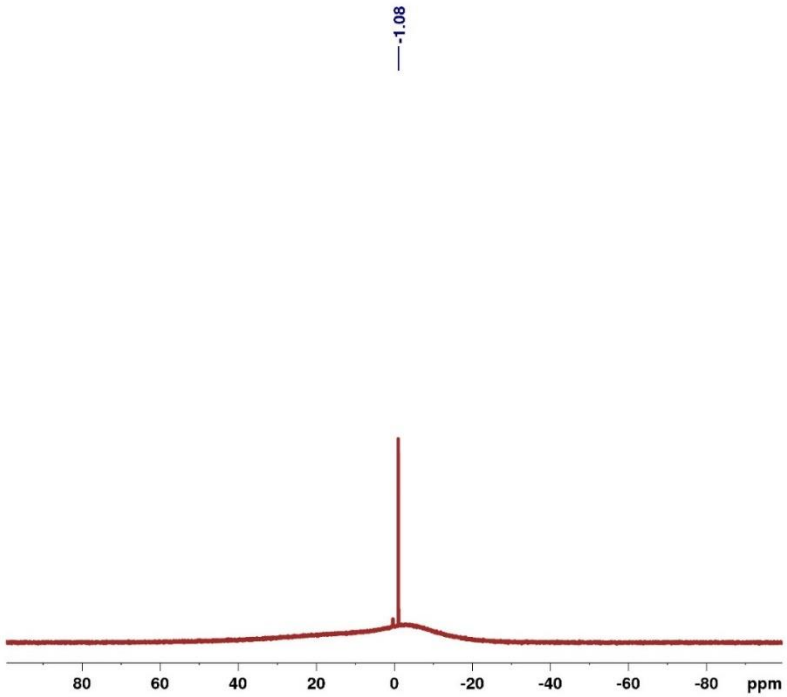

Figure 2.11. ^{11}B NMR spectrum of **2.2** in $CDCl_3$ at room temperature.

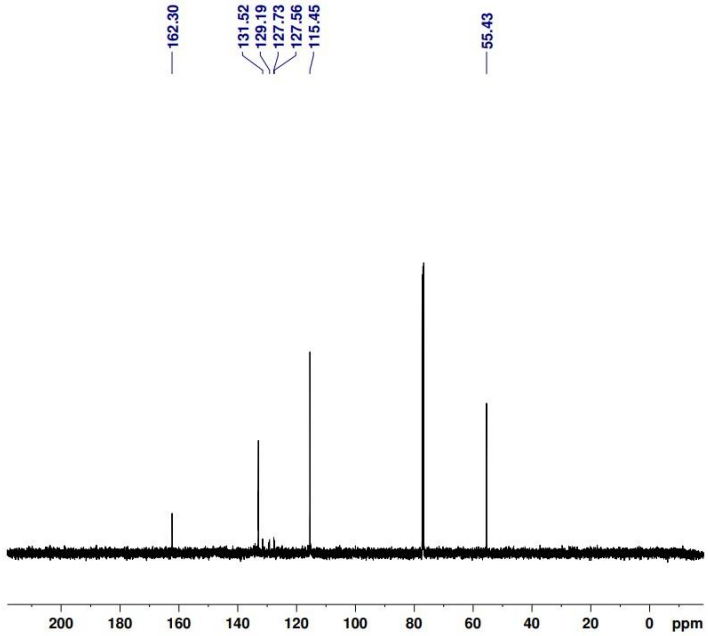

Figure 2.12. ^{13}C NMR spectrum of **2.2** in $CDCl_3$ at room temperature.

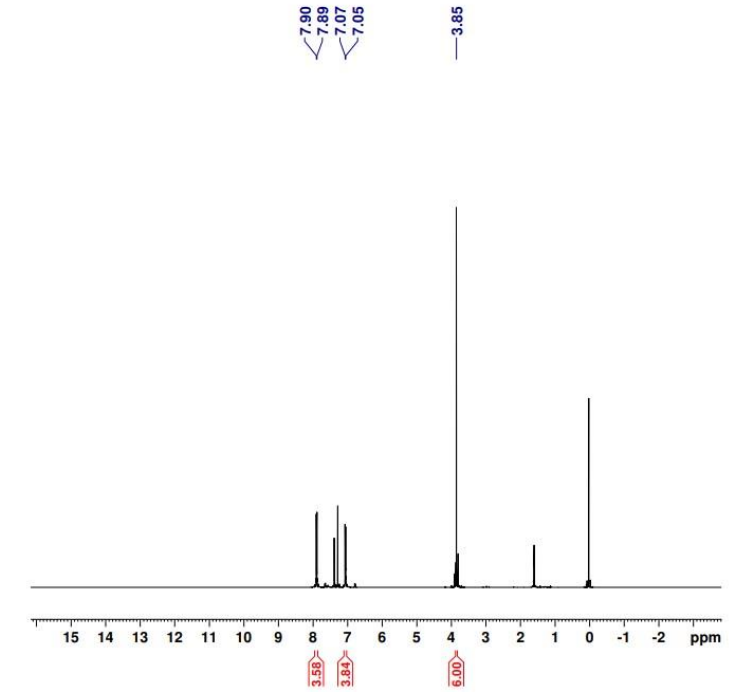

Figure 2.13. ^{1}H NMR spectrum of **2.2** in $CDCl_3$ at room temperature.

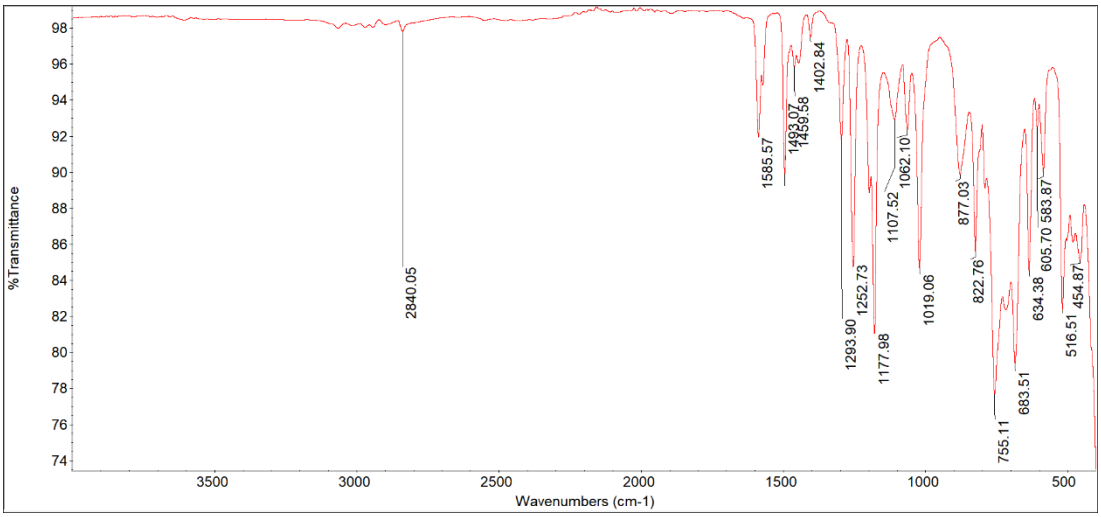

Figure 2.14. FT-IR spectrum of comppf 2.2

ESI mass spectral analysis of compound 2.3

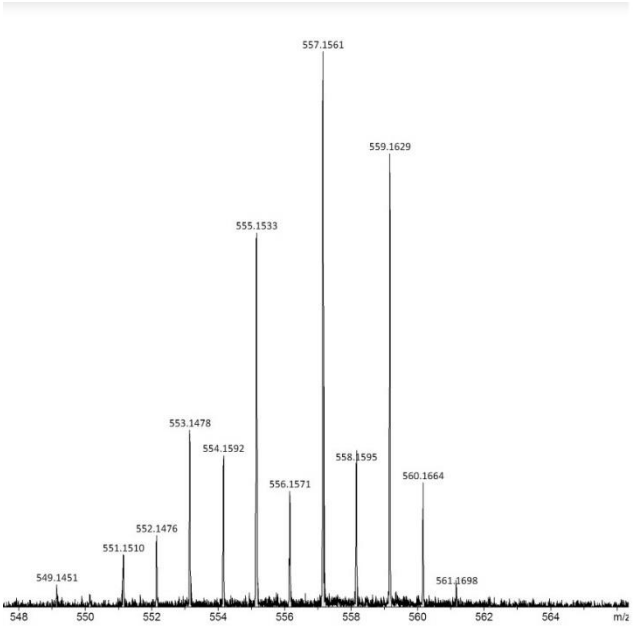

Figure 2.15.

Table 2.5 Crystal data and structure refinement for **2.4**

Identification code	**2.4**
Empirical formula	$C_{80}H_{80}B_4F_{16}O_{16}Se_4Te_4$
Formula weight	2470.92
Temperature/K	100.0(2)
Crystal system	tetragonal
Space group	P4/n
a/Å	19.8704(5)
b/Å	19.8704(5)
c/Å	14.8286(4)
α/°	90
β/°	90
γ/°	90
Volume/Å^3	5854.8(3)
Z	2
ρ_{calc}g/cm^3	1.402
μ/mm^{-1}	2.303
F(000)	2392.0
Crystal size/mm^3	0.08 × 0.06 × 0.06
Radiation	MoKα (λ = 0.71073)
2Θ range for data collection/°	3.994 to 53.98
Index ranges	-25 ≤ h ≤ 24, -24 ≤ k ≤ 24, -18 ≤ l ≤ 18
Reflections collected	35407
Independent reflections	6106 [R_{int} = 0.1233, R_{sigma} = 0.1443]
Data/restraints/parameters	6106/255/282
Goodness-of-fit on F^2	1.097
Final R indexes [I>=2σ (I)]	R_1 = 0.1089, wR_2 = 0.3336
Final R indexes [all data]	R_1 = 0.1937, wR_2 = 0.3658
Largest diff. peak/hole / e Å^{-3}	3.40/-1.12

Table 2.6 Bond lengths for 2.4.

Atom	Atom	Length/Å	Atom	Atom	Length/Å
Te1	O1[1]	2.180(10)	C16	C19	1.40(2)
Te1	O2	2.161(10)	C1	C2	1.32(2)
Te1	C7	2.088(15)	C1	C6	1.36(3)
Te1	C14	2.115(15)	C10	C11	1.40(2)
Se1	O1	1.715(10)	C10	C9	1.41(2)
Se1	O2	1.705(9)	C8	C9	1.41(2)
Se1	C1	1.843(17)	C11	C12	1.43(2)
F4	B1	1.31(2)	C15	C17	1.39(2)
F3	B1	1.38(3)	F2	B1	1.30(3)
O4	C10	1.30(2)	C18	C17	1.44(2)
O4	C13	1.43(2)	C18	C19	1.33(2)
C7	C8	1.320(19)	B1	F1	1.34(3)
C7	C12	1.45(2)	C2	C0AA	1.60(3)
C14	C16	1.33(2)	C6	C1AA	1.34(3)
C14	C15	1.38(2)	C5	C1AA	1.44(3)
O3	C18	1.34(2)	C5	C0AA	1.28(3)
O3	C20	1.42(3)			

Table 2.7 Bond Angles for 2.4.

Atom	Atom	Atom	Angle/°	Atom	Atom	Atom	Angle/°
O2	Te1	O1[1]	170.0(4)	O4	C10	C9	122.5(18)
C7	Te1	O1[1]	85.5(5)	C11	C10	C9	118.8(16)
C7	Te1	O2	86.1(5)	C7	C8	C9	122.0(15)
C7	Te1	C14	97.0(6)	C10	C11	C12	118.7(17)
C14	Te1	O1[1]	89.0(5)	C14	C15	C17	122.4(16)
C14	Te1	O2	86.7(5)	C11	C12	C7	119.4(14)
O1	Se1	C1	97.3(6)	C8	C9	C10	120.8(16)
O2	Se1	O1	101.6(4)	O3	C18	C17	123.6(18)
O2	Se1	C1	97.0(7)	C19	C18	O3	117.7(18)
Se1	O1	Te1[2]	114.1(5)	C19	C18	C17	118.7(17)
Se1	O2	Te1	116.5(5)	C15	C17	C18	115.7(17)
C10	O4	C13	122.0(17)	C18	C19	C16	124.2(18)
C8	C7	Te1	122.7(12)	F4	B1	F3	115.3(14)
C8	C7	C12	119.3(15)	F4	B1	F1	117(3)
C12	C7	Te1	116.8(11)	F2	B1	F4	114(2)
C16	C14	Te1	120.8(12)	F2	B1	F3	107(2)
C16	C14	C15	121.1(14)	F2	B1	F1	94.6(19)

C15	C14	Te1	118.0(11)	F1	B1	F3	106(2)
C18	O3	C20	114.1(18)	C1	C2	C0AA	116.7(19)
C14	C16	C19	117.4(16)	C1AA	C6	C1	123(2)
C2	C1	Se1	116.7(15)	C0AA	C5	C1AA	125(2)
C2	C1	C6	120.9(18)	C6	C1AA	C5	116(2)
C6	C1	Se1	120.7(14)	C5	C0AA	C2	114(2)
O4	C10	C11	118.4(18)				

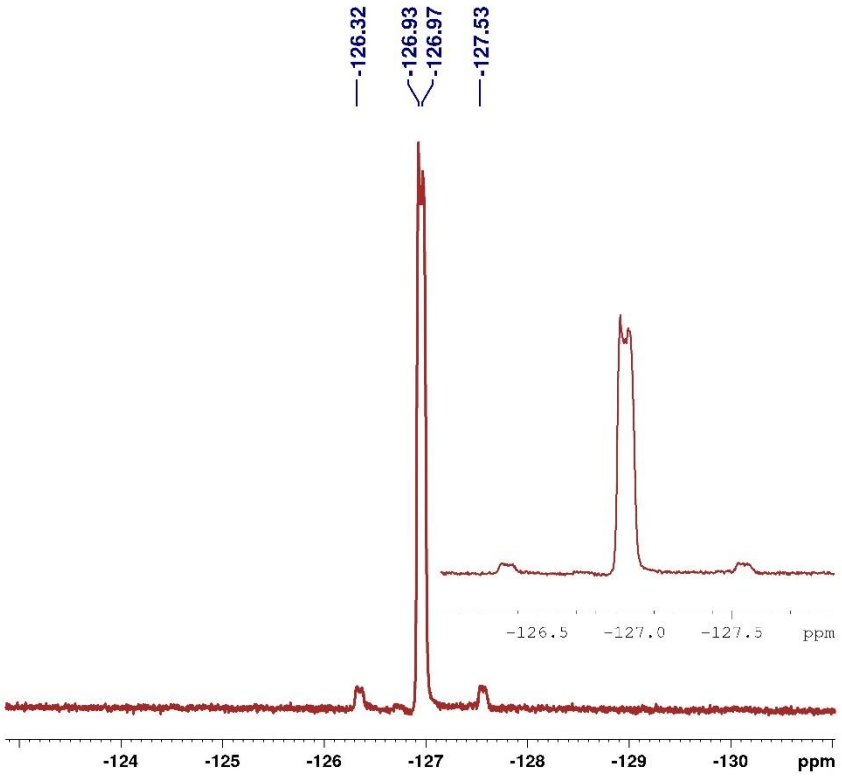

Figure 2.16. ^{19}F NMR spectrum of **2.4** in $CDCl_3$ at room temperature.

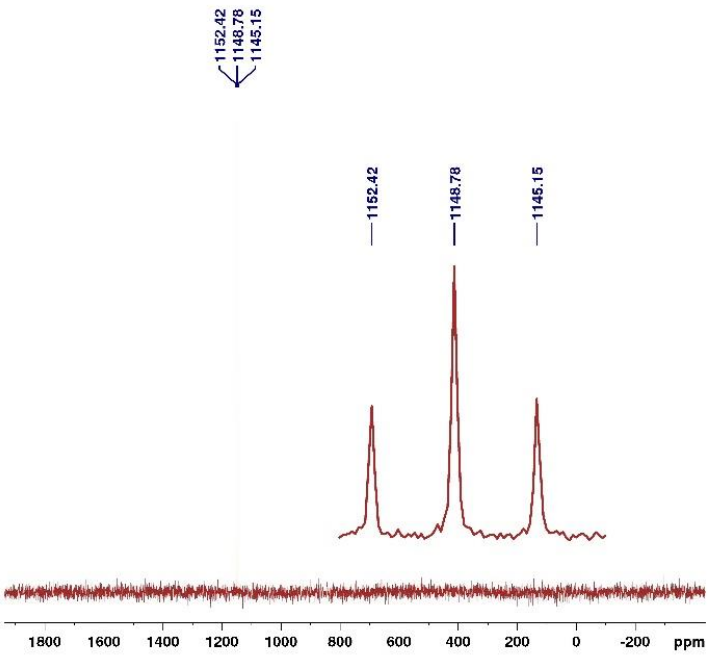

Figure 2.17. ^{125}Te NMR spectrum of **2.4** in $CDCl_3$ at room temperature.

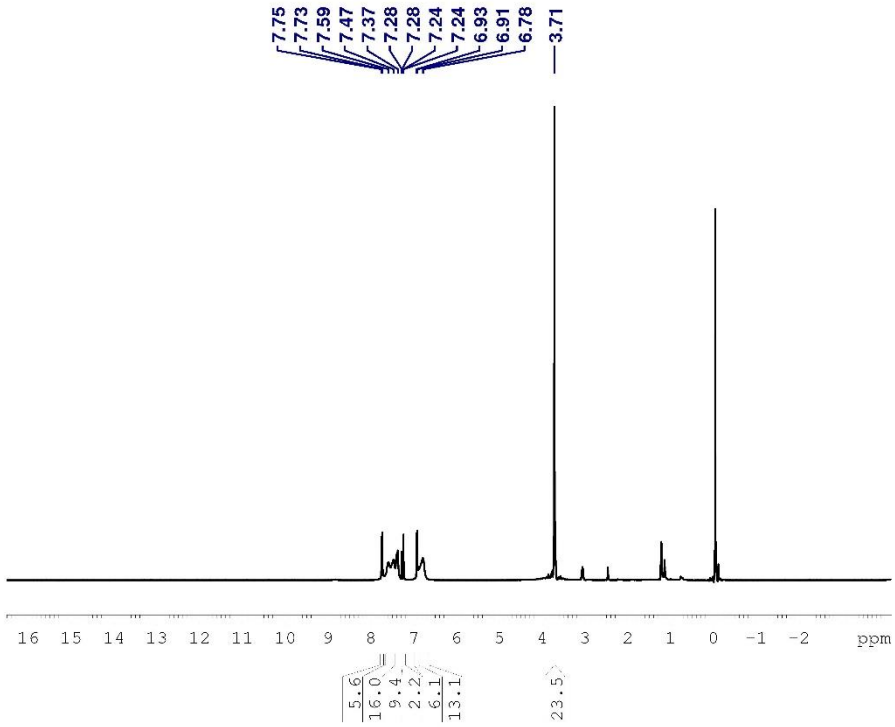

Figure 2.18. ^{1}H NMR spectrum of **2.4** in $CDCl_3$ at room temperature.

IR spectra of 2.4

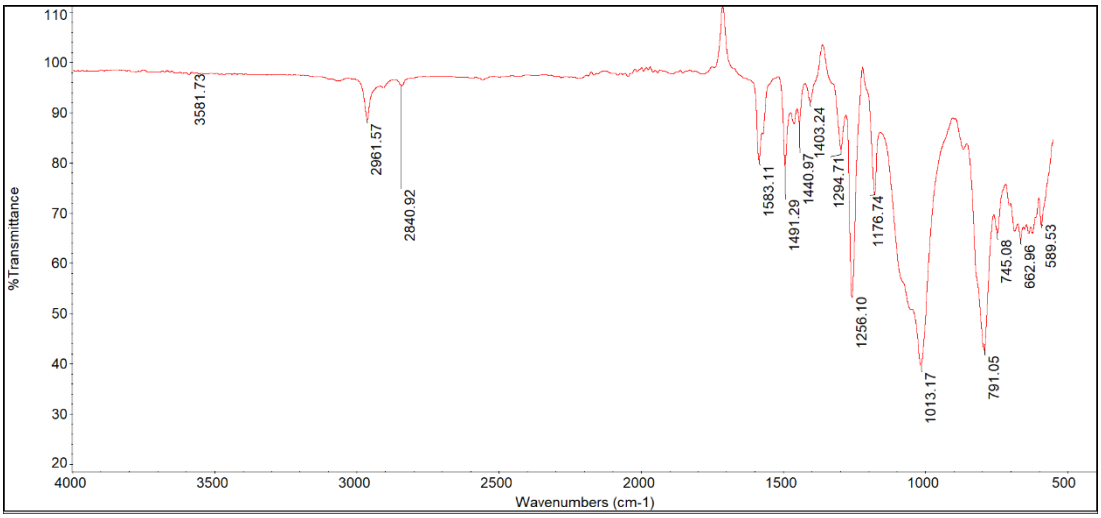

Figure 2.19

References

1. (a). R. Gleiter, G. Haberhauer, D. B. Werz, F. Rominger and C. Bleiholder, *Chem Rev*, 2018, 118, 2010–2041. (b). N. Biot, D. Romito and D. Bonifazi, *Cryst Growth Des*, 2021, **21**, 536–543. (c). N. Biot and D. Bonifazi, *Coord Chem Rev*, 2020, 413. (d). P. C. Ho, J. Lomax, V. Tomassetti, J. F. Britten and I. Vargas-Baca, , DOI:10.1002/chem.202101425Part. (e). P. C. Ho, P. Szydlowski, J. Sinclair, P. J. W. Elder, J. Kübel, C. Gendy, L. M. Lee, H. Jenkins, J. F. Britten, D. R. Morim and I. Vargas-Baca, *Nat Commun*, DOI:10.1038/ncomms11299. (f). G. Haberhauer and R. Gleiter, *Angewandte Chemie - International Edition*, 2020, **59**, 21236–21243. (g). A. F. Cozzolino, P. J. W. Elder and I. Vargas-Baca, *Coord Chem Rev*, 2011, 255, 1426–1438.
2. (a). Huacheng Zhanga, Ruqiang Zoub, Yanli Zhao *Coord Chem Rev*,. 2015, **292** 74–90.
3. O. Carugo, G. Resnati and P. Metrangolo, *ACS Chem Biol*, *ACS Chem. Biol.*2021, **16**, 9, 1622–1627, DOI:10.1021/acschembio.1c00441.
4. Graham E. Garrett, Elisa I. Carrera, Dwight S. Seferos and Mark S. Taylor, : Chem. Commun., 2016, 52, 988
5. (a). K. Kobayashi, N. Deguchi, E. Horn and N. Furukawa, *Angewandte Chemie - International Edition*, 1998, **37**, 984–986. (b). K. Kobayashi, N. Deguchi, O. Takahashi, K. Tanaka, E. Horn, O. Kikuchi and N. Furukawa, *Angewandte Chemie - International Edition*, 1999, **38**, 1638–1640. (c). K. Kobayashi, H. Izawa, K. Yamaguchi, E. Horn, N. Furukawa, *Chem. Commun.* 2001, 1428. (d). J. Beckmann, D. Dakternieks, A. Duthie, N. A. Lewcenko, C. Mitchell, M. Schürmann, *Z. Anorg. Allg. Chem*. 2005, **631,** 1856.
6. (a). V. Chandrasekhar, R. Thirumoorthi, *Inorg. Chem*. 2009, **48**, 10330. (b). N. K. Srungavruksham and V. Baskar, *Eur. J. Inorg. Chem*., 2012, 136-142 (c). N. K. Srungavruksham and V. Baskar, *Dalton Transactions*, 2015, **44**,

4554– 4569. (d). Ramesh K. Metre, Subrata Kundu, Dipankar Sahoo, and Vadapalli Chandrasekhar. *Organometallics,* 2014, **33**, 2380−2383. (e). Alcock, N. W.; Culver, J.; Roe, S. M. *J. Chem. Soc., Dalton Trans*. 1992, 1477. (f). Alcock, N. W.; Harrison, W. D. *J. Chem. Soc., Dalton Trans*. 1982, 1421. (g). Kenji Kobayashi, Hiroyuki Izawa, Kentaro Yamaguchi, Ernst Hornc and Naomichi Furukawaa, *Chem. Commun*., 2001, 1428–1429. (h). Jens Beckmann Jens Bolsinger, Johann Spandl, *Journal of Organometallic Chemistry*, 2008, **693**, 957–964.

7. (a). Jens Beckmann, Dainis Dakternieks, Andrew Duthie, Naomi A. Lewcenko, and Cassandra Mitchell, *Angew. Chem. Int. Ed*. 2004, **43**, 6683 – 6685. (b). Jens Beckmann, Jens Bolsinger, and Andrew Duthie, *Z. Anorg. Allg. Chem*. 2010, 636, 765–769.
8. (a). A. F. Gushwa, Y. Belabassi, J. L. Montchamp and A. F. Richards, *J. Chem. Crystallogra.* 2009, **39**, 337-347. (b). J. Bergman, *Tetrahedron*, 1972, **28**, 3323.
9. (a). G. M. Sheldrick, *Acta Crystallogr C Struct Chem*, 2015, **71**, 3–8. (b). O. v. Dolomanov, L. J. Bourhis, R. J. Gildea, J. A. K. Howard and H. Puschmann, *J Appl Crystallogr*, 2009, **42**, 339–341.
10. S. Alvarez, Dalton Trans., 2013, 42, 8617–8636.
11. Cordero, B. et al. Covalent radii revisited. *Dalton Trans*. 2008, 2832–2838.
12. B. Zhou and F. P. Gabbaï, *Chem Sci*, 2020, **11**, 7495–7500.
13. B. Zhou and F. P. Gabbaï, *J Am Chem Soc*, 2021, **143**, 8625–8630.
14. (a). Kirij, N. V., Yagupolskii, Y. L., Tyrra, W., Pantenburg, I. & Naumann, D. The structure of tris(trifluoromethyl)tellurium fluoride dimethylformamide, [$Te(CF_3)_3$-DMF(m-F)]. Z. Anorg. Allg. Chem. 633, 943–945 (2007). (b). H. Zhu, P. P. Zhou, and Y. Wang, *Nat Commun*, DOI:10.1038/s41467-022-31293-5.
15. (a) K. B. Borisenko, M. Broschag, I. Hargittai, T. M. Klapötke, D. Schröder, A. Schulz, H. Schwarz, I. C. T. Oetting and P. S. White, J. Chem. Soc., Dalton

Trans., 1994, 2705; (b) W. Nakanishi, S. Hayashi, A. Sakaue, G. Ono and Y. Kawada, J. Am. Chem. Soc., 1998, 120, 3635. (c). N. K. Srungavruksham and V. Baskar, *Dalton Transactions*, 2015, **44**, 4554– 4569.

Chapter 3

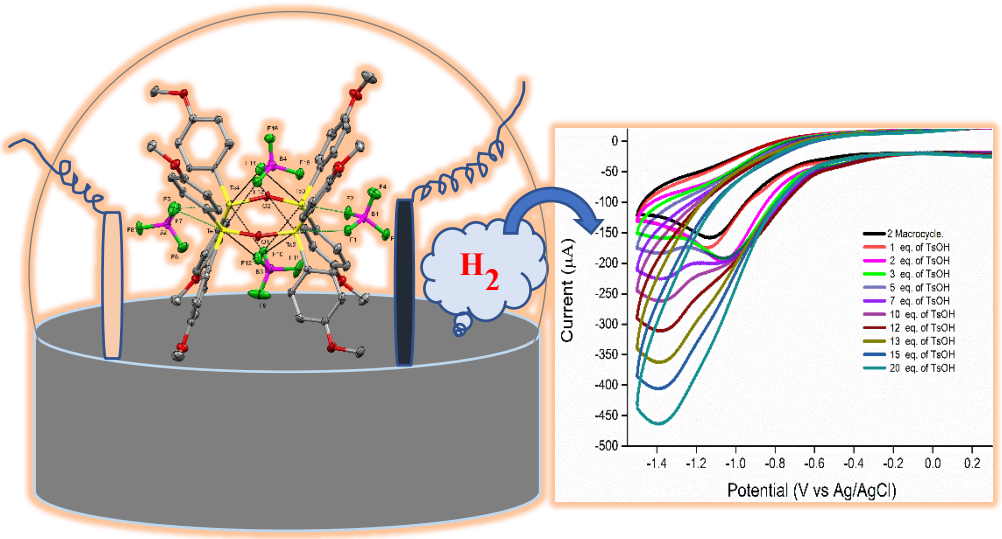
H2
Current (μA)
Potential (V vs Ag/AgCl)
0
-50
-100
-150
-200
-250
-300
-350
-400
-450
-500
-1.4
-1.2
-1.0
-0.8
-0.6
-0.4
-0.2
0.0
0.2
2 Macrocycle
1 eq. of TsOH
2 eq. of TsOH
3 eq. of TsOH
5 eq. of TsOH
7 eq. of TsOH
10 eq. of TsOH
12 eq. of TsOH
13 eq. of TsOH
15 eq. of TsOH
20 eq. of TsOH

Chapter 3

Electrocatalytic Hydrogen Evolution Mediated by an Organotelluroxane Macrocycle Stabilized through Secondary Interactions

The macrocycle is synthesized as the chloride abstraction from bis(p-methoxyphenyl) tellurium dichloride (1) by silver salts $AgMX_4$ ($MX_4 = BF_4^-$, and ClO_4^-) results in situ formed di-cationic tetraorganoditelluroxane units two such units are held together by two weak anions μ_2-MX_4 bridging to create a 12-membered di-cationic macrocycle $[(p\text{-}MeO\text{-}C_6H_4)_2Te)_2(\mu\text{-}O)(\mu_2\text{-}F_2BF_2)_2]^{2+}$ (3.2), $[(p\text{-}MeO\text{-}C_6H_4)_2Te)_2(\mu\text{-}O)(\mu_2\text{-}O_2ClO_2)_2]^{2+}$ (3.3) stabilized via Te-(μ_2-BF_4/ClO_4), secondary interactions. Two more μ-MX_4 anions present above and below the macrocycle plane to balance the charge. The same reaction at higher temperatures led to the formation of telluronium salts R_3TeX [X= BF_4^- (3.4), ClO_4^- (3.5)] as a significant product. The BF_4^- anion containing macrocycle and telluronium salt was monitored with ^{19}F NMR. The HRMS confirmed the stability of all the compounds in the solution state. Homogeneous electrocatalytic proton reduction is reported using organotellurium macrocycle as electrocatalysis employed in an organic medium with the addition of para-toluene sulfonic acid.

3.1 Introduction

The global energy demand is increasing day by day, while the primary energy source are fossil fuels, whose abundance is on the decline continuously. Also, using fossil fuel energy is undesirable for the earth's environment. Hence, there is a need to shift from dependency on fossil fuels to sustainable options such as renewable/clean energy. Hydrogen gas is more promising for fulfilling energy demands near future. The evolution of hydrogen through homogeneous electrocatalysis is one of the ways. Earth abundant metals and chalcogenide-stabilized transition compounds have been employed as homogenous electrocatalysts for hydrogen evolution in nonaqueous solutions.[1] The organochalcogen compounds as electrophilic sites have long been known for secondary bonding interactions with electron-rich anion/ Lewis bases resulting in applications in the fields of catalysis[2], biology[3], anion transport[4], host-guest chemistry/ supramolecular chemistry[5], in the synthesis of organic and organometallic compounds, used as moderate oxygen transfer reagents.[6] The chalcogens act as secondary bonding interaction centers, as shown by their VSEPR geometry in oxidation states (II) and (IV), which typically have two positions. These characteristics make it possible to achieve chelation and the production of a planar complex of tellurium (IV) cations, which exhibit stronger Lewis' acidity and higher ion transport activity in comparison to tellurium compounds including Te (II). Among Group 16 elements (Lewis's acidity order O < S < Se < Te), tellurium is the softest, heaviest, and most electropositive chalcogen forming the strongest and shortest secondary bonding interactions with oxygen, nitrogen, and chlorine atoms.[7] Presence of an electron-withdrawing group enhances the electropositive region on tellurium, leading to much stronger secondary bond interaction. Kobayashi and Furukawa et al. reported bis-diaryltellurium (IV) oxide dicatation by inserting an oxygen atom.[8] These tellurium cations can react with nucleophiles.[9] Beckmann et al. studied the reactivity of diorganotellurium oxide towards strong acids like diphenyl phosphinic acid and

weak acids such as triflic acid leading to the formation of tetraorganoditelluroxane along with anions which shows extensive secondary Te---O interactions.[10] Also, diorgano tellurium dihalide reaction with protic acids such as cyclic phosphinic acid has been explored.[11] Recently, Gabbai et al. developed novel Lewis acidic receptors which work as catalysts with telluronium ions as an active site.[12] The group also reported the oxidative alkylation of diaryl tellurides $[Mes(C_6F_5)TeMe]^+$ and $[(C_6F_5)_2TeMe]^+$ from $Mes(C_6F_5)Te$, $[(C_6F_5)_2Te$, respectively.[13] The formation of complexes and the transport of chloride ions across phospholipid bilayers may be possible with these newly discovered telluronium salts. Recently, bistelluronium dicatation obtained as tetrafluoroborate salt and its catalytic properties have been studied.[14] Our group has been involved in the preparation of the tellurium macrocycle of organotellurium with benzene seleninic acid[15], which formed a 12- membered inorganic macrocycle made up of two tetraorgano telluroxane moieties assembled with two selenates to form dicationic $Te_4Se_2O_4$ macrocyclic core stabilized with Te---X (X = spherical anions Cl, Br, and I). Subsequently, the anion exchange reaction of the 12-membered macrocycle with different anions shows variable geometry around the central atom.[16] Synthesis of Telluronium salts is known in the literature.[17] Here, we present the synthesis and structural characterization of 12-membered tellurium macrocycles where weak anions such as ClO_4^-, and BF_4^- act as μ_2- bridging and capping ligands and isolation of homoleptic Telluronium salts, obtained through the milder synthetic methodology. One of the macrocycles shows the electrocatalytic activity towards proton reduction.

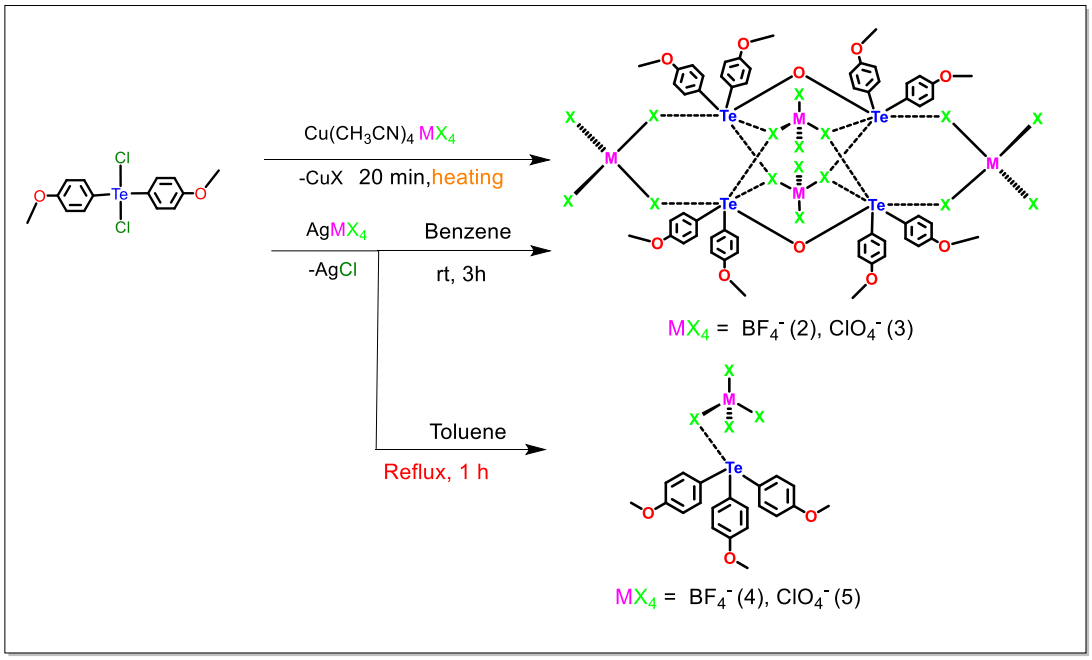

Scheme 3.1. Synthetic procedure for 3.2-3.5

3.2 Experimental section

3.2.1 Reagents and general procedures

Chemicals $TeCl_4$, $AgBF_4$, and $AgClO_4.xH_2O$ (Caution! Silver perchlorate is a hazardous and potentially explosive chemical, it causes chemical burns when exposed to skin or eye burns and must be handled in fume wood with care) were purchased from Sigma Aldrich Ltd. Solvents and other general reagents were purchased from a commercial source and purified according to standard procedure. Bis-(p-methoxyphenyl) Tellurium dichloride and $[Cu(CH_3CN)_4]BF_4$ and $[Cu(CH_3CN)_4]ClO_4$ was synthesized according to the previously reported procedure.[19] The yields of all compounds were calculated based on Bis-(p-methoxyphenyl) Tellurium dichloride for isolated crystals. These dried samples (free of benzene and toluene solvents) were subjected to spectroscopic and electrochemical analysis.

3.2.1 Instrumentation

Infrared spectra were recorded with a NICOLET Is5 FTIR spectrometer. Single crystal X-ray data for 5 was collected at 298 K and carried out with a Bruker smart apex CCD area detector system. [λ (Mo Kα) = 0.71073 Å] with a graphite monochromator. The data were reduced using APEX-2, and the structures were solved using SHELXS-97 and OLEX-2-1.2 and were refined using the program SHELXl-2018/7. The Remaining three single-crystal X-ray data were collected at 100K carried out by Rigaku Oxford Xta- Lab synergy diffractometer with the graphite monochromator with a Mo Kα (λ=0.71073 Å) microfocus sealed tube operated at 50 kV and 1mA. The data was solved and refined using OLEX software 2-1.2. 20 ^{1}H, ^{13}C, ^{125}Te, ^{11}B, and ^{19}F NMR spectra were recorded with Bruker AVANCE III 400 and 500 instruments. CCDC (2160462-2160465) for 2, 3, 4, and 5 Contain the supplementary crystallographic data for this paper. These can be obtained free of charge from the Cambridge crystallographic data center via www.ccdc.cam.ac. Uk/data request/cif.

3.2.2 Synthetic procedure for 3.2 and 3.3

Silver salt was weighed in a glove box in a round bottom flask sealed with a rubber septum and covered with aluminum foil: to this, 5 ml of benzene was injected and was kept for stirring for 5 minutes, then, a solution of Bis-(p-methoxyphenyl) Tellurium dichloride (p-$OMeC_6H_6)_2TeCl_2$ in benzene was injected at ambient temperature, and it was kept for continuous stirring for 6 hours, The solution was filtered to remove AgCl (precipitate) formed during reactions. The filtrate 2 was crystalized by a diffusion method and 3 by an evaporation method, both of which, after weeks, gave block-like crystals suitable for a single-crystal X-ray diffractometer studies. From copper salts: $[Cu(CH_3CN)_4]BF_4$ and $[Cu(CH_3CN)_4]ClO_4$ salt was added to a hot benzene solution of Bis-(p-methoxyphenyl) Tellurium dichloride (p-$OMe-C_6H_6)_2TeCl_2$ and the stirring was continued for 20 minutes. The filtrate was concentrated in a vacuum, and the white crystalline powder in good yield was separated.

[{(p-$OMeC_6H_4$)$_2$Te}$_2$(μ-O)(μ-BF_4)(μ-BF_4)]$_2$ (3.2):

Bis-(p-methoxy phenyl) Tellurium dichloride (p-OMe-C_6H_6)$_2$$TeCl_2$(0.20 g, 0.49 mmol), silver tetrafluoroborate (0.19 g, 0.97 mmol), yield: 0.14g (66%) based on Bis-(p-methoxy phenyl) Tellurium dichloride. MP: 208-210 °C. $C_{56}H_{56}B_4F_{16}O_{10}Te_4$ (1746.65): ^{1}H NMR (500 MHz, CDCl3, ppm): δ 7.99 (d), δ 7.04(d), δ 3.87 (s). ^{13}C NMR (125 MHz, CDCl3, ppm): δ 162.26, δ 135.44, δ 125.23, δ 115.61, δ 55.57.; ^{19}F NMR (471.6 MHz, CDCl3, ppm) δ -109.24, δ -127.07.; ^{11}B NMR (160.77 MHz, CDCl3, ppm) δ - 0.98.; ^{125}Te NMR (158.22 MHz CDCl3, ppm): δ 1148.78 (t, J=573 Hz); IR:2836.0 (w), 2427.8 (m), 1581.3(s), 1489.9 (s), 1458.9 (s), 1439.6 (m), 1401.9 (s), 1293.8 (s), 1250.5 (s), 1176.2 (m), 1058.9 (m), 1019.5 (s), 819.9 (s), 739.6 (m), 684.9 (s), 588.7 (s), 512.2 (s), 473.8 (s).

[{(p-$OMeC_6H_4$)$_2$Te}$_2$(μ-O)(μ-ClO_4)(μ-ClO_4)]$_2$ (3.3):

Bis-(p-methoxy phenyl) Tellurium dichloride (*p*-OMe-C_6H_6)$_2$$TeCl_2$ (0.19 g, 0.47 mmol), $AgClO_4.xH_2O$ (0.27 g, 0.93 mmol) yield: 0.16 g (76%) based on Bis(*p*-methoxy phenyl) Tellurium dichloride. MP: 204-206 °C. $C_{56}H_{56}Cl_4O_{26}Te_4$ (1797.24): ^{1}H NMR (400 MHz, CDCl3, ppm): δ 7.81(S, 16H), δ 7.00 (d, 16 H), δ 3.84(S, 24); ^{13}C NMR (100 MHz, CDCl3, ppm): δ 162.53, 135.26, 128.38, 115.64, 55.57; ^{125}Te NMR (158.22 MHz CDCl3, ppm):δ 1500; IR : 3097.3(m), 3078.3(m), 3014.7(m), 2970.3 (m), 2938.5 (m), 2840.0 (m), 2566.8(m), 2373.0(m), 1580.9(s), 1491.7(s), 1458.0(s), 1435.8(s), 1407.2(m), 1302.4(s),1256.2(s), 1178.3(s), 1083.5(s), 922.5(m), 822.4(s), 790.3(m), 708.4(s), 681.0(s), 616.1(s), 591.8(s), 510.8(s) 476.0(m).

3.2.3 Synthetic procedure for 3.4 and 3.5

To Bis-(para-methoxy phenyl) tellurium dichloride dissolved in 20 mL of toluene was added to silver salts in a round bottom flask kept for one hour reflux. After the one-hour reaction mixture was filtered, and the filtrate contained a variety of compounds, macrocycle, and telluronium salt. The remaining sticky solid in the round bottom flask was added to 20 ml of acetonitrile and filtered. This filtrate contains only telluronium

salt; Block-like crystals were obtained via the evaporation method from the filtrate in weeks.

$(p\text{-}OMeC_6H_4)_3TeBF_4$) (3.4):

Bis-(p-methoxy phenyl) Tellurium dichloride (p-OMe-$C_6H_6)_2TeC_{l2}$(0.20g, 0.24 mmol), silver tetrafluoroborate (0.18 g, 0.96 mmol), yield: 0.12g (45%) based on Bis-(p-methoxy phenyl) Tellurium dichloride. MP: 202-204 °C. $C_{21}H_{21}BF_4O_3Te$ (535.79): ^{1}H NMR (500 MHz, $CDCl_3$, ppm): δ 7.48 (d, 6H), δ 7.05 (d, 6H), δ 3.82 (S, 9H); ^{13}C NMR (125 MHz, CDCl3, ppm): δ162.24, 135.47, 125.26, 115.61, 55.58.; ^{19}F NMR (471.6 MHz, CDCl3, ppm) -147.72; 11B NMR (160.77 MHz, CDCl3, ppm) -0.96 ^{125}Te NMR (158.22 MHz CDCl3, ppm): δ 744.50 (d); IR: 2961.0 (w), 2085.2(w), 1719.4(m), 1643.3(s), 1449.1(m), 1258.4(s), 1013.7(s), 794.0(s), 744.8(m), 696.2(m).

$(p\text{-}OMe\ C_6H_4)_3TeClO_4$) (3.5):

Bis-(p-methoxy phenyl) Tellurium dichloride (p-OMe-$C_6H_6)_2TeCl_2$ (0.10g, 0.24 mmol), $AgClO_4.H_2O$ (0.094 g, 0.48 mmol) yield: 0.06 g (45%) based on Bis (p-methoxy phenyl) Tellurium dichloride. MP:200-202 °C. $C_{21}H_{21}ClO_7Te$ (548.44): ^{1}H NMR (400 MHz, CDCl3, ppm): δ 7.52 (d, 6H), δ 7.08 (d, 6H), δ 3.88 (S, 9H); ^{13}C NMR (100MHz, CDCl3, ppm): δ 162.53, 135.26, 128.38, 115.64, 55.57; ^{125}Te NMR (158.22 MHz CDCl3, ppm): δ 744 (S); IR: 3547.9(w), 3059.4(m), 2961.6(m), 1583.2(m), 1488.0(m), 1435.4(m), 1299.2(m), 1258.7(s), 1051.3(w), 1012.9(w), 854.8(m), 796.3(s), 747.7(s), 698.3(s), 615.9(s), 556.0(s), 533.5(m), 506.4(m), 442.5(m).

3.3 Results and discussion

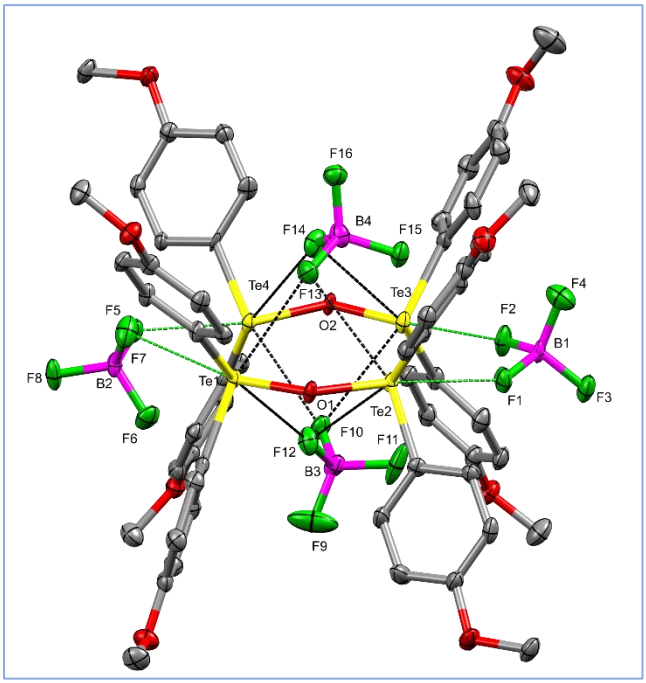

Figure 3.1 Solid state molecular crystal structure of 2, hydrogen atoms, and benzene solvate are omitted for clarity. Te shows interactions with Fluorine atoms., and thermal ellipsoids are drawn at 40% probability

Organotelluroxane of tetrafluoroborate was obtained through the reaction of bis (p-methoxyphenyl) tellurium dichloride (1) with copper salts Cu(CH3CN)4BF4 and silver tetrafluoroborate (AgBF4) benzene. $[(p\text{-}MeO\text{-}C_6H_4)_2Te)_2(\mu\text{-}O)(\mu_2\text{-}F_2BF_2)_2]^{2+}.3C_6H_6$ (3.2), (Figure 3.1) and with copper salts/silver perchlorate hydrate $Cu(CH3CN)_4ClO_4/(AgClO_4.H2O)$ for$[(pMeO\text{-}C_6H_4)_2Te)_2(\mu\text{-}O)(\mu_2\text{-}O_2ClO_2)_2]^{2+}$ $3C_6H_6$ (3.3) (crystal structure in SI) in moderate yields (Scheme 3.1). Both 2 and 3 are structurally quite similar (isomorphic) and crystalize 3.2 and 3.3 in monoclinic space group *P 1 21/C1*. These structures comprise two tetraorganoditelluroxane dicationic units connected by anions acting as μ2-bridging ligands (BF_4 and ClO_4) arranged in a 12-membered macrocyclic dicationic core fashion. The other counter anions are accommodating above and below of macrocycle for the charge balance through Te-(μ_2-BF_4)-Te (3.2), Te-(μ_2-ClO_4)-Te (3.3), secondary bonding interactions. 3.2 and 3.3 are the first examples of telluroxanes arranged in a macrocyclic fashion containing two distinct chemical motifs: R_2Te-- F—B—F—TeR_2 (3.2), R_2Te--O—Cl—O—TeR_2 (3.3), and an Organotelluroxane R_2Te —O—TeR_2. The solution ^{125}Te NMR of 3.2 is supposed to show a quartet since three fluorine atoms

surround each tellurium. One of the fluorine is from a bridging ligand other two are from capping ligands, despite this showing two different coupling environments for ^{125}Te and ^{19}F NMR spectra. Due to the distorted pseudo-octahedral coordination environment around every tellurium in 3.2 and 3.3 (Figure 1 inside) macrocycles, two fluorine from capping BF_4^- anions and two para (methoxyphenyl phenyl) groups situated each other 161° making equatorial positions in the bridging BF_4^- anions and oxygen bridging between two telluroxane units axially situated at 173°. The presence of two fluorine atoms in the equatorial position de-shields the tellurium and causes the ^{125}Te NMR spectrum to split into a triplet at 1147.18 ppm with a coupling constant of 570 Hz (1J Te---F = 573 Hz). The nuclei ^{125}Te NMR and axial fluorine coupling indicate a tellurium spectrum into a doublet that is somewhat up-filed at 1085.46 ppm with a coupling constant of 624 Hz. Similarly (Figure. 3.2a), the ^{19}F NMR spectrum of 3.2 in $CDCl_3$ shows two singlets' resonances at -126.60 ppm and another singlet slightly at down filed at -108. 81. These ^{19}F NMR spectra appeared along with the ^{125}Te NMR satellite peaks (125.83, 127.36, and 107.98, 109.64 ppm, respectively) (Figure. 3.2b). The existence of the BF^{4-} group in macrocycle 3.2 is shown by a signal in the ^{11}B NMR spectrum measured in CDCl3. This peak is located at -0.9 ppm. The solution ^{125}Te NMR and ^{19}F NMR spectrum of telluronium salt of

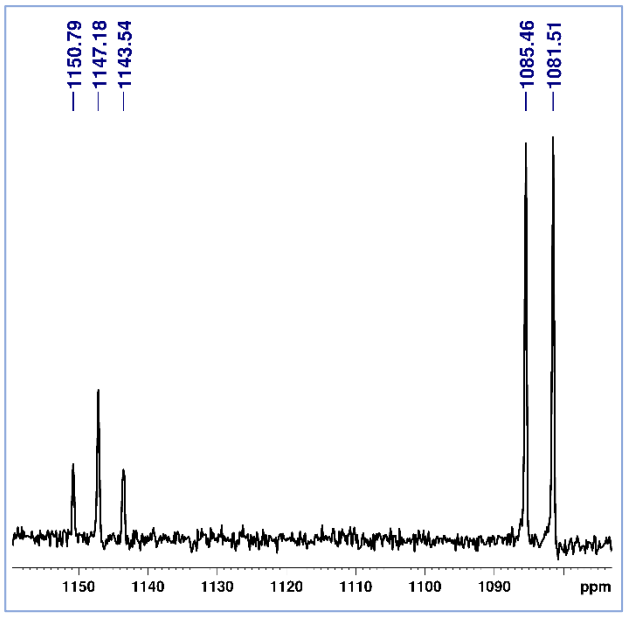

Figure 3.2. Solution of (a). ^{125}Te NMR of 3.2 showing a triplet and doublet, (b). ^{19}F NMR of 3.2 showing two singlets along with satellite peaks, respectively.

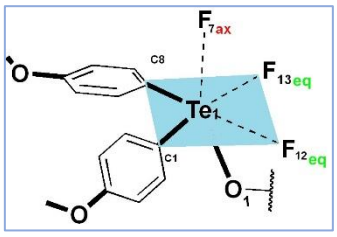

3.4 show resonances at 744.67 and at = -147.63 ppm in CDCl3, respectively (supporting info). In solution, ^{19}F NMR natural abundance of 100 % and nuclear spin quantum number of F is I =1/2 evince ^{19}F NMR spectroscopy highly suitable for observation of formation and stability of the products. The ^{19}F NMR spectrum of 3.2 and 3.4 able to be optimized. In previous reports, strong Lewis's base-like cyclic phosphinates and phenyl selenate act as bridging between two like cyclic phosphinates and phenyl selenate act as bridging between two lewis acidic tetraorgano ditelluroxane units, while in this work, weak bases Bridging ligands (RPO_2^{2-} , SeO_2^{-}> ClO_4^{-} , BF_4^{-}) like ClO_4^{-}, BF_4^{-} are working as bridging ligands

The HRMS study shows a peak corresponding to M^{+} 2 benzene + $3H^{+}$ ion at 1909.00 [$C_{56}H_{56}B_4F_{16}O_{10}Te_4.2C_6H_6$ $3H^{+}$] for 3.2 and M^{+} 3.3 benzene + Na^{+} ion at 2056.83 [$C_{56}H_{56}Cl_4O_{26}Te_4.3$ C_6H_6 Na^{+}] for 3.3. This matches with the simulated HRMS pattern of 3.2 and 3.3. The benzene unit present corresponds to the number of benzene solvent

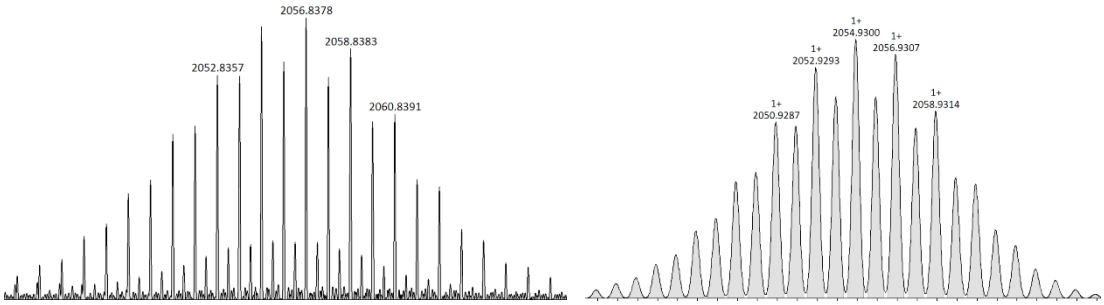

Figure 3.4 Experimental (left) and simulated (right) ESI-MS of 3.3

molecules that crystallized in 3.2 and 3.3, respectively. This suggests structural stability of the macrocycles in solution. Interestingly in both mass spectra, a common mass cluster is 361.00 [(p-MeO-C_6H_4)$_2$TeOH]$^{+}$ is present, and in very low intensity, a peak corresponding to telluronium salt [(p-MeO-C_6H_4)$_3$Te]$^{+}$ (451.05) is observed along with several other mass clusters; most intense mass cluster at 719.00 is assigned to dipositive 12-membered $Te_4O_2B_2F_8$ [$Te_4O_2(BF_4)_2$]$^{+}$ macrocyclic core of 3.2 and 744.99 corresponds to dipositive 12- membered $Te_4O_{10}Cl_2$ [$Te_4O_2(ClO_4)_2$] + macrocyclic core of 3.3. Compounds 3.4 and 3.5 peaks at 451.05, corresponding to

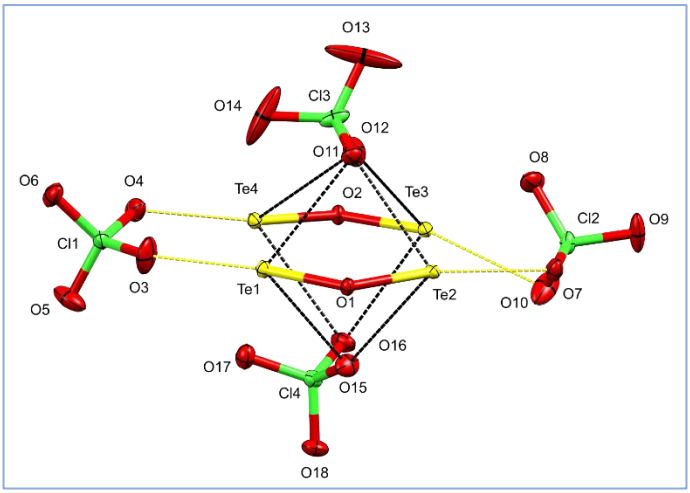

Figure 3.5. (a) solid-state molecular crystal structure of 4, (Left), (b) solid-state molecular crystal structure of 5 (Right), hydrogen atoms are omitted for clarity; Thermal ellipsoids are drawn at 40% probability.

telluronium cations. An interesting observation of the difference between macrocycles and telluronium salts is that they are dissociated in the solution state, unlike the macrocycle, which does not dissociate. A solution of Bis-(p-methoxy phenyl) tellurium dichloride in toluene is stirred at elevated temperature with respective silver salts to form homoleptic telluronium salts, (p-methoxy phenyl Tris) telluronium tetrafluoroborate $(p\text{-}OMeC_6H_4)_3TeBF_4$ (3.4) and Tris (p-methoxy phenyl) telluronium perchlorate $(p\text{-}OMeC_6H_4)_3TeClO_4$ (3.5). The plausible formation of triorganotelluronium salt from a diorganotellurium dihalide starting material has been explained in our earlier report.[18] The distance between Tellurium and weakly coordinating anions Te- --F is 2.96 Å and Te---O 3.05 Å, falling in the reported literature ranges. Single crystal structure analysis X-ray crystal structures of 3.2-3.5 were determined using single-crystal X-ray analysis. The selected bond length and bond angles are presented in the spectroscopic and analytical part. The compounds 3.2 and 3.3 crystallize in the monoclinic space group *P 1 21/c1*, and telluronium salts 3.4 and 3.5 crystalize in triclinic *P-1*. 2 and 3.3 are isostructural and contain two bis tetraorganotelluroxane dicationic units; also, it has 3.4 BF_4^- anions and 3.4 ClO_4^- anions for 3.2 and 3.3 respectively. The anions are connected via Te-$\mu_2BF_4^-$Te (3.2), Te-$\mu_2ClO_4^-$Te (3.3) bridging, and through secondary Te- --F (3.2), Te---O (3.3) interactions, the distance is 2.60 and 2.63. The mean angles Te-O-Te of 3.2 and 3.3 are 125.3(1)° and 122.4(1)° respectively. the F-Te-O of 2 and O-Te-O of 3 angles are 173° and 169°., respectively. Each of the four counterions

interacts with Te atoms of the paired dicationic telluraxane through their fluorine atom (3.2) in the range of 2.607, 2.636, and 3.018 Å and an oxygen atom (3.3) 2.637, 2.657 to 3.335 Å considerable amount shorter than the total of the Vander Waals radii, which is (Te and F vdw (Te—F) = 3.45 Å) and (Te and O vdw (Te—O) = 3.60 Å) respectively. Interestingly of the four Te…F secondary interactions present in macrocycle 3.1, three (Te---F) of those are shorter than the recently reported molecules.[14] The coordination environment around tellurium atoms in the (3.1) and (3.2) is a distorted pseudo-octahedral by taking into secondary interactions with fluoride (3.1) and oxygen (3.2).

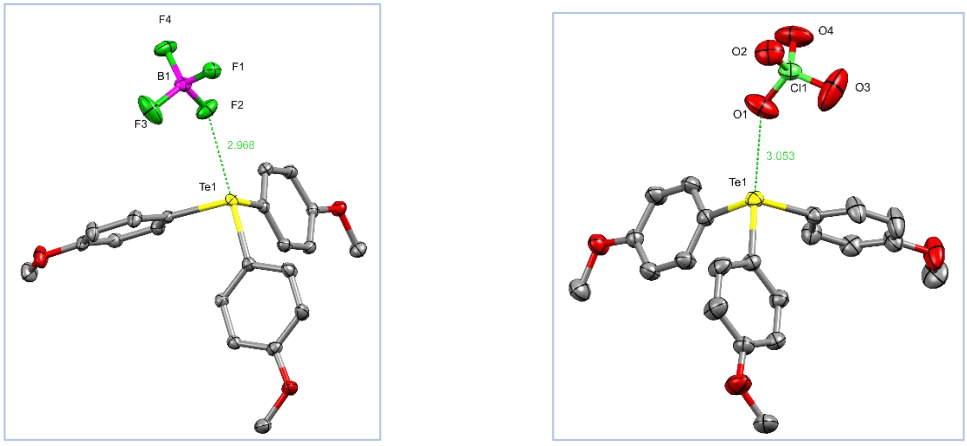

3.6. solid-state molecular crystal structure of 3.3, Te shows interactions with O atoms. Anisyl group attached to Te and hydrogen atoms and benzene solvates are omitted for clarity; thermal ellipsoids are drawn at 40 ٪ probability.

In comparison, Pseudo trigonal pyramid geometry is present around the Tellurium atom in telluronium salts (3.3) and (3.4). It is important to note that though in Scheme 1 the macrocycle is prepared in benzene and the telluronium salt in toluene, we did observe that both the products formed in two solvents but predominately in benzene 12-membered macrocycle was isolated. In toluene, triorganotelluronium salt was obtained. The oxidation state of the tellurium atoms in the compounds has been calculated using bond valence sum (BVS) calculations.

3.4 Electrocatalytic hydrogen evolution by macrocycle 3.2

Homogeneous cyclic voltammogram (CV) experiments were carried out using macrocycle 3.2 (as a representative example) in the three-electrode system furnished using a glassy carbon (GC) working electrode (= 3 mm) and a platinum wire auxiliary electrode, and an Ag/AgCl (3 M) as a reference electrode under nitrogen environment at ambient temperature. Tetra butyl ammonium perchlorate (TBAP) containing acetonitrile solution (100 mM) was employed as a supporting electrolyte and used to prepare a 1 mM concentration of macrocycle 3.2 solutions for a homogeneous electrocatalytic hydrogen evolution reaction (HER). 100 mV/s scan rate was used to carry out the CV experiments, and all the potential was reported here with respect to the Ag/AgCl. The para-toluene sulfonic acid (TsOH) was employed as a proton source for catalytic HER. (Figure. 3.7) evidences the tellurium-based redox as well as catalytic HER activity. The CV of macrocycle 3.2 (without TsOH addition) has shown an electrochemical redox response around -1.15 V vs Ag/AgCl of perhaps assigned to the tellurium, and the electrochemically reduced tellurium further reduces the proton

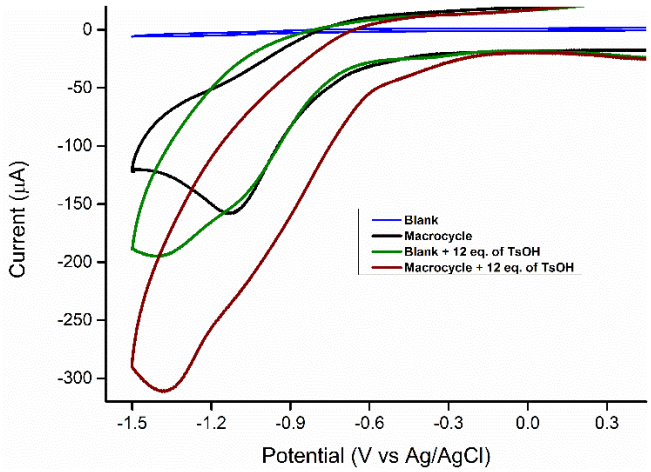

Figure 3.7 Cyclic voltammogram of **Blank** (blue)**, macrocycle 3.2** (black), blank with 12 eq. equivalents of para-Toluene sulfonic acid as a proton source, and Macrocycle 3.2 with 12 eq. of TsOH. Electrocatalytic conditions 1 mM of the 3.2 in acetonitrile in the presence of 100 mM TBAP as supporting electrolyte at a scan rate of 100 mV s^{-} in an inert atmosphere using a three-electrode configuration.

into molecular hydrogen. It is noteworthy to mention that, upon gradual addition of TsOH into the electrochemical cell shown, the enhancement in the cathodic current confirms the catalytic HER along with 170 mV anodic shift in HER onset potential under operation conditions.

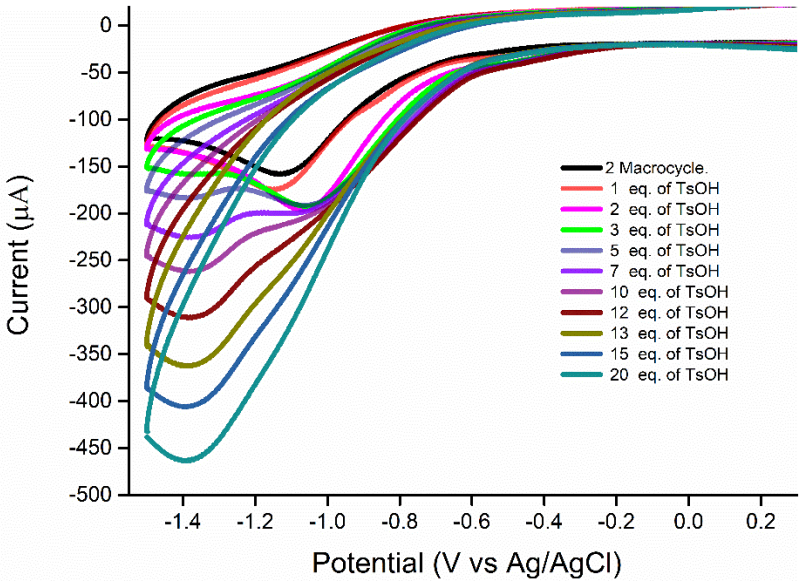

Figure. 3.8 Cyclic voltammogram of macrocycle 3.2 (block), and in the presence of 1 to 20 equivalents of para-toluene sulfonic acid as a proton source. Electrocatalytic conditions 1 mM of the macrocycle 3.2 in acetonitrile in the presence of 100 mM TBAP as supporting electrolyte, CV collected with a scan rate of 100 mV/s in an inert atmosphere using a three-electrode configuration.

bulk electrolysis experiments were conducted in homogeneous and heterogeneous ways. Both methods demonstrate that macrocycle **3.2** was able to catalyze proton reduction. The experiments were carried out in a homemade three-electrode system. Carbon paper as a working and auxiliary electrode, a silver/ silver chloride (Ag/AgCl) (3 M) as a reference electrode under argon environment purging for 30 minutes at ambient temperature. Tetra butyl ammonium perchlorate (TBAP) containing acetonitrile solution (100 mM) was employed as a supporting electrolyte and used to prepare a 1 mM concentration of macrocycle **3.2** solutions with a proton source. The linear sweep voltammetry was recorded by sweeping the potential between 0 and -1 V vs Ag/Ag^{+} at a scan rate of 10 mV/s (Figure 1a). The increase in current was observed immediately after the start of the potential scan indicating the reduction of the proton. Two broad peaks (Pre-waves) appeared before -1 V indicating the possibility of two

reductions during the scan. On the other hand, a broad reduction wave was observed while the potential was swept in the same potential window in the absence of a proton source for the macrocycle **3.2**. With this information in hand, we propose the mechanism of proton reduction in (Scheme 3.2)

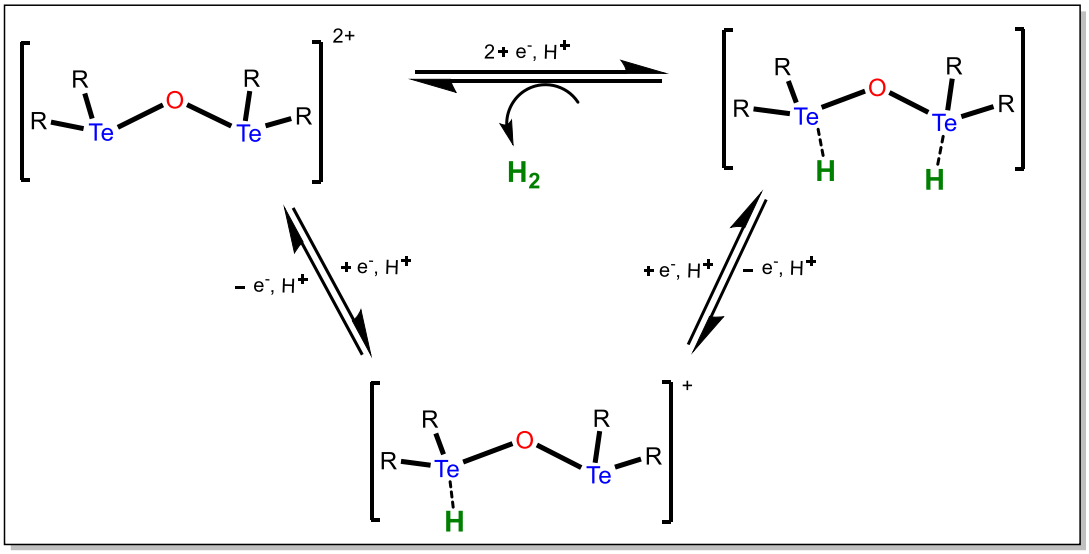

Scheme 3.2: Proton reduction reaction mechanism of macrocycle 3.2

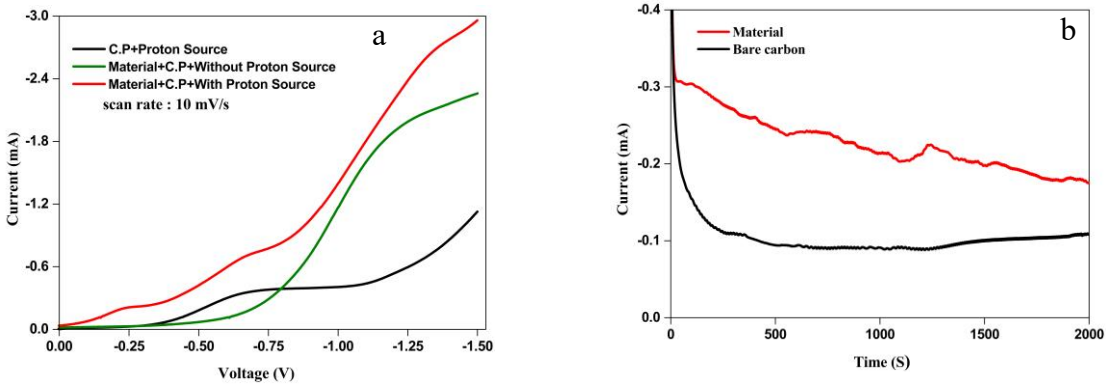

Figure 3.9: (a) Linear sweep voltammetry of solution comprising tellurium complex, *p*-toluene sulfonic acid, and electrolyte in acetonitrile. (b) Chronoamperometry profile of the same solution while holding the potential at -0.68 V vs Ag/Ag^{+}.

The potential required to attain a current density of 0.5 mA is 0.55 V in the case of macrocycle **3.2**. However, the current did not reach 0.5 mA while using bare carbon paper (C.P) as an electrode. This indicates the electrocatalytic behavior of the macrocycle **3.2**. We carried out chronoamperometry using the homemade electrochemical setup. The applied potential was -0.68 V, which is the potential of the second reduction wave. The experiment was carried out for 2000 s (Figure 3.8b). The hydrogen gas generated during the electrochemical reaction was quantified using gas chromatography and found to be 0.01 µL. the details about heterogeneous method analysis details given in supporting information.

3.5 Conclusions

In this chapter, we have demonstrated that an organotelluroxane macrocycle acting as active site ([(*p*-$OMeC_6H_4)_2Te(\mu$-O)]) towards HER activity. The compound [{(*p*-$OMeC_6H_4)_2Te\}_2(\mu$-O)(µ-BF_4)(µ-BF_4)]$_2$ **(3.2)** is the first organotellurium containing catalyst for electrochemical hydrogen evolution. Plausible mechanism has been proposed for proton reduction based on the Linear Sweep Voltammetry (LSV) plots which shows two pre-waves corresponding to two successive reductions. Various techniques including CV, LSV, bulk electrolysis have been employed *in the* hydrogen evolution process.

Analytical and Spectroscopic data

Section – 1: Crystallographic information of compounds 3.2-3.5

	$C_{56}H_{56}B_4F_{16}O_{10}Te_4$	$C_{56}H_{56}Cl_4O_{26}Te_4$	$C_{21}H_{21}BF_4O_3Te$	$C_{21}H_{21}ClO_7Te$
F.wt g/mol^{-1}	1942.92	1992.47	535.79	548.43
T, K	100.0(2)	100.0(2)	106(9)	285
Crystal system	Monoclinic	Monoclinic	Triclinic	Triclinic
Space group	*P 1 21/c 1*	*P 1 21/c 1*	*P -1*	*P -1*
Crystal size mm^3	0.32 × 0.25 × 0.16	0.1 × 0.08 × 0.08	0.8 × 0.12 ×0.1	0.09 × 0.08 × 0.06
a, Å	17.0516(2)	17.1420(1)	10.2455(2)	10.3196(4)
b, Å	17.0082(3)	17.2042(1)	10.5162(2)	10.7682(5)
c, Å	26.0697(4)	26.0805(2)	10.9829(2)	11.1672(5)
α, deg	90	90	110.245(2)	111.398(1)
β, deg	97.065(1)	97.419(1)	97.955(1)	96.827(1)
γ, deg	90	90	104.283(1)	104.125(1)
V, $Å^3$	7503.2(2)	7627.13(9)	1042.82(4)	1090.36(8)
Z	4	4	2	2
D_{calcd} Mg/m^3	1.720	1.735	1.706	1.670
μ, mm^{-1}	1.635	1.734	1.482	1.526
F(000)	3800.0	3924.0	528.0	544.0
Theta range, deg	3.72 to 49.998	3.94 to 53.874	4.078 to 53.924	5.878 to 61.102
Index ranges	$-20 \le h \le 20$ $-20 \le k \le 20$ $-30 \le l \le 30$	$-21 \le h \le 21$ $-21 \le k \le 21$ $-32 \le l \le 32$	$-13 \le h \le 13$ $-13 \le k \le 13$ $-13 \le l \le 13$	$-14 \le h \le 14$ $-15 \le k \le 15$ $-15 \le l \le 15$
Total reflns	67629	80531	15561	58169
Ind. reflns / R(int)	13201/0.0817	15871/0.0230	4326/0.0318	6644/0.0298
Data/restraints/ parameters	13201/0/954	15871/0/954	4326/0/274	6644/0/274

Completeness to θ_{max}, %	100	96.1	95.4	99.6
GooF(F^2)	1.039	1.141	1.051	1.043
R_1/wR_2 [I>2σ(I)]	R_1 = 0.0594, wR_2 = 0.1427	R_1 = 0.0246, wR_2 = 0.0521	R_1 = 0.0267, wR_2 = 0.0597	R_1 = 0.0223, wR_2 = 0.0550
R_1/wR_2 [all data]	R_1 = 0.0741, wR_2 = 0.1499	R_1 = 0.0266, wR_2 = 0.0528	R_1 = 0.0294, wR_2 = 0.0610	R_1 = 0.0281, wR_2 = 0.0574
Largest diff peak/hole, e.Å^{-3}	3.36/-1.45	1.28/-1.02	1.30/-0.72	0.44/-0.51

Table S1. Crystallographic information of compounds 3.2-3.5.

Section – 2: ORTEP diagram of compound 3.2

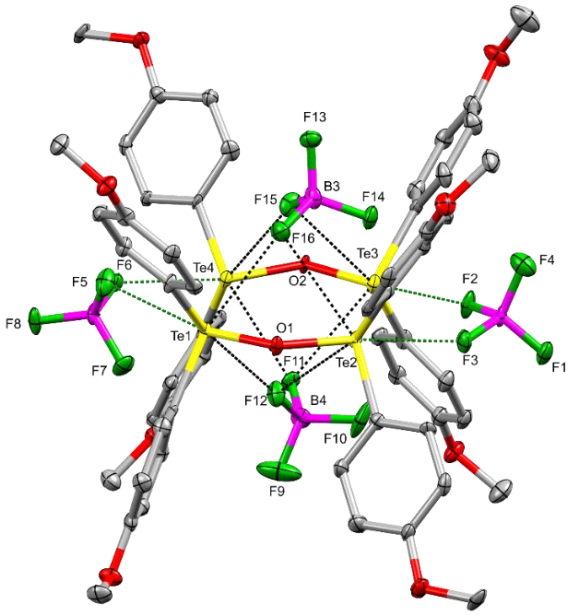

Figure S1. ORTEP diagram of **3.2**. The thermal ellipsoids are shown at a 40% probability level. Solvent molecule and all hydrogen atoms were omitted for clarity.

Section – 3: Te-F (BF_4) interaction distances of compound 3.2

Table S2. Bridging anion Interaction with Tellurium [Å].

Te(1)-F(5)	3.018
Te(2)-F(3)	2.636
Te(3)-F(2)	2.607
Te(4)-F(6)	2.623

Table S3. Capping anion Interaction with Tellurium [Å].

Te(1)-F(12)	2.800
Te(1)-F(16)	2.891
Te(2)-F(12)	2.937
Te(2)-F(16)	2.937
Te(3)-F(15)	3.079
Te(3)-F(11)	2.943
Te(4)-F(11)	2.840
Te(4)-F(15)	3.028

Section – 4: Bond lengths and bond angles for compound 3.2

Table S4. Selected bond lengths [Å] and angles [°] for **3.2**

Te(1)-O(1)	1.942(4)
Te(2)-O(1)	1.961(4)
Te(3)-O(2)	1.958(4)
Te(4)-O(2)	1.947(4)
Te(1)-O(1)-Te(2)	125.2(2)
Te(3)-O(2)-Te(4)	122.2(2)

ESI mass spectral analysis of compound 3.2

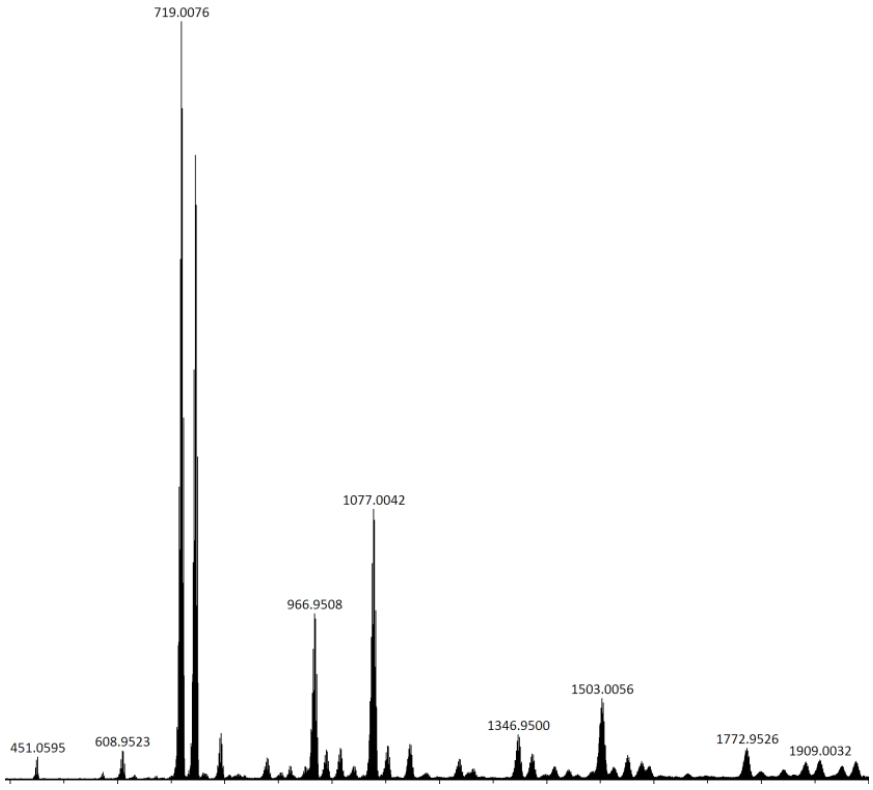

Section – 6: ^{125}Te, ^{19}F, ^{11}B, ^{1}H, ^{13}C NMR spectral analysis of compound

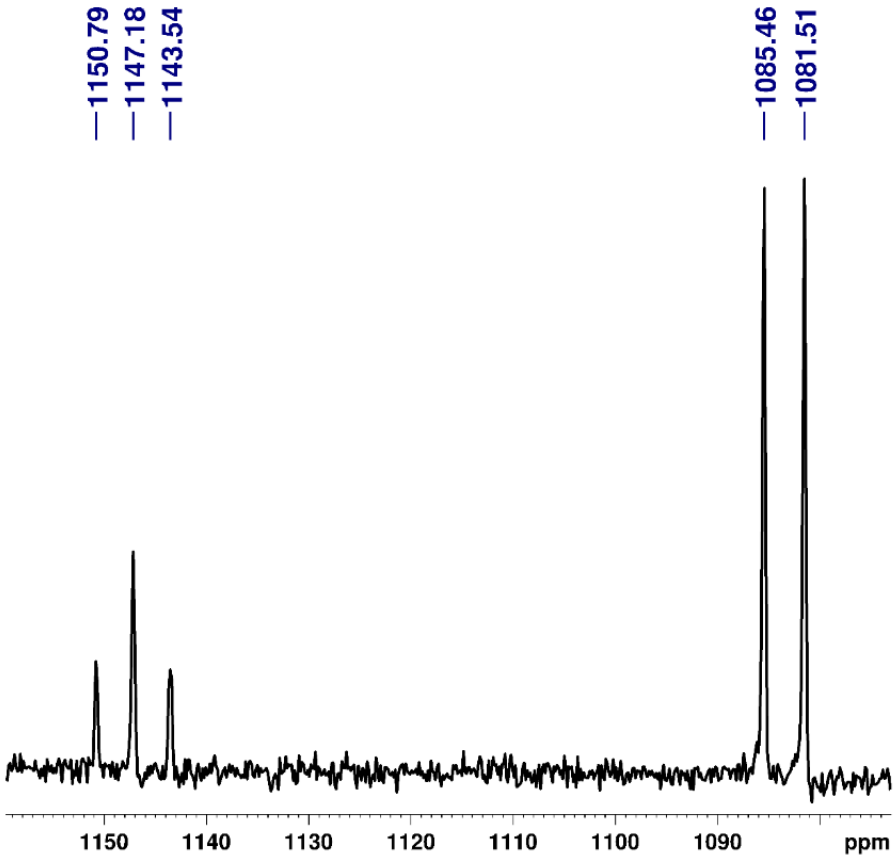

Figure S3. ^{125}Te NMR spectrum of **3.2** in $CDCl_3$ at room temperature.

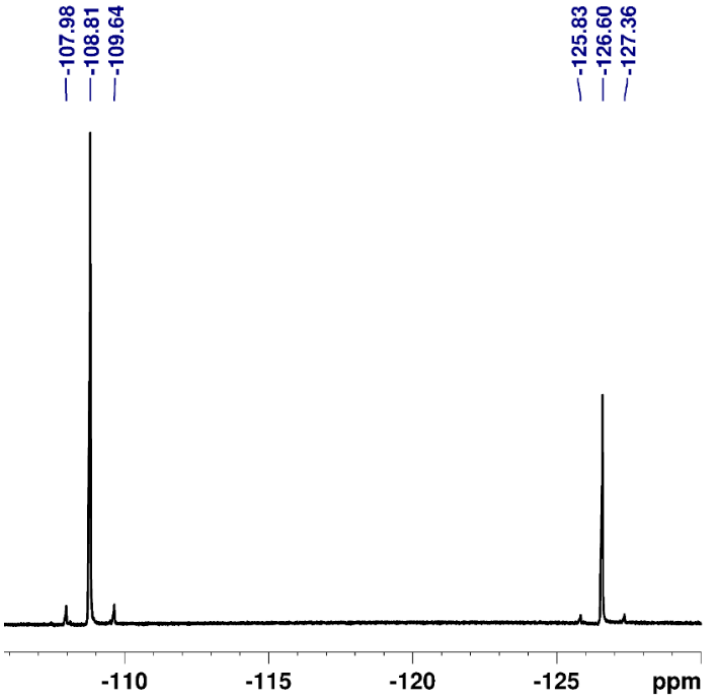

Figure S4. ^{19}F NMR spectrum of **3.2** in $CDCl_3$ at room temperature.

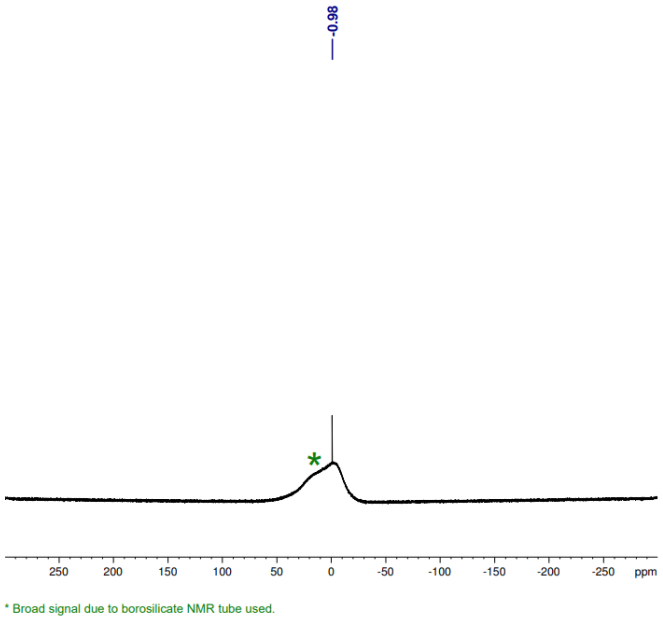

Figure S5. ^{11}B NMR spectrum of **3.2** in $CDCl_3$ at room temperature.

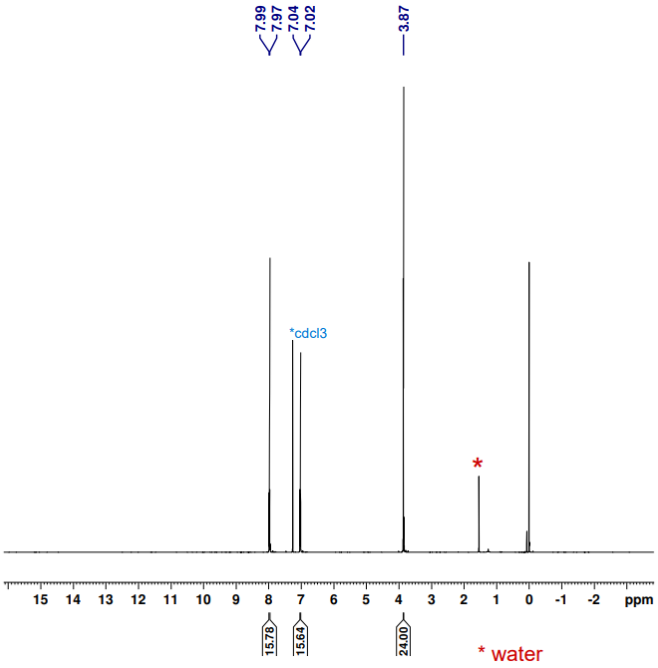

Figure S6. ^{1}H NMR spectrum of **3.2** in $CDCl_3$ at room temperature.

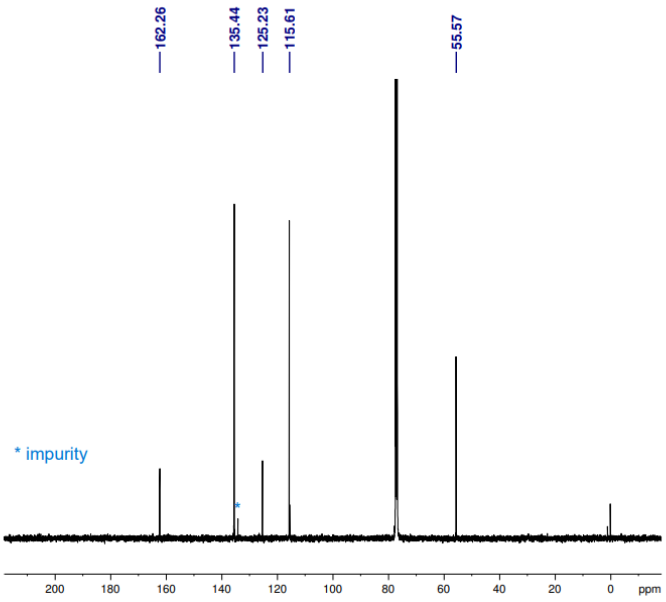

Figure S7. ^{13}C NMR spectrum of **3.2** in $CDCl_3$ at room temperature.

Section – 7: FT-IR spectral analysis of compound 3.2

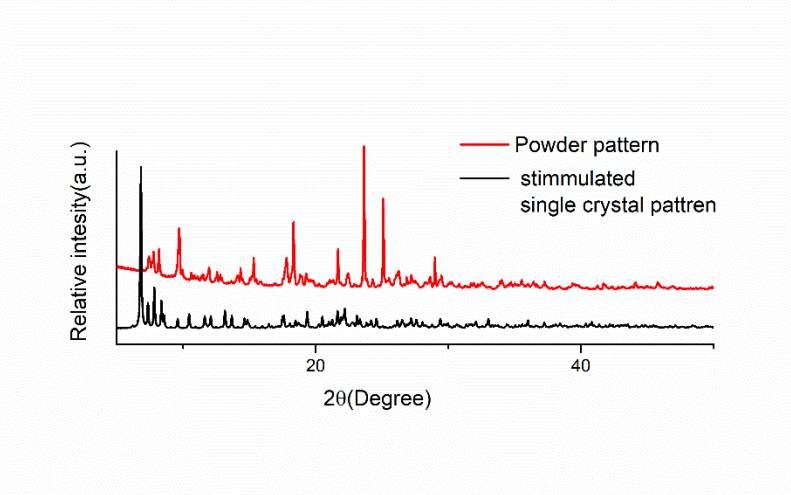

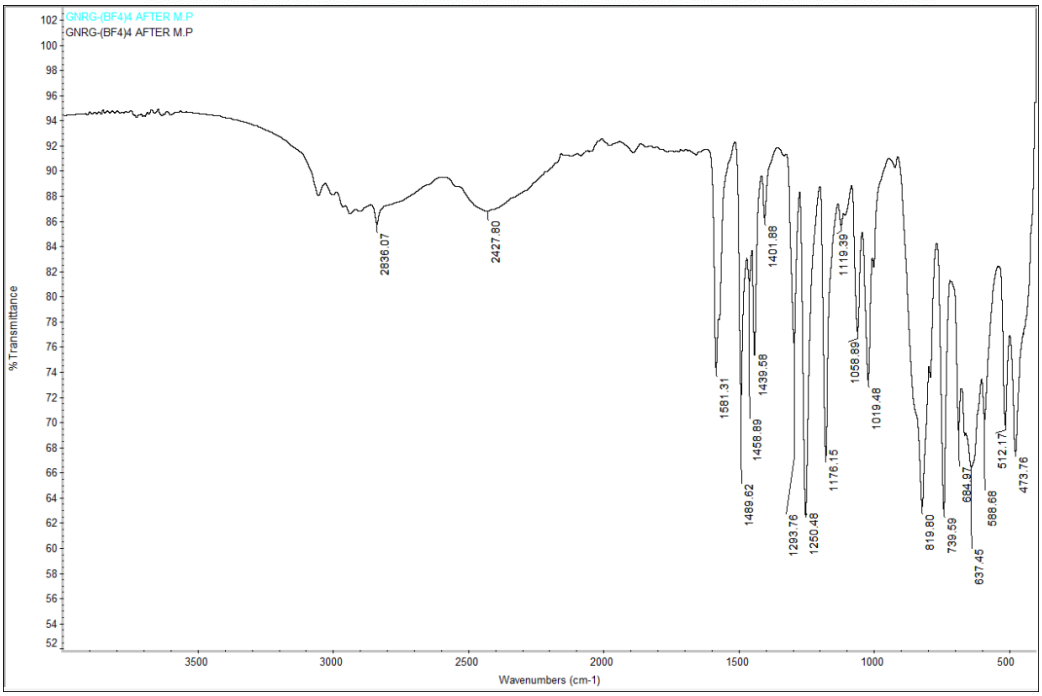

Figure S8. FT-IR spectrum of 3.2

Section – 8: ORTEP diagram of compound 3.3

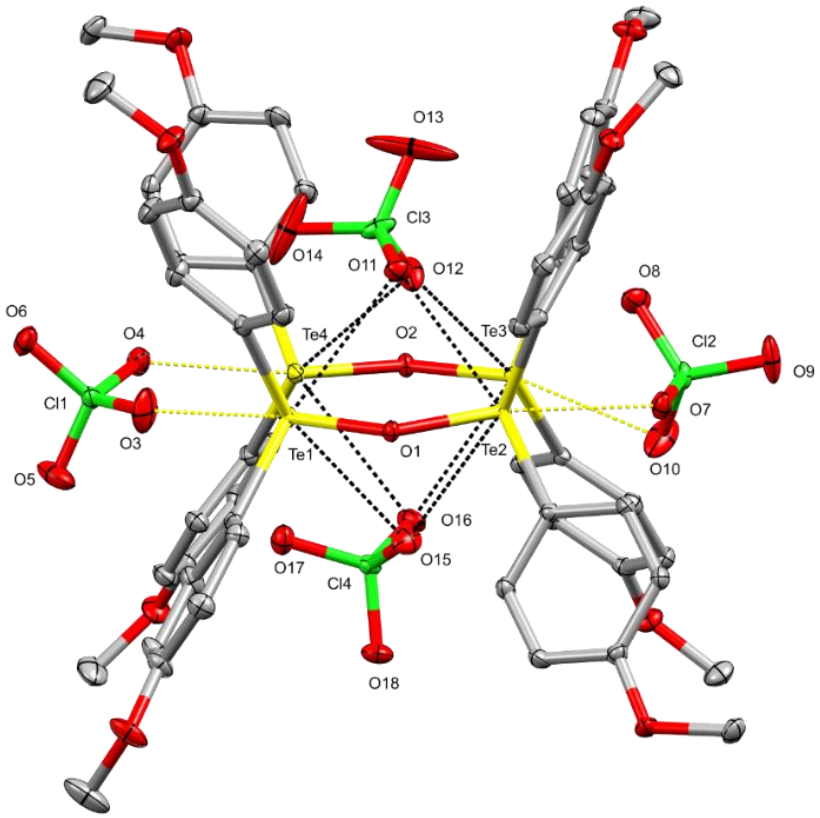

Figure S9. ORTEP diagram of **3.3** The thermal ellipsoids are shown at a 40% probability level. Solvent molecule and all hydrogen atoms were omitted for clarity.

Section – 9: Te-O (perchlorate) interaction distances of compound 3.3

Table S5. Bridging anion (perchlorate) Interaction with Tellurium [Å].

Te(1)-O(3)	2.658
Te(2)-O(7)	2.636
Te(3)-O(11)	3.084
Te(4)-O(4)	2.685
Te(1)-O(3)	2.658

Table S6. Capping anion (perchlorate) Interaction with Tellurium [Å].

Te(1)-O(11)	2.963
Te(1)-O(15)	3.099
Te(2)-O(11)	2.885
Te(2)-O(15)	3.085
Te(3)-O(12)	2.841
Te(3)-O(16)	2.911
Te(4)-O(12)	2.955
Te(4)-O(16)	3.081

Section – 10: Bond lengths and bond angles of compound 3.3

Table S7. Selected bond lengths [Å] and angles [°] for **3.3**

Te(1)-O(1)	1.9487(18)
Te(2)-O(1)	1.9602(17)
Te(3)-O(2)	1.9434(18)
Te(4)-O(2)	1.9677(17)
Te(1)-O(1)-Te(2)	122.01(9)
Te(3)-O(2)-Te(4)	124.77(9)
Te(2)-O(1)	1.9602(17)
Te(3)-O(2)	1.9434(18)

Section – 11: ESI mass spectral analysis of compound 3.3

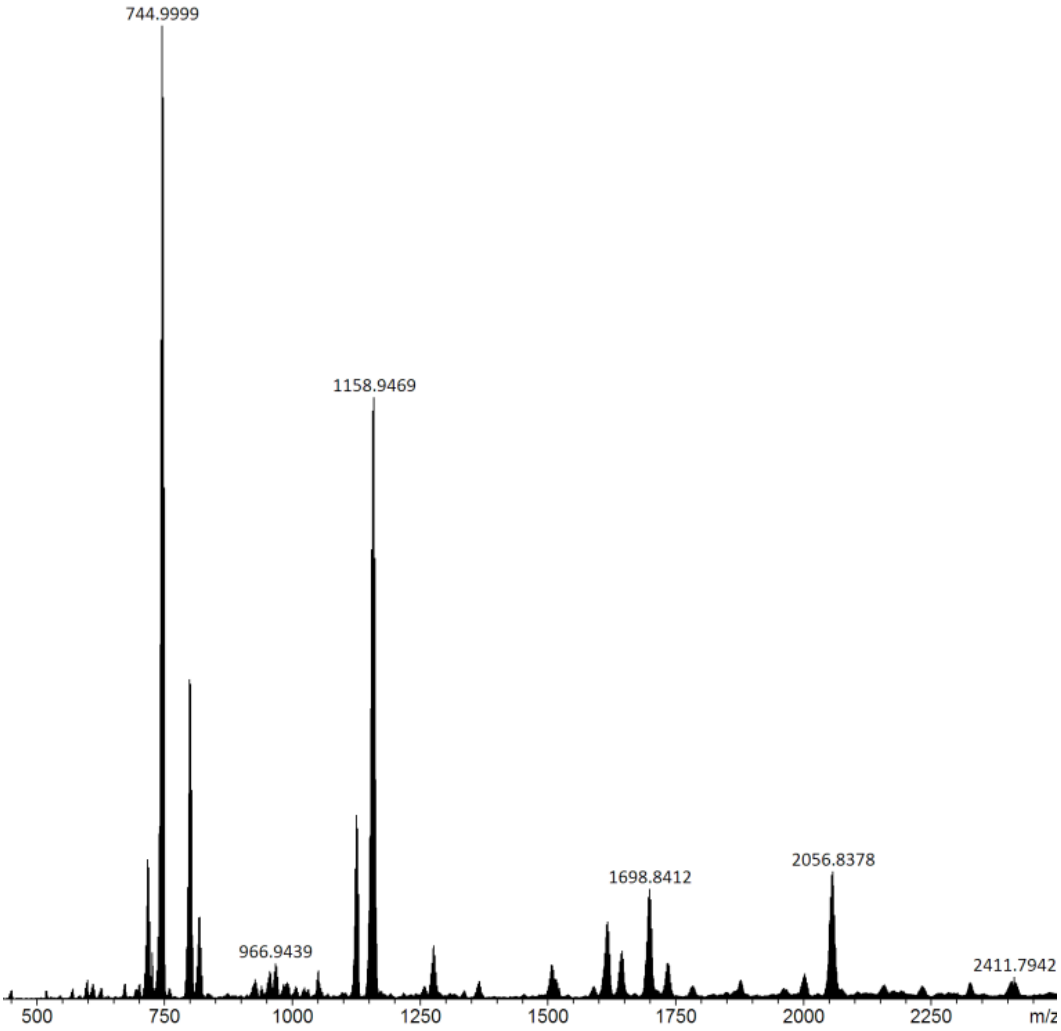

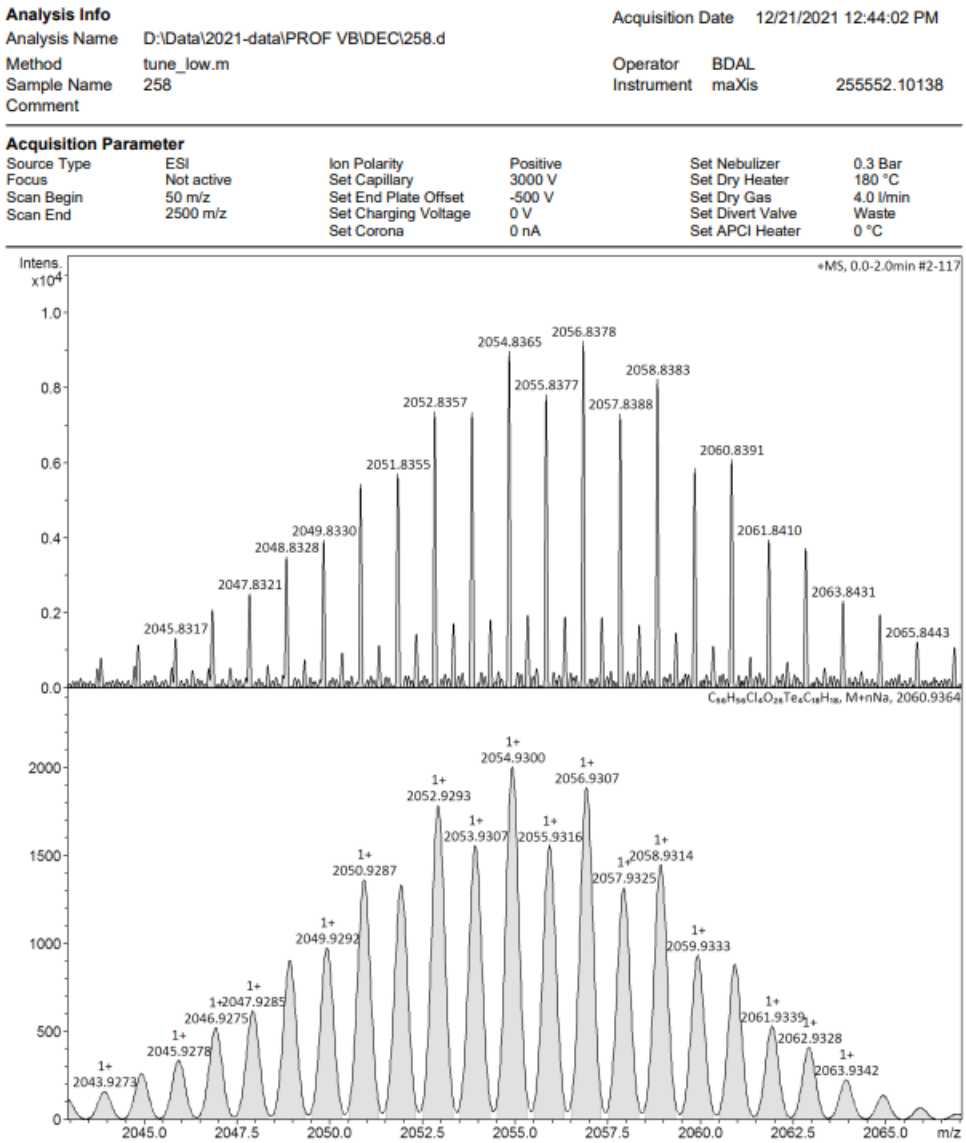

Figure S11. ESI mass spectra of **3.3** experimental above and simulated below

Section – 12: ^{1}H, ^{13}C NMR spectral analysis of compound 3

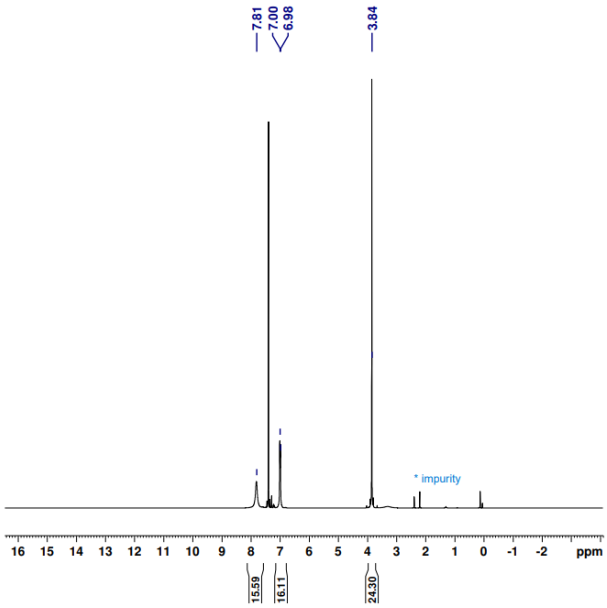

Figure S12. ^{1}H NMR spectrum of **3.3** in $CDCl_3$ at room temperature.

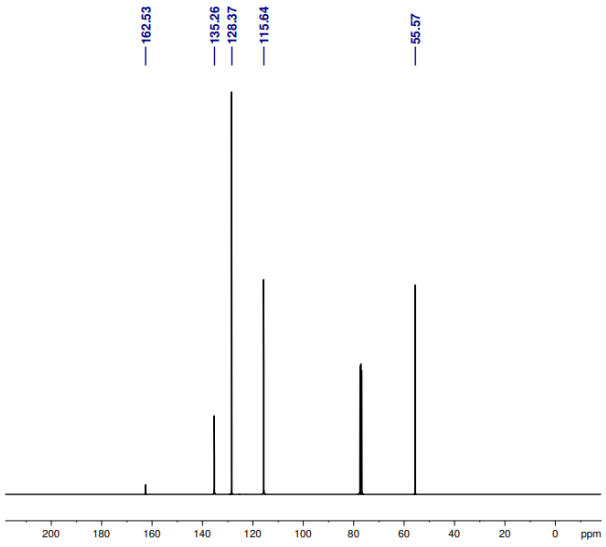

Figure S13. ^{13}C NMR spectrum of **3.3** in $CDCl_3$ at room temperature.

Section – 13: FT-IR spectral analysis of compound 3

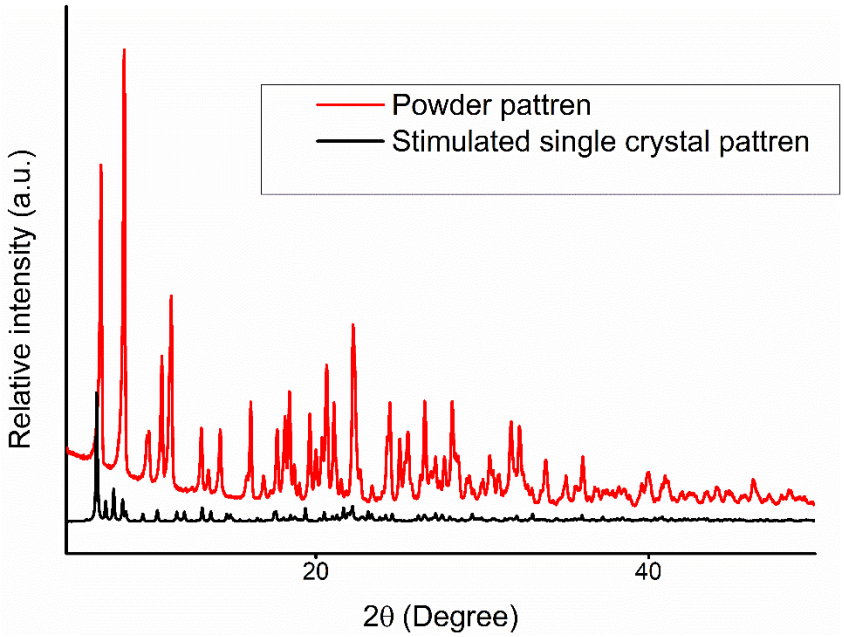

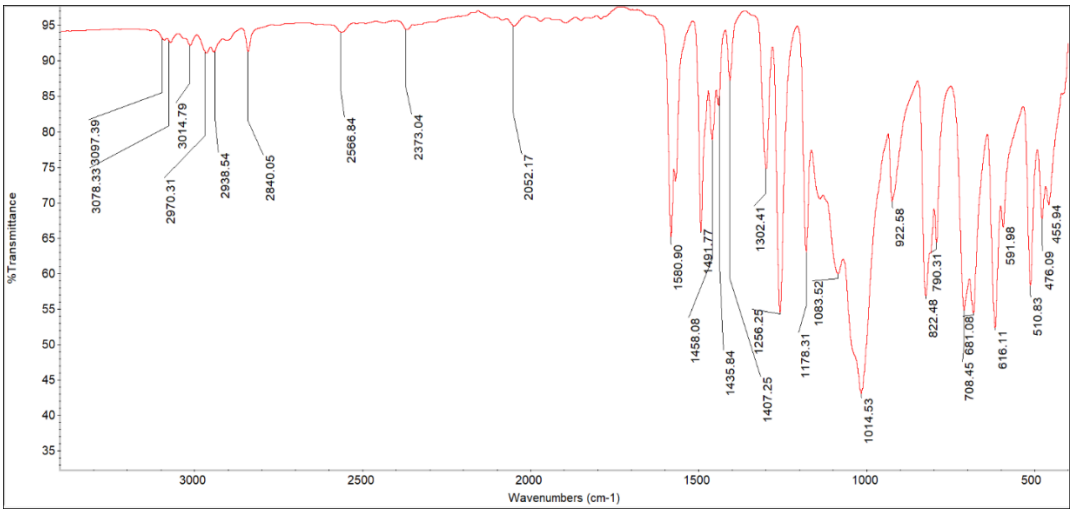

Figure S14. FT-IR spectrum of compound **3.3**

Section – 14: ORTEP diagram of compound 3.4

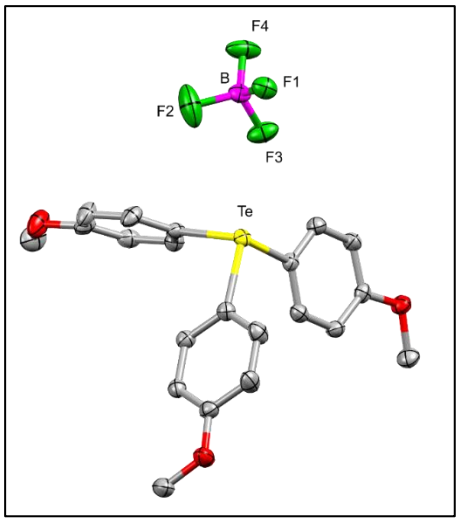

Figure S15. ORTEP diagram of **3.4** The thermal ellipsoids are shown at a 40% probability level. All hydrogen atoms omitted for clarity.

Section – 15: Te-F (BF_4) interaction distances, bond lengths and bond angles of compound 3.4

Table S8. Interaction [Å], Bond lengths [Å] and angles [°] for **3.4**

Te(1)--F(1))	3.031
Te(1)-C(1))	2.100(3)
Te(1)-C(8))	2.101(3)
Te(1)-C(15))	2.117(3)
C(1)-Te(1)-C(8)	95.31(10)
C(1)-Te(1)-C(15)	97.45(10)
C(8)-Te(1)-C(15)	94.95(10)

Section – 16: ESI mass spectral analysis of compound 3.4

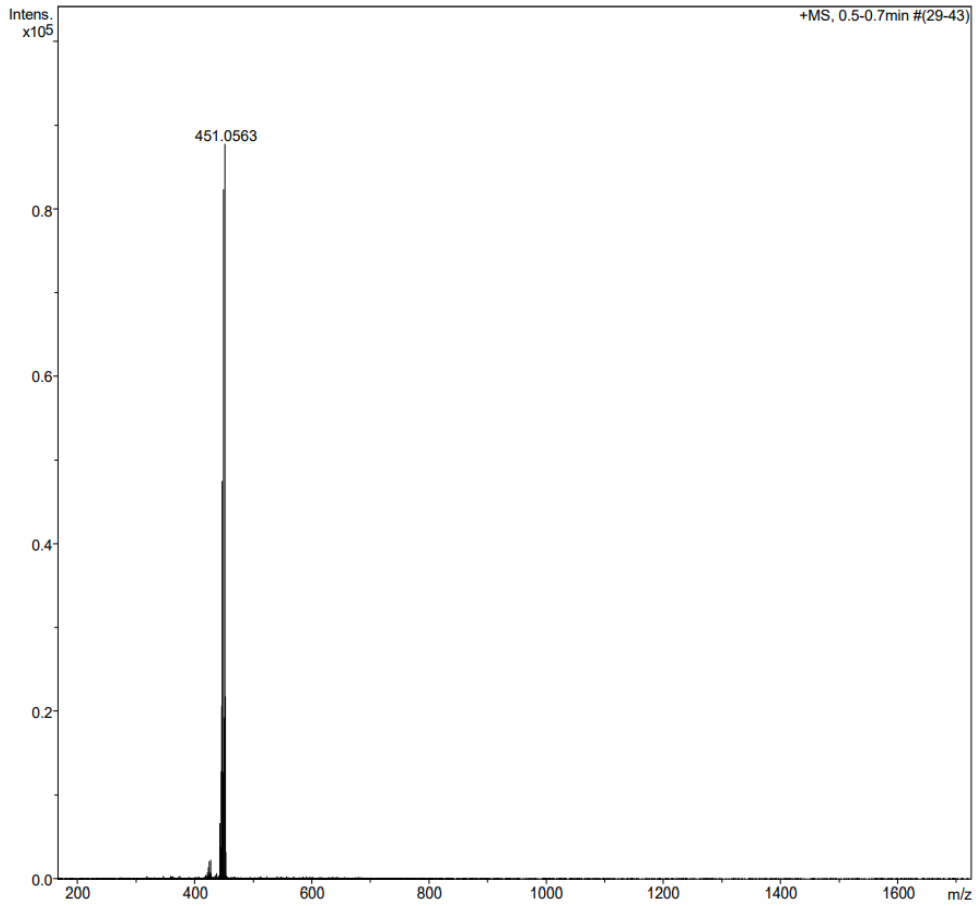

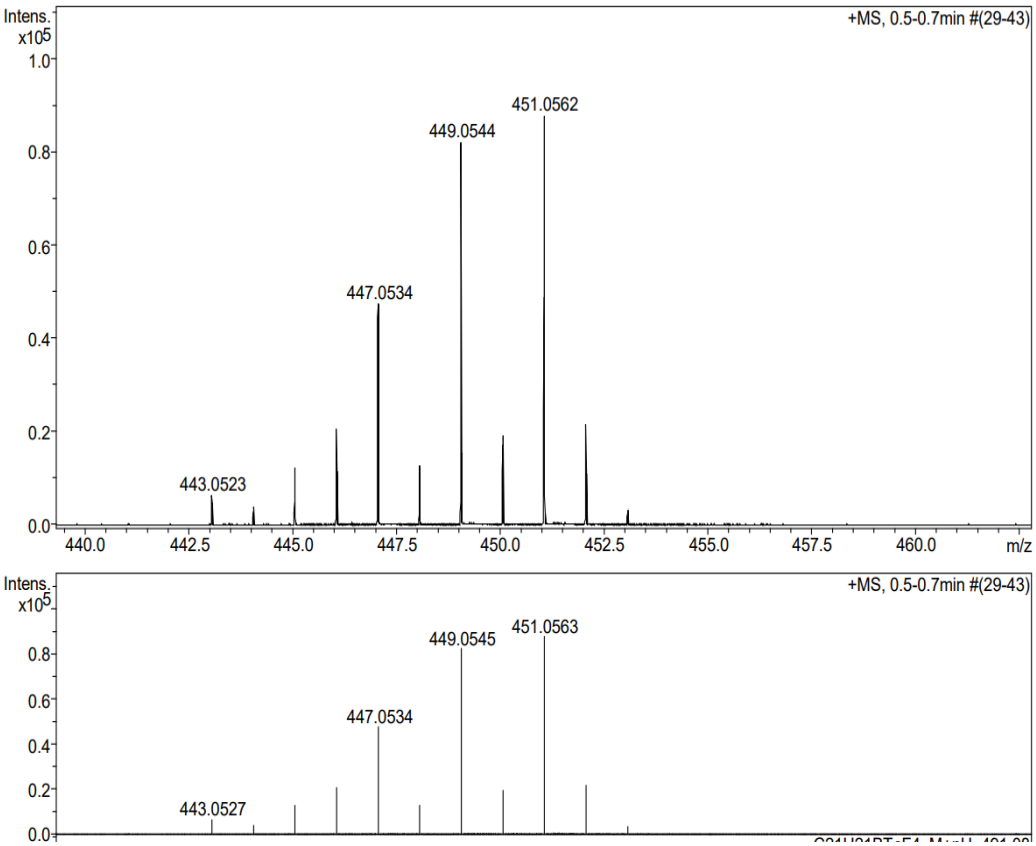

Figure S16. ESI mass spectra of **3.4** (experimental)

Section – 17: ^{125}Te ^{19}F, ^{11}B, ^{1}H, ^{13}C NMR spectral analysis of compound

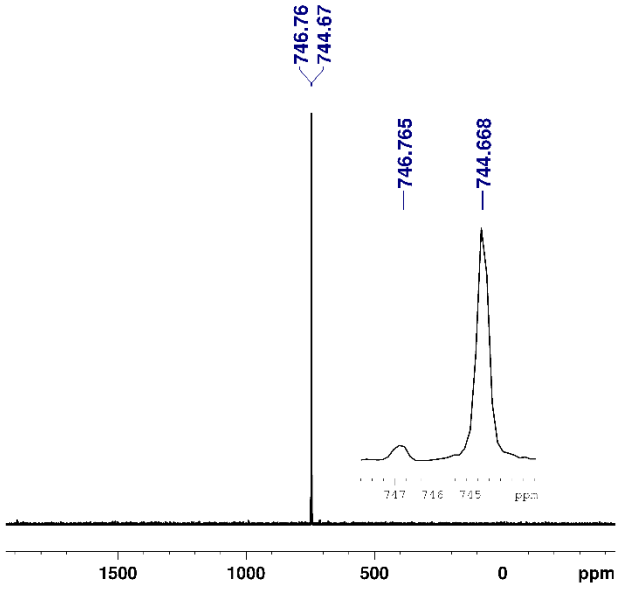

Figure S18. ^{125}Te NMR spectrum of **3.4** in $CDCl_3$ at room temperature.

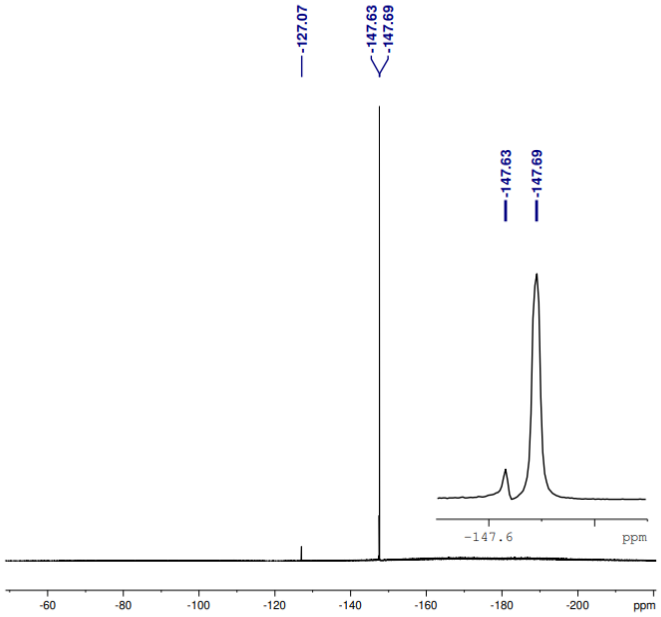

Figure S19. ^{19}F NMR spectrum of **3.4** in $CDCl_3$ at room temperature.

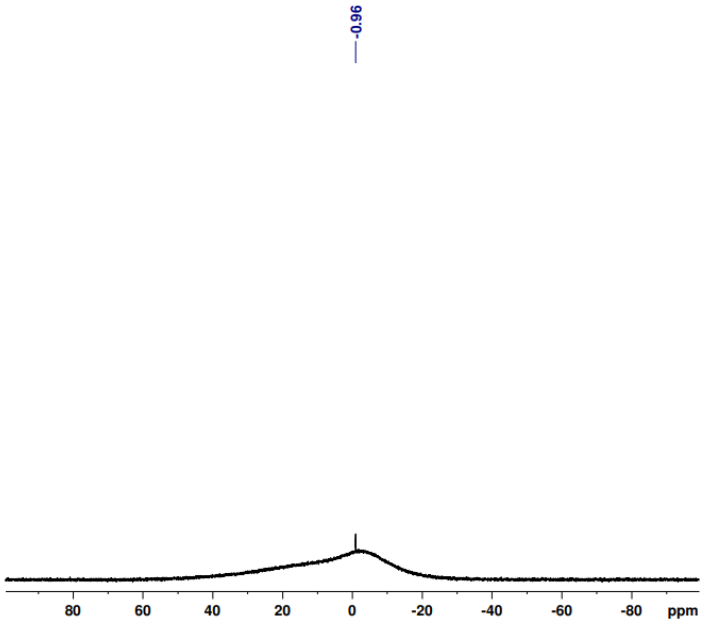

Figure S20. ^{11}B NMR spectrum of **3.4** in $CDCl_3$ at room temperature.

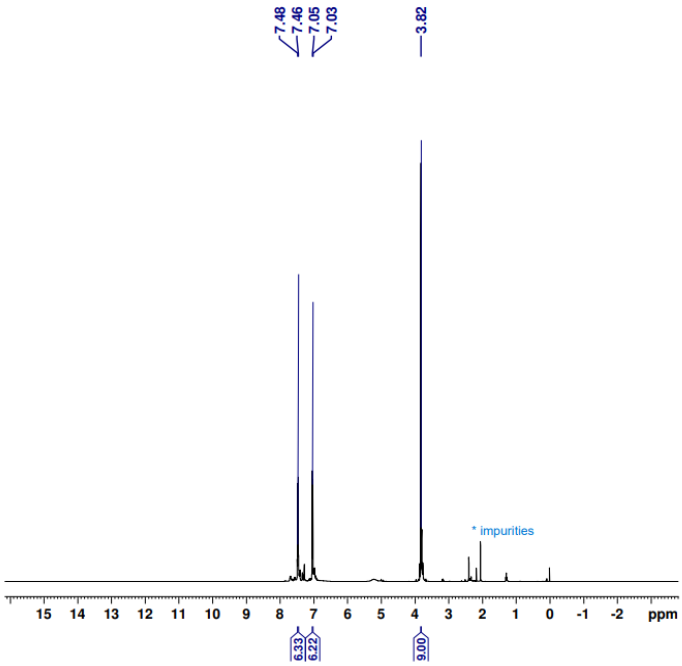

Figure S21. ^{1}H NMR spectrum of **3.4** in $CDCl_3$ at room temperature.

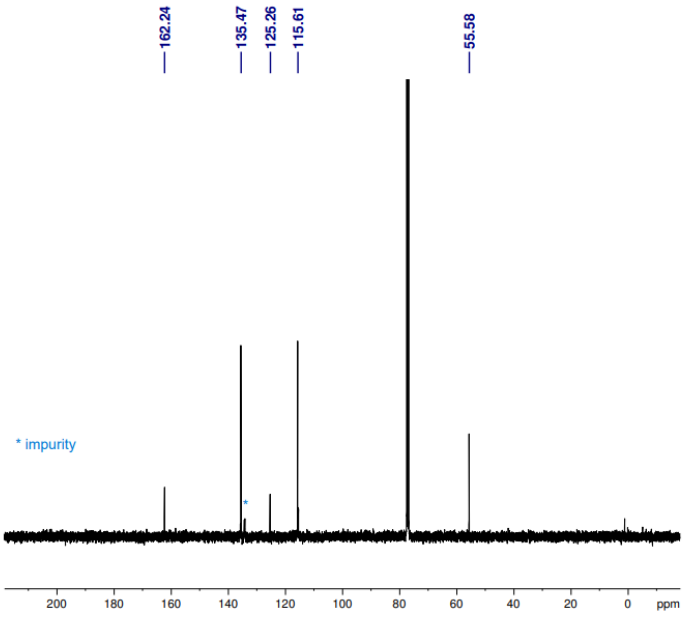

Figure S22. ^{13}C NMR spectrum of **3.4** in $CDCl_3$ at room temperature.

Section – 18: FT-IR spectral analysis of compound 3.4

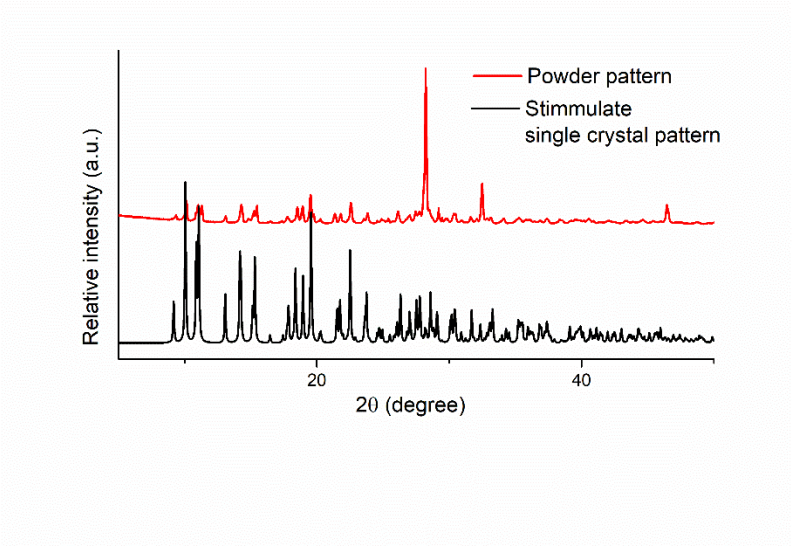

figureS23: PXRD data of compound 3.4

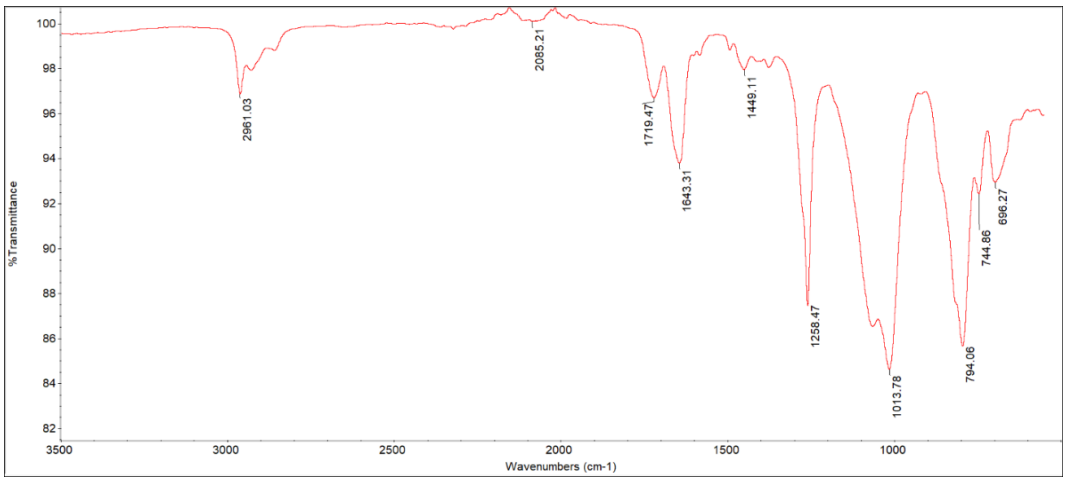

Figure S23a. IR spectrum of compound **3.4**

Section – 19: ORTEP diagram of compound 3.5

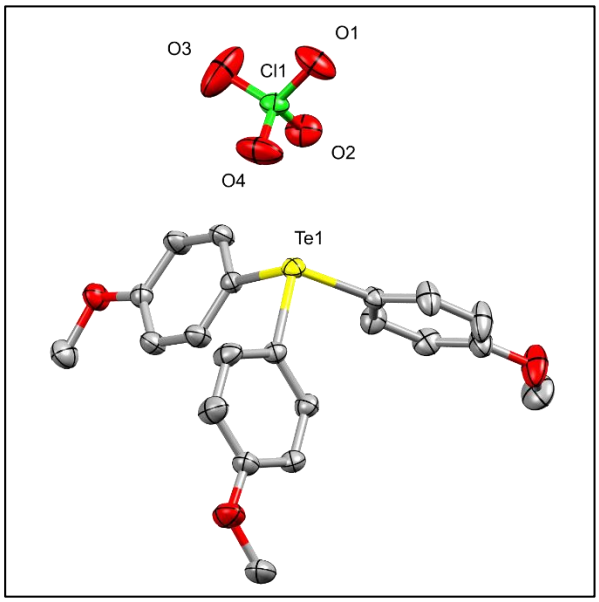

Figure S24. ORTEP diagram of **3.5** The thermal ellipsoids are shown at a 40% probability level. All hydrogen atoms omitted for clarity.

Section – 20: Te-O (perchlorate) interaction distances, bond lengths and bond angles of compound 3.5

Table S9. Interactions [Å], selected bond lengths [Å] and angles [°] for **3.5**

Te(1)--O(2)	3.164
Te(1)-C(7)	2.1025(16)
Te(1)-C(1)	2.1034(16)
Te(1)-C(15)	2.1186(16)
C(7)-Te(1)-C(1)	95.61(6)
C(7)-Te(1)-C(15)	95.20(6)
C(1)-Te(1)-C(15)	97.47(6)

Section – 21: ESI mass spectral analysis of compound 3.5

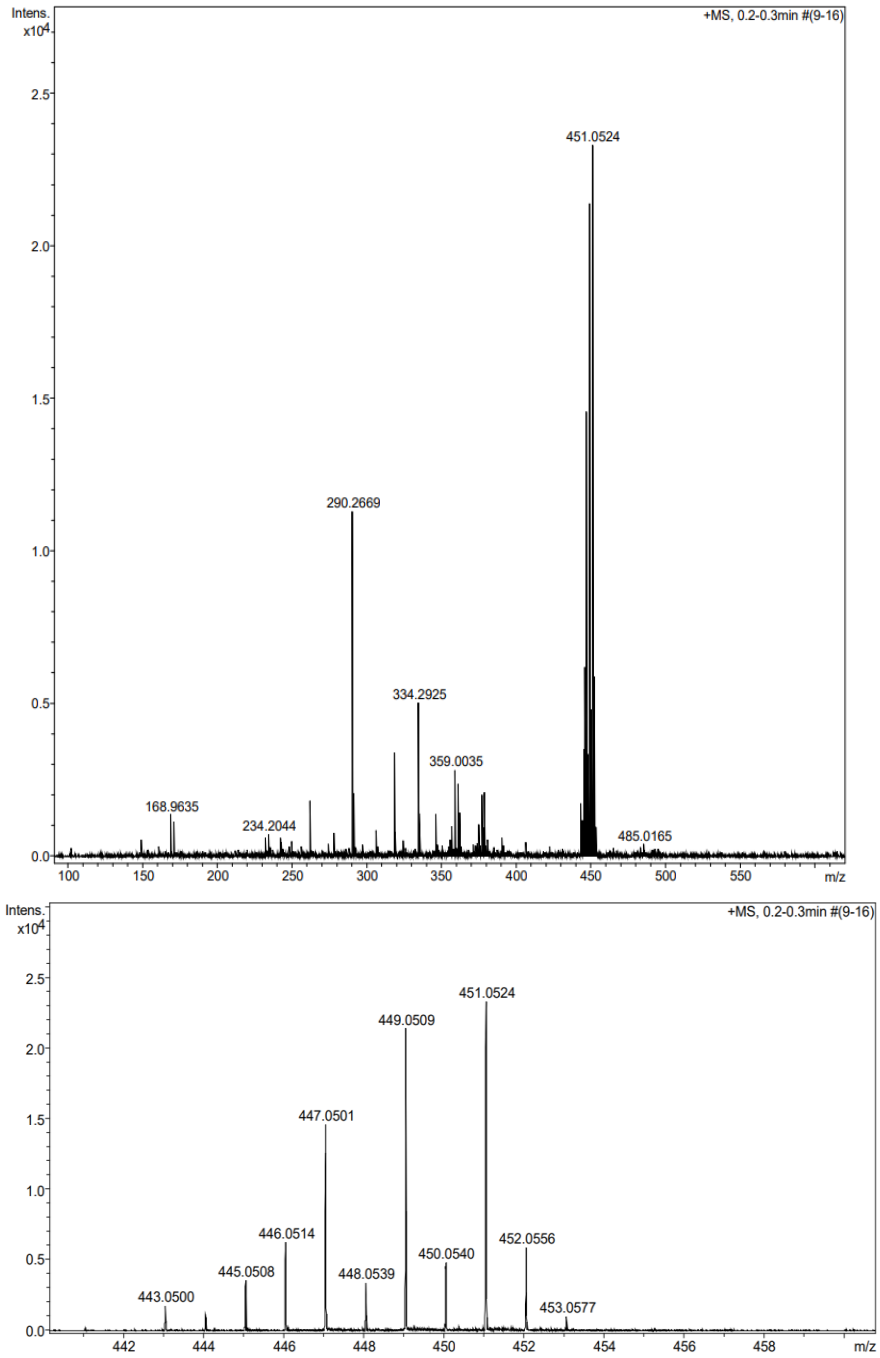

Figure S25. ESI mass spectra of **3.5**

Section – 22: ^{125}Te NMR spectral analysis of compound 3.5

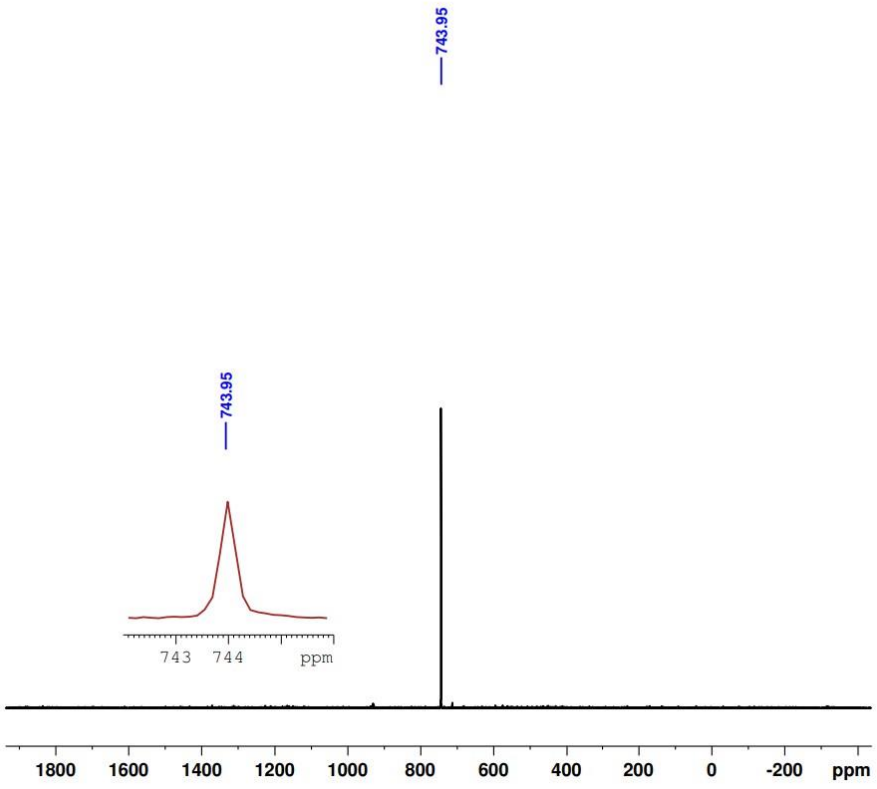

Section – 23: FT-IR spectral analysis of compound 3.5

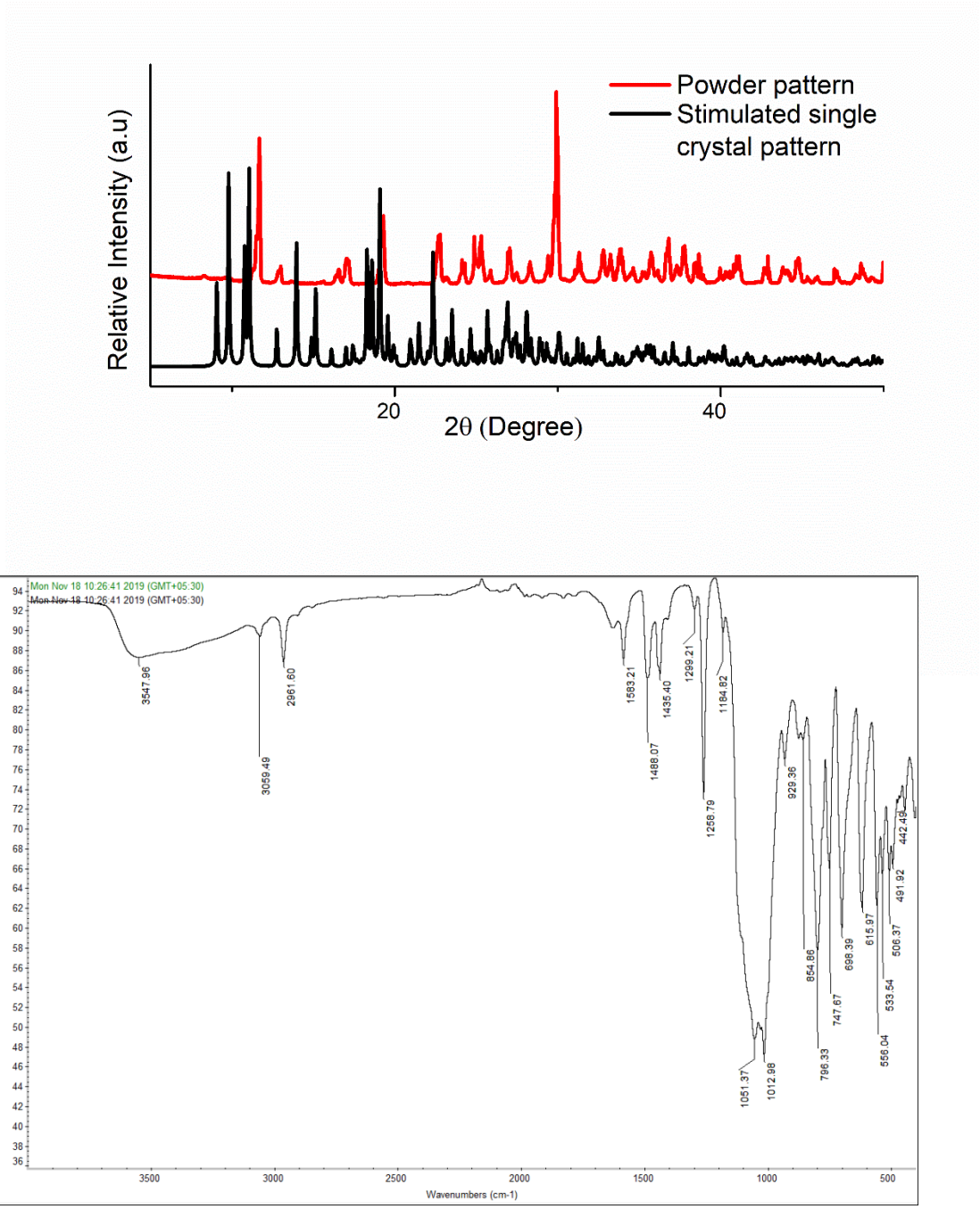

Figure S26. FT-IR spectrum of compound **3.5**

Section – 23: Bond valence calculation

Bond valence calculation. Numbers in brackets

after atom symbols are at.no., r and c -

see O"Keeffe and Brese, J.A.C.S. 1991, 113, 3226

[{(*p*-OMeC$_6$H$_4$)$_2$Te}$_2$(μ-O)(μ-BF$_4$)(μ-BF$_4$)]$_2$

.....Te1

Te (52, 1.40, 2.72)		Rij	Dij	Vij
-O	(8, .63, 3.15)	2.03	1.94	1.26
-C	(6, .78, 2.00)	2.17	2.09	1.23
-C	(6, .78, 2.00)	2.17	2.08	1.26

Bond valence sum for Te 3.76

.....Te2

Te (52, 1.40, 2.72)		Rij	Dij	Vij
-O	(8, .63, 3.15)	2.03	1.96	1.20
-C	(6, .78, 2.00)	2.17	2.10	1.22
-C	(6, .78, 2.00)	2.17	2.07	1.30

Bond valence sum for Te 3.72

.....Te3

Te (52, 1.40, 2.72)		Rij	Dij	Vij
-O	(8, .63, 3.15)	2.03	1.96	1.21
62				
-C	(6, .78, 2.00)	2.17	2.10	1.21
-C	(6, .78, 2.00)	2.17	2.10	1.22

Bond valence sum for Te 3.64

.....Te4

Te (52, 1.40, 2.72) Rij Dij Vij

-O (8, .63, 3.15) 2.03 1.95 1.24

-C (6, .78, 2.00) 2.17 2.11 1.17

-C (6, .78, 2.00) 2.17 2.07 1.31

Bond valence sum for Te 3.7

[{(*p*-OMeC$_6$H$_4$)$_2$Te}$_2$(μ-O)(μ-ClO$_4$)(μ-ClO$_4$)]$_2$

.....Te1

Te (52, 1.40, 2.72) Rij Dij Vij

-O (8, .63, 3.15) 2.03 1.95 1.24

-C (6, .78, 2.00) 2.17 2.10 1.22

-C (6, .78, 2.00) 2.17 2.11 1.18

Bond valence sum for Te 3.64

.....Te2

Te (52, 1.40, 2.72) Rij Dij Vij

-O (8, .63, 3.15) 2.03 1.96 1.20

-C (6, .78, 2.00) 2.17 2.10 1.21

-C (6, .78, 2.00) 2.17 2.08 1.27

Bond valence sum for Te 3.69

.....Te3

Te (52, 1.40, 2.72) Rij Dij Vij

119

-O (8, .63, 3.15) 2.03 1.94 1.26

-C (6, .78, 2.00) 2.17 2.10 1.20

-C (6, .78, 2.00) 2.17 2.09 1.24

Bond valence sum for Te 3.70

.....Te4

Te (52, 1.40, 2.72) Rij Dij Vij

-O (8, .63, 3.15) 2.03 1.97 1.17

-C (6, .78, 2.00) 2.17 2.09 1.25

-C (6, .78, 2.00) 2.17 2.10 1.20

Bond valence sum for Te 3.63

(*p*-OMeC$_6$H$_4$)$_3$TeBF$_4$

.....Te1

Te (52, 1.40, 2.72) Rij Dij Vij

-C (6, .78, 2.00) 2.17 2.10 1.20

-C (6, .78, 2.00) 2.17 2.10 1.20

-C (6, .78, 2.00) 2.17 2.12 1.15

Bond valence sum for Te 3.56

(*p*-OMe C$_6$H$_4$)$_3$TeClO$_4$

.....Te1

Te (52, 1.40, 2.72) Rij Dij Vij

-C (6, .78, 2.00) 2.17 2.10 1.19

-C (6, .78, 2.00) 2.17 2.10 1.19

-C (6, .78, 2.00) 2.17 2.12 1.14

Bond valence sum for Te 3.53

Reference:

1 (a). C. Tard and C. J. Pickett, *Chem Rev*, 2009, **109**, 2245–2274. (b). S. Kal, A. S. Filatov and P. H. Dinolfo, *Inorg Chem*, 2014, **53**, 7137–7145. (c). M. Raj and S. K. Padhi, *New Journal of Chemistry*, 2022, **46**, 6027–6038. (d). S. Lin, S. Banerjee, M. T. Fortunato, C. Xue, J. Huang, A. Yu. Sokolov and C. Turro, *J Am Chem Soc*, 2022, **144**, 20267–20277. (e). A. Rahaman, G. C. Lisensky, J. Browder-Long, D. A. Hrovat, M. G. Richmond, E. Nordlander and G. Hogarth, *Dalton Transactions*, 2020, **49**, 7133–7143.

2 (a). L. Vogel, P. Wonner and S. M. Huber, *Angewandte Chemie*, 2019, **131**, 1896–1907. (b). J. Bamberger, F. Ostler and O. G. Mancheño, *ChemCatChem*, 2019, 11, 5198–5211. (c). K. Selvakumar and H. B. Singh, *Chem Sci*, 2018, 9, 7027–7042. (d). K. T. Mahmudov, M. N. Kopylovich, M. F. C. Guedes Da Silva and A. J. L. Pombeiro, *Dalton Transactions*, 2017, 46, 10121–10138. (e). M. Breugst, D. von der Heiden and J. Schmauck, *Synthesis (Germany)*, 2017, 49, 3224–3236. (f). B. Zhou and F. P. Gabbaï, *J Am Chem Soc*, 2021, **143**, 8625–8630. (g). R. Weiss, E. Aubert, P. Pale and V. Mamane, *Angewandte Chemie - International Edition*, 2021, **60**, 19281–19286. (h). Q. Zhang, Y. Y. Chan, M. Zhang, Y. Y. Yeung and Z. Ke, *Angewandte Chemie - International Edition*, DOI:10.1002/anie.202208009. (i). Y. You, K. Ahsan and M. R. Detty, *J Am Chem Soc*, 2003, **125**, 4918–4927.

3 O. Carugo, G. Resnati and P. Metrangolo, *ACS Chem Biol*, DOI:10.1021/acschembio.1c00441.

4 (a). L. E. Bickerton, A. Docker, A. J. Sterling, H. Kuhn, F. Duarte, P. D. Beer and M. J. Langton, *Chemistry - A European Journal*, 2021, **27**, 11738–11745. (b). L. M. Lee, M. Tsemperouli, A. I. Poblador-Bahamonde, S. Benz, N. Sakai, K. Sugihara and S. Matile, *J Am Chem Soc*, 2019, **141**, 810–814. (c). A. Docker, C. H. Guthrie, H. Kuhn and P. D. Beer, *Angewandte Chemie - International Edition*, 2021, **60**, 21973–21978. (d). S. Benz, M. Macchione, Q. Verolet, J.

Mareda, N. Sakai and S. Matile, *J Am Chem Soc*, 2016, **138**, 9093–9096. (e). B. Zhou and F. P. Gabbaï, *Chem Sci*, 2020, **11**, 7495–7500.

5 (a). R. Gleiter, G. Haberhauer, D. B. Werz, F. Rominger and C. Bleiholder, *Chem Rev*, 2018, 118, 2010–2041. (b). N. Biot, D. Romito and D. Bonifazi, *Cryst Growth Des*, 2021, **21**, 536–543. (c). N. Biot and D. Bonifazi, *Coord Chem Rev*, 2020, 413. (d). P. C. Ho, J. Lomax, V. Tomassetti, J. F. Britten and I. Vargas-Baca, , DOI:10.1002/chem.202101425Part. (e). P. C. Ho, P. Szydlowski, J. Sinclair, P. J. W. Elder, J. Kübel, C. Gendy, L. M. Lee, H. Jenkins, J. F. Britten, D. R. Morim and I. Vargas-Baca, *Nat Commun*, DOI:10.1038/ncomms11299. (f). G. Haberhauer and R. Gleiter, *Angewandte Chemie - International Edition*, 2020, **59**, 21236–21243. (g). A. F. Cozzolino, P. J. W. Elder and I. Vargas-Baca, *Coord Chem Rev*, 2011, 255, 1426–1438.

6 L. Engman, Synthetic Applications of Organotellurium Chemistry, 1985, vol. 18.

7 (a). P. Wonner, T. Steinke, L. Vogel and S. M. Huber, *Chemistry - A European Journal*, 2020, **26**, 1258–1262. (b). P. Wonner, A. Dreger, L. Vogel, E. Engelage and S. M. Huber, *Angewandte Chemie*, 2019, **131**, 17079–17083.

8 K. Kobayashi, N. Deguchi, E. Horn and N. Furukawa, *Angewandte Chemie - International Edition*, 1998, **37**, 984–986.

9 K. Kobayashi, N. Deguchi, O. Takahashi, K. Tanaka, E. Horn, O. Kikuchi and N. Furukawa, *Angewandte Chemie - International Edition*, 1999, **38**, 1638–1640. (b). K. Kobayashi, H. Izawa, K. Yamaguchi, E. Horn and N. Furukawa, *Chemical Communications*, 2001, **1**, 1428–1429.

10 J. Beckmann, D. Dakternieks, A. Duthie, N. A. Lewcenko, C. Mitchell and M. Schürmann, *Z Anorg Allg Chem*, 2005, **631**, 1856–1862.

11 V. Chandrasekhar and R. Thirumoorthi, *Inorg Chem*, 2009, **48**, 10330–10337.

12 H. Zhu, P. P. Zhou, and Y. Wang, *Nat Commun*, DOI:10.1038/s41467-022-31293-5.

13 B. Zhou and F. P. Gabbaï, *Chem Sci*, 2020, **11**, 7495–7500.

14 B. Zhou and F. P. Gabbaï, *J Am Chem Soc*, 2021, **143**, 8625–8630.

15 N. K. Srungavruksham and V. Baskar, *Eur J Inorg Chem*, 2012, 136–142.

16 N. K. Srungavruksham and V. Baskar, *Dalton Transactions*, 2015, **44**, 4554–4569.

17 (a). J. Jeske, W. W. du Mont, F. Ruthe, P. G. Jones, L. M. Mercuri and P. Deplano, *Eur J Inorg Chem*, 2000, 1591–1599. (b). Y. Mutoh, T. Murai, and S. Yamago, *J Am Chem Soc*, 2004, **126**, 16696–16697. (c). R. Oilunkaniemi, J. Pietikäinen, R. S. Laitinen and M. Ahlgrén, *Cation-anion interactions in triphenyl telluronium salts. The crystal structures of* $(Ph_3\ Te)_2\ [MCl_6]$ *(M=Pt, Ir),* $(Ph_3Te)[AuCl_4]$*, and* $(Ph_3\ Te)(NO_3)\cdot HNO_3$, 2001, vol. 640.

18 N. K. Srungavruksham and V. Baskar, *Dalton Transactions*, 2015, **44**, 6358–6362.

19 (a). J. Bergman, *a novel synthesis of biaryls*, Pcrgamon Press, 1972, vol. 28. (b) C. Li, W. Li, A. F. Henwood, D. Hall, D. B. Cordes, A. M. Z. Slawin, V. Lemaur, Y. Olivier, I. D. W. Samuel and E. Zysman-Colman, *Inorg Chem*, 2020, **59**, 14772–14784. (c). By csoregh, P. Kierkegaard and R. Norrestam, *Acta Crsta, 1975, B31, 314.*

20 (a). G. M. Sheldrick, *Acta Crystallogr C Struct Chem*, 2015, **71**, 3–8. (b). O. v. Dolomanov, L. J. Bourhis, R. J. Gildea, J. A. K. Howard and H. Puschmann, *J Appl Crystallogr*, 2009, **42**, 339–341.

Chapter 4

Chapter 4

Star-shaped Te(VI)-Te(VI) complex and an octanuclear heterometallic Te_2Sb_6 oxo cluster

The reaction of telluric acid with di-organotellurium di chloride (R_2TeCl_2) and tri-organoantimony dichloride (R_3SbCl_2) has been carried out in binary solvent using solvothermal synthesis method and isolated high phase purity two novel mixed valent tellurium (VI) containing clusters $Te^{VI}[OTe^{IV}(p\text{-}MeOC_6H_4)_2Cl]_6$ (R = p-$MeOC_6H_4$) (**4.1**) and $[Te(\mu_2\text{-}O_5SbPh_3)(OSbh_3Cl)]_2$ (**4.2**). The products have been analyzed using standard spectroscopic and analytical methods and optical band gap measurements discussed in this chapter.

4.1 Introduction:

Heavier main group organometallic compounds have been used as molecular precursors in the field of material chemistry[1-2] and electrochemistry[3]. Metal ions when present in varying oxidation state has a profound effect on the properties and functions of the assembled complexes. Chandrashekar *et al.* have reported tellurasiloxane clusters $Te_6Si_4O_{12}$ and $Te_6Si_6O_{15}$ exhibiting interesting molecular architectures.[4] Organoantimony(V) compounds have been used as staring material for synthesizing multinuclear clustes by treating with various protic acid.[5-7] The first organotellurium compound was synthesized by hydrolysis of $C_8H_8Te[S_2P(OEt)_2]$, which contained both tellurium (IV) and tellurium (VI).[8] Later M. Driess et. al synthesized $[(Me_3SiO)_8Te_2O_2]$ and $[(Me_4Si_2O_2)_3Te]$ by reaction of $Te(OH)_6$ with $Me_3SiNEt_2$and $Me4Si_2(NEt_2)_2$ respectively.[9] Beckmann and his co-workers reported organo group

containig tellurostannoxane. Tellurates forms adducts with phosphate, sulphate, and urea through hydrogen bonding interactions.[10-11] Mono-substituted tellurate clusters demonstarted H_2 evolutiuon via photo- decomposition route.[12] In generally tellurate (TeO_6^-) ions have been used as exllent luminous capabilities after Mn_4^+ incorporation.[14]

The triphenylantimony(V) derivatives are substantially more chemically stable and have been used to develop covalent oxide materials. The triphenyl antimony (Ph_3Sb^{+2}) cations interactions with oxianions are essential for the formation of either discrete oxoclusters or polymers. From our group we have reported isolation of eight membered organoantimony rings incorporating a phosphorus or selenium[15] atom. Tetraorganoditelluroxane moiety have been shown to stabilize organoantimony based POM structure.[16] Here in, non-aqueous medium has been employed for synthesizing two mixed vallent organo tellurate clusters.. SCXRD studies has revealed the formation of interesting molecular architectures in solid state. The synthesis and structural analysis of the compounds are discussed in this chapter.

4.2 Experimental section

4.2.1 Reagents and general procedures

Chemicals $TeCl_4$, $Te(OH)_6$, Ph_3Sb were purchased from Sigma Aldrich Ltd. Solvents and other general reagents were purchased from a commercial source and purified according to standard procedure. Bis-(p-methoxyphenyl) Tellurium dichloride and triphenyl antimony dichloride was synthesized according to the previously reported procedure.[17-18] The yields of clusters were calculated based on telluric acid for isolated crystals and were used under high vacuum for one hour before being subjected to spectroscopic and analytical analysis.

4.2.1 Instrumentation

Infrared spectra were recorded with a NICOLET Is5 FTIR spectrometer. Single crystal X-ray data were collected at 293 K carried out by Rigaku Oxford Xta- Lab synergy diffractometer with the graphite monochromator with a Mo Kα (λ=0.71073 Å) microfocus sealed tube operated at 50 kV and 1mA. The data was solved and refined using OLEX software 2-1.2. 20 CCDC (2260626 and 2260969) for 4.1 and 4.2

4.2.2 General synthetic procedure

R_2TeCl_2 is dissolved in acetonitrile, then added to 1 ml of telluric acid (0.1 mol/L DMF) solution is added to reaction mixture. Triethyl amine is added then and kept for stirring at room temperature. The solution was sealed and heated gradually to 90 °C for two hours and continued for 24 hours, then cooled to 25°C over a period of 48 hours. The reaction mixture was filtered and colorless crystals suitable for SCXRD was isolated from the reaction mixture solution. Crystals were grown from acetonitrile/ DMF and methanol/ DMF mixture for compound 4.1 and 4.2 respectively.

4.3 Results and Discussion:

Under solvothermal conditions, we synthesized two novel clusters by reacting telluric acid with bis (*p*-methoxyphenyl) tellurium dichloride, yielding compound (4.1) $Te^{VI}[OTe^{IV}(p\text{-}MeOC_6H_4)_2Cl]_6$ (R = *p*-$MeOC_6H_4$) and triphenyl antimony trichloride gives compound (4.2) $[Te(\mu_2\text{-}O_5SbPh_3)(OSbh_3Cl)]_2$ in the presence of trimethylamine using bainary solvent as a medium. 4.1 and 4.2 were obtained as colorless crystals. The compound 4.1 and 4.2 were characterized by standard spectroscopic and analytical methods. Both the compounds have poor solubility in common organic solvents such as acetonitrile, chloroform, dichloromethane DMF, DMSO, and methanol. Telluric acid infrared spectra show a strong broad band spectra at 2950 cm^- of OH. Te=O has two medium bands at 1215 and 1124 cm^-, and a weak band at 632 cm^-. These telluric acid spectra when compared with synthesized clusters $Te^{VI}[OTe^{IV}(p\text{-}MeOC_6H_4)_2Cl]_6$ (1) and $[Te(\mu_2\text{-}O_5SbPh_3)_2\ (OSbPh_3Cl)]_2$ (2) a strong

broad band disappeared in synthesized clusters due to O—H bond cleavage, and forming Te—O—Te (1) and Te—O—Sb (2) bond formed. The IR spectrum of 4.1 and 4.2 the band in the range from 801 to 580 cm^{-1} mainly results from the Te—O, Sb—O, and aromatic groups. The thermal properties of 4.1 and 4.2 organo metal tellurate cluster was studied by thermogravimetric analysis (TGA) in an N_2 atmosphere from 30 to 800. The TGA studies of 4.1 and 4.2 organo metal tellurate cluster revealed that stability up 285 °C and 277 °C respectively. 1 and 2 crystals collected from Teflon tube to make fine powder

for powder X-ray diffraction data for the conformation of phase purity bulk of compounds.

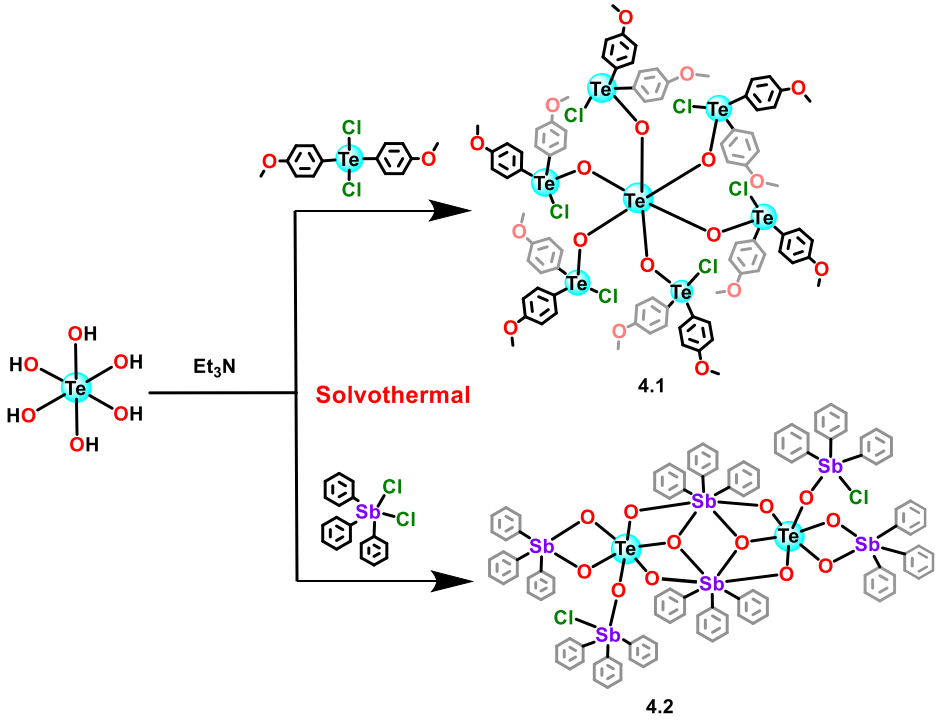

Scheme 4.

4.3.1 X-ray single crystal analysis 4.1 to 4.2

Compound 4.1 crystallize in crystal system of triclinic in space group *p-1* and has an octahedrally Te (VI) atom present in the center which is connected to Six Te (IV)

atoms through oxo linkage. The Te (IV) ion are tetra-coordinated in geometry. X-ray crystal structural data and refinement details are given in (**Table 1**) below. Compound **4.1** molecular structure in the solid-state molecular single crystal structural analysis shows the asymmetric unit on complete growth giving a discrete $Te^{VI}[OTe^{IV}(p\text{-}MeOC_6H_4)_2Cl]_6$ molecules. In the compound (**4.1**), the centre element tellurium (VI) is connected to six oxygen atoms, giving a high symmetric octahedral connectivity with an average bond distance of Te(VI)—O is 1.928 (15) Å when compared to bond distance of telluric acid (TeO_6H_6) of Te—O is less(1.901 Å). These six oxygens further connected to six tellurium atoms each [O—Te(IV)] with an average diastnce of 2.0563 (16) Å is longer distance when compare with Te(VI)—O, overally these oxygens are acting as bridging atom between Te(VI) and Te(IV), Te(VI)—O—Te(IV). Te(IV) connected to two (*p*-methoxy phenyl) groups perpendicularly and one chloride axially (**Figure 1**). Bond angle Te(VI)—O—Te(IV) is 124.51º (8) this parameter falls in the literrature range $Te^{VI}[OTe^{IV}(C_8H_8)(Edtp)]_6$ is 121.4º and Te(OTeF5) is 139.0º.[8,19] The geometry around Te(VI) octaherdal shown (Figure c) with polyhedral representaion and Packing diaram of in uint cell six molecules arranged in circle mode shown in (Figure 1d).

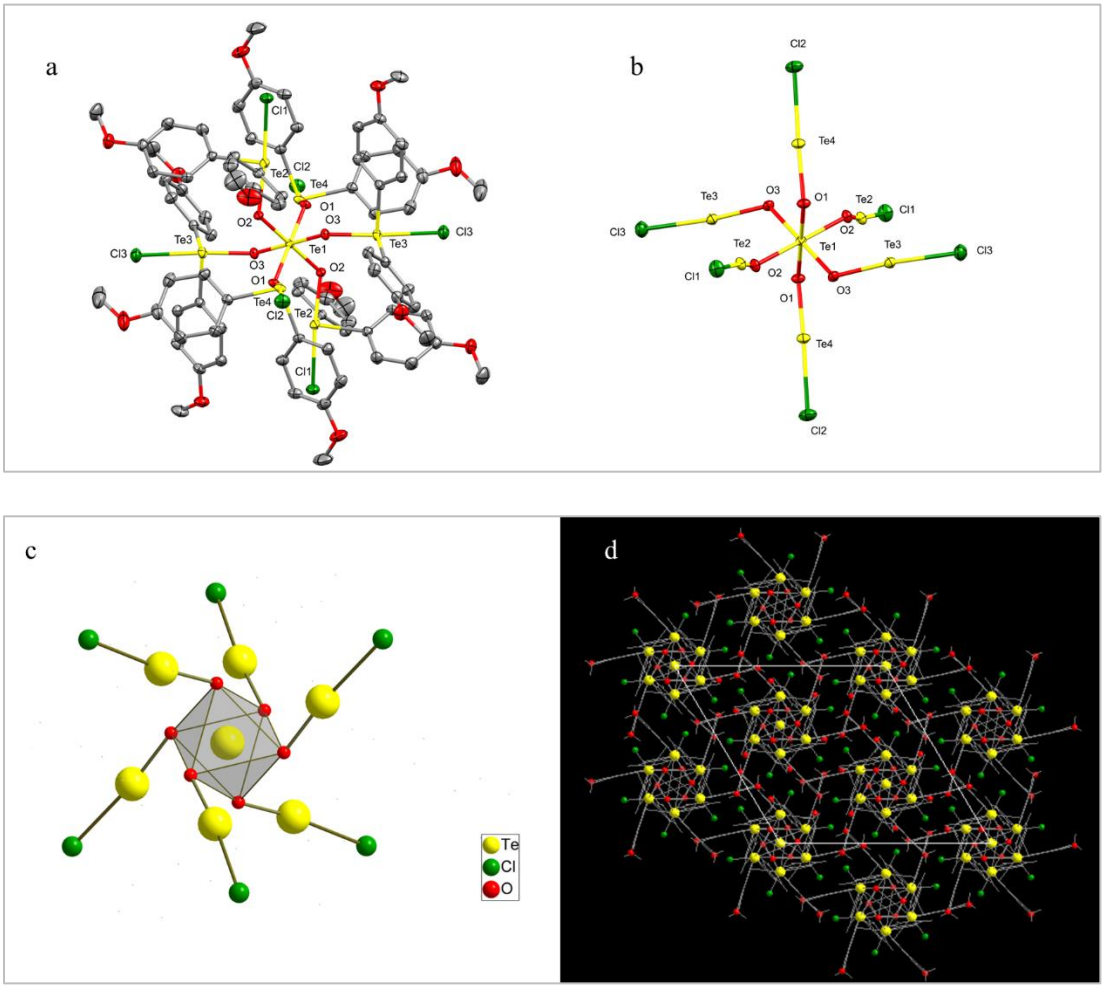

Figure 1. Solid state molecular crystal structure of 4.1, (a), and its core structure (b) hydrogen atoms are omitted for clarity. Thermal ellipsoids are drawn at 40% probability. (c) Octahedral geometry around central Te atom polyhedral representation, (d) packing diagram in a unit cell.

The molecular structure of compound 4.2 $[Te(\mu_2\text{-}O_5SbPh_3)_2(OSbPh_3Cl)]$ (**Figure 2**) is as follows. It contains a central butterfly type of a Te_2Sb_2 fragment held together by two μ_3-bridging oxygenated and four μ_2-bridging oxygen atom $[Te(\mu_3\text{-}O)(\mu_2\text{-}O)_2SbPh_3]_2$. This central butterfly core is flatted on each side by two Sb (V) atoms. One of the Sb(V) atom is bound to Te(VI) atom through two μ_2-bridging oxygen forming a four membered ring $[Te(\mu\text{-}O)_2Sb]_2$ while the other antimony is a pendant

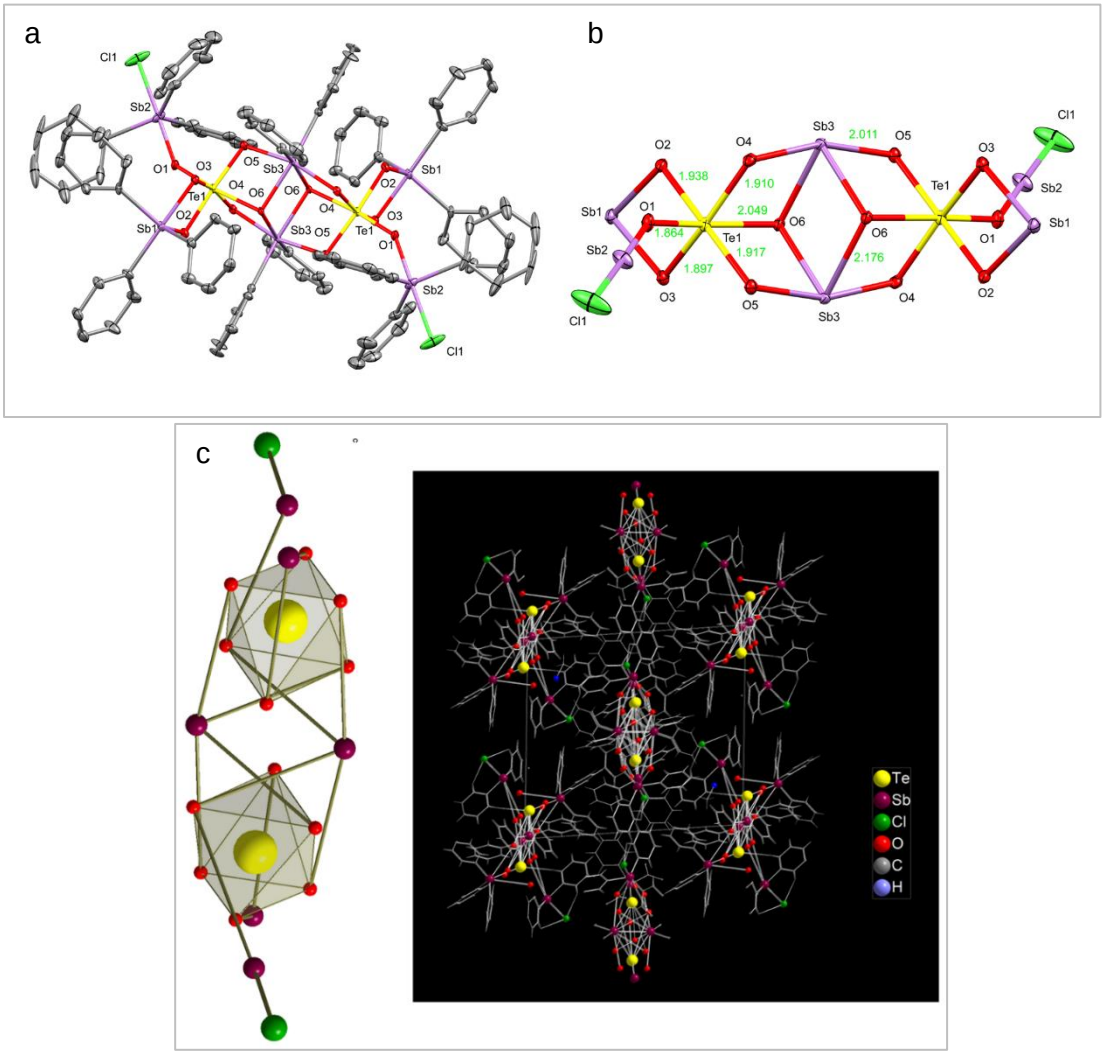

Figure 2. (a) Solid state molecular crystal structure of 4.2, (b) its core structure, (c) Polyhedral representation and packing diagram of unit cell. all hydrogen atoms are omitted for clarity. Thermal ellipsoids are drawn at 40% probability.

atom connected through oxygen (Te-O-Sb) of the Te(VI) atom of the central unit makes the overall Te_2Sb_6 oxo cluster. Selected metric parameters given in analytical data. Each Te atom is here coordinated by six oxygen atoms, geometry around this tellurium is slightly distorted octahedral [TeO_6] and around antimony in pentagonal bipyramid [SbC_3O_4]. The butterfly core antimony atoms coordinated to four oxygens

and three phenyl rings overall 7, while the other four Sb atoms 5- coordinated. The selected metric parameter given in the supporting information (**Table S4**). The bond distance between tellurium to oxygen, antimony to oxygen in the butterfly core fall in the range of (Te—O) 1.91 Å-2.05 Å, and (Sb_3—O) 2.10 Å-2.71 Å. The bond angles of Te—O—Sb is in the range of 91.58º (13) to 129.30º (12) (**Figure 2b**). The other three more oxygens from each tellurium bond distance in the range 1.86 Å-2.01 Å, out of this three two oxygen are connected one antimony forming a four membered ring [Te(μ-$O)_2$Sb] in this ring bond angle of Te_1—O_2—Sb_1 is 102.89º, here antimony contains three phenyl rings. Bond angle of pendant unit Te_1—O—Sb_1 is 144º, here antimony contains chloride alonfg with three phenyl rings. All this bond distances and bond angle are comparable erlier repoted literratute range.[16,20] Since this cluster are not soluble in any other organic solvents and mixture of organic solvent, the characterization carried out using solid state techniques such as powder Xray diffraction, UV absorption spectra (**Figure. S6**).

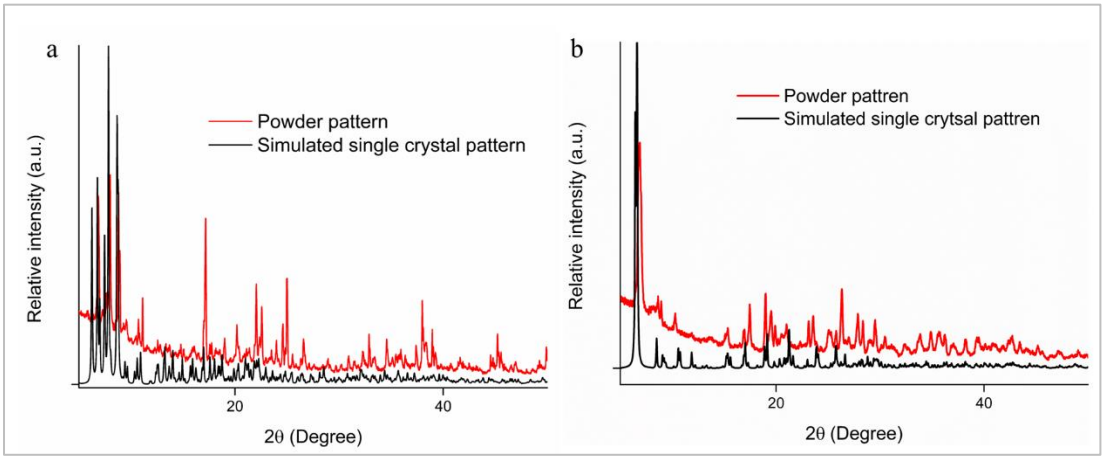

Figure 3. Simulated and index powder X-ray diffraction pattern of 4.1 (a) and 4.2 (b).

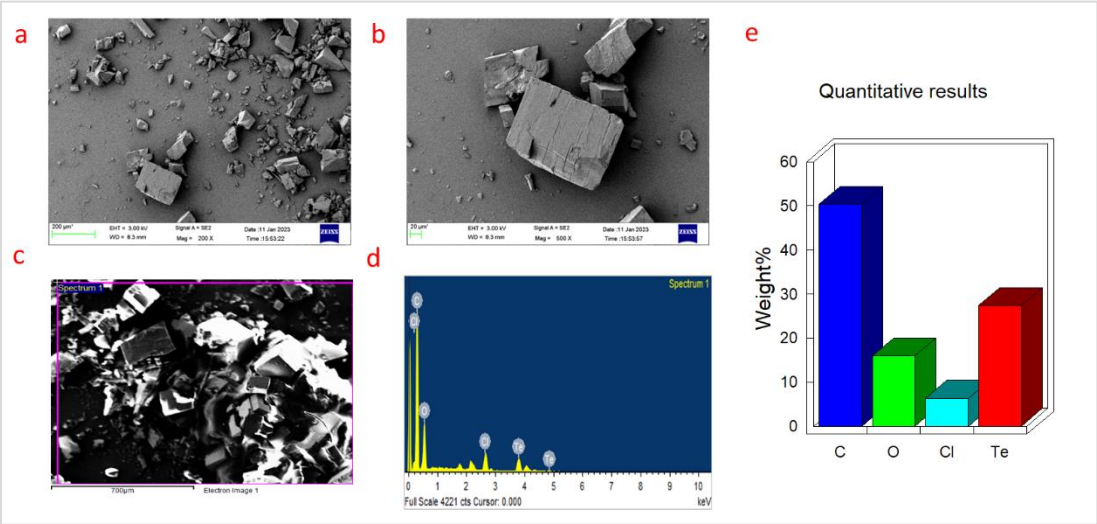

(a). SEM EDAX image of 4.1, (b). Crystal surface, (c) Area used for quantitative elemental finding, (d). Identified elements, (e). Elements weight % of cluster 4.1

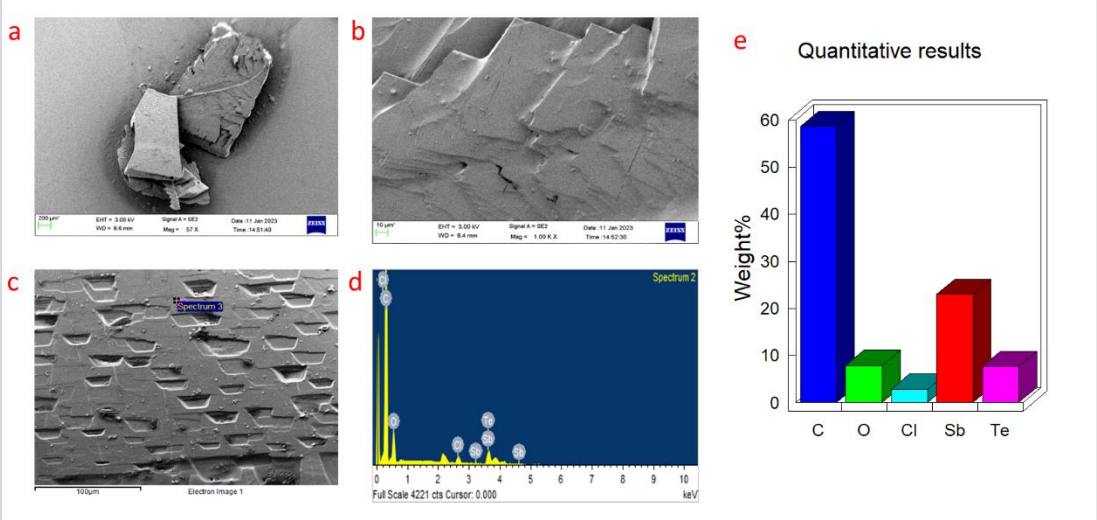

(a). SEM image of 4.1, (b). Crystal surface, (c) Area used for quantitative elemental finding, (d). Identified elements, (e). Elements weight % of cluster 4.2

4.4 Optical studies

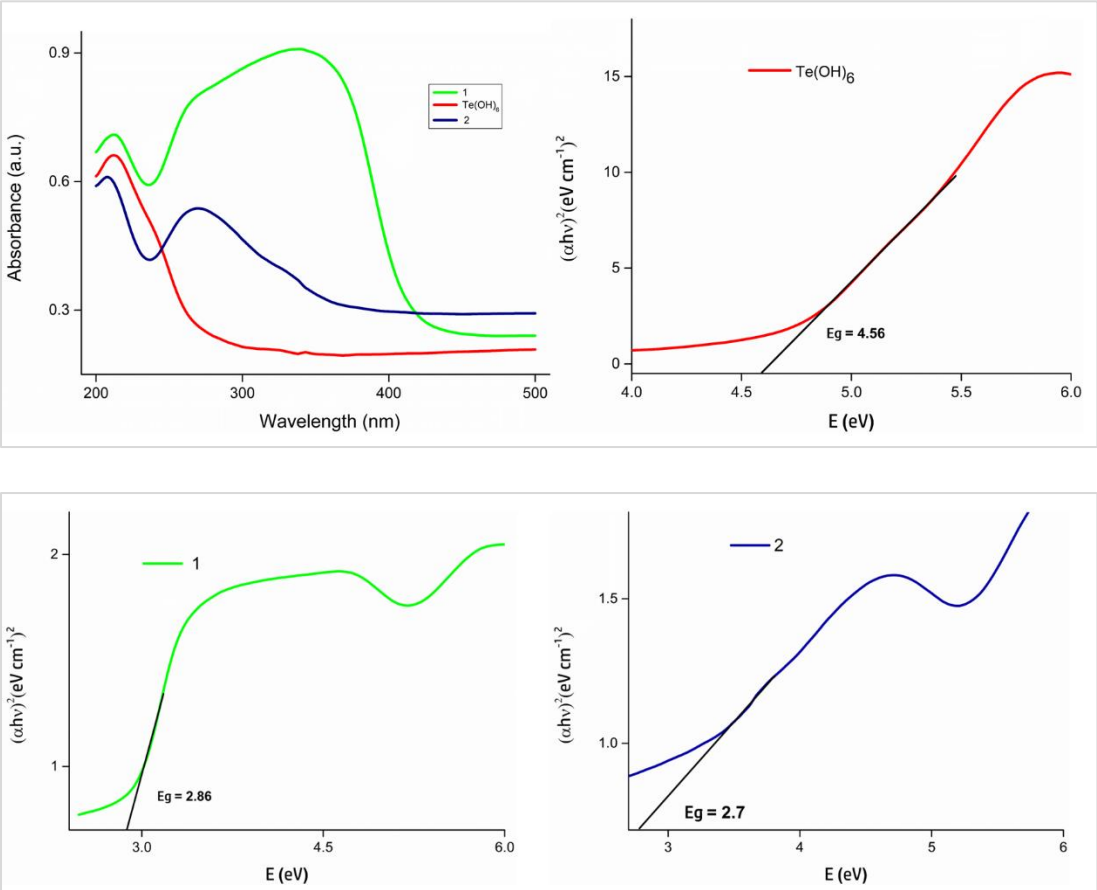

Figure 4. Solid state UV- visible spectroscopy graph of Telluric acid, 4.1 (1), and (4.2) 2 and Tauc plots of telluric acid, (4.1) 1 and (4.2) .

UV-visible absorption spectra in solid states were recorded 200 to 500 nm wave length range for studying of telluric acid, 4.1 and 4.2 clusters. The optical band gap (Eg) values of 4.1 and 4.2 calculated and compared with telluric acid by using Tauc equation.

$$(\alpha h\nu)^{1/n} = A(h\nu - Eg)$$

Eg = Band gap

A = Constant

h = Plank constant

ν = photons frequency

α = Absorption Co-efficient

The type of electron transition is denoted by the 'n' factor, whereas n values of either 1/2 or 2 indicate the direct and indirect energy band gaps, respectively.[21] Between (αhυ)2 and hυ, a graph was plotted. It was possible to calculate the optical bandgap (E_g) through the process of extrapolating the tangent lines to the X-axis (also known as equaling 0). The energy band gap is obtained from the fundamental peak's linear fit. The x-coordinate (abscissa) for the slope that is located below the fundamental absorption peak is determined using a linear fit. The energy band gap is shown by the junction of the two linear fitting curves. Therefore, the estimate of bandgaps using this baseline technique is correct. All semiconducting materials with little absorption can be employed with this technique. The resultant band gap values may be skewed during this approach is used to materials (surface modified, doped, defected, or bulk) that display a considerable absorbance at energies below band gap energy (Eg).[22] The direct band gap (E_g) of the telluric acid $Te(OH)_6$ is 4.56 eV. The calculated band gap has been observed for $Te^{VI}[OTe^{IV}(p\text{-}MeOC_6H_4)_2Cl]_6$ (4.1) is 2.86 eV and $[Te(\mu_2\text{-}O_5SbPh_3)_2(OSbPh_3Cl)]_2$ (4.2) is 2.7 eV. When moving from telluric acid [Te(OH)6] to main group binary metal mixed valent clusters, a discernible narrowing of the band gap can be seen.

4.5 Infrared spectroscopy analysis for4.1 and 4.2:

The Fourier transform infrared spectroscopy (FTIR) used to record spectra with a "NICOLET Is5 FTIR spectrometer in the range of 400- 4000". Telluric acid infrared spectra show a strong broad band spectra at 2950 cm^- of OH. Te=O has two medium bands at 1215 and 1124 cm^-, and a weak band at 632 cm^-. These telluric acid spectra

when compared with synthesized clusters $Te^{VI}[OTe^{IV}(p\text{-}MeOC_6H_4)_2Cl]_6$ (4.1) and $[Te(\mu_2\text{-}O_5SbPh_3)_2\,(OSbPh_3Cl)]_2$ (4.2) a strong broad band disappeared in synthesized clusters due to O—H bond cleavage, and forming Te—O—Te (4.1) and Te—O—Sb (4.2) bond formed. The IR spectrum of 4.1 and 4.2 the band in the range from 801 to 580 cm^{-1} mainly results from the Te—O, Sb—O, aromatic groups.

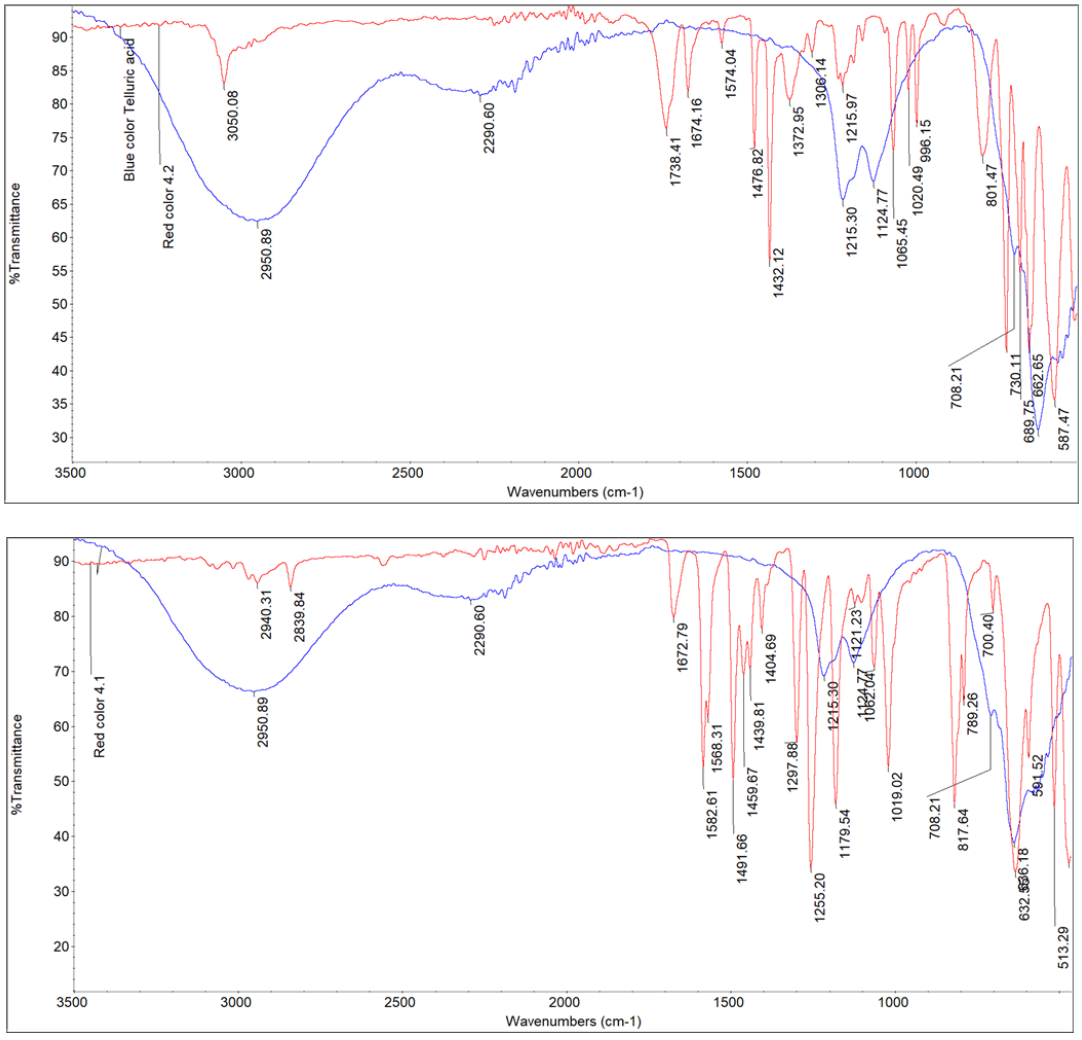

Figure 5. Infrared spectra of cluster 4.1 (above), 4.2 below

4.6 Thermal analysis:

The thermal properties of 4.1 and 4.2 organo metal tellurate cluster was studied by thermogravimetric analysis (TGA) in an N_2 atmosphere from 30 to 800. The TGA curve shown in the Figure 6. The TGA studies of 4.1 and 4.2 organo metal tellurate cluster revealed that stability up 285 $^{\circ}$C and 277 $^{\circ}$C respectively.

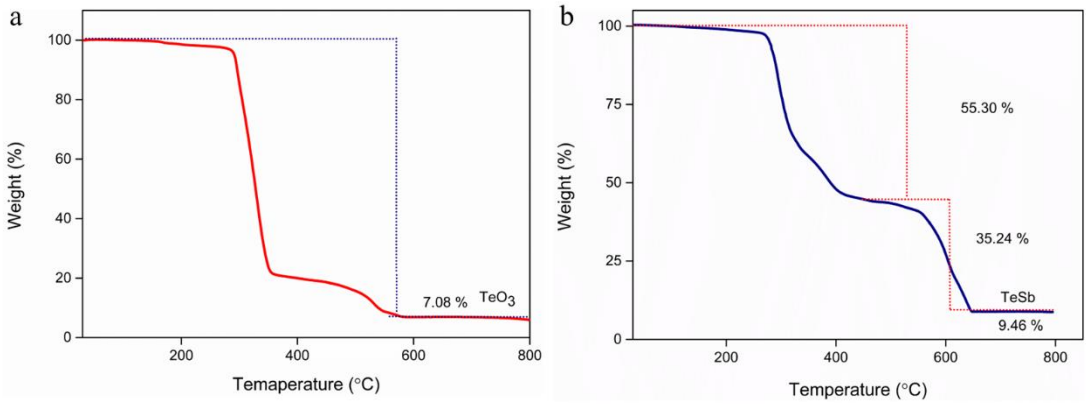

Figure 6. Thermogravimetric analysis 4.1 (a) and 4.2 (b).

4.7 Conclusion

we synthesized high phase purity two novel mixed valent containing main group metal organotellurium and organoantimony with tellurates forming clusters by solvothermal method in non-aqueous medium by using organic binary solvent. The isolated compound 4.1 has octahedral tellurate connected to diorganotellurium chloride $[TeO_6(TeR_2Cl)_6]$ and butterfly (Te-μ-O_2SbPh_3) core contain novel octanuclear cluster. These synthesized mixed valent metal clusters solid state structural characterization detailed in this paper. These synthesized mixed valent metal clusters optical properties investigated.

Analytical and Spectroscopic data

Table S1. Crystallographic information of compounds 4.1 and 4.2

Identification code	4.1	4.2
Empirical formula	$C_{84}H_{80}Cl_6O_{18}Te_7$	$C_{92}H_{73}Cl_2O_{12}Sb_6Te_2$
Formula weight	2483.38	2468.15
Temperature/K	293.36(14)	115(1)
Crystal system	triclinic	triclinic
Space group	P-1	P-1
a/Å	13.49630(10)	13.01540(10)
b/Å	13.61670(10)	18.86980(10)
c/Å	13.69790(10)	20.1970(2)
α/°	91.8480(10)	83.5220(10)
β/°	90.3450(10)	82.2410(10)
γ/°	100.1340(10)	75.5650(10)
Volume/Å^3	2476.60(3)	4743.54(7)
Z	1	2
ρ_{calc}g/cm^3	1.665	1.728
μ/mm^{-1}	2.253	2.400
F(000)	1194.0	2374.0
Crystal size/mm^3	0.1 × 0.1 × 0.08	0.1 × 0.08 × 0.04
Radiation	MoKα (λ = 0.71073)	MoKα (λ = 0.71073)
2Θ range for data collection/°	3.918 to 53.95	3.75 to 53.972
Index ranges	-16 ≤ h ≤ 17, -16 ≤ k ≤ 17, -16 ≤ l ≤ 17	-16 ≤ h ≤ 16, -22 ≤ k ≤ 23, -24 ≤ l ≤ 25

Reflections collected	42754	107173
Independent reflections	10322 [R_{int} = 0.0163, R_{sigma} = 0.0162]	19724 [R_{int} =0.0419, R_{sigma} = 0.0335]
Data/restraints/parameters	10322/882/530	19724/1993/1055
Goodness-of-fit on F^2	1.098	1.061
Final R indexes [I>=2σ (I)]	R_1 = 0.0287, wR_2 = 0.1109	R_1 = 0.0518, wR_2 = 0.1313
Final R indexes [all data]	R_1 = 0.0315, wR_2 = 0.1130	R_1 = 0.0587, wR_2 = 0.1366
Largest diff. peak/hole / e $Å^{-3}$	2.07/-0.82	4.67/-3.99

Table S2. Bond Lengths for 4.1

Atom	Atom	Distance		Atom	Atom	Distance
Te1	O3	1.9284(15)		C6	C1	1.374(4)
Te1	O3[1]	1.9284(15)		O5	C27	1.356(4)
Te1	O1[1]	1.9272(15)		O5	C30	1.433(5)
Te1	O1	1.9272(15)		C24	C29	1.386(4)
Te1	O2	1.9262(15)		C24	C25	1.381(4)
Te1	O2[1]	1.9262(15)		C43	C42	1.389(4)
Te2	Cl1	2.5859(7)		C39	C40	1.378(4)
Te2	O2	2.0563(16)		C35	C36	1.370(4)
Te2	C8	2.096(3)		C35	C34	1.389(4)
Te2	C6	2.104(3)		C29	C28	1.389(4)
Te4	Cl2	2.6025(7)		C28	C27	1.374(4)
Te4	O1	2.0518(15)		C40	C41	1.386(4)
Te4	C16	2.094(3)		C5	C4	1.374(4)
Te4	C24	2.097(2)		C34	C33	1.384(4)
Te3	Cl3	2.5943(7)		C21	C20	1.385(4)
Te3	O3	2.0597(16)		C33	C32	1.385(4)
Te3	C31	2.101(2)		C10	C11	1.384(5)
Te3	C38	2.108(3)		C2	C3	1.374(4)
O9	C34	1.358(3)		C2	C1	1.388(4)
O9	C37	1.437(4)		C13	C12	1.369(4)
O8	C41	1.360(3)		C41	C42	1.378(4)
O8	C44	1.424(4)		C3	C4	1.380(4)
O6	C3	1.359(3)		O7	C11	1.563(7)
O6	C7	1.418(4)		O7	C0AA	0.811(13)

C31	C36	1.392(4)		C27	C26	1.385(5)
C31	C32	1.381(3)		C25	C26	1.373(4)
C8	C9	1.382(4)		O4	C19	1.352(4)
C8	C13	1.384(4)		O4	C23	1.372(6)
C16	C21	1.376(4)		C12	C11	1.386(5)
C16	C17	1.388(4)		C17	C18	1.368(4)
C9	C10	1.376(4)		C11	C0AA	1.752(13)
C38	C43	1.379(4)		C20	C19	1.377(5)
C38	C39	1.391(4)		C19	C18	1.399(5)
C6	C5	1.388(4)				

Table S3. Bond Angles for 4.1.

Atom	Atom	Atom	Angle/°		Atom	Atom	Atom	Angle/°
$O3^1$	Te1	O3	180.0		C1	C6	Te2	119.5(2)
O1	Te1	$O3^1$	88.86(7)		C1	C6	C5	119.4(2)
O1	Te1	O3	91.14(7)		C27	O5	C30	118.0(3)
$O1^1$	Te1	O3	88.86(7)		C29	C24	Te4	120.42(19)
$O1^1$	Te1	$O3^1$	91.14(7)		C25	C24	Te4	119.6(2)
O1	Te1	$O1^1$	180.0		C25	C24	C29	119.9(3)
O2	Te1	$O3^1$	90.98(7)		C38	C43	C42	120.3(3)
O2	Te1	O3	89.01(7)		C40	C39	C38	119.8(3)
$O2^1$	Te1	$O3^1$	89.02(7)		C36	C35	C34	120.3(3)
$O2^1$	Te1	O3	90.99(7)		C35	C36	C31	120.0(2)
O2	Te1	$O1^1$	91.42(7)		C24	C29	C28	119.9(3)
$O2^1$	Te1	$O1^1$	88.58(7)		C27	C28	C29	119.9(3)
O2	Te1	O1	88.58(7)		C39	C40	C41	120.4(3)

O2[1]	Te1	O1	91.42(7)		C4	C5	C6	119.8(3)
O2[1]	Te1	O2	180.0		O9	C34	C35	115.7(3)
O2	Te2	Cl1	172.81(5)		O9	C34	C33	124.3(2)
O2	Te2	C8	86.98(8)		C33	C34	C35	120.0(3)
O2	Te2	C6	89.03(8)		C16	C21	C20	120.6(3)
C8	Te2	Cl1	87.10(7)		C34	C33	C32	119.5(2)
C8	Te2	C6	97.76(10)		C9	C10	C11	119.4(3)
C6	Te2	Cl1	87.72(7)		C31	C32	C33	120.5(3)
O1	Te4	Cl2	172.19(5)		C3	C2	C1	119.5(3)
O1	Te4	C16	87.36(8)		C12	C13	C8	119.4(3)
O1	Te4	C24	88.49(8)		O8	C41	C40	114.9(3)
C16	Te4	Cl2	86.99(7)		O8	C41	C42	125.3(3)
C16	Te4	C24	98.30(10)		C42	C41	C40	119.8(3)
C24	Te4	Cl2	87.00(7)		O6	C3	C2	125.0(3)
O3	Te3	Cl3	173.28(5)		O6	C3	C4	115.2(3)
O3	Te3	C31	87.07(8)		C2	C3	C4	119.8(3)
O3	Te3	C38	88.45(8)		C0AA	O7	C11	89.3(11)
C31	Te3	Cl3	87.80(7)		C5	C4	C3	120.7(3)
C31	Te3	C38	96.97(10)		O5	C27	C28	123.9(3)
C38	Te3	Cl3	87.88(7)		O5	C27	C26	116.1(3)
Te1	O3	Te3	123.23(8)		C28	C27	C26	119.9(3)
Te1	O1	Te4	123.91(8)		C26	C25	C24	119.9(3)
Te1	O2	Te2	124.51(8)		C19	O4	C23	118.4(4)
C34	O9	C37	117.5(2)		C6	C1	C2	120.7(3)
C41	O8	C44	117.9(3)		C41	C42	C43	119.9(3)
C3	O6	C7	118.6(3)		C13	C12	C11	120.2(3)
C36	C31	Te3	118.27(18)		C25	C26	C27	120.5(3)
C32	C31	Te3	122.10(19)		C18	C17	C16	119.4(3)

C32	C31	C36	119.6(2)		C10	C11	O7	107.9(4)
C9	C8	Te2	116.96(19)		C10	C11	C12	120.4(3)
C9	C8	C13	120.6(3)		C10	C11	C0AA	135.3(4)
C13	C8	Te2	122.4(2)		O7	C11	C0AA	27.6(3)
C21	C16	Te4	117.2(2)		C12	C11	O7	131.7(4)
C21	C16	C17	120.2(3)		C12	C11	C0AA	104.3(4)
C17	C16	Te4	122.6(2)		C19	C20	C21	119.4(3)
C10	C9	C8	120.0(3)		O4	C19	C20	125.6(4)
C43	C38	Te3	120.2(2)		O4	C19	C18	114.6(3)
C43	C38	C39	119.8(2)		C20	C19	C18	119.8(3)
C39	C38	Te3	120.03(19)		C17	C18	C19	120.6(3)
C5	C6	Te2	121.09(19)		O7	C0AA	C11	63.1(11)

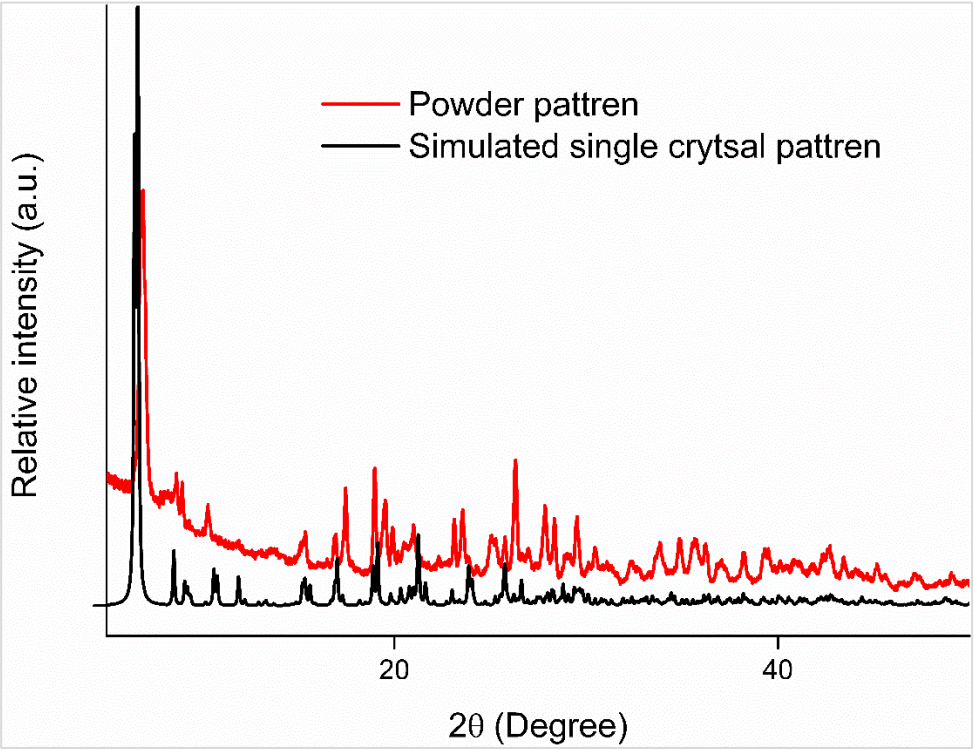

Figure S2: Powder X-ray diffraction pattern of a bulk sample of 1 compared to the simulated powder pattern extracted from single-crystal diffraction data.

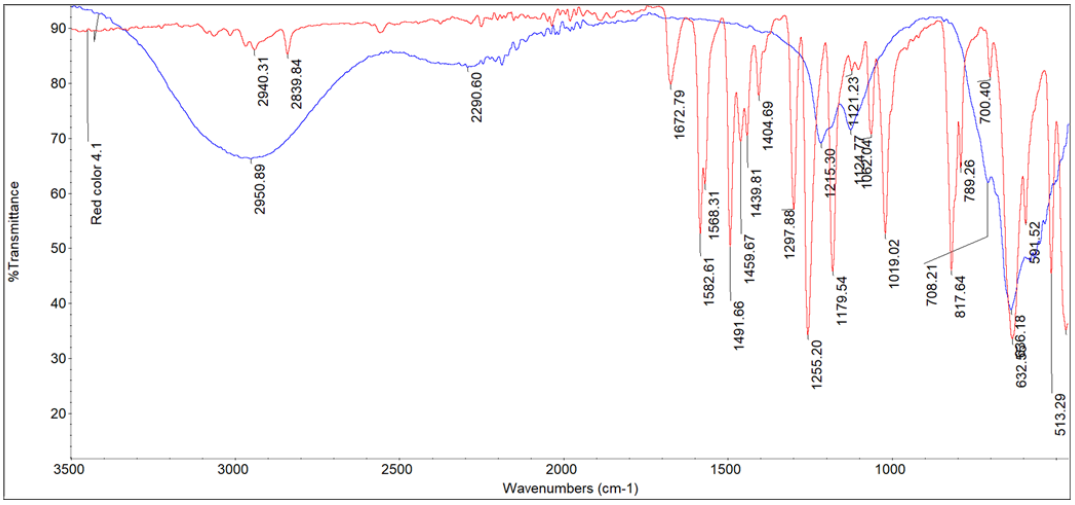

Figure S3. Infrared spectra of cluster 4.1

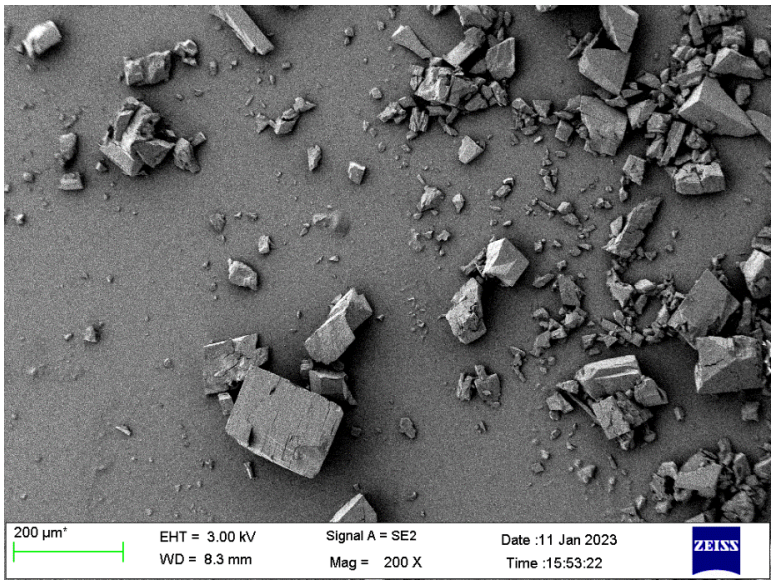

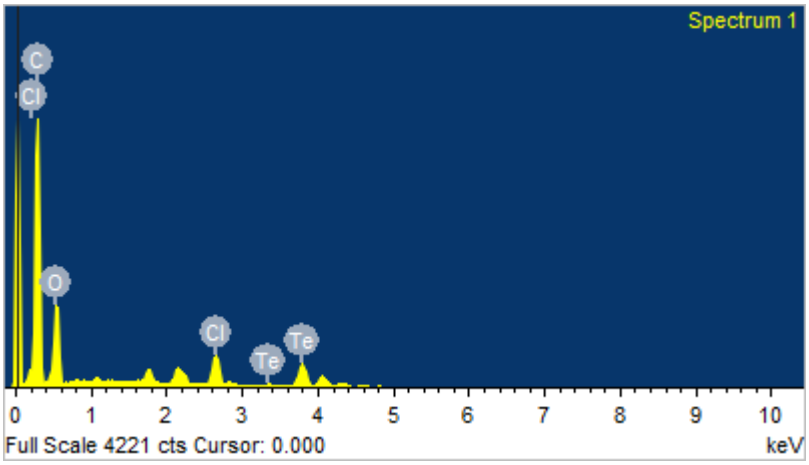

Quantitative results

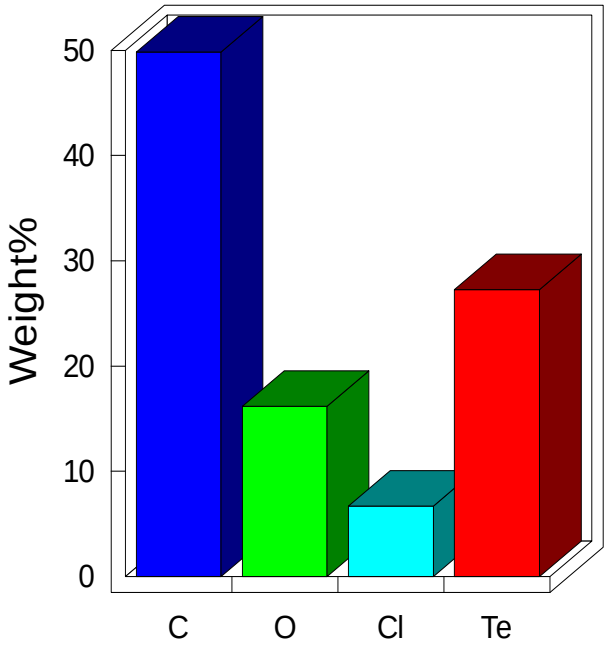

Element	Calculated weight%	Measured weight% from EDAX analysis
C	40.60	40.01
O	11.60	11.26
Cl	8.58	8.42
Te	35.98	35.82
H	3.23	Not Detected

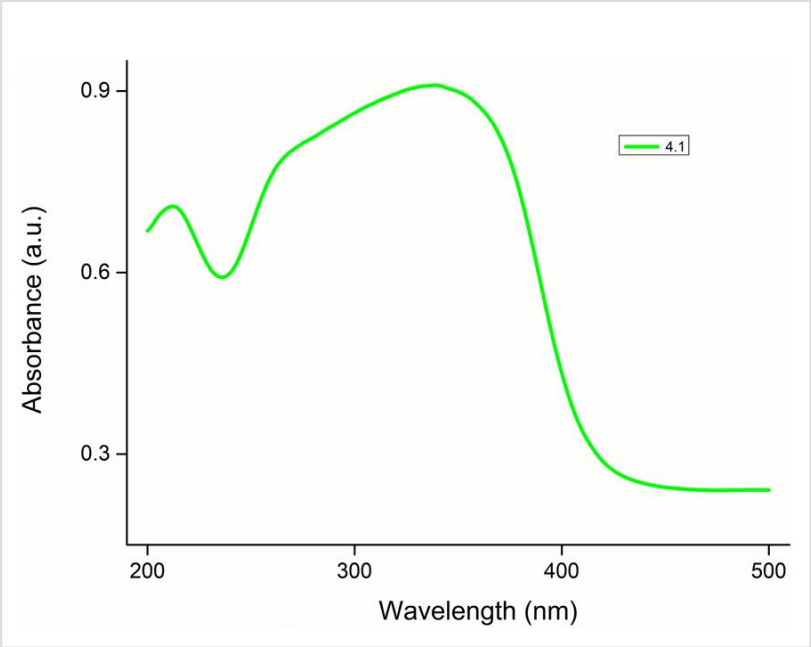

Figure S6: Solid-state UV-vis absorption spectrum of Cluster 4.1

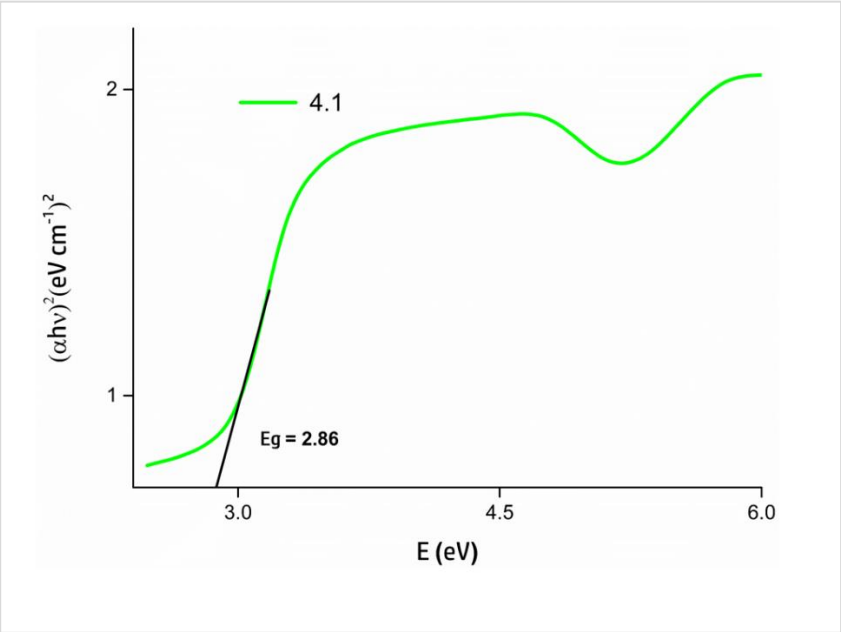

Figure S7: Tauc plot of of Cluster 4.1

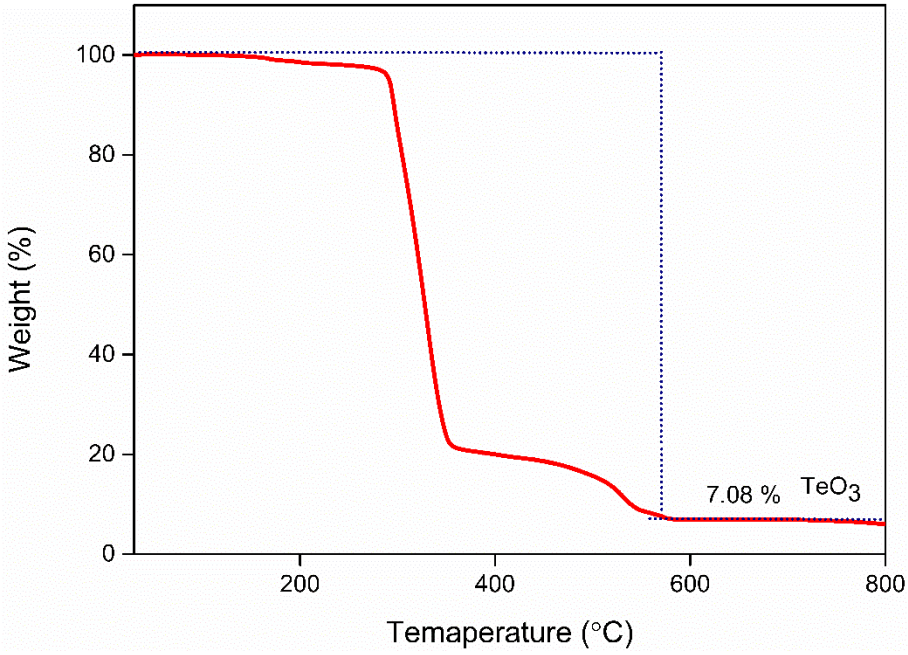

Figure 6. Thermogravimetric analysis of 4.1.

Table 4. Bond Lengths, bond Angles for 4.2

Atom	Atom	Length/Å	Atom	Atom	Atom	Angle/°
Te1	Sb3[1]	3.1566(5)	Sb3	Te1	Sb3[1]	65.869(14)
Te1	Sb3	3.1418(5)	Sb1	Te1	Sb3	122.231(16)
Te1	Sb1	3.0669(5)	Sb1	Te1	Sb3[1]	115.332(16)
Te1	O6	2.048(4)	O6	Te1	Sb3[1]	43.23(12)
Te1	O4	1.911(4)	O6	Te1	Sb3	42.38(11)
Te1	O5	1.917(4)	O6	Te1	Sb1	96.09(11)
Te1	O2	1.938(4)	O4	Te1	Sb3[1]	37.19(13)
Te1	O3	1.896(4)	O4	Te1	Sb3	89.31(13)
Te1	O1	1.863(4)	O4	Te1	Sb1	127.63(13)
Sb3	O6	2.135(4)	O4	Te1	O6	80.04(17)
Sb3	O6[1]	2.176(4)	O4	Te1	O5	94.83(18)
Sb3	O4[1]	2.001(4)	O4	Te1	O2	88.62(18)
Sb3	O5	2.011(4)	O5	Te1	Sb3[1]	91.58(13)
Sb3	C83	2.123(6)	O5	Te1	Sb3	37.94(13)
Sb3	C84	2.119(6)	O5	Te1	Sb1	136.36(13)
Sb1	O2	1.990(4)	O5	Te1	O6	80.22(17)
Sb1	O3	2.094(4)	O5	Te1	O2	173.13(19)
Sb1	C55	2.098(7)	O2	Te1	Sb3[1]	87.58(13)
Sb1	C61	2.116(7)	O2	Te1	Sb3	136.43(13)
Sb1	C49	2.153(7)	O2	Te1	Sb1	39.27(13)
Sb2	Cl1	2.495(2)	O2	Te1	O6	94.57(17)
Sb2	O1	2.013(5)	O3	Te1	Sb3[1]	132.74(14)
Sb2	C72	2.096(8)	O3	Te1	Sb3	91.81(13)
Sb2	C90	2.101(8)	O3	Te1	Sb1	42.21(13)
Sb2	C66	2.089(1	O3	Te1	O6	91.87(18)

			O3	Te1	O4	166.65(19)
			O3	Te1	O5	94.21(18)
			O3	Te1	O2	81.41(18)
			O1	Te1	Sb3	131.17(14)
			O1	Te1	Sb3^{1}	129.21(15)
			O1	Te1	Sb1	94.46(14)
			O1	Te1	O6	169.29(18)
			O1	Te1	O4	92.02(19)
			O1	Te1	O5	93.41(19)
			O1	Te1	O2	92.40(19)
			O1	Te1	O3	97.2(2)
			Te1	Sb3	Te1^{1}	114.133(14)
			O6^{1}	Sb3	Te1^{1}	40.13(11)
			O6^{1}	Sb3	Te1	84.13(11)
			O6	Sb3	Te1	40.29(11)
			O6	Sb3	Te1^{1}	84.41(11)

Atom	**Atom**	**Atom**	**Angle/°**
O6	Sb3	O6^{1}	74.85(17)
O4^{1}	Sb3	Te1	129.30(12)
O4^{1}	Sb3	Te1^{1}	35.24(12)
O4^{1}	Sb3	O6	89.31(16)
O4^{1}	Sb3	O6^{1}	75.03(16)
O4^{1}	Sb3	O5	162.55(17)
O4^{1}	Sb3	C83	92.7(2)
O4^{1}	Sb3	C84	100.2(2)
O5	Sb3	Te1	35.87(12)
O5	Sb3	Te1^{1}	131.67(12)
O5	Sb3	O6^{1}	91.76(16)

O5	Sb3	O6	76.06(16)
O5	Sb3	C83	98.2(2)
O5	Sb3	C84	91.0(2)
C83	Sb3	Te1	97.23(17)
C83	Sb3	Te1^{1}	127.93(19)
C83	Sb3	O6^{1}	164.8(2)
C83	Sb3	O6	96.3(2)
C84	Sb3	Te1^{1}	92.67(17)
C84	Sb3	Te1	125.78(17)
C84	Sb3	O6	159.2(2)
C84	Sb3	O6^{1}	89.7(2)
C84	Sb3	C83	101.6(2)
O2	Sb1	Te1	38.06(12)
O2	Sb1	O3	75.46(17)
O2	Sb1	C55	117.7(2)
O2	Sb1	C61	126.8(2)
O2	Sb1	C49	88.1(2)
O3	Sb1	Te1	37.46(12)
O3	Sb1	C55	91.7(2)
O3	Sb1	C61	85.9(2)
O3	Sb1	C49	162.1(2)
C55	Sb1	Te1	109.62(18)
C55	Sb1	C61	112.1(3)
C55	Sb1	C49	102.3(3)
C61	Sb1	Te1	107.99(19)
C61	Sb1	C49	98.8(3)
C49	Sb1	Te1	125.55(19)

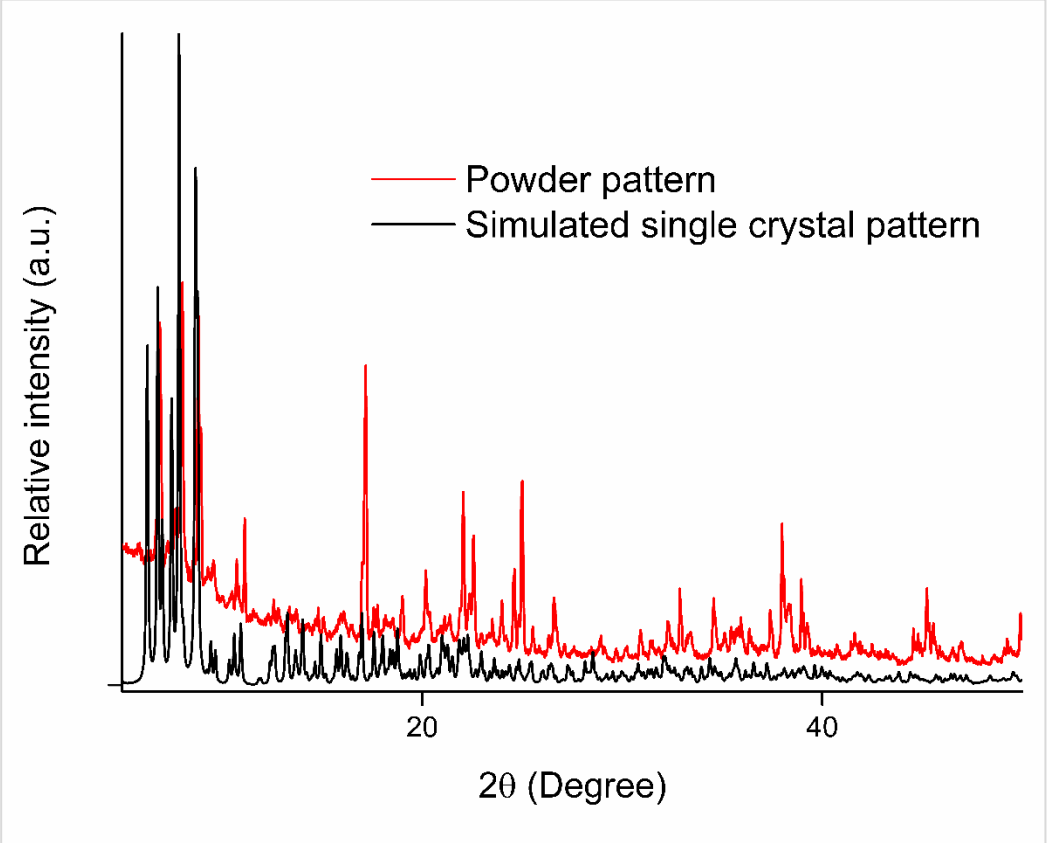

Figure S9: Powder X-ray diffraction pattern of a bulk sample of 4.2 compared to the simulated powder pattern extracted from single-crystal diffraction data.

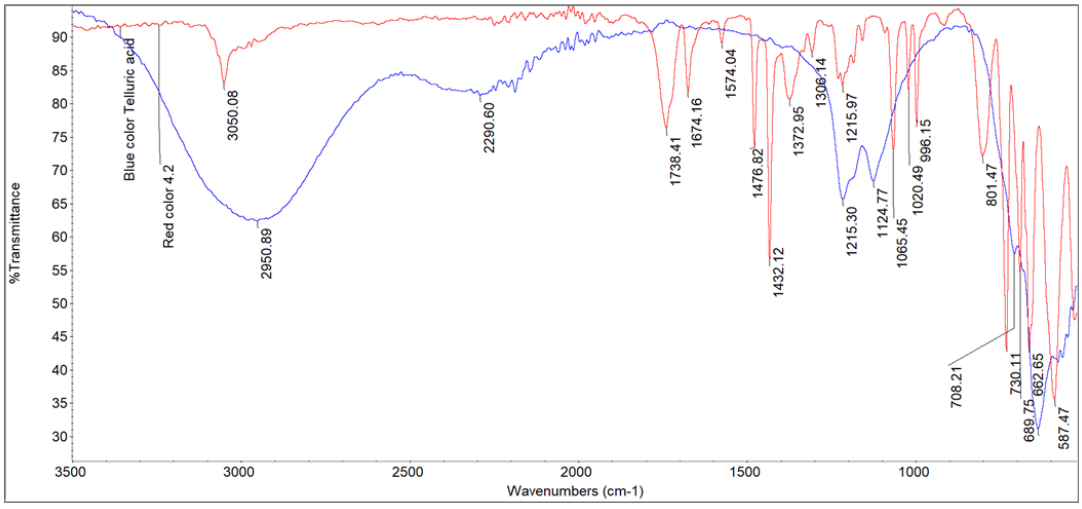

Figure S10. Infrared spectra of cluster 4.1

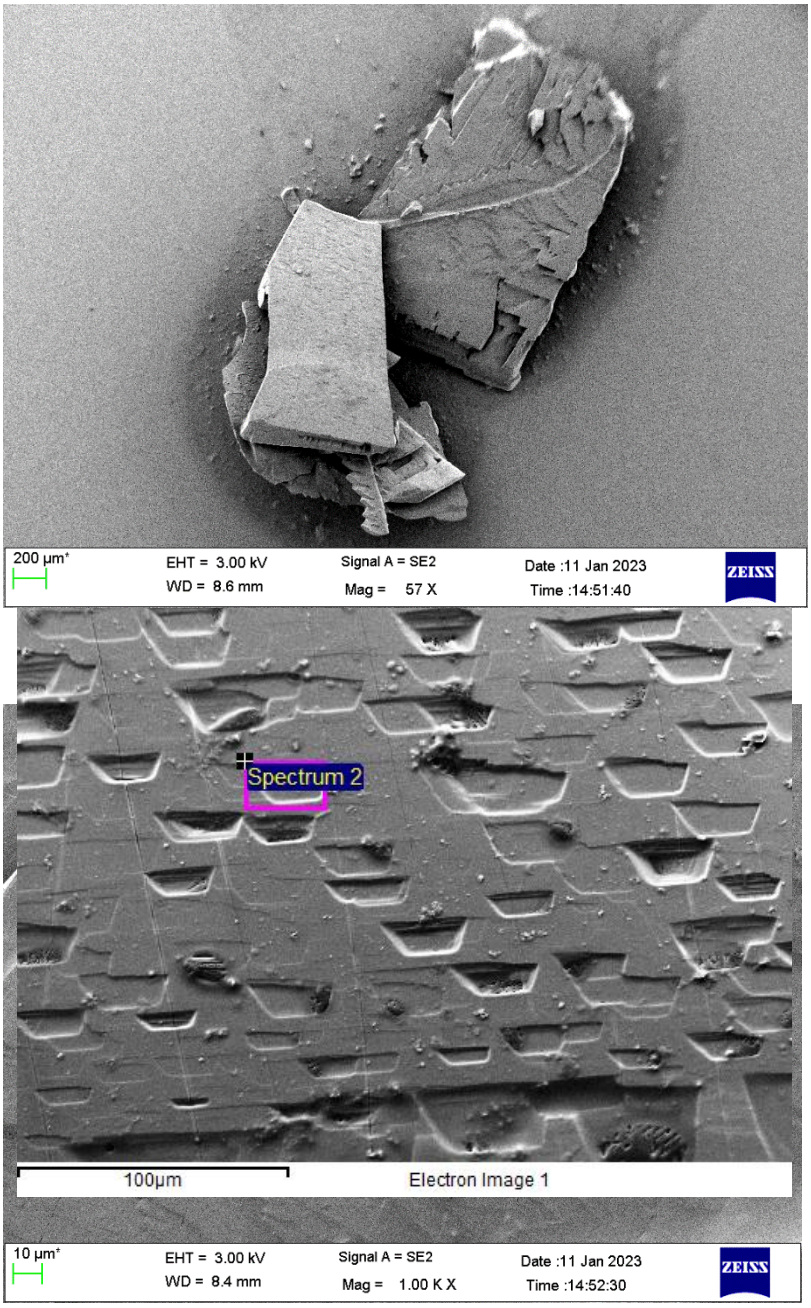

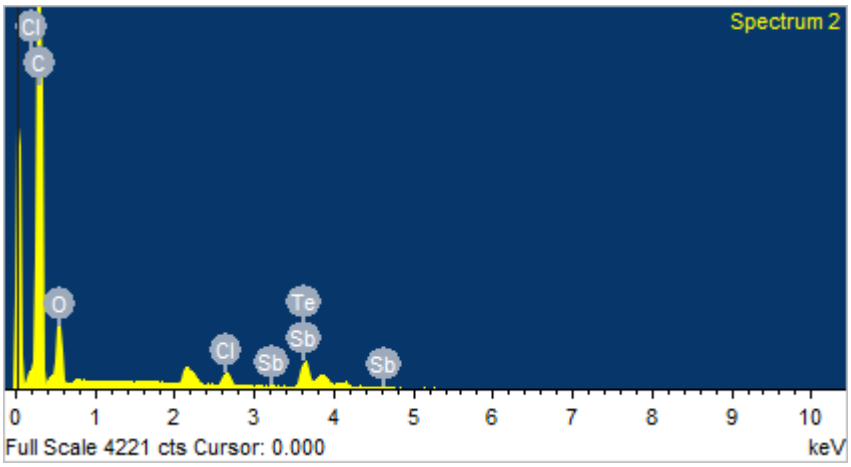
Spectrum 2
Cl
C
O
Cl
Sb
Te
Sb
Sb
0
1
2
3
4
5
6
7
8
9
10
Full Scale 4221 cts Cursor: 0.000
keV

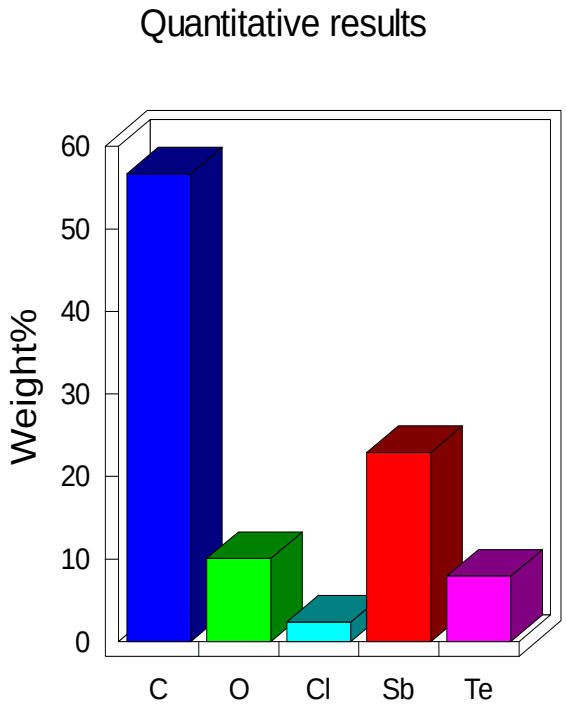

Figure S11: EDAX spectrum of cluster **4.2**.

Element	Calculated weight%	Measured weight% from EDAX analysis
C	45.52	45.32
O	7.93	7.92
Cl	2.90	2.87
Sb	30.10	30.01
Te	10.52	10.42
H	3.03	3.01

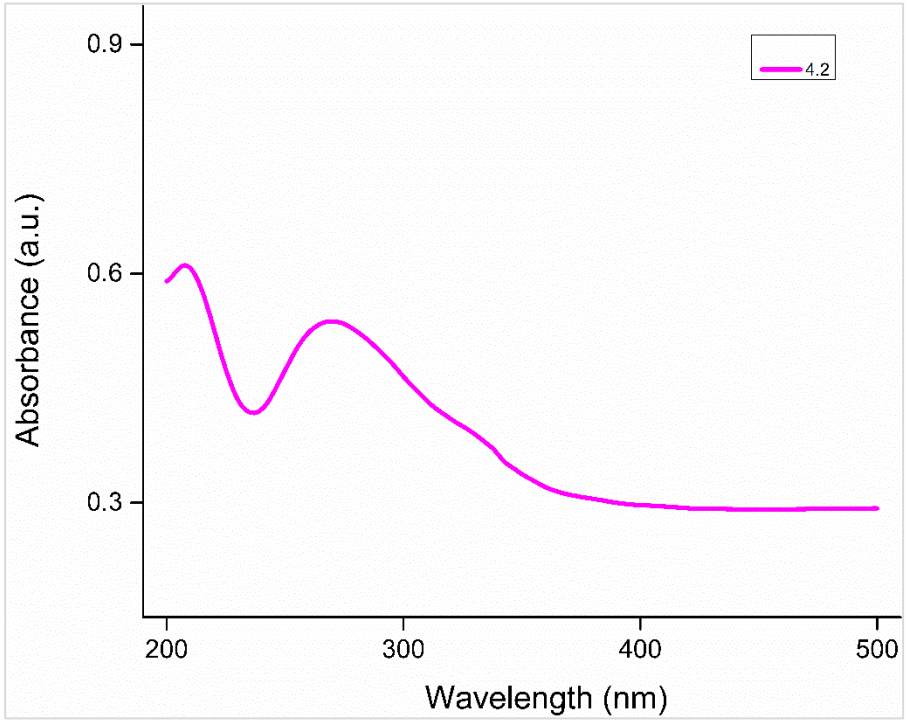
0.9
0.6
0.3
Absorbance (a.u.)
4.2
200
300
400
500
Wavelength (nm)

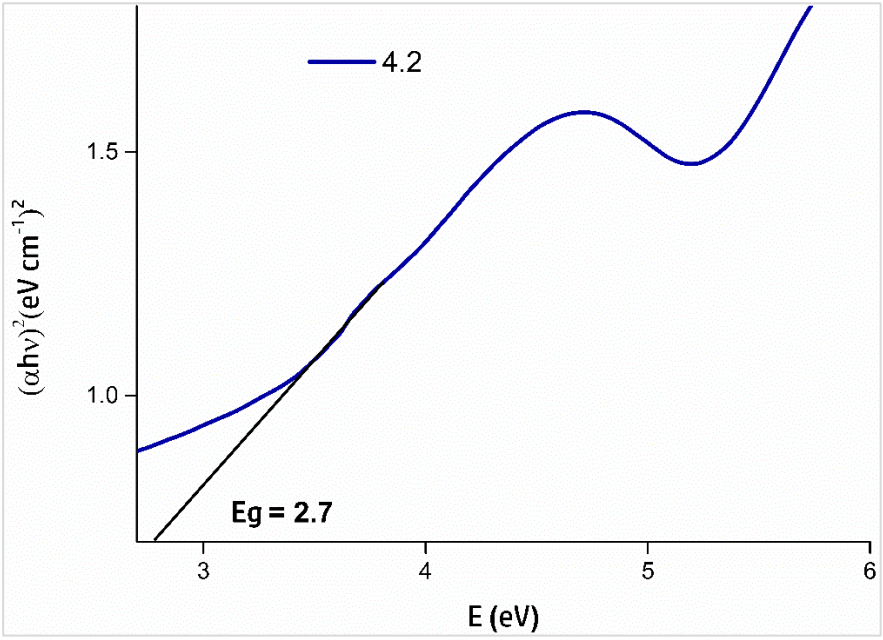
4.2
1.5
1.0
$(\alpha h\nu)^2(eV\ cm^{-1})^2$
Eg = 2.7
3
4
5
6
E (eV)

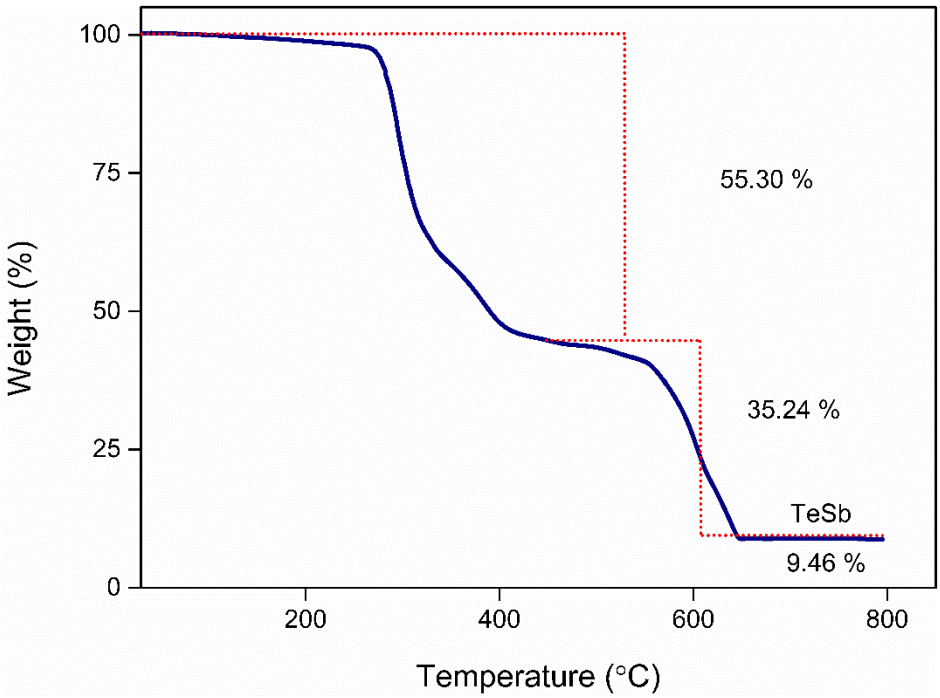

Figure 6. Thermogravimetric analysis and 4.2.

References:

1. R. J. Gilliard and C. W. Chiu, 2020 An Update on the "Organometallic Chemistry of the Main-Group Elements", *Organometallics*, **39**, 4123-4126.
2. M. R. Friedfeld, J. L. Stein and B. M. Cossairt, 2017 Main-Group-Semiconductor Cluster Molecules as Synthetic Intermediates to Nanostructures, *Inorg Chem*, **56**, 8689-8697.
3. A. Rahaman, G. C. Lisensky, J. Browder-Long, D. A. Hrovat, M. G. Richmond, E. Nordlander and G. Hogarth, 2020 Electrocatalytic proton-reduction behaviour of telluride-capped triiron clusters: tuning of overpotentials and stabilization of redox states relative to lighter chalcogenide analogues, *Dal Trans*, **49**, 7133-7143.
4. V. Chandrasekhar and R. Thirumoorthi, 2009 Tellurasiloxane cages containing $Te_6Si_4O_{12}$ and $Te_6Si_6O_{15}$ frameworks, *Inorg Chem*, **48**, 6236-6241.
5. M. A. Said, K. C. Kumara Swamy, D. M. Poojary, A. Clearfield, M. Veith and V. Huch, 1996 Dinuclear and Tetranuclear Cages of Oxodiphenylantimony Phosphinates: Synthesis and Structures, *Inorg Chem*, **35**, 3235-3241.
6. M. A. Said, K. C. K. Swamy, K. Babu, K. Aparna and M. Nethaji, 1995 Diphenylantimony(V) oxo/chloro carboxylates and phosphinates: crystal structures of $\{SbPh_2Cl[O_2P(C_6H_{11})_2]\}_2O$ and $[SbPh_2(O_2CPh)_2]_2O$, *J. Chem. Soc, Dalton Trans*, DOI: 10.1039/dt9950002151, 2151.
7. K. C. Kumara Swamy, M. A. Said and M. Netaji, 1999 A heptacoordinated mononuclear diphenylantimony carboxylate, *J. Chem. Crystallogr*, **29**, 1103-1106.
8. D. Dakternieks, R. Digiacomo, R. W. Gable and B. F. Hoskins, 1988 Observation of Secondary Bonding in Solution - Synthesis, Nmr-Studies, and the Crystal-Structure of $[C_8H_8Te[S_2P(OEt)_2]$, *J. Am. Chem. Soc*, **110**, 6541-6546.

9. M. Driess, C. v. Hänisch and K. Merz, 1999 The First Orthotelluric Acid Polysilylesters: Synthesis and Crystal Structure of $[(Me_3SiO)_8Te_2O_2]$ and $[(Me_4Si_2O_2)_3Te]$, *Z Anorg Allg Chem*, **625**, 493-496.
10. J. Beckmann, D. Dakternieks, J. O'Connell, K. Jurkschat and M. Schürmann, 2002 The First Well-Defined Tellurastannoxanes: the X-ray Structure oftrans-$[(Bu_3SnO)_2\{CH_2(Ph_2SnO)_2\}_2Te]$, *Eur. J. Inorg. Chem*, **2002**, 1484-1487.
11. J. Beckmann, M. Hesse, H. Poleschner and K. Seppelt, 2007 Formation of mixed-valent aryltellurenyl halides RX2TeTeR, *Angew Chem Int Ed Engl*, **46**, 8277-8280.
12. D. Tran Qui, J. Vicat and A. Durif, 1984 Structure of telluric acid–glycine (1:2) monohydrate, $Te(OH)_{6.2}$ $C_2H_5NO_2.H_2O$, at 120 K and determination of hydrogen positions, *Acta Crystallogr. C Struct. Com*, **40**, 181-184.
13. J. H. Son, J. Wang, F. E. Osterloh, P. Yu and W. H. Casey, 2014 A tellurium-substituted Lindqvist-type polyoxoniobate showing high H(2) evolution catalyzed by tellurium nanowires via photodecomposition, *Chem Commun (Camb)*, **50**, 836-838.
14. K. Li, H. Lian and R. V. Deun, 2018 Site occupancy and photoluminescence properties of a novel deep-red-emitting phosphor $NaMgGdTeO_6:Mn^{4+}$ with perovskite structure for w-LEDs, *J. Luminescence*, **198**, 155-162.
15. N. K. Srungavruksham and V. Baskar, 2013 Organoantimony(V) Phosphinates, Phosphonates, and Seleninates, *Eur. J. Inorg. Chem*, **2013**, 4345-4352.
16. N. K. Srungavruksham and V. Baskar, 2015 assembling anionic Sb(V)/(III) containing poly-oxo-stibonates stabilized by triphenyl tellurium cations, *Dalton Trans*, **44**, 6358-6362.
17. (a). A. F. M. M. Rahman, T. Murafuji, M. Ishibashi, Y. Miyoshi and Y. Sugihara, 2005 *J. Organomet. Chem.*, 690, 4280. (b). J. Bergman, 1972 *a novel synthesis of biaryls*, Pcrgamon Press, , vol. **28**.

18. Rahman A F M M, Murafuji T, Ishibashi M, MiyoshiY and Sugihara Y 2004 Effect of π-accepting substituent on the reactivity and spectroscopic characteristics of triarylbismuthanes and triarylbismuth dihalides *J. Organomet. Chem.* **689** 3395
19. H. Pritzkow and K. Seppelt, 2002 Crystal and molecular structure of tellurium(VI) tetrakis [oxopentafluorotellurate(VI)] difluoride, *Inorg. Chem*, **16**, 2685-2687.
20. K. V. Domasevitch and G. A. Senchyk, 2021 Tris[tri-phenyl-antimony(V)]hexa(mu-oxido)-tellurium(VI): a mol-ecular complex with six Te-O-Sb bridges, *Acta Crystallogr E Crystallogr Commun*, **77**, 1229-1233.
21. Pankove, J. I. Optical Processes in Semiconductors; Courier Corporation, 1971.
22. P. Makula, M. Pacia and W. Macyk, *J. Phys. Chem. Lett*, 2018, **9**, 6814-6817.

checkCIF (basic structural check) running

Checking for embedded fcf data in CIF ...
No extractable fcf data in found in CIF

checkCIF/PLATON (basic structural check)

You have not supplied any structure factors. As a result the full set of tests cannot be run.
THIS REPORT IS FOR GUIDANCE ONLY. IF USED AS PART OF A REVIEW PROCEDURE FOR PUBLICATION, IT SHOULD NOT REPLACE THE EXPERTISE OF AN EXPERIENCED CRYSTALLOGRAPHIC REFEREE.

You have not supplied any structure factors. As a result the full set of tests cannot be run.
No syntax errors found. CIF dictionary
Please wait while processing .... Interpreting this report
Structure factor report

Datablock: Compound-5

Bond precision:	C-C = 0.0220 A		Wavelength=0.71073
Cell:	**a=15.3504(5)**	**b=16.2441(5)**	**c=16.3271(5)**
	alpha=82.150(2)	beta=89.207(3)	gamma=84.745(2)
Temperature:	100 K		

	Calculated	Reported
Volume	4016.1(2)	4016.1(2)
Space group	P -1	P -1
Hall group	-P 1	-P 1
Moiety formula	C168 H172 O30 P6 Te6, 2(C7 H8)	C168 H172 O30 P6 Te6, 2(C7 H8)
Sum formula	C182 H188 O30 P6 Te6	C182 H188 O30 P6 Te6
Mr	3806.76	3806.73
Dx,g cm-3	1.574	1.574
Z	1	1
Mu (mm-1)	1.210	1.210
F000	1922.0	1922.0
F000'	1920.20	
h,k,lmax	15,16,16	15,16,16
Nref	8420	8356
Tmin,Tmax	0.897,0.908	0.754,1.000
Tmin'	0.897	

Correction method= # Reported T Limits: Tmin=0.754
Tmax=1.000 AbsCorr = MULTI-SCAN
Data completeness= 0.992 Theta(max)= 20.815
R(reflections)= 0.0671(5256) wR2(reflections)= 0.1888(8356)
S = 1.030 Npar= 1031

PLATON version of 06/07/2023; check.def file version of 30/06/2023

Datablock Compound-5 - ellipsoid plot

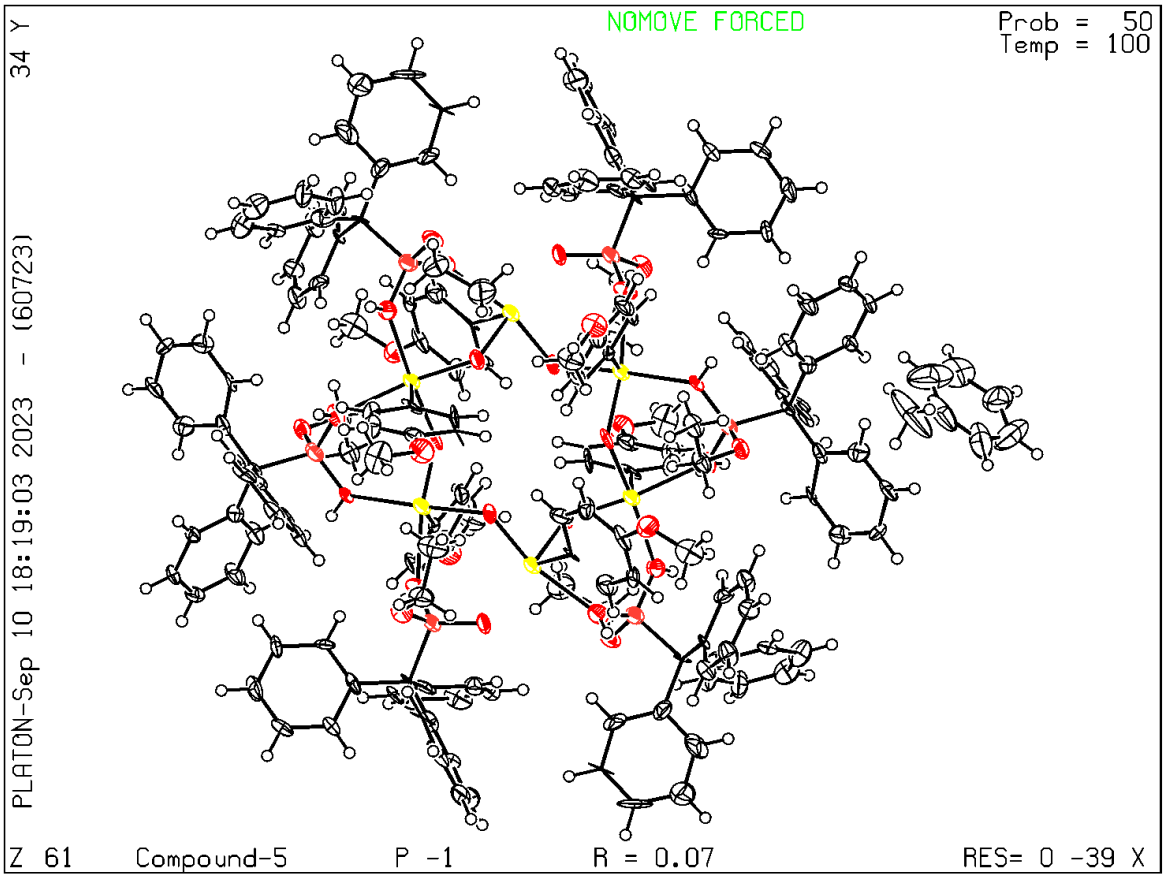

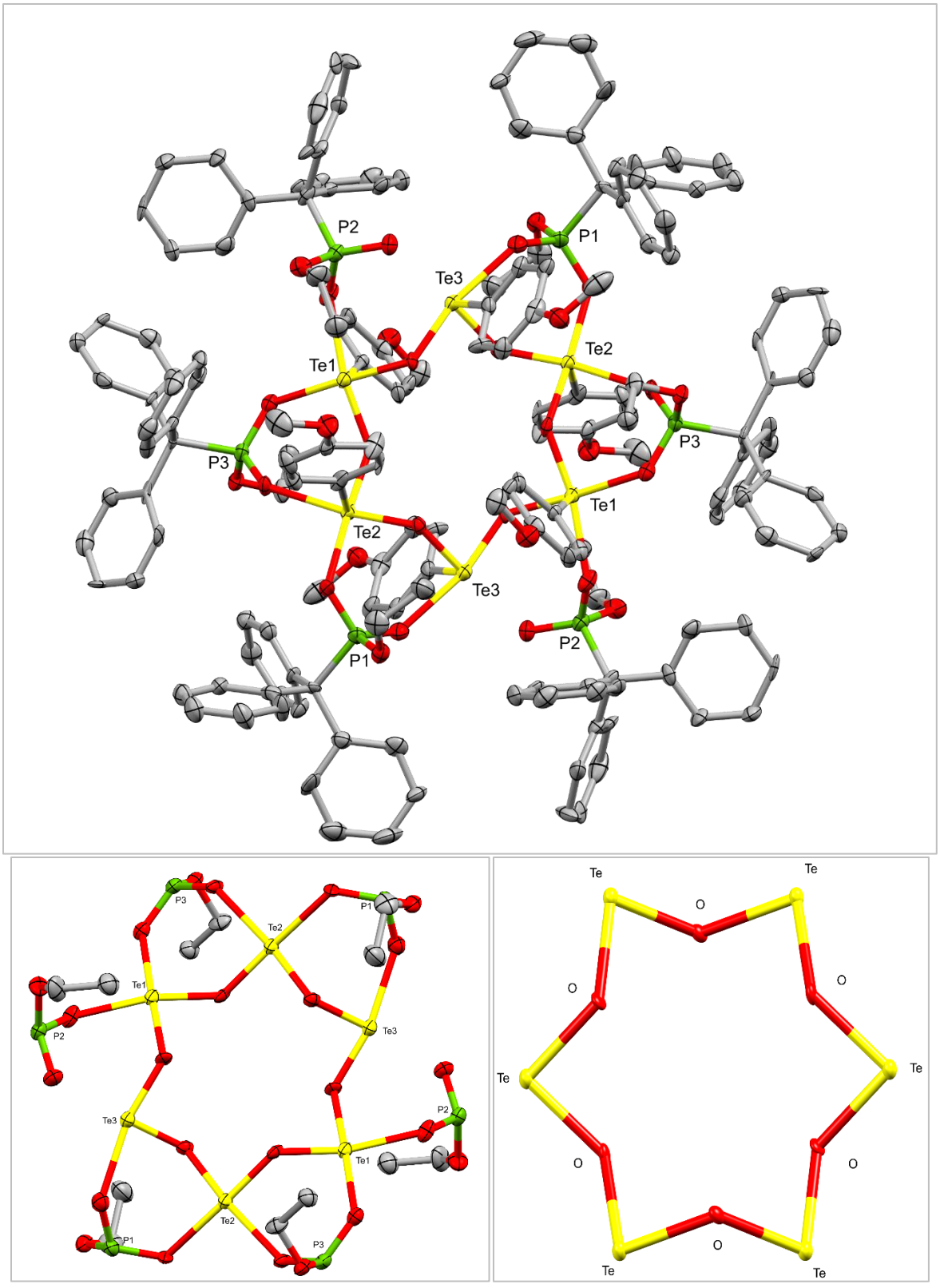

Figure. E1. Solid state molecular crystal structure of compound 5 (top), its core structure (left below) and star shape core (right below) hydrogen atoms are omitted for clarity. Thermal ellipsoids are drawn at 50% probability.

Datablock: Compound-6

```
Bond precision:     C-C = 0.0311 A              Wavelength=0.71073
Cell:         a=23.20900    b=16.62600    c=26.62700
              alpha=90      beta=114.3400 gamma=90
Temperature:  100 K
```

	Calculated	Reported
Volume	9361.382	9361
Space group	C 2/c	C 1 2/c 1
Hall group	-C 2yc	-C 2yc
Moiety formula	C82 H68 O14 P2 Te4, 2(C6 H5), 2(C6 H2), 2(Cl)	0.8(C94 H78 O14 P2 Te4), 1.6(Cl), 1.6(C6 H2)
Sum formula	C106 H82 Cl2 O14 P2 Te4	C84.80 H72 Cl1.60 O11.20 P1.60 Te3.20
Mr	2222.96	1784.81
Dx,g cm-3	1.577	1.583
Z	4	5
Mu (mm-1)	1.390	1.391
F000	4408.0	4440.0
F000'	4403.20	
h,k,lmax	30,21,34	28,21,34
Nref	10822	9754
Tmin,Tmax	0.779,0.858	0.374,1.000
Tmin'	0.736	

```
Correction method= # Reported T Limits: Tmin=0.374
Tmax=1.000 AbsCorr = MULTI-SCAN
Data completeness= 0.901       Theta(max)= 27.536
R(reflections)= 0.0801( 5629)                wR2(reflections)=
                                             0.2573( 9754)
 S = 1.064            Npar= 575
```

PLATON version of 06/07/2023; check.def file version of 30/06/2023

Datablock Compound-6 - ellipsoid plot

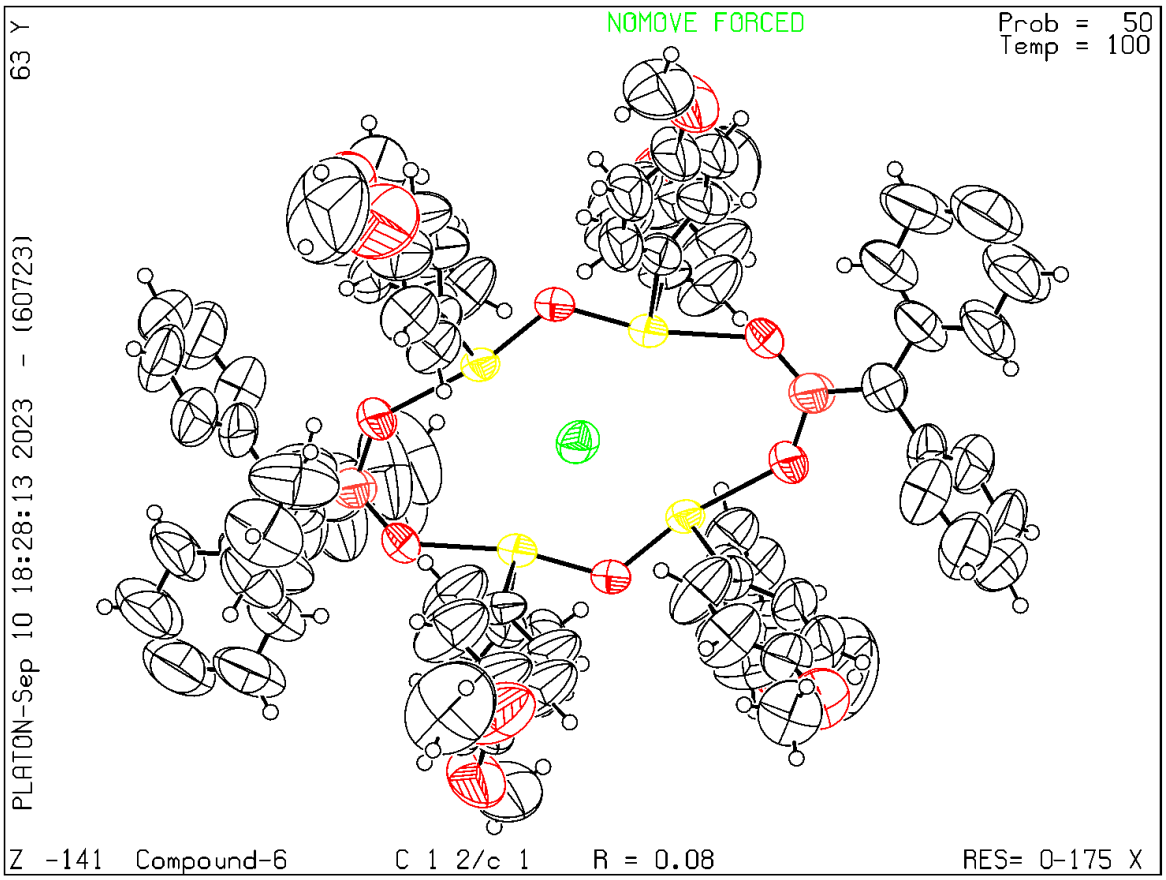

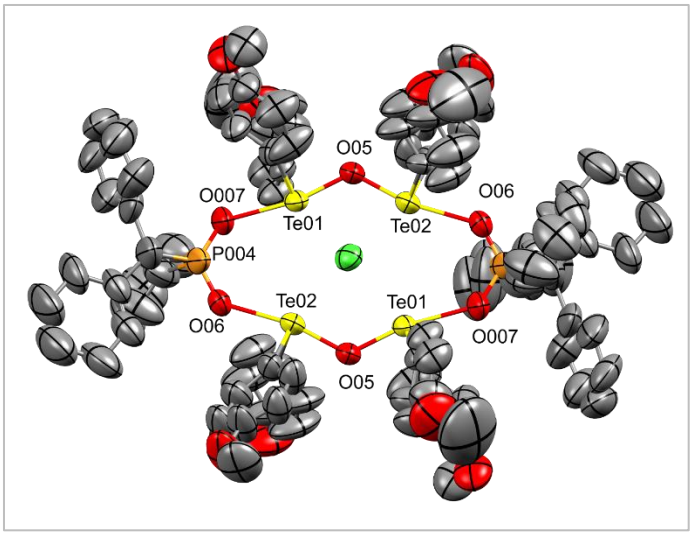

Figure. E2. Solid state molecular crystal structure of compound 6, hydrogen atoms are omitted for clarity. Thermal ellipsoids are drawn at 50% probability.

Datablock: Compound-7

```
Bond precision:      C-C = 0.0441 A              Wavelength=0.71073
Cell:          a=23.3222(9)  b=16.7196(3)     c=26.6409(7)
               alpha=90      beta=111.915(4)  gamma=90
Temperature:   136 K
                    Calculated                      Reported
Volume              9637.6(6)                       9637.6(5)
Space group         C 2/c                           C 1 2/c 1
Hall group          -C 2yc                          -C 2yc
Moiety formula      C40 H35 O6 P Te2, C6 H6, C6     2(C188 H172 O28 P4 Te8), 8(N
                    H3, N O3, C H3 O, H             O3), 8(C6 H3), 8(H)
Sum formula         C53 H48 N O10 P Te2             C424 H384 N8 O80 P8 Te16
Mr                  1145.09                         9160.73
Dx,g cm-3           1.578                           1.578
Z                   8                               1
Mu (mm-1)           1.304                           1.304
F000                4576.0                          4576.0
F000'               4570.24
h,k,lmax            29,21,33                        29,21,32
Nref                10502                           10043
Tmin,Tmax           0.882,0.925                     0.708,1.000
Tmin'               0.878
Correction method= # Reported T Limits: Tmin=0.708
Tmax=1.000 AbsCorr = MULTI-SCAN
Data completeness= 0.956       Theta(max)= 26.979
R(reflections)= 0.1179( 6475)                  wR2(reflections)=
                                               0.4062( 10043)
 S = 1.556             Npar= 497
```

PLATON version of 06/07/2023; check.def file version of 30/06/2023

Datablock Compound-7 - ellipsoid plot

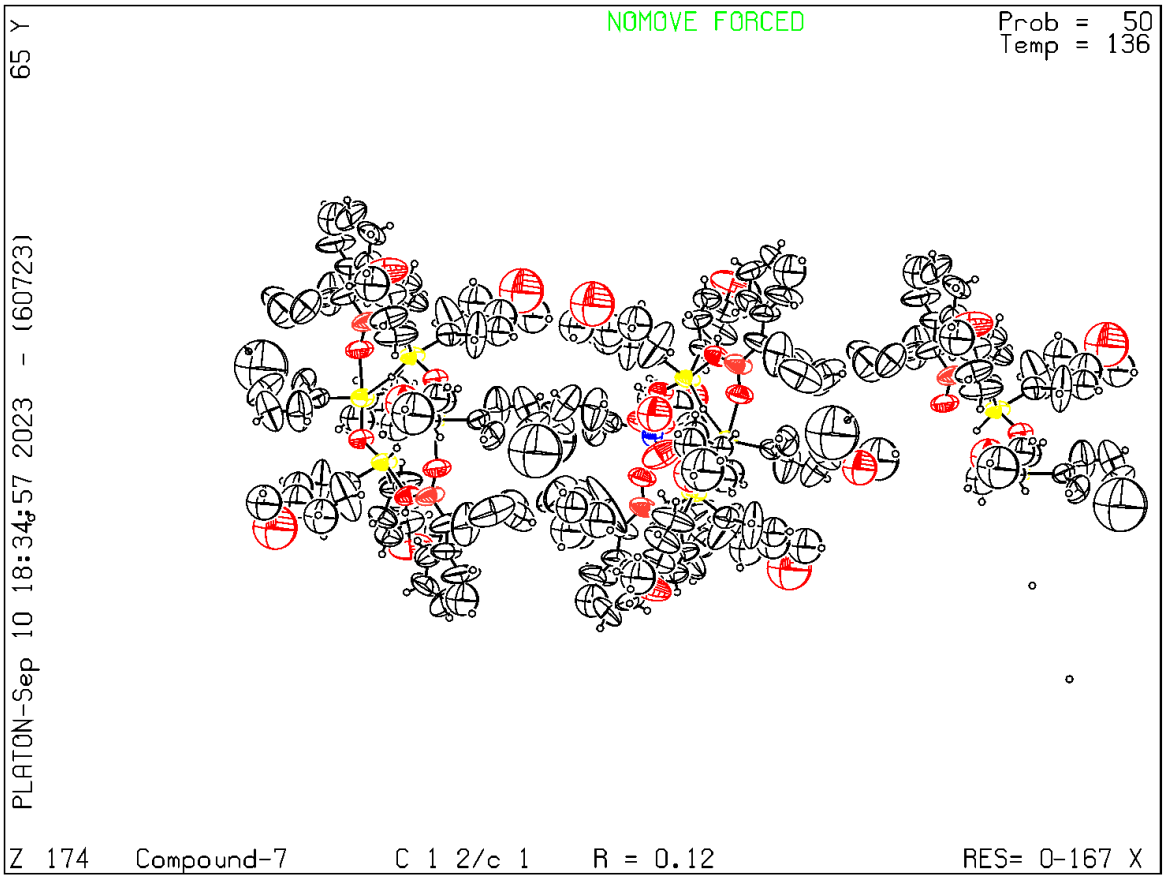

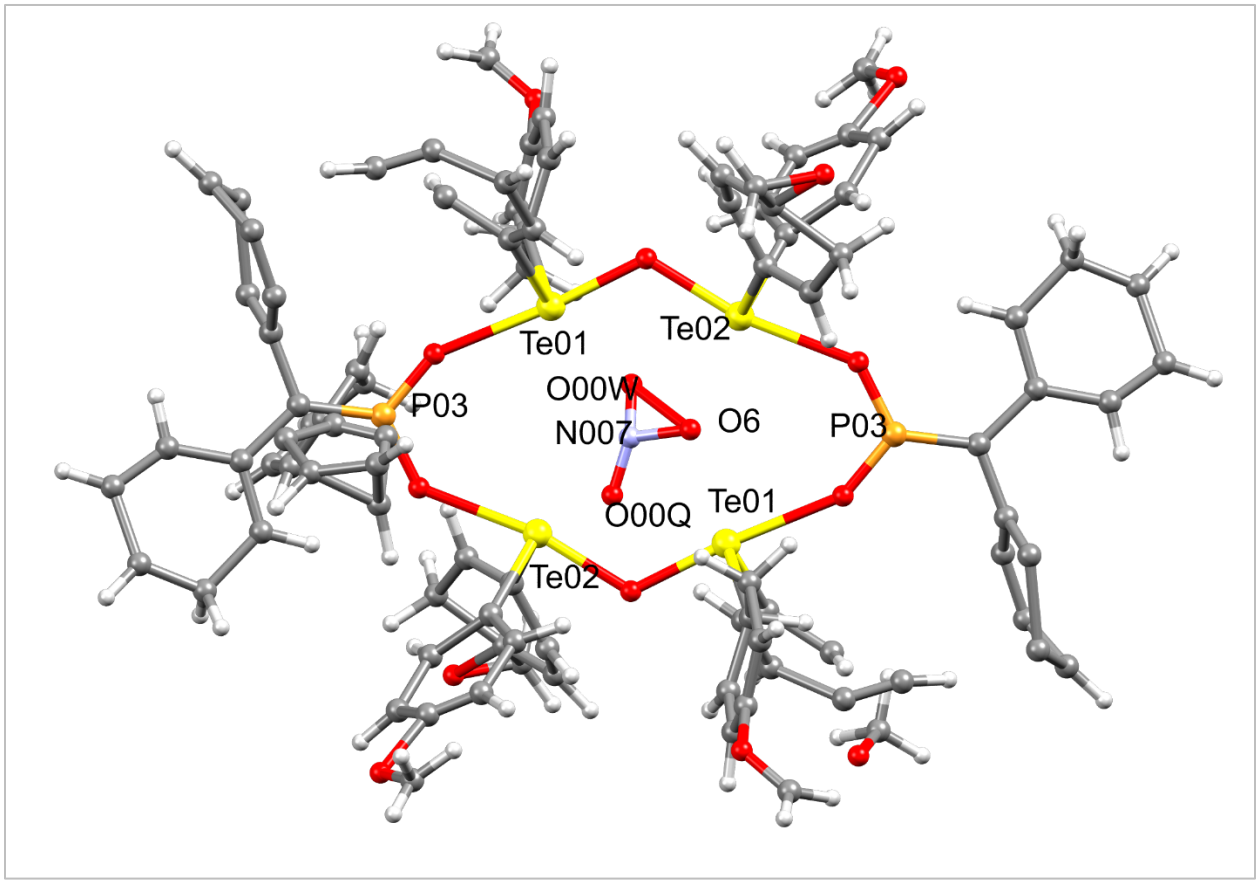

Figure. E3. Solid state molecular crystal structure of compound 7. Thermal ellipsoids are drawn at 50% probability.

Datablock: Compound-8

Bond precision:	C-C = 0.0088 A		Wavelength=0.71073
Cell:	a=7.6701(3)	b=7.4722(2)	c=22.6515(7)
	alpha=90	beta=90	gamma=90
Temperature:	293 K		
	Calculated		Reported
Volume	1298.22(7)		1298.21(7)
Space group	P n m a		P n m a
Hall group	-P 2ac 2n		-P 2ac 2n
Moiety formula	C7 H7 Cl4 O Te, H3 N		C7 H7 Cl4 O Te, H3 N
Sum formula	C7 H10 Cl4 N O Te		C7 H10 Cl4 N O Te
Mr	393.56		393.56
Dx,g cm-3	2.014		2.014
Z	4		4

```
Mu (mm-1)          3.084                          3.084
F000               748.0                          748.0
F000'              748.42
h,k,lmax           9,9,28                         9,9,28
Nref               1522                           1474
Tmin,Tmax          0.744,0.940                    0.217,1.000
Tmin'              0.735
Correction method= # Reported T Limits: Tmin=0.217
Tmax=1.000 AbsCorr = MULTI-SCAN
Data completeness= 0.968       Theta(max)= 26.942
R(reflections)= 0.0435( 1292)                  wR2(reflections)=
                                               0.1166( 1474)
 S = 1.077             Npar= 87
```

PLATON version of 06/07/2023; check.def file version of 30/06/2023

Datablock Compound-8 - ellipsoid plot

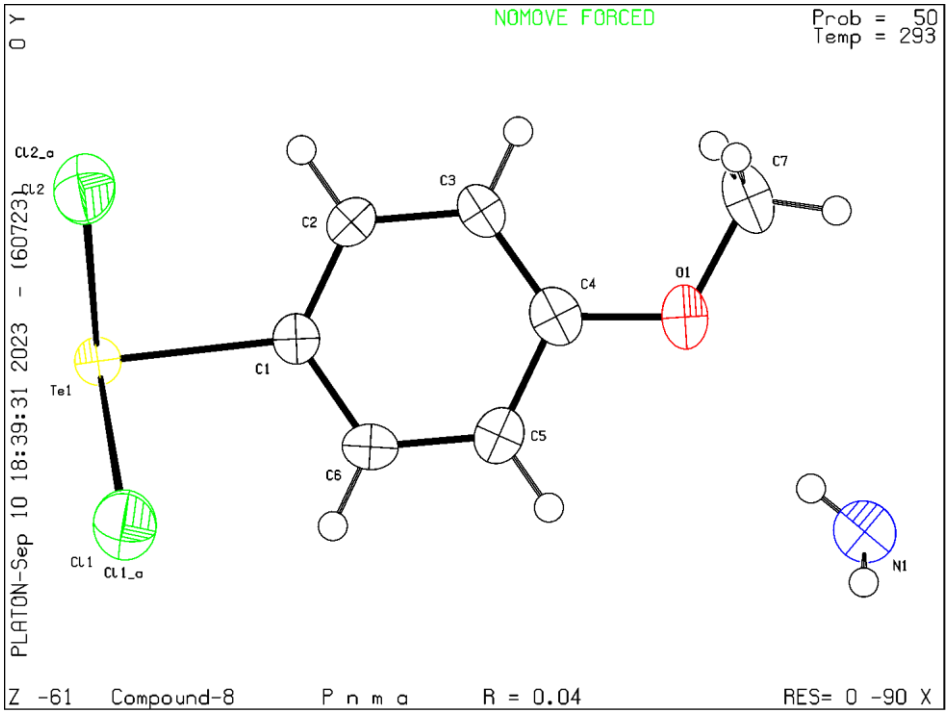

Figure. E4. Solid state molecular crystal structure of compound 8. Thermal ellipsoids are drawn at 50% probability.

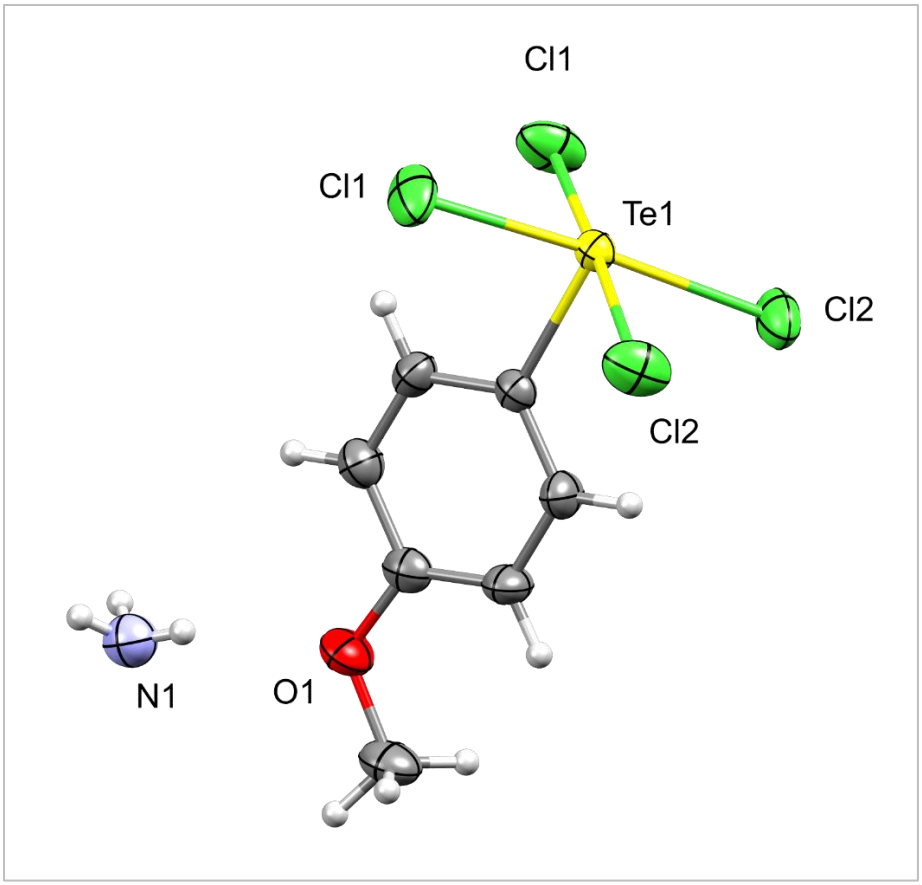
Cl1
Cl1
Te1
Cl2
Cl2
N1
O1

Future Scope of the Thesis

In the thesis, we have worked on synthesis of the 12-membered organotelluroxane 2(Te-O-Te), telluronium salts and organotellurium clusters using *bis*-(*p*-methoxy phenyl) tellurium dichloride with various silver salts and telluric acid respectively. These synthesized organotelluroxane macrocycle working as electrocatalyst for the hydrogen evolution by proton reduction using external proton source of PTSA. Using similar synthetic strategies one can synthesize 2 (Te-O-Te-O-Te) telluroxane motifs containing macrocycle which may increase the electrocatalytic efficiency for hydrogen production. In the chapter-4 chloro biding cluster synthesized one can synthesize bromo, Iodo-binding cluster to decrease bond gaps.

Publications

1. Pilli V V N Kishore, Junaid Ali, **Gujju Narsimhulu** and Viswanathan Baskar. Investigations on the reactivity of aryl antimony halides with N,O-donor ligands. ***J. Chem. Sci.*** **2018**, 130:100; https://doi.org/10.1007/s12039-018-1495-3
2. **Gujju Narsimhulu**, Calvin Samuel, Satish Phalani, Sai Hemant Kumar Dasari, *Krishnamoorthy Kothandam*, Viswanathan Baskar. Electrocatalytic hydrogen evolution mediated by an organotelluroxane stabilized through secondary interactions. (*Manuscript Submitted for peer review ID:* DT-ART-08-2023-002746.
3. **Gujju Narsimhulu**, and Viswanathan Baskar. Organotellurium macrocycle and telluronium salts (*Manuscript under preparation*)
4. **Gujju Narsimhulu**, and Viswanathan Baskar. Star-shaped Te(VI)-Te(IV) complex and an octanuclear Te_2Sb_6 heterometallic oxo cluster. (*Manuscript Submitted for peer review ID:* JCSC-D-23-00505

Posters and oral presentations

1. Presented a poster National Conference "New Frontiers in Chemical Sciences (NFCS-2018)" at Department of Chemistry Indian Institute of Technology Bombay 13 to 14 December 2018 (Won the Best Poster Award)
2. Attended National Conference "47th National Seminar on crystallography -2019". At Department of Atomic Energy, Government of India in association of Board of Nuclear in Science, Baba Atomic Research Center Bombay
3. Presented a poster in International Conference "Modern Trends in Inorganic Chemistry (MTICXVIII)" at Department of Chemistry Indian Institute of Technology Guwahati from 11 to 14 December 2019
4. Presented a poster. in "Inhouse symposium Chemfest-2019" School of Chemistry University of Hyderabad Gachibowli, Hyderabad Telangana 500046
5. Presented a poster at in-house symposium Chemfest-2020 School of Chemistry University of Hyderabad Gachibowli, Hyderabad Telangana-500046. (Won the Best Poster Award)

6. An oral presentation "Organotellurium Macrocycles and Telluronium salt stabilized by Weak Anions" at in-house symposium Chemfest-2021 School of Chemistry University of Hyderabad Gachibowli, Hyderabad Telangana-500046.

Synthesis and Application of Organotelluroxane Macrocycles and Clusters

by Gujju Narsimhulu

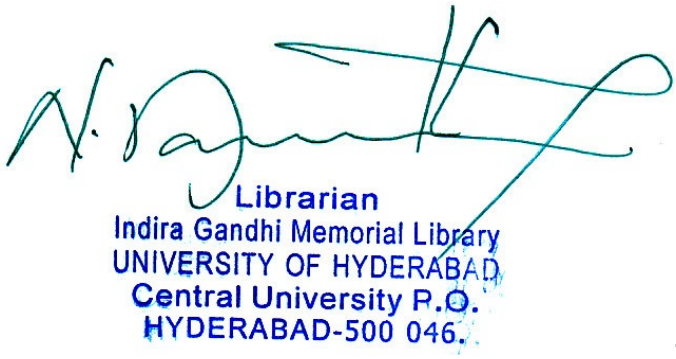

Submission date: 12-Sep-2023 11:09AM (UTC+0530)
Submission ID: 2163894519
File name: Thesis_for_Plagarism_check.docx (762.01K)
Word count: 9458
Character count: 55352

Synthesis and Application of Organotelluroxane Macrocycles and Clusters

ORIGINALITY REPORT

7%	4%	6%	1%
SIMILARITY INDEX	INTERNET SOURCES	PUBLICATIONS	STUDENT PAPERS

PRIMARY SOURCES

1	pubs.rsc.org Internet Source	2%
2	Vadapalli Chandrasekhar, Ramalingam Thirumoorthi. "Halide-Capped Tellurium-Containing Macrocycles", Inorganic Chemistry, 2009 Publication	1%
3	repository.ias.ac.in Internet Source	1%
4	Jens Beckmann, Dainis Dakternieks, Jenny O'Connell, Klaus Jurkschat, Markus Schürmann. "The First Well-Defined Tellurastannoxanes: the X-ray Structure oftrans-[(Bu3SnO)2{CH2(Ph2SnO)2}2Te]", European Journal of Inorganic Chemistry, 2002 Publication	<1%
5	www.researchgate.net Internet Source	<1%

6	Benyu Zhou, François P. Gabbaï. "Redox-controlled chalcogen-bonding at tellurium: Impact on Lewis acidity and chloride anion transport properties", Chemical Science, 2020 Publication	<1 %
7	He, Gang, Olena Shynkaruk, Melanie W. Lui, and Eric Rivard. "Small Inorganic Rings in the 21st Century: From Fleeting Intermediates to Novel Isolable Entities", Chemical Reviews Publication	<1 %
8	Jens Beckmann, Dainis Dakternieks, Andrew Duthie, François Ribot, Markus Schürmann, Naomi A. Lewcenko. " New Insights into the Structures of Diorganotellurium Oxides. The First Polymeric Diorganotelluroxane [(-MeOC H) TeO] ", Organometallics, 2003 Publication	<1 %
9	www.nature.com Internet Source	<1 %
10	Benyu Zhou, François P. Gabbaï. "Anion Chelation via Double Chalcogen Bonding: The Case of a Bis-telluronium Dication and Its Application in Electrophilic Catalysis via Metal–Chloride Bond Activation", Journal of the American Chemical Society, 2021 Publication	<1 %
11	core.ac.uk Internet Source	

		<1 %
12	Jerod M. Kieser, Leighton O. Jones, Nathan J. Lin, Matthias Zeller, George C. Schatz, Suzanne C. Bart. " Synthesis and Characterization of Tellurium Catecholates and Their -Oxide Adducts ", Inorganic Chemistry, 2021 Publication	<1 %
13	Matthias A. Grasser, Tobias Pietsch, Jan Blasius, Oldamur Hollóczki, Eike Brunner, Thomas Doert, Michael Ruck. "Coexistence of Tellurium Cations and Anions in Phosphonium-Based Ionic Liquids", Chemistry – A European Journal, 2021 Publication	<1 %
14	hdl.handle.net Internet Source	<1 %
15	livrepository.liverpool.ac.uk Internet Source	<1 %
16	Aayushi Arora, Preeti Oswal, Anupama Datta, Arun Kumar. "Complexes of metals with organotellurium compounds and nanosized metal tellurides for catalysis, electrocatalysis and photocatalysis", Coordination Chemistry Reviews, 2022 Publication	<1 %

17	Rudolf Pietschnig, Stefan Spirk. "The chemistry of organo silanetriols", Coordination Chemistry Reviews, 2016 Publication	<1 %
18	Tyler A. Sullens, Thomas E. Albrecht-Schmitt. " Structure and Properties of the Thorium Vanadyl Tellurate, Th(VO) (TeO)(H O) ", Inorganic Chemistry, 2005 Publication	<1 %
19	harvest.usask.ca Internet Source	<1 %
20	www.rsc.org Internet Source	<1 %
21	Manfred Scheer, Mehdi Elsayed Moussa, Stefan Welsch, Matthias Lochner, Eugenia Peresypkina, Alexander Virovets. "Organometallic-Organic Hybrid Polymers Assembled from Pentaphosphaferrocene, Bipyridyl Linkers and CuI Ions", European Journal of Inorganic Chemistry, 2018 Publication	<1 %
22	Vigato, P.A.. "The challenge of cyclic and acyclic schiff bases and related derivatives", Coordination Chemistry Reviews, 200410 Publication	<1 %
23	Vadapalli Chandrasekhar, Arun Kumar, Mrituanjay D. Pandey. "Imine-functionalized,	<1 %

fluorescent organomercury and -tellurium compounds", Journal of Organometallic Chemistry, 2010
Publication

24	www.funcas.es Internet Source	<1 %

Exclude quotes	On	Exclude matches	< 14 words
Exclude bibliography	On		